Investigation of the interaction between corticomuscular coherence, motor precision and perceived difficulty in wrist flexion and extension

By

Nikhil Vishwas Divekar
BSc (ENG) Mechatronics
DVKNIK001

SUBMITTED TO THE UNIVERSITY OF CAPE TOWN
In partial fulfilment of the requirements for the degree

MSc (MED) Biomedical Engineering

Faculty of Health Sciences

UNIVERSITY OF CAPE TOWN

Date of Submission: 28th August 2012

Supervisor: Dr. Lester R. John
Department: Human Biology, Faculty of Health Sciences, University of Cape Town

DECLARATION

I, Nikhil Vishwas Divekar, hereby declare that the work on which this dissertation is based is my original work (except where acknowledgements indicate otherwise) and that neither the whole work nor any part of it has been, is being, or is to be submitted for another degree in this or any other university.

I empower the university to reproduce for the purpose of research either the whole or any portion of the contents in any manner whatsoever.

Signature: Signed by candidate

Date: 28th August 2013

ABSTRACT

Motivation: Recently, behavioural (motor precision) differences were reported between isometric wrist flexion and extension. Neurophysiological as well as clinical differences have also been reported between these antagonistic movements. Corticomuscular coherence (CMC), i.e. the frequency specific temporal coupling between the electroencephalogram (EEG) and electromyogram (EMG) recorded during isometric force production, reflects the functional connectivity between cortex and muscle. A single muscle (flexor digitorum superficialis) study suggests a positive correlation between 15-35 Hz (beta) CMC and motor precision of the muscle. Yet, no study has simultaneously compared CMC and motor precision between wrist flexion and extension. Task perceived difficulty, which is a perceptual variable, may influence both motor precision and CMC, but has not been studied yet. The main aim of the present study was to investigate the interaction between CMC, motor precision and perceived difficulty in isometric wrist flexion and extension tasks.

Methods: Simultaneous recordings of EEG, EMG and wrist joint torque were made from fifteen healthy subjects who performed 10 repetitions of alternating isometric wrist flexion and extension tasks at 15% of their maximum voluntary contraction (MVC) torque levels. CMC (peak CMC, peak frequency, frequency width, CMC area), as well as associated variables related to cortical activity (normalised EEG alpha and beta powers), muscle activity (normalised EMG beta power), behaviour (motor precision, < 5 Hz torque fluctuation, beta torque fluctuation, MVC) and perception (task perceived difficulty) were calculated and statistically compared between wrist flexion and extension tasks. Motor precision was calculated by quantifying differences between target and actual torque recordings using the mean square error method. Subjects rated the perceived difficulty levels for both tasks on a scale of 1-5 (1 being very easy and 5 being very difficult).

Results: Isometric wrist flexion was associated with significantly lower peak CMC (peak was in the beta band), peak frequency, frequency width, CMC area, normalised EMG beta power, torque fluctuation (<5Hz and beta band) and perceived difficulty ratings; but significantly higher MVC and motor precision compared to extension. Normalised EEG alpha and beta powers were not significantly different between flexion and extension.

Conclusions: An inverse relationship was found between beta CMC (peak CMC and CMC area) and motor precision when comparing isometric wrist flexion and extension; contrary to the direct relationship found in the prior single muscle study. Better functional suitability, long term usage adaptation and lower perceived difficulty of wrist flexion compared to extension may explain the inversion of the beta CMC - motor precision relationship. Further, the lower normalised EMG beta power of the flexors may help explain their lower torque fluctuations (higher precision). Future work would be based on testing the relationship between beta CMC, normalised EMG beta power and torque fluctuation, in an intra-muscle, intra-task scenario, to factor out the variables of muscle and task.

Significance: This study adds to the literature relating CMC and motor precision by including the functionally different, antagonistic wrist flexors and extensors. Further, this study contributes to the general CMC literature by introducing perceived difficulty as one of the variables that potentially influences CMC.

ACKNOWLEDGEMENTS

I would like to thank Dr. L.R. John for his guidance throughout the project, S. Stoeckigt for helping with the design of the electroencephalography system; L. Webb and J. Joseph for assistance with data recording; K. Mauff (Statistical Department, University of Cape Town) for statistical support; C. Harris (Mechanical Workshop, University of Cape Town) for support in construction of the testing manipulandum; R. Seletani and A. Sayed for assistance with the SolidWorks design of the testing manipulandum and J. Pitman for providing the fundamental calibration hardware and software that was used for calibrating the EEG and EMG systems.

I would like to thank my parents and family for their continuous love and support not only during this project but throughout my life.

Last but not the least I would like to thank my dearest Krishna-Balaram and dedicate this dissertation to them.

PUBLICATIONS AND CITATIONS

The core of the work presented in this dissertation has been published (Divekar and John, 2013). The publication received editorial recognition (Ushiyama and Ushiba, 2013) in which the important findings and their contribution to the debate on the relationship between corticomuscular coherence (CMC) and motor precision were further emphasised. There is also a second citation (Chow and Stokic, 2013). The original publication (Divekar and John, 2013) and editorial (Ushiyama and Ushiyba, 2013) are attached at the end of this dissertation after the appendices.

1. **Divekar NV**, John LR. Neurophysiological, behavioural and perceptual differences between wrist flexion and extension related to sensorimotor monitoring as shown by corticomuscular coherence. Clin Neurophysiol. 2013 Jan; 124 (1): 136–47.

2. Ushiyama J, Ushiba J. Resonance between cortex and muscle: A determinant of motor precision? Clin Neurophysiol. 2013 Jan; 124 (1): 5–7.

3. Chow JW, Stokic DS. Impaired force steadiness is associated with changes in force frequency composition in subacute stroke. Neuroscience. 2013 Jul 9; 242 (0): 69–77.

TABLE OF CONTENTS

LIST OF FIGURES

LIST OF ABBREVIATIONS

AT	Actual torque
CL	Confidence level
CMC	Corticomuscular coherence
CMRR	Common mode rejection ratio
CNS	Central nervous system
CPG	Central pattern generator
CSD	Current source density
CV	Coefficient of variation
DAC	Digital to analogue converter
DAQ	Data acquisition
DRL	Driven right leg
ECRB	Extensor carpi radialis brevis
ECRL	Extensor carpi radialis longus
ECU	Extensor carpi ulnaris
ED	Extensor digitorum
EEG	Electroencephalography/Electromyogram
EMG	Electromyography/Electromyogram
EOG	Electrooculography/Electrooculogram
EPSP	Excitatory post synaptic potential
ESD	Electrostatic discharge (ESD)
fc	Cut-off frequency

FCR	Flexor carpi radialis
FCU	Flexor carpi ulnaris
FDS	Flexor digitorum superficialis
fMRI	Functional magnetic resonance imaging
GABA	Gamma-Aminobutyric acid
GTO	Golgi tendon organ
GUI	Graphical user interface
HP	High precision
IED	Inter electrode distance
IPSP	Inhibitory post synaptic potential
LCD	Liquid crystal display
LMN	Lower motor neuron
LP	Low precision
MCU	Microcontroller unit
MEG	Magnetoencephalography
MEP	Motor evoked potential
MI	Primary motor cortex
MRCP	Movement related cortical potential
MSE	Mean square error
MVC	Maximum voluntary contraction
PC	Personal computer
PCB	Printed circuit board

PL	Palmaris longus
PMC	Premotor cortex
PPC	Posterior parietal cortex
PSD	Power spectral density
PSP	Post synaptic potential
SCI	Serial communication interface
SPI	Serial peripheral interface
SI	Primary somatosensory cortex
SII	Secondary somatosensory cortex
SMA	Supplementary motor area
TT	Target torque
USB	Universal serial bus

1 INTRODUCTION

The general field of interest of the present study is the functional role of corticomuscular coherence (CMC) especially in relation with motor precision and perceived difficulty. The findings of various behavioural (motor precision), neurophysiological and clinical differences between wrist flexion and extension provided the impetus for the study. The subject of the present study was investigating the interaction between CMC, motor precision and perceived difficulty between wrist flexion and extension.

1.1 Motivation

Wrist flexors and extensors are antagonistic sets of muscles which although being anatomically close (same joint), seem to be functionally apart. A recent study by Salonikidis et al. (2011) reported that isometric wrist flexion was performed with higher motor precision than extension based on the coefficient of variation (CV) of torque output. The motor precision differences between wrist flexors and extensors also appear to be valid when these muscle groups are involved in more complex movements. For example in sports such as Tennis, there is higher precision and faster learning of forehand strokes (primarily involving flexors) compared to backhand strokes (primarily involving extensors) in beginners (Mavvidis et al., 2010). Furthermore, neurophysiological differences (Cheney and Fetz, 1980; Mink and Thach, 1991; de Noordhout et al., 1999; Yue et al., 2000; Chye et al., 2010) as well as clinical differences (Lieberman, 1986; Duncan and Badke, 1987; Pfann et al., 2004; Little and Massagli, 2007; Vallence et al., 2012) have been reported between wrist flexion and extension in both primates and in humans and emphasise the importance of studying the wrist joint

Motor control in humans involves a significant amount of information exchange between the central nervous system (CNS) and the peripheral nervous system (PNS). Electroencephalography (EEG) can be used to measure neuronal activity at the cortical level of the CNS (Sabate et al., 2012). Electromyography (EMG) can be used to measure muscle activity which indirectly reflects the activity of the neurons of the PNS (Farina et al., 2013). A property of neurons to fire rhythmically i.e. neuronal oscillation has been observed at the cortical level (Pfurtscheller et al., 1996; Sabate et al., 2012) as well as at the muscular level

(Kilner et al., 2002; Farina et al., 2013) using the above mentioned techniques. Interestingly, studies have also demonstrated the existence of significant frequency specific temporal coupling between these cortical and muscular oscillatory activities during steady state muscle force production (Conway et al., 1995; Tatsuya Mima and Hallett, 1999; Chakarov et al., 2009; Ushiyama, Suzuki, et al., 2011). CMC is a measure of the degree of this coupling at a given frequency. This makes CMC a unique tool for probing the motor system as it allows simultaneous analysis of distant (central-peripheral) neural sites.

Although the exact functional role of CMC is still not fully understood (Baker, 2007; Witham et al., 2011), proposed theories associate it with promoting of the existing steady motor state (Gilbertson et al., 2005; Matsuya et al., 2013) and facilitation of efficient sensorimotor monitoring of the peripheral system (Witham et al., 2011). The proposed functional roles seem to match the results of Kristeva et al. (2007), who reported a direct relationship between beta CMC and motor precision, in a study involving isometric force compensation by a single (finger flexor) muscle. In this study, the higher precision periods were associated with significantly higher beta band CMC as well as significantly higher EEG beta band spectral power compared to the lower precision periods. Muscle function (posture or fine movement) and muscle training have also been shown to modulate CMC levels (Ushiyama et al., 2010); however, this study did not simultaneously measure precision levels. In a pre-fatigue post-fatigue comparison study, a positive correlation was found between beta CMC, beta EMG discharge and force fluctuation in the motor system (inversely related to motor precision) (Ushiyama, Katsu, et al., 2011). This actually suggests an overall inverse beta CMC-motor precision relationship although the confounding effect of fatigue could have caused this inversion.

Cognition has been shown to modulate CMC. Kristeva et al. (2002) showed a positive correlation between attention and beta CMC while Schoffelen et al. (2005) showed a positive correlation between the level of preparedness and 40-70 Hz (gamma) CMC. In line with these findings, it is possible that differences in the perceived difficulty of a force maintenance task arising from inherent differences between two muscle groups (e.g. inherent differences between wrist flexors and extensors) may induce cognitive alterations (e.g. in the level of attention and/or level of preparedness) that in turn would modulate CMC.

1.2 Rationales

Although there is a suggested link between CMC and motor precision, no study has investigated these variables simultaneously in wrist flexors and extensors, which are antagonistic muscle groups with not only behavioural (motor precision) differences, but also neurophysiological and clinical differences between them. Also, the potential correlation between task perceived difficulty (a perceptual variable), CMC and motor precision has not been explored previously.

1.3 Aim

The main aim of the present study was to investigate the interaction between CMC, motor precision and perceived difficulty in isometric wrist flexion and extension tasks.

1.4 Objectives

In order to achieve the aim, variables related to CMC, motor precision and perceived difficulty were measured and compared between high precision demanding isometric wrist flexion and extension tasks. Overall, the variables could be grouped into neurophysiological, behavioural and perceptual sections and are listed below with the actual variable names used in the study given in brackets:-

Neurophysiological Variables

1. Peak CMC (CMC_{MAX})
2. Peak CMC frequency (FP)
3. Significant CMC frequency width (FW)
4. Significant CMC area (CMC_{AREA})
5. Normalised EEG alpha power (EEGα-PSD)
6. Normalised EEG beta power (EEGβ-PSD)
7. Normalised EMG beta power (EMGβ-PSD)

Behavioural variables

8. Motor precision (PRECISION)
9. Low-frequency band (< 5 Hz) torque fluctuation (Torque-low-PSD)
10. Beta band (15 - 35 Hz) torque fluctuation (Torqueβ-PSD)
11. Maximum voluntary contraction (MVC)

Perceptual variable

12. Perceived task difficulty (Perceived difficulty rating)

1.5 Hypothesis

It is hypothesised that compared to isometric wrist extension, isometric wrist flexion will be performed with higher motor precision as well as higher beta CMC; thus confirming the previously suggested direct relationship between motor precision and beta CMC and hence explaining the higher motor precision for isometric wrist flexion previously reported.

1.6 Significance of the study

This CMC comparison between the antagonistic wrist muscles may help to improve our understanding of the functional role of CMC especially in relation to motor precision and perceived difficulty, and also provide insight into the underlying causes of the functional differences reported between wrist flexors and extensors.

1.7 Scope of the study

The present study is limited to the study of the right wrist in 15 right handed human subjects, using EEG, EMG and torque measurement techniques. Only neurologically normal healthy subjects will be used during the study. Isometric contraction of the wrist in only two directions i.e. wrist extension and wrist flexion directions will be examined. This study is also limited to one intensity level of isometric contraction per direction; i.e. 15 % of the maximum voluntary contraction level of each direction. Further, only the agonist muscles for each direction will be analysed i.e. only the wrist extensors during wrist extension and only the wrist flexors during wrist flexion will be analysed.

1.8 Plan of development

Section 2 (BACKGROUND) outlines the basic anatomy and physiology of the motor system and the basics of the electrophysiological measurement techniques i.e. EEG and EMG used to probe it at the central and peripheral levels respectively. This information provides a framework for the subsequent sections and may be skipped by the advanced reader.

Section 3 (LITERATURE REVIEW) provides a detailed survey of the related literature, and contains technical, conceptual as well as perspective information related to the present study. It thereby also supports the present study's motivation, rationales, aims and objectives that are mentioned above.

Section 4 (EXPERIMENTAL APPARATURS) provides details on the concept, design, construction and calibration of the experimental apparatus that facilitated the appropriate testing of the objectives of the present study.

Section 5 (EXPERIMENTAL METHODOLOGY) describes the subjects, experimental paradigm, data recording, data analysis and statistical analysis carried out to test the objectives of the present study.

Section 6 (RESULTS) contains the results of the comparisons of the variables (listed under the objectives) between wrist flexion and extension in both a qualitative and quantitative form.

Section 7 (DISCUSSION) explores the possible factors that could have influenced the obtained results.

Section 8 (CONCLUSIONS) rounds up the outcomes of the present study, outlines the limitations of the study as well as discusses future work.

2 BACKGROUND

The information presented in section 2 outlines the basic anatomy and physiology of the motor system (section 2.1) and the basics of the electrophysiological measurement techniques i.e. EEG (section 2.2) and EMG (section 2.3) used to probe it at the central and peripheral levels respectively. This section may be skipped by the advanced reader knowing that references are made back to it where needed from the subsequent sections.

2.1 Motor system basics

The information presented in section 2.1 is primarily acquired from a medical physiology textbook (Guyton and Hall, 2006), an online motor systems textbook (Knierim, 2013) and a motor systems website (University of Wisconsin-Madison, 2009). Additional references are added in text where necessary. The motor system is described here in a 'bottom-up' fashion; starting at the level of the muscle (section 2.1.1), then the spinal cord (section 2.1.2), following on to the descending motor pathways to the spinal cord (section 2.1.3) and ending with the cerebral cortex (section 2.1.4). Additional structures which are considered 'side-loops' i.e. the basal ganglia and cerebellum are also subsequently described in sections 2.1.5 and 2.1.6 respectively.

2.1.1 Muscle activation and sensing

2.1.1.1 Lower motor neurons (LMNs)

At the lowest level of the motor system, an extrafusal muscle fibre contracts to produce force. A muscle is composed of numerous such extrafusal muscle fibres, which are able to contract in union to produce an overall larger force. The contraction of a single extrafusal muscle fibre is controlled by the activation of a single alpha lower motor neuron (LMN) which innervates it; see Figure 2.1. An alpha LMN originates from the ventral root of the spinal cord. A single alpha LMN is able to innervate multiple extrafusal muscle fibres simultaneously by branching of its axon into smaller terminal branches, each of which innervates a single extrafusal muscle fibre. A motor unit is a single alpha LMN and all of the extrafusal muscle fibres it innervates. The number of extrafusal muscle fibres innervated by a single alpha LMN is its innervation ratio. Muscles involved in fine control (e.g. extraocular muscles) have a lower innervation ratio, whereas muscles involved in coarse control (e.g. proximal muscles of the limb) have a higher innervation ratio.

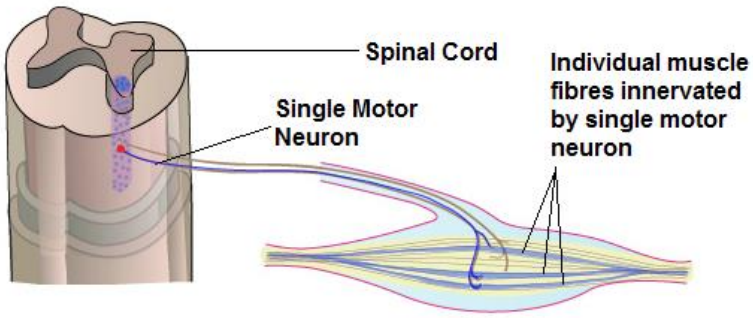

Figure 2.1 Innervation of muscle by motor neurons. Modified from online textbook (Knierim, 2013).

A terminal branch of an alpha LMN forms a neuromuscular junction with the motor end plate of the extrafusal muscle fibre near its midpoint. An action potential originating at the spinal level travels down the main axon of the alpha LMN and down all the terminal axons that innervate individual extrafusal muscle fibres. Upon reaching the neuromuscular junction, the action potential causes the release of a chemical transmitter called acetylcholine into the synaptic cleft (gap between terminal axon and motor end plate). Acetylcholine in turn excites the extrafusal muscle fibre causing it to contract.

The amount of force produced by the extrafusal muscle fibres in a motor unit depends on a number of factors including the rate of firing of action potentials down the motor neuron. A single action potential causes a single twitch of the muscle. If a subsequent action potential occurs after the muscle has returned back to its basal state then the muscle will twitch again, producing the same amount of force as the first twitch. However, if the firing rate is such that the subsequent action potential occurs before the muscle has fully returned to its resting state, then a greater twitch force results as compared to the first (the two muscle contractions summate). A further increase in firing rate will result in a further increase in twitch force until a limit is reached. This is referred to as muscle tetanus.

Multiple alpha LMNs can innervate a single muscle. The collection of all alpha LMNs innervating a single muscle is called a motor neuron pool. An alpha LMN responds to or is controlled by inputs from three sources i.e. sensory inputs from the dorsal root of the spinal cord, spinal interneurons and descending tracts from higher centres like the brain stem and cerebral cortex. In a motor neuron pool, the smaller motor units are activated before the larger ones. This is referred to as the size principle.

2.1.1.2 Muscle spindles and Golgi tendon organs (GTOs)

A muscle also has various sensory mechanisms e.g. Golgi tendon organs (GTOs) and muscle spindles, that serve to detect various properties of the muscle e.g. tension and length of muscle; see Figure 2.2.

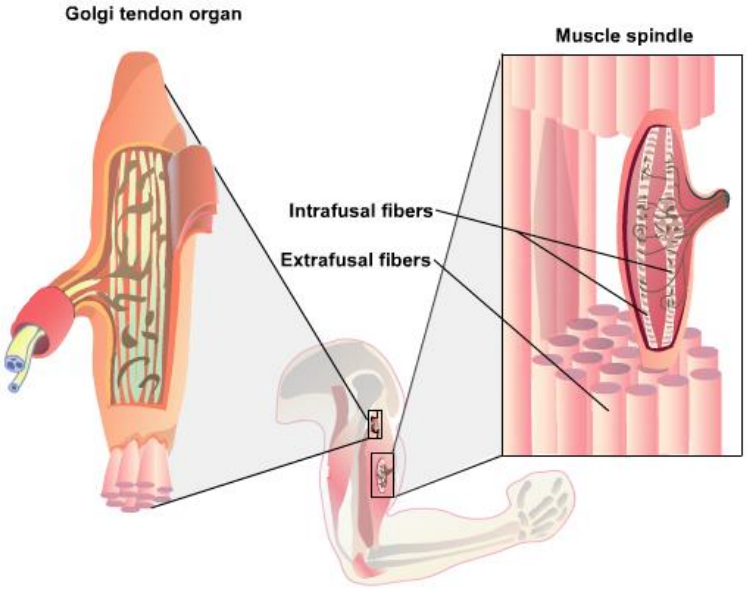

Figure 2.2 Golgi tendon organ (left) and muscle spindle containing intrafusal muscle fibres (right). Modified from online textbook (Knierim, 2013).

Along with extrafusal muscle fibres, which contract to produce force, a muscle also has intrafusal muscle fibres, which serve a sensory purpose. Approximately 6-8 such intrafusal muscle fibres are contained in a single muscle spindle that runs parallel to the extrafusal muscle fibres. There are 3 types of intrafusal muscle fibres that are contained in each muscle spindle i.e. dynamic nuclear bag fibre, static nuclear bag fibre and nuclear chain fibre; see Figure 2.3.

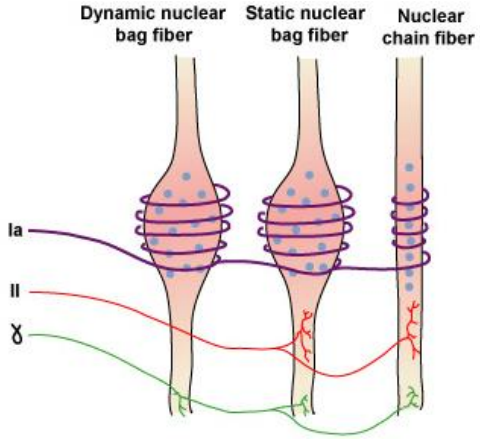

Figure 2.3 Types of intrafusal muscle fibres and their innervation. Modified from online textbook (Knierim, 2013).

The dynamic nuclear bag fibre type is sensitive to the rate of change in a muscle's length or muscle velocity. The static nuclear bag fibre and nuclear chain fibre types are sensitive to the instantaneous length of the muscle. Sensory neuron Ia innervates all three intrafusal fibre types and hence conveys information about the muscles length as well as rate of change in length. Sensory neuron II innervates the static nuclear bag fibre type and nuclear chain fibre type and hence conveys information about only the instantaneous length of the muscle. Sensory neurons Ia and II enter the dorsal root of the spinal cord. All three types of intrafusal muscle fibres are also innervated by the gamma LMN. The gamma LMN which is controlled by the cerebral cortex controls the sensitivity of the intrafusal fibres. Another sensory mechanism apart from the muscle spindle is the Golgi tendon organ (GTO); see Figure 2.4.

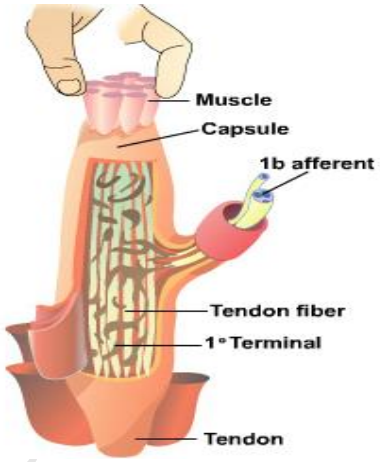

Figure 2.4 Golgi tendon organ (GTO) responds to tension in a muscle. Modified from online textbook (Knierim, 2013).

Unlike the intrafusal fibres which run parallel to the extrafusal muscle fibres, the GTO is in series with the muscle, between the muscle and its tendon. The GTO is sensitive to the stretch or tension in a muscle. The GTO is innervated by sensory neuron Ib which enters the dorsal root of the spinal cord.

2.1.2 Neuronal circuits of the spinal cord

Spinal reflexes form the basic building blocks of motor control as they can be accomplished without intervention from higher centres of the CNS like the cerebral cortex (although they may be modulated by these higher centres). A spinal reflex typically begins with an input stimulus from a sensory neuron e.g. Ia sensory neuron, and ends with the activation of a LMN as a response. There are typically only 1-2 synapses between the sensory and motor neurons, thus making a reflex rapid.

2.1.2.1 Stretch reflex

The stretch reflex is the simplest reflex; see Figure 2.5. It works to resist the lengthening (stretching) of a muscle. By doing so it allows weight bearing muscles to automatically adjust to changes in load without involving higher centres of the CNS. When a muscle is stretched, Ia sensory fibres which detect changes in length of the intrafusal muscle fibres (nuclear bag and nuclear chain) synapse onto and excite the alpha LMN of the same (homonymous) muscle causing it to contract. This is autogenic excitation. This is a monosynaptic reflex and therefore extremely fast (the synaptic delay being ~ 1 ms while the entire reflex delay being ~ 50 ms). Ia sensory fibres may also synapse with LMNs of muscles that are synergistic (carry out the same function) to the homonymous muscle. Furthermore, Ia sensory fibres synapse with and excite Ia inhibitory interneurons that then inhibit the alpha LMNs of muscles that are antagonistic (carry out the opposite function) to the homonymous muscle. This is reciprocal innervation.

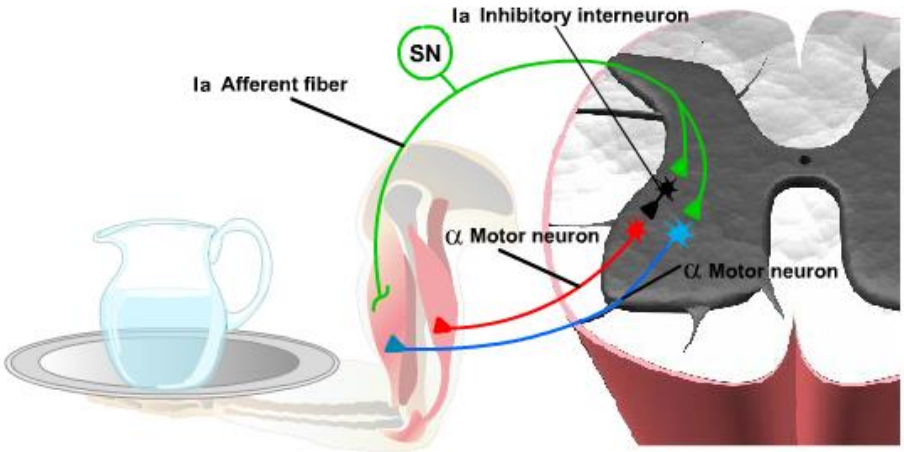

Figure 2.5 Simple stretch reflex showing autogenic excitation and reciprocal innervation. Modified from online textbook (Knierim, 2013).

2.1.2.2 Inverse stretch reflex

The opposite of the stretch reflex is the inverse stretch reflex; see Figure 2.6. This reflex functions so as to prevent over-contraction of a muscle leading to tendon damage. Ib sensory fibres which carry information about the tension in a muscle from the muscle's GTO, synapse onto Ia inhibitory interneurons which in turn inhibit the alpha LMNs of the same (homonymous) muscle. This is autogenic inhibition.

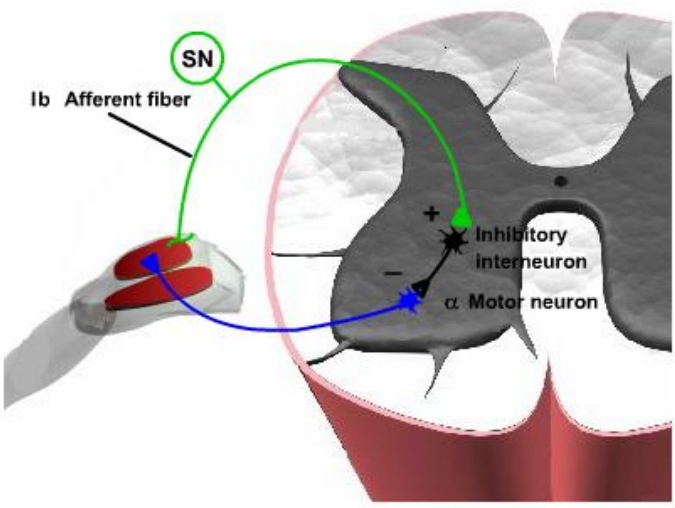

Figure 2.6 Inverse stretch reflex acts to dampen muscle activation. Modified from online textbook (Knierim, 2013).

2.1.2.3 Renshaw inhibition

Apart from the Ia inhibitory interneuron, a Renshaw cell also provides a form of inhibition to the alpha LMN; see Figure 2.7. Also see discussion section (7.1.4) that describes the unique type of Renshaw inhibition for wrist flexors and extensors. The Renshaw cell provides negative feedback to the alpha LMN. It receives excitatory input from the collateral of an alpha LMN axon and inhibits that same alpha LMN. This recurrent inhibition mechanism works so that an increase in excitation of the alpha LMN results in an increase in its inhibition by the Renshaw cell. This mechanism prevents prolonged over-activation of a muscle which could lead to symptoms like muscle tetanus. Renshaw cells also synapse onto and inhibit Ia inhibitory interneurons of the antagonist muscles i.e. they disinhibit the antagonist.

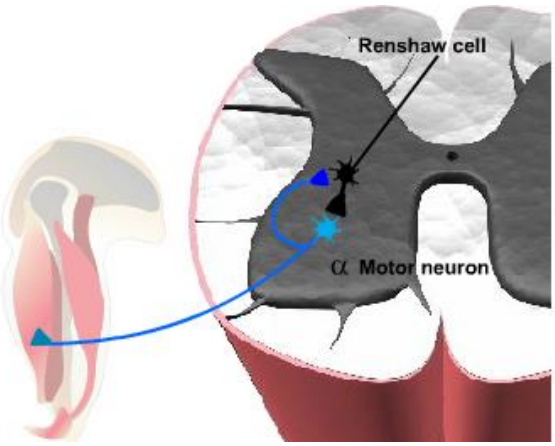

Figure 2.7 Renshaw cell inhibiting the same alpha neuron that excited it. Modified from online textbook (Knierim, 2013).

2.1.2.4 Withdrawal reflex

A well-known spinal protective reflex is the flexion/withdrawal reflex; see Figure 2.8. C and delta sensory fibres (Group III) relay information such as heat and pain back to the spinal cord via the dorsal root. These sensory fibres synapse onto both excitatory and inhibitory interneurons such that the alpha LMNs of the flexor muscles are excited and their antagonists i.e. the extensors are inhibited. Upon presentation of a noxious stimulus to the end of a limb (e.g. a pin prick on the foot) the withdrawal reflex is activated and results in a rapid flexion of the limb (e.g. hamstring will contract pulling the foot up).

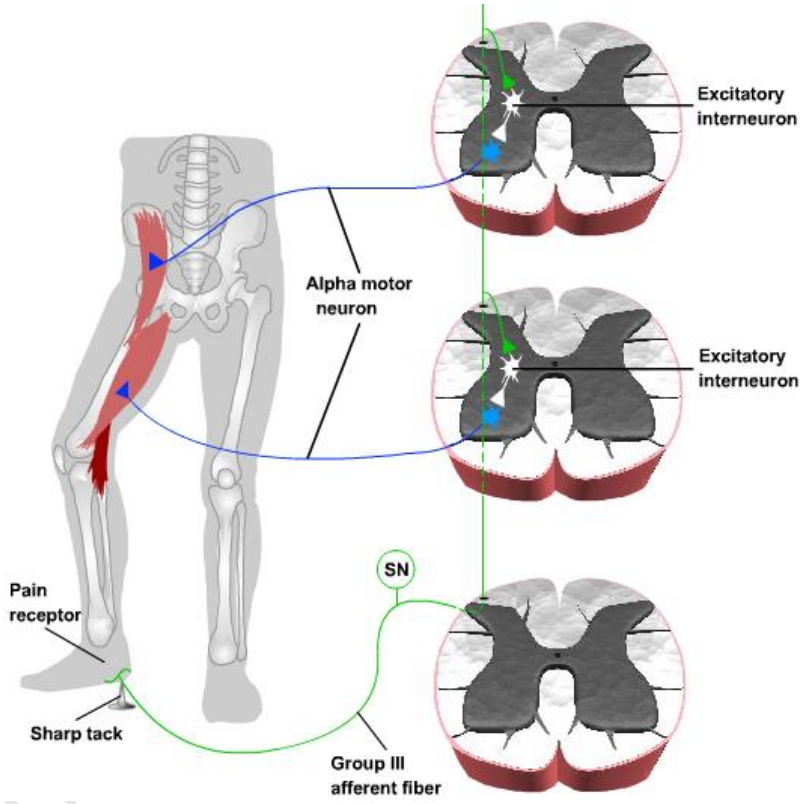

Figure 2.8 Neuronal activation in a withdrawal reflex after a painful stimuli. Modified from online textbook (Knierim, 2013).

2.1.2.5 Central pattern generators

At the level of the spinal cord there exist independent sets of neuronal circuits called central pattern generators (CPGs); see Figure 2.9. CPGs orchestrate rhythmic force production by the muscles. CPGs are activated by a tonic input from higher centres in the CNS like the brain stem and the cortex (see section 2.1.4) via the descending pathways (see section 2.1.3). The basic mechanism of a CPG involves alternate activation/inhibition of agonist/antagonist muscle sets at a particular frequency. Basic day to day movements that involve repetitive actions e.g. walking are thought to be orchestrated by CPGs.

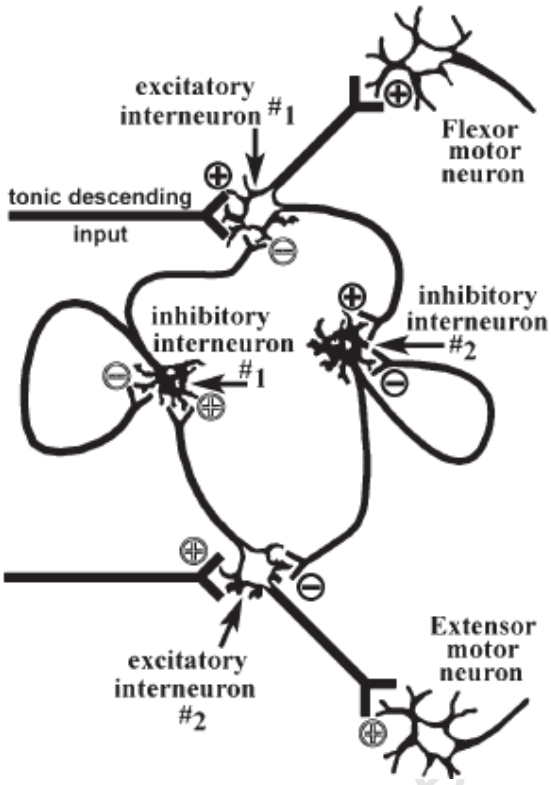

Figure 2.9 Central pattern generator network showing alternating agonist/antagonist activation/inhibition. Adapted from motor systems website (University of Wisconsin-Madison, 2009).

2.1.3 Descending motor pathways to the spinal cord

At the spinal level basic reflex actions can take place independently of the higher centres of the CNS. However, voluntary movements are initiated at higher levels of the CNS e.g. at the cortical level (see section 2.1.4). The commands for these voluntary movements that are generated at the higher CNS levels descend down to the spinal level where they are put into effect by the neurons of the spinal cord (LMNs, interneurons etc.). Various descending pathways exist to facilitate the transmission of commands from various supraspinal structures to the spinal level.

The descending pathways to the spinal cord are divided into the lateral and medial groups; see Figure 2.10. The lateral group consists of the lateral corticospinal tract and rubrospinal tract. The medial group consists of the vestibulospinal tracts (medial and lateral), reticulospinal tracts (pontine and medullary), the tectospinal tract and the anterior corticospinal tract. The lateral group is responsible for mediating fine control of distal musculature whereas the medial group is responsible for balance, posture and coarse control of axial and proximal musculature.

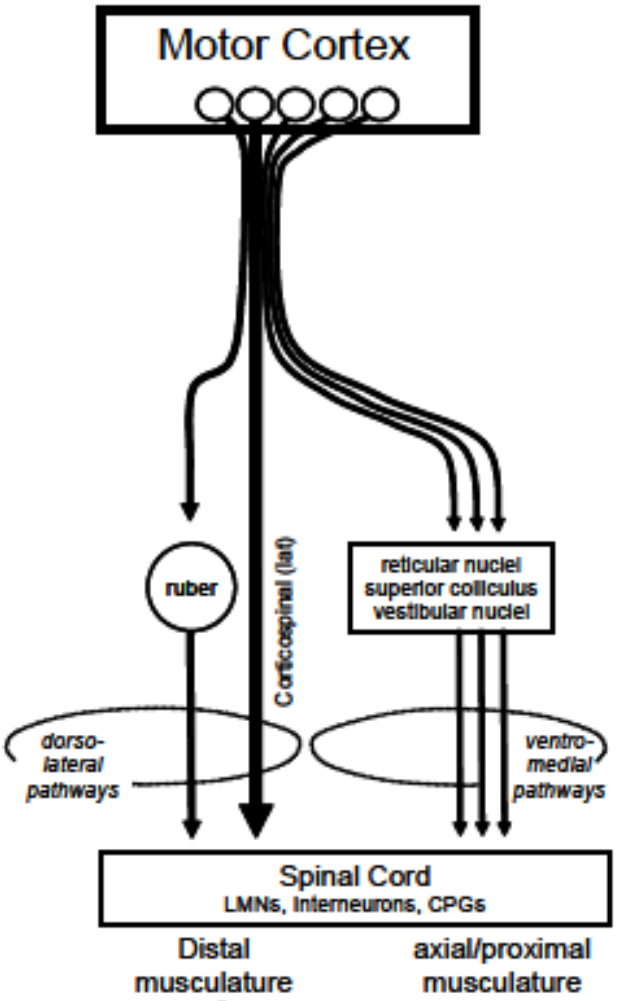

Figure 2.10 Summary of descending motor pathways from the cortex. Adapted from motor systems website (University of Wisconsin-Madison, 2009).

2.1.3.1 Corticospinal pathway

The corticospinal pathway is the primary pathway that carries voluntary movement commands to the spine; see Figure 2.11. It originates in the motor cortex. The axons of motor projection collect in the internal capsula which then courses through various structures in the mid brain. At the level of the medulla, the axons form the medullary pyramids (this tract is also called the pyramidal tract). At the level of the caudal medulla, the tract splits into two sections. 90% of the axons cross over to the contralateral side at the pyramidal decussation and form the lateral corticospinal tract. 10% of the axons form the anterior corticospinal tract, the majority of which cross over to the contralateral side at the spinal segment at which they terminate, while some terminate ipsilaterally. The axons in the lateral corticospinal tract terminate in synapses with either the LMNs or interneurons at the ventral horn of the spinal cord. The axons in the anterior corticospinal tract terminate in

synapses with either the LMNs or interneurons at the anterior horn of the spinal cord. The lateral corticospinal tract is responsible for direct voluntary control of distal musculature e.g. that of the hands and wrists, whereas the anterior corticospinal tract is for proximal musculature. The speciality of the corticospinal tract is the monosynaptic connections of some of its axons to the alpha LMNs. These direct connections between the cortex and the alpha LMNs result in the very fine control of muscles. The percentage of the axons in this tract making monosynaptic corticospinal connections is much higher in humans and primates as compared to other mammals. This reflects on the finer dexterity of the distal musculature in humans and primates e.g. higher dexterity of the digits of the hand as compared to other mammals.

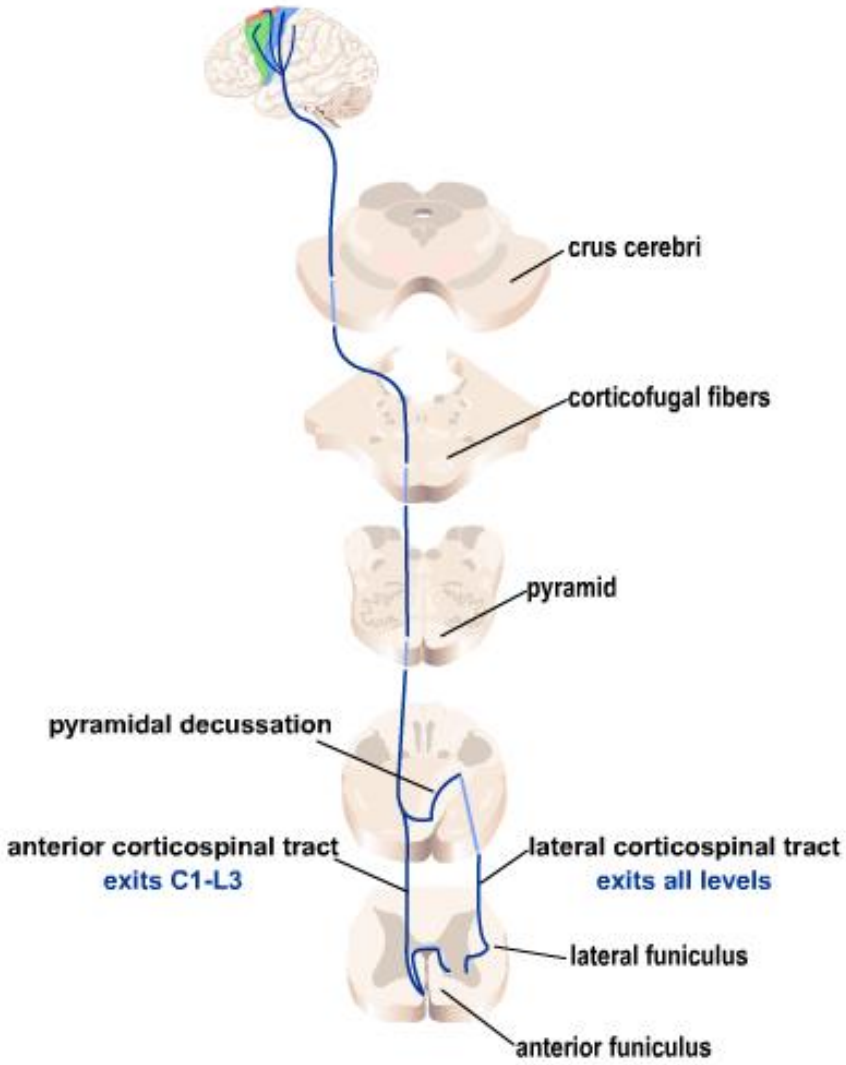

Figure 2.11 Anterior and lateral corticospinal tracts, origin and termination. Modified from online textbook (Knierim, 2013).

2.1.3.2 Rubrospinal pathway

The rubrospinal tract originates at the red nucleus and its axons after crossing over to the contralateral side terminate at all levels of the spinal cord. It is a minor tract in humans whereas it plays a major role in primates. Its activation causes facilitation of flexor muscles and inhibition of extensor muscles. This tract is an alternative means of voluntary muscle control to the corticospinal tract. The red nucleus receives most of its input from the cerebellum and thus the rubrospinal tract may also be responsible for transmission of learned motor commands from the cerebellum to the musculature.

2.1.3.3 Vestibulospinal pathways

The vestibulospinal tracts, both medial and lateral originate from the vestibular nuclei. The lateral terminates at LMNs and interneurons at all levels of the spinal cord whereas the medial terminates at levels C1 to T6. Minute changes in the body's position are detected by the verstibular nuclei. The vestibulospinal tracts mediate muscle control necessary to compensate for these changes in body position and maintain balance and posture. The lateral vestibulospinal tract excites antigravity muscles. The medial verstibulospinal tract excites muscles of the neck to maintain head position.

2.1.3.4 Reticulospinal pathways

The pontine and medullary reticulospinal tracts originate from the pontine and medullary reticular formations respectively and provide input to both proximal and axial musculature at all levels of the spinal cord; as well as to distal musculature (Riddle et al., 2009; Riddle and Baker, 2010). The pontine reticulospinal tract excites anti-gravity spinal reflexes, whereas the medullary reticulospinal tract inhibits anti-gravity spinal reflexes. The recently found monosynaptic as well as disynaptic connections to distal musculature of the upper limb in addition to proximal musculature implies a parallel influence from corticospinal as well as reticulospinal tracts on distal musculature (Riddle et al., 2009; Riddle and Baker, 2010).

2.1.3.5 Tectospinal tract

Relatively less has been studied about this tract in humans. Nevertheless, it originates from the superior colliculus of the midbrain and after crossing over to the contralateral side it terminates mainly on the cervical section of the spinal cord. It is believed to be involved in head movements related to visual stimuli.

2.1.4 Cerebral Cortex

The highest level of the motor hierarchy is at the cerebral cortex; see Figure 2.12. The cerebral cortex has numerous gyri and sulci that are used as anatomical landmarks. Anterior to the central sulcus is the motor cortex. Posterior to the central sulcus is the somatosensory cortex. The motor cortex is divided into the primary motor cortex (MI), premotor cortex (PMC) and supplementary motor area (SMA). The somatosensory cortex is divided into primary and secondary somatosensory cortices (SI and SII respectively). Each area has a different role to play.

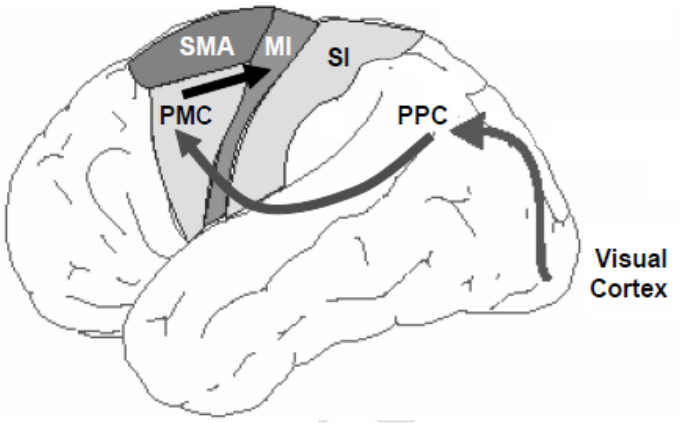

Figure 2.12 Motor cortices (MI, SMA and PMC) and primary somatosensory cortex (SI). Modified from motor systems website (University of Wisconsin-Madison, 2009).

2.1.4.1 Primary motor cortex (MI)

The MI is responsible for the final execution of movements. It is located in the precentral gyrus rostral to the central sulcus and covers Brodmann area 4 (see APPENDIX A). It is somatotopically organised as different areas of the MI represent different body parts. The face representation is the most lateral, followed by the upper limbs, trunk and lower limbs being the most medial. The MI encodes information related to execution of basic movements to the LMNs (electric stimulation of the MI with electrodes resulted in activation of a simple movement of a body part). Encoded information sent to the LMNs includes specifics on:

- Direction of movement – Corticospinal neurons have been shown to be specific to the particular direction of joint movement e.g. monkey studies have found corticospinal neurons that fire either during wrist flexion or extension.
- Force of movement – The rate of firing of corticospinal neurons has been shown to be correlated to the force produced by the target muscle.

- Extent of movement – The rate of firing of some corticospinal neurons has been found to be correlated to the distance of movement, i.e. the distance from the starting position to the target position.
- Speed of movement – The velocity profile of a movement has been shown to be correlated to the firing rate profile of some corticospinal motor neurons.

2.1.4.2 Premotor cortex (PMC)

The PMC lies anterior to the MI and is part of Brodmann area 6 (see APPENDIX A). Stimulation of the PMC results in more complex movements involving multiple joints as compared to stimulation of the MI. Stimulation of different regions of the PMC results in different types of complex movements. For example, monkeys move their arm in a defensive like position or towards their mouth akin to eating when their PMC is stimulated in different areas. The PMC is also responsible in the planning/preparation stage before a movement is performed. This includes selecting the correct motor plan for the intended action. This motor plan is then conveyed to the MI which then executes actions via the LMNs.

The PMC is also involved in sensorimotor integration via communication with other association centres in the brain. For example, a visual cue (e.g. an apple) is detected by the retina and is processed by the visual cortex. This visual information travels to the posterior parietal cortex (PPC), which processes the cue's accurate location in extrapersonal space. The PPC then signals this information to the PMC, which then selects the correct motor plan to reach that object. This motor plan is then conveyed to the MI which executes it via the LMNs.

2.1.4.3 Supplementary motor area (SMA)

The SMA lies anterior to MI and medial to the PMC and is part of Brodmann area 6 (see APPENDIX A). The SMA is involved with internally generated movement and movement sequences. SMA cells were found that were specific (increased firing) for a particular movement sequence and not another in which different SMA cells were active. The SMA thus stores motor programs for various movement sequences. The correct motor program for the intended movement sequence is then conveyed to the MI which executes it via the LMNs. The SMA cells were found to be active also during imagined motor sequences.

2.1.4.4 Primary somatosensory cortex (SI)

The SI lies posterior to the central sulcus, specifically, at the post-central gyrus; see Figure 2.12. It constitutes of Brodmann areas 3, 1 and 2 (see APPENDIX A). It receives sensory information from different body parts. Sensory information received includes the mechanoreceptive, thermoreceptive and pain sense categories. Under the mechanoreceptive category are the tactile and position senses. Tactile senses include touch, pressure and vibration whereas the position senses include static position and rate of movement. Position senses are facilitated by afferents from muscle spindles. These afferents travel up the Dorsal Column – Medial Lemniscal pathway of the spinal cord through the ventrobasal complex of the thalamus to finally project to SI and the secondary somatosensory cortex (SII) which covers Brodmann areas 5 and 7 (see APPENDIX A). The SI can relay this positional information of the joints to the MI which in turn controls their movements.

2.1.5 Basal ganglia

The basal ganglia are one of the two "side loops" of the motor system, the second one being the cerebellum. The term side loop is used as these nuclei don't execute movements (done by the cortex) but play a role in the control/modulation of the execution.

2.1.5.1 Basal ganglia anatomy

Anatomically, the basal ganglia are a group of nuclei located in the telencephalon region of the brain. These are the caudate nucleus, putamen, globus pallidus (external and internal), subthalmic nucleus and substantia nigra. The thalamus although not part of the basal ganglia, is a component that takes part in the communication between the cortex and basal ganglia.

The neurons in the caudate nucleus and putamen (together termed the striatum) receive afferents from various parts of the cortex including the motor cortex. The striatal neurons project this cortical input to the globus pallidus which in turn projects to the motor thalamaus (ventral anterior nucleus and ventral lateral nucleus) which ultimately projects back on the motor cortex, thus forming a loop. The subthalmic nucleus forms a sub loop with the globus pallidus and the substantia nigra sends efferents to the striatum.

2.1.5.2 Functions of the basal ganglia

The basal ganglia are able to both excite and inhibit cortical nuclei though two pathways. These are the direct and indirect pathways; see Figure 2.13. Although these pathways involve various structures of the basal ganglia, as well as various combinations of excitatory-inhibitory projections, the net effect of the direct pathway is excitatory whereas the net effect of the indirect pathway is inhibitory. The projections of the substantia nigra onto the striatum (via the nigrostriatal pathway) have the effect of exciting the direct pathway (increasing its excitatory effect on cortical neurons) and inhibiting the indirect pathway (decreasing its inhibitory effect on cortical neurons). Both effects ultimately count towards an increase in excitation of cortical neurons.

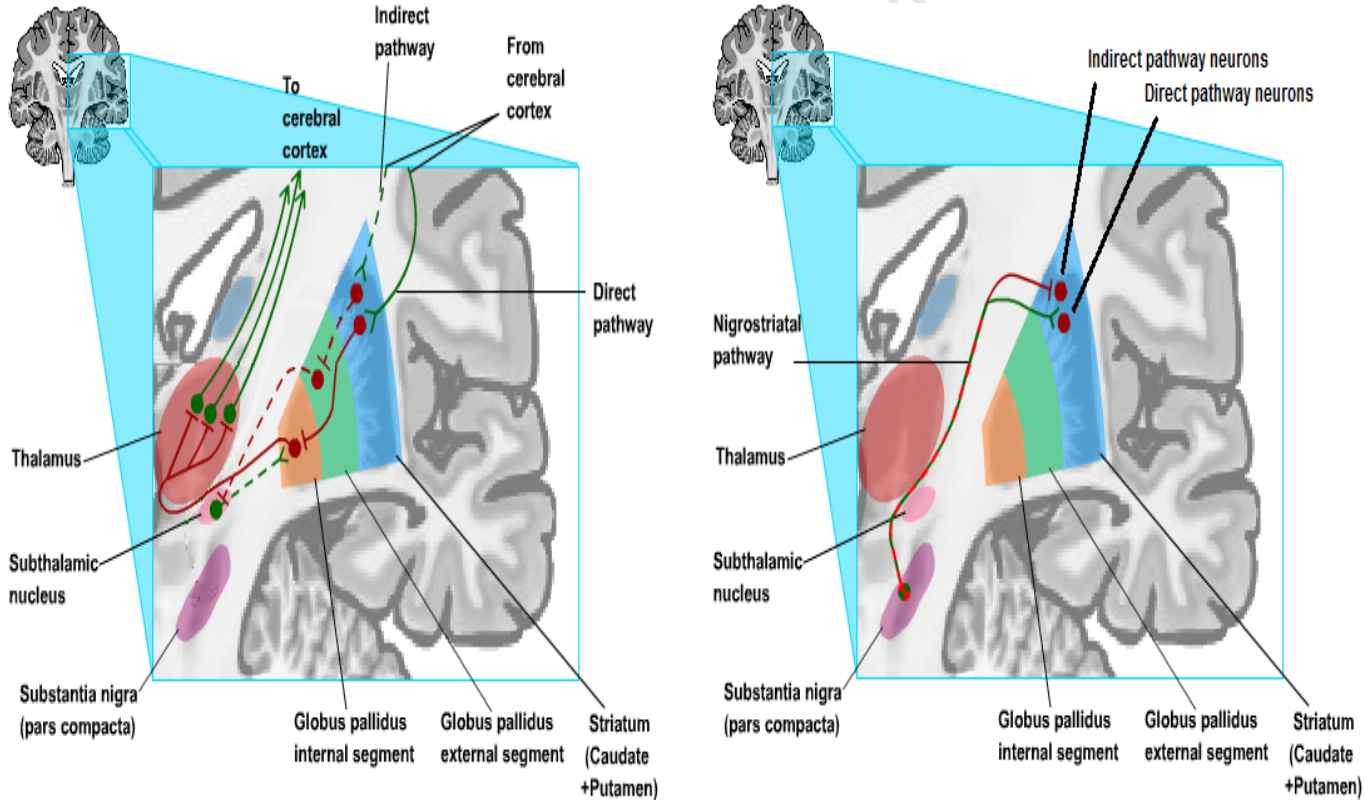

Figure 2.13 Direct and indirect pathways of the basal ganglia (left). Nigrostriatal pathway of the basal ganglia (right). Green tracts represent excitatory projections whereas red represent inhibitory. Modified from online textbook (Knierim, 2013).

It is generally accepted that a balance is needed between activation of the direct and indirect pathways for normal motor functioning. The motor cortex stores motor programs for execution of certain actions. There is evidence that shows the direct and indirect pathways are utilised by the motor cortex to select the appropriate motor program for the required motor task; see Figure 2.14. The indirect pathway is used to inhibit all non-relevant

motor programs whereas the direct pathway selects (excites) the appropriate motor program.

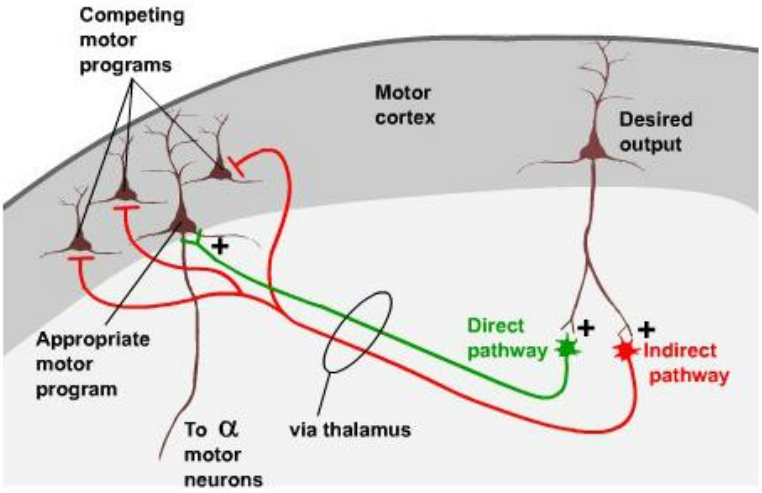

Figure 2.14 Basal ganglia involvement in selecting appropriate motor programs. Modified from online textbook (Knierim, 2013).

2.1.6 Cerebellum

2.1.6.1 Anatomical components of the cerebellum

The cerebellum is a structure underlying the occipital and temporal lobes of the cerebral cortex. It consists of more than 50% of the total neurons in the brain, although its volume is close to 10% of the total brain. The cerebellum can be divided into two parts, the deep cerebellar nuclei and the cerebellar cortex. The deep cerebellar nuclei are the only source of output from the cerebellum. The deep cerebellar nuclei include the fastigial nuclus, interposed nucleus, dentate nucleus and the vestibular nucleus. These nuclei receive afferents from and provide efferents to various other structures including the spinal cord, vestibular nuclei and cerebral cortex. They also receive afferents from the cerebellar cortex. The various afferent and efferent connections in the cerebellum (i.e. interconnections between exterior brain structures, deep cerebellar nuclei and cerebellar cortex) can be divided into three tracts or bundles, the cerebellar peduncles. They are the inferior, middle and superior cerebellar peduncles; see Figure 2.15.

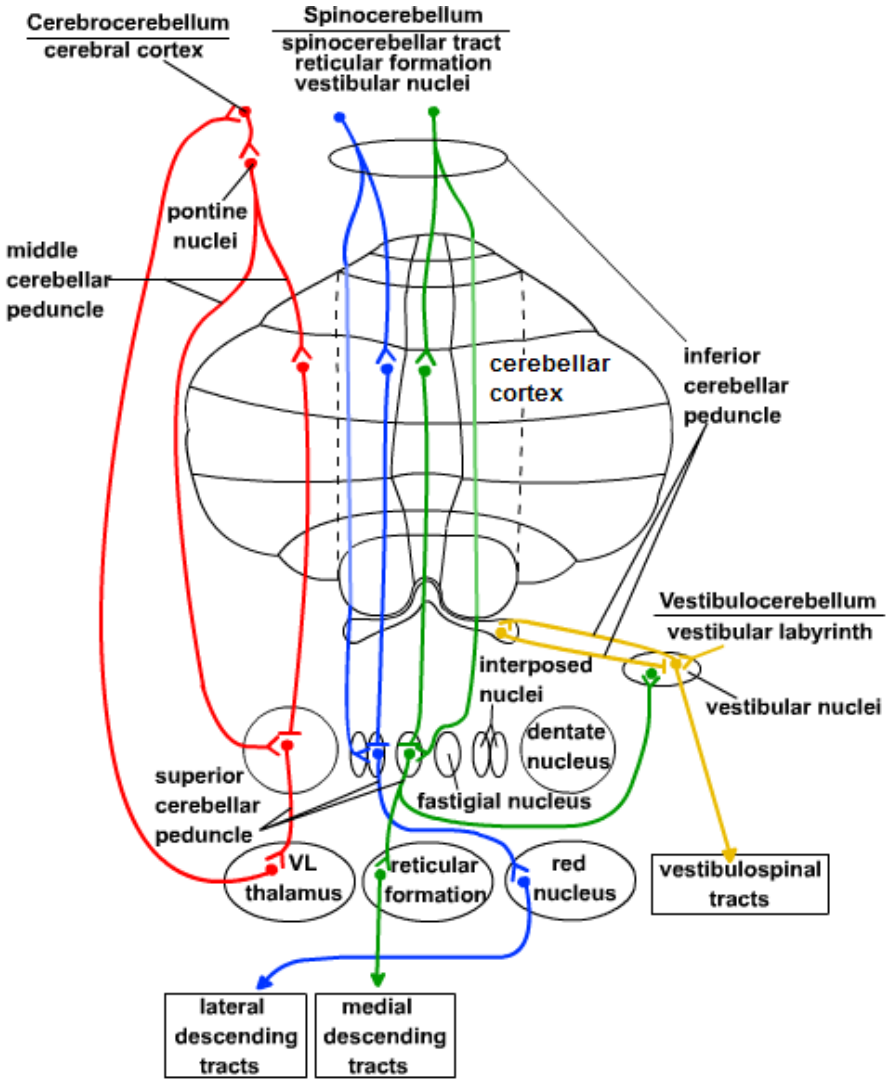

Figure 2.15 Input and output pathways of cerebellum. Modified from online textbook (Knierim, 2013).

The cerebellar cortex is divided into 3 lobes (anterior, posterior and flocculonodular) and three regions (vermis, intermediate zone and lateral hemisphere). The cerebellar cortex also has 3 layers, the innermost being the granule cell layer (consists the majority of neurons of the cerebellum), then the purkinje cell layer and lastly the modular layer. The purkinje cells are the only source of output from the cerebellar cortex; see Figure 2.16. These cells make inhibitory synapses onto the deep cerebellar nuclei (which are the only source of output from the entire cerebellum). The purkinje cells in turn receive synaptic input from granule cells as well as climbing fibre cells. The granule cells receive input from mossy fibres which in turn receive input from various other structures in the brain. The climbing fibre cells originate solely from the inferior olive.

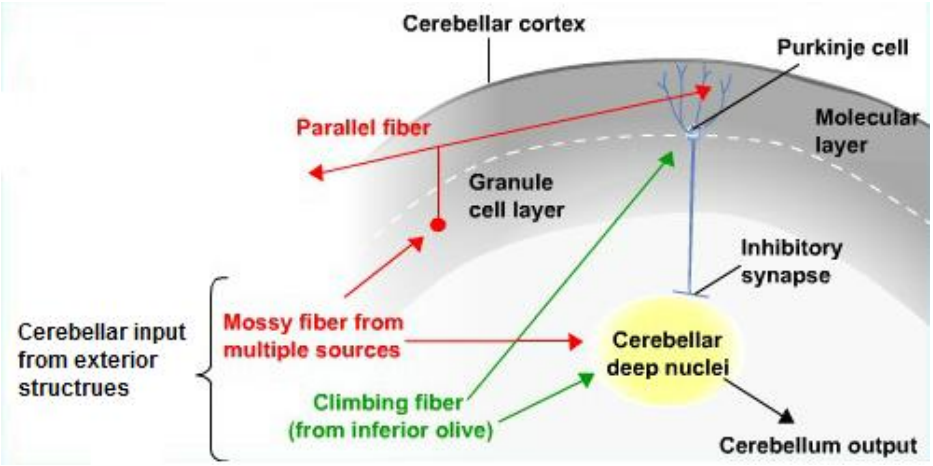

Figure 2.16 Cerebellar circuitry showing interconnections between cerebellar deep nuclei and cerebellar cortical cells. Modified from online textbook (Knierim, 2013).

2.1.6.2 Cerebellar functions

As the cerebellum receives input and sends output to various structures in the brain, it can be functionally divided into three major parts related to these structures. These are the spinocerebellum, vestibulocerebellum and the cerebrocerebellum. The spinalcerebellum is involved in the integration of sensory input with motor commands to produce adaptive motor coordination. The vestibulocerebellum is involved with vestibular reflexes and in postural maintenance. The cerebrocerebellum is involved in the planning and timing of movements as well as the cerebellar cognitive functions. The cerebellum receives afferents from the cerebral cortex via the pontine nuclei and sends efferents back to the cerebral cortex via the thalamus.

2.1.6.3 Proposed model of the cerebellum in motor control

Motor related tasks such as balance, posture and sequential movements are maintained by the cerebellum by modulating the motor commands that control the appropriate motor neurons for the tasks, such that the desired motor state (e.g. position and velocity of a limb) is satisfied. This is done by comparing the desired motor state to the continuous sensory inputs the cerebellum receives from vestibular nuclei and proprioceptive sensors e.g. muscle spindles, Golgi tendon organs (GTOs), skin tactile receptors and joint receptors. The cerebellum can thus also be modelled as a feed-forward control mechanism. Feed-forward control is especially necessary in fast alternating movements e.g. playing the piano.

2.2 EEG detection theory

The information presented in section 2.2 is primarily acquired from a clinical neurophysiology textbook (Daube and Rubin, 2009).

EEG is based on detecting the electrical potentials produced by the activity of the neurons of the cortex. The human cortex has approximately 100 billion neurons interconnected in a network by approximately 10^{14} synapses. Typically an action potential travels down the axon of a neuron reaching the presynaptic terminal where it elicits the release of a neurotransmitter into the synaptic cleft, hence communicating with the postsynaptic neuron (Figure 2.17 shows the process of synaptic transmission).

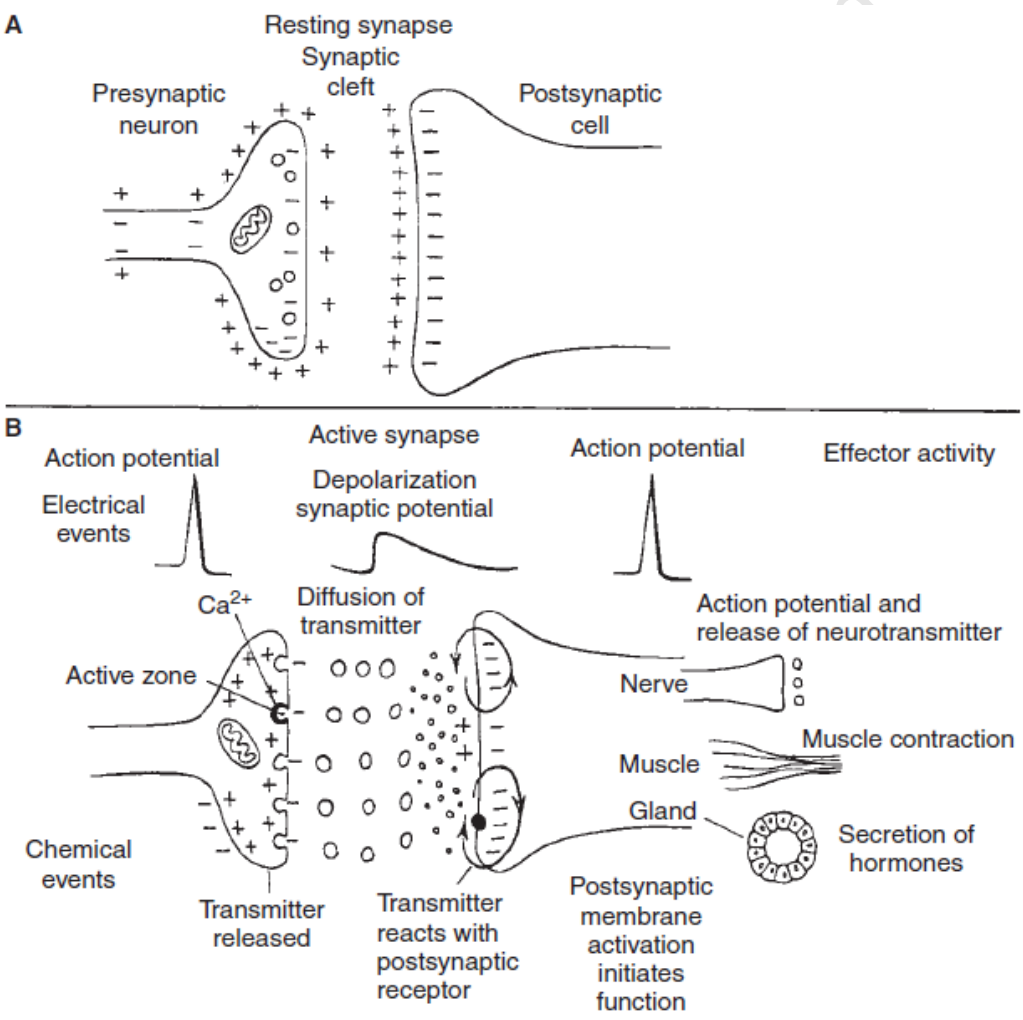

Figure 2.17 Synaptic transmission. A: - Resting synapse where the presynaptic and postsynaptic membranes are normally polarised. B: - Active synapse where an action potential invades the axon terminal and depolarizes it, resulting in the release of neurotransmitter from the terminal, causing local current flow at the postsynaptic membrane (Daube and Rubin, 2009).

The type of neurotransmitter released depends on the type of neuron. For example an inhibitory neuron may elicit the release of a gamma-Aminobutyric acid (GABA) neurotransmitter whereas an excitatory neuron may elicit the release of Glutamate. The neurotransmitter causes a postsynaptic potential (PSP), which is a local change in potential across the membrane of the postsynaptic neuron. The PSP can be either an excitatory postsynaptic potential (EPSP) or inhibitory postsynaptic potential (IPSP) depending on the type of neurotransmitter. An EPSP causes depolarisation of the postsynaptic membrane whereas an IPSP will cause hyperpolarisation. The EPSPs and IPSPs can summate both spatially and temporally. If the summated EPSP is large enough (higher than the threshold) an action potential is elicited which travels down the axon of the postsynaptic neuron. Figure 2.18 illustrates this for EPSPs.

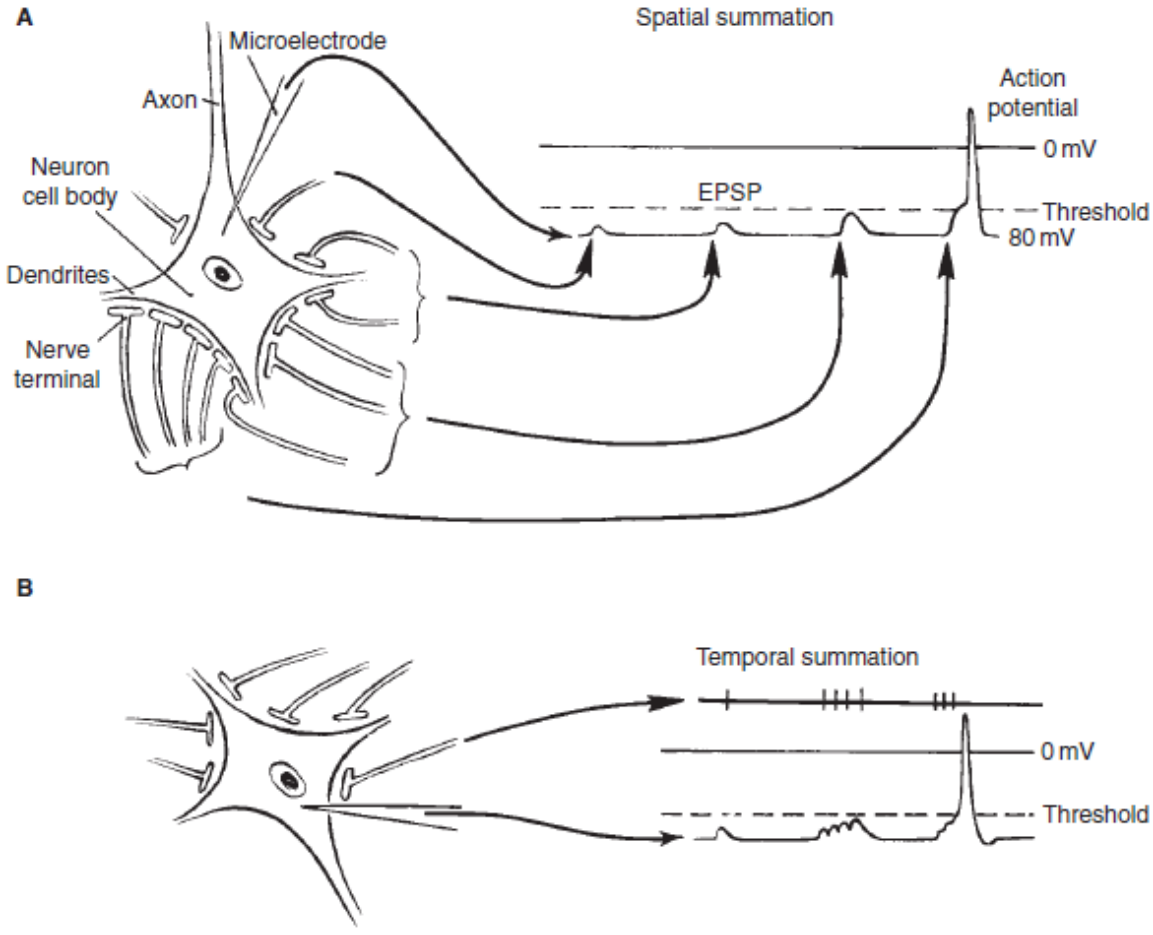

Figure 2.18 Summation of local potentials. A - Spatial summation occurs when more nerve terminals discharge neurotransmitters to produce a larger EPSP. B - Temporal summation occurs when a nerve terminal discharges more rapidly to produce a larger EPSP (Daube and Rubin, 2009).

Using conventional (i.e. positive charge) flow, an EPSP is associated with an inward flow of current (into the cell membrane) and is termed as a current sink; an IPSP is associated with an outward flow of current (out of the cell membrane) and is termed as a current source. This synaptic trans-membrane current flow is accompanied by an opposite outward (for an EPSP) or inward (for an IPSP) flow of current at another location along the dendritic tree. These are called the passive current sources or sinks; see Figure 2.19.

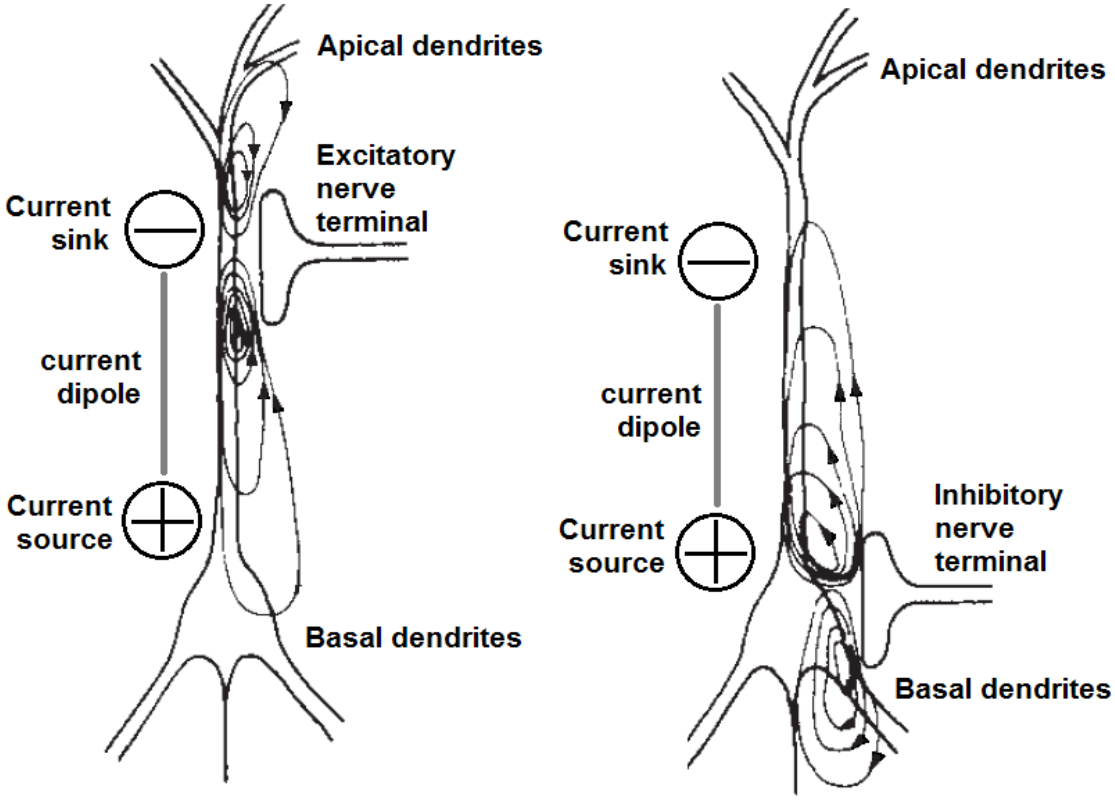

Figure 2.19 Electric dipole created by post synaptic potential. Left: - Excitatory synapse. Right: - Inhibitory synapse. Current direction is shown by arrows (Daube and Rubin, 2009).

Together, the combination of a current source and sink on a dendritic tree produces an electric dipole (similar to a battery). The electric dipole produces current fields in a conductive medium; which also produce voltage fields (perpendicular to the current fields) as shown in Figure 2.20.

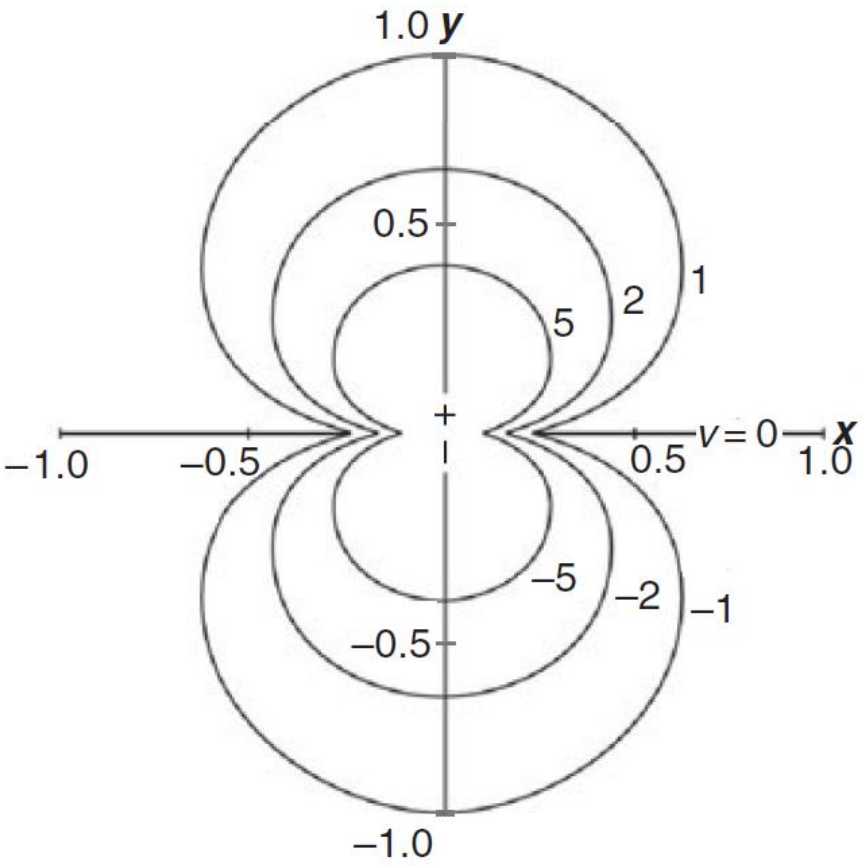

Figure 2.20 Voltage isopotential lines of an electric dipole (Daube and Rubin, 2009).

EEG electrodes are able to pick up the difference in voltage between two points in the voltage field. If the two points are on an isopotential line, no voltage difference will be picked up. Considering the isopotential lines of a current dipole shown in Figure 2.20, it is evident that the voltage difference picked up depends on the measuring system (bipolar or referential) and the location of the electrodes with respect to the dipole. Figure 2.21 illustrates the potentials recorded along parallel and perpendicular lines to the dipole axis, as a function of position along the lines. The effect of varying the distance between the lines and the dipole axis is also illustrated (solid curve, 1 cm; dashed curve, 2 cm; dotted curve, 3 cm), as well as the effect of using a bipolar or monopolar (referential) recording system.

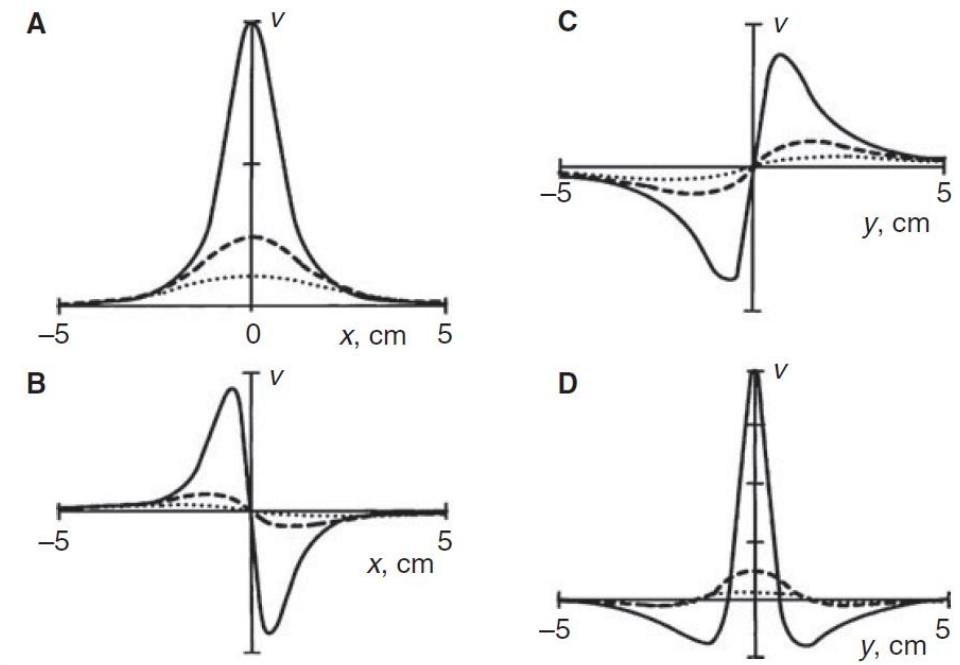

Figure 2.21 Potentials recorded along a line located at various distances from a current dipole (solid curve, 1 cm; dashed curve, 2 cm; dotted curve, 3 cm) as a function of position along the line. A: - Referential recording with the line perpendicular to dipole axis. B: - Bipolar recording for line perpendicular to dipole axis. C: - Referential recording with the line parallel to dipole axis. D: - Bipolar recording for line parallel to dipole axis (Daube and Rubin, 2009).

In each of the 4 cases (A,B,C and D), a greater voltage difference is picked up closer to the source (dipole), as can be seen from the solid, dashed and dotted lines; the voltage difference diminishes with the square of the distance from the source. In the case of the orientation of the dipole axis being reversed (rotated by 180 degrees), the diagrams shown in Figure 2.21 would be flipped about the horizontal axis. At the cortical level, the orientation of the dipole axis can be flipped by two factors, i.e. the location of the synapse on the dendritic tree (apical or basal) and the type of synapse (excitatory or inhibitory); see Figure 2.22

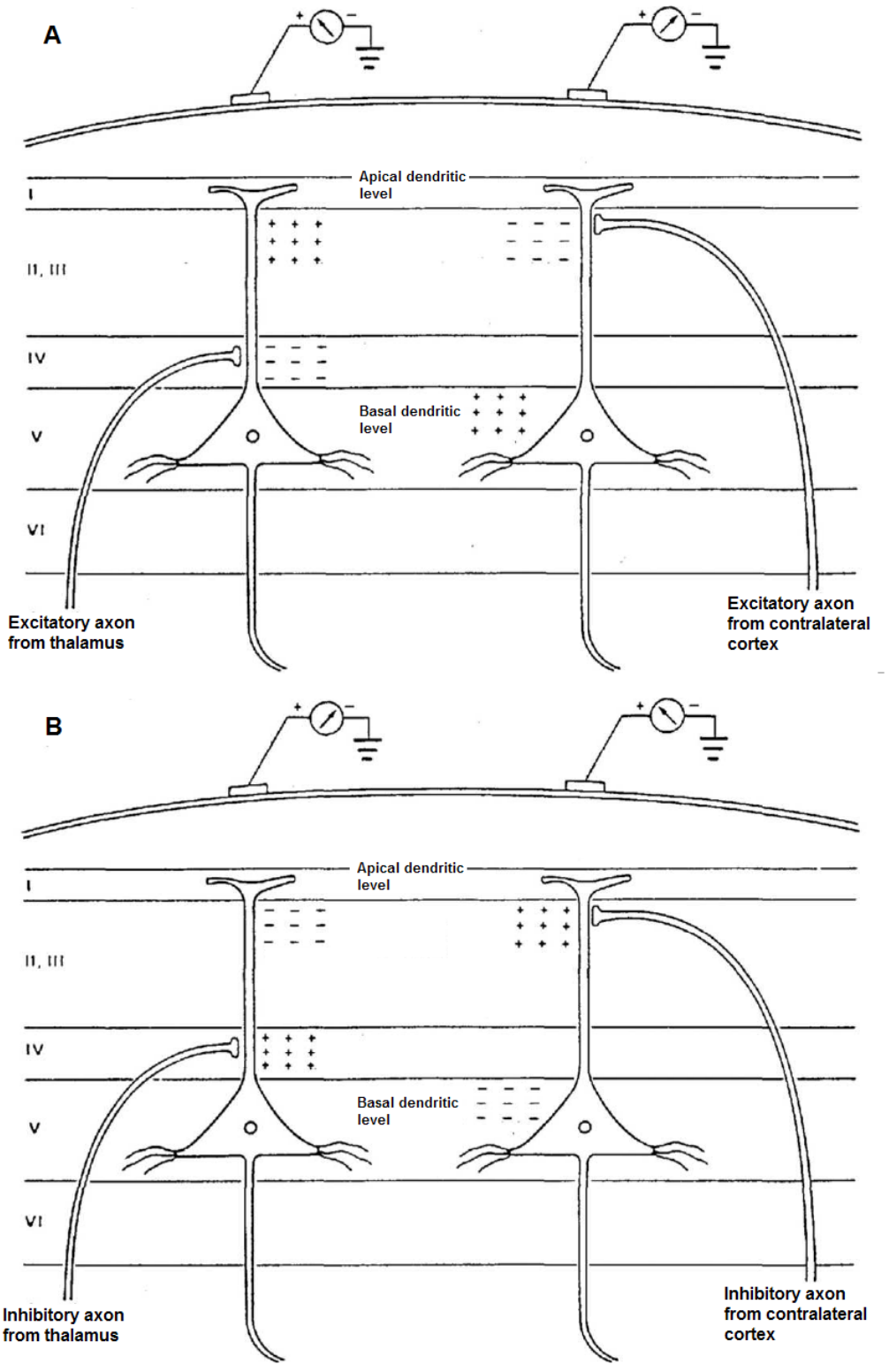

Figure 2.22 Scalp voltage polarity change due to location and type of synapse. A: - Excitatory synapses on two different locations on the dendritic tree. B: - Inhibitory synapses on two different locations on dendritic tree (Daube and Rubin, 2009).

The EPSPs or IPSPs from the pyramidal neurons of the cortex are the major sources of measurable scalp EEG. This is because the dendrites of the pyramidal neurons are aligned and are perpendicular to the scalp surface. This allows summation of local potentials (PSPs) so that they can be measured at the scalp level. Action potentials on the other hand are too short for effective constructive interference that would allow them to be measured on the surface. Further, the axons of the pyramidal cells are not aligned so that the action potentials do not summate.

2.3 EMG detection theory

The information presented in section 2.3 is primarily acquired from a clinical neurophysiology textbook (Daube and Rubin, 2009) and a medical physiology textbook (Guyton and Hall, 2006); additional references are specified where necessary.

EMG is based on measuring the electrical activity produced by muscles during their contraction. A nerve terminal from an alpha motor neuron invaginates into a muscle fibre near its midpoint, forming a neuromuscular junction; see Figure 2.23.

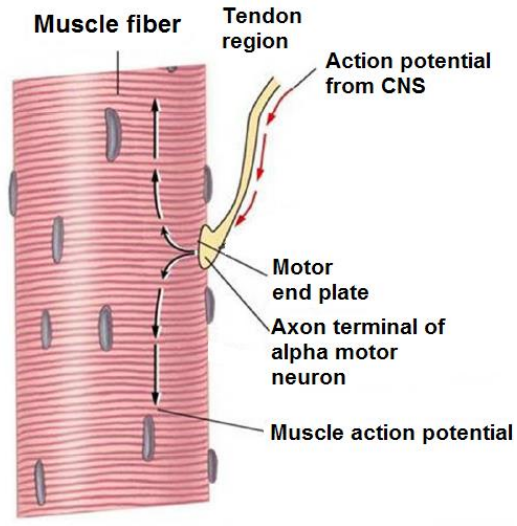

Figure 2.23 Muscle action potential (Guyton and Hall, 2006).

On arrival of a neuronal action potential at the motor end plate, acetylcholine is released into the synaptic cleft. Acetylcholine-gated ion channels on the muscle fibre membrane then open in response, and an influx of sodium ions occurs into the muscle fibre. This in effect causes local depolarisation of the muscle fibre membrane and is called the end plate

potential. If threshold end plate potential is reached, an action potential is elicited. This action potential is similar to the neuronal action potential; however, it travels in two opposite directions along the length of the muscle fibre starting off from the neuromuscular junction at which it was initiated. The action potential causes the sarcoplasmic reticulum to release large quantities of calcium ions. The calcium ions in turn initiate the attractive forces between the contractile elements of the muscle fibre (actin and myosin filaments), and contraction occurs. After a fraction of a second, the calcium ions are pumped back into the sarcoplasmic reticulum and thus contraction ceases until the arrival of another action potential.

An action potential travelling along a muscle fibre can be modelled as a traveling tripole. A tripole has a voltage field potential in a conductive homogenous medium as shown in Figure 2.24.

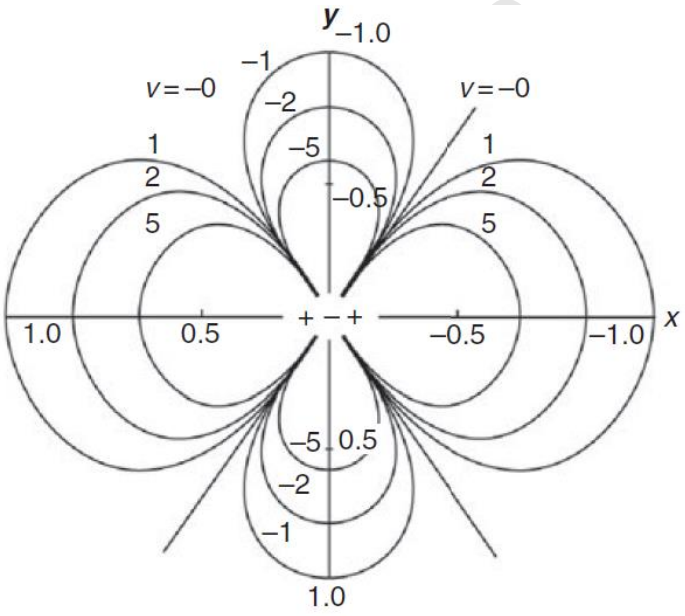

Figure 2.24 Voltage field configuration of a tripole. This is an approximation of an action potential (Daube and Rubin, 2009).

Increasing proximity to the source will result in higher amplitude of electric potential recorded between the electrodes. Figure 2.25 shows an illustration of a travelling action potential from a single muscle fibre recorded at the surface using bipolar electrodes.

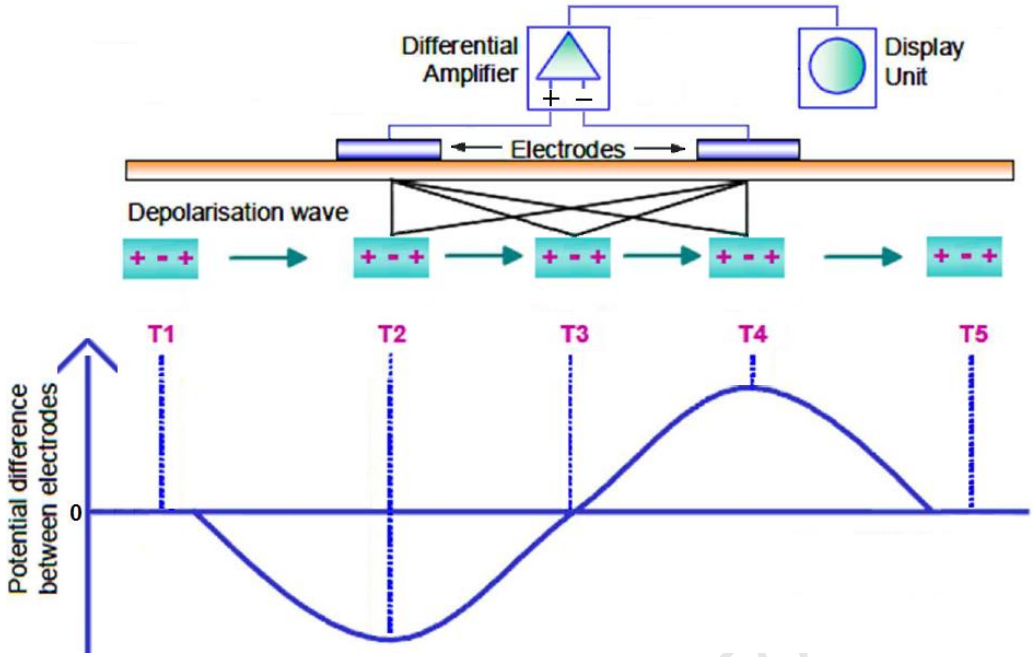

Figure 2.25 An action potential travelling along a muscle fibre membrane recorded using bipolar electrode measurement system (Kumar and Mital, 1996).

In practise during surface EMG measurements, action potentials from all muscle fibres in a motor unit will summate and this summation is what is recorded on the bipolar electrodes; see Figure 2.26. This summation results in a triphasic waveform to be recorded.

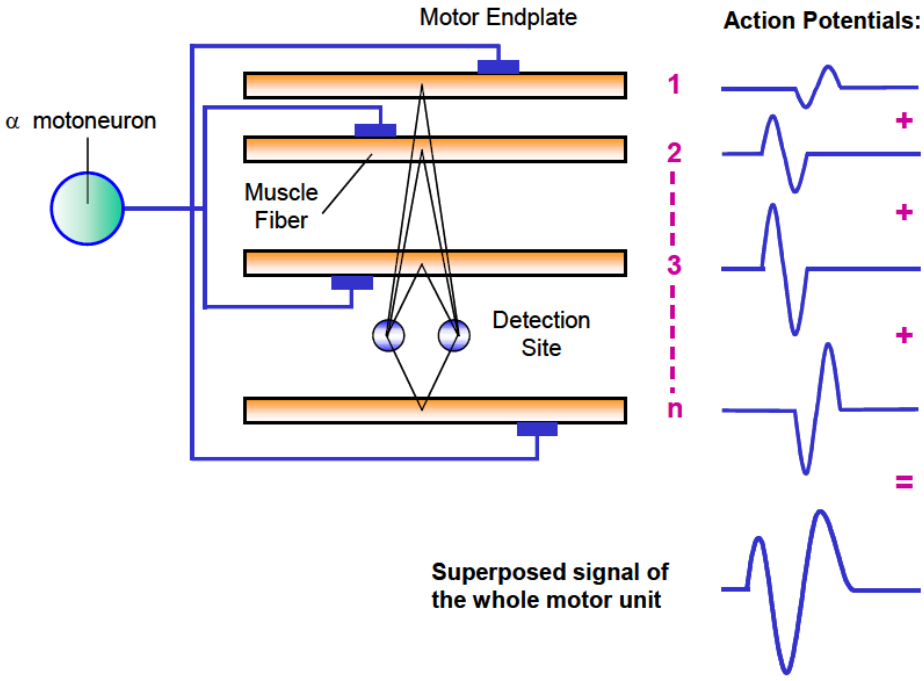

Figure 2.26 Summation of action potentials from multiple muscle fibres innervated by a single alpha motor neuron resulting in a triphasic waveform (Basmajian, 1974).

3 LITERATURE REVIEW

Section 3 is an extended survey of related prior texts and contains technical, conceptual as well as perspective information related to the present study.

Section 3.1 covers the functional differences between wrist flexion and extension starting with a brief description of the musculature of the wrist joint (section 3.1.1), and then reviews: the behavioural (motor precision) differences (section 3.1.2), neurophysiological differences (section 3.1.3) and finally the clinical differences (section 3.1.4) between wrist flexion and extension.

Section 3.2 covers CMC, starting with a description of oscillatory neuronal activity (section 3.2.1) and an overview of CMC (section 3.2.2). Subsequent subsections critically review: the past and current outlooks on how CMC is mediated (section 3.2.3), factors that can co-vary with or modulate CMC including motor precision and cognition (section 3.2.4) and finally the functional models of CMC that are currently standing (section 3.2.5).

3.1 Functional differences between wrist flexion and extension

Flexors and extensors of the wrist joint form an antagonistic pairing. Behavioural (motor precision), neurophysiological as well as clinical differences in their control of movement by the CNS are reported in the literature. A brief outlook on the biomechanics of the wrist is given in the next subsection before reviewing these differences in the subsections that follow it.

3.1.1 Biomechanics of the wrist joint

Section 3.1.1 is mainly taken from a review of wrist control in humans (Bawa et al., 2000). There are 6 major superficial muscles that are specific to the wrist joint; see Figure 3.1 (posterior view of the forearm) and Figure 3.2 (anterior view of the forearm). These are the wrist flexors: - Flexor Carpi Radialis (FCR), Palmaris Longus (PL), Flexor Carpi Ulnaris (FCU) and wrist extensors: - Extensor Carpi Radialis Longus (ECRL), Extensor Carpi Radialis Brevis (ECRB) and Extensor Carpi Ulnaris (ECU). However, other muscles which are not specific only to the wrist e.g. Extensor Digitorum (ED) and Flexor Digitorum Superficialis (FDS) also produce forces about the wrist joint.

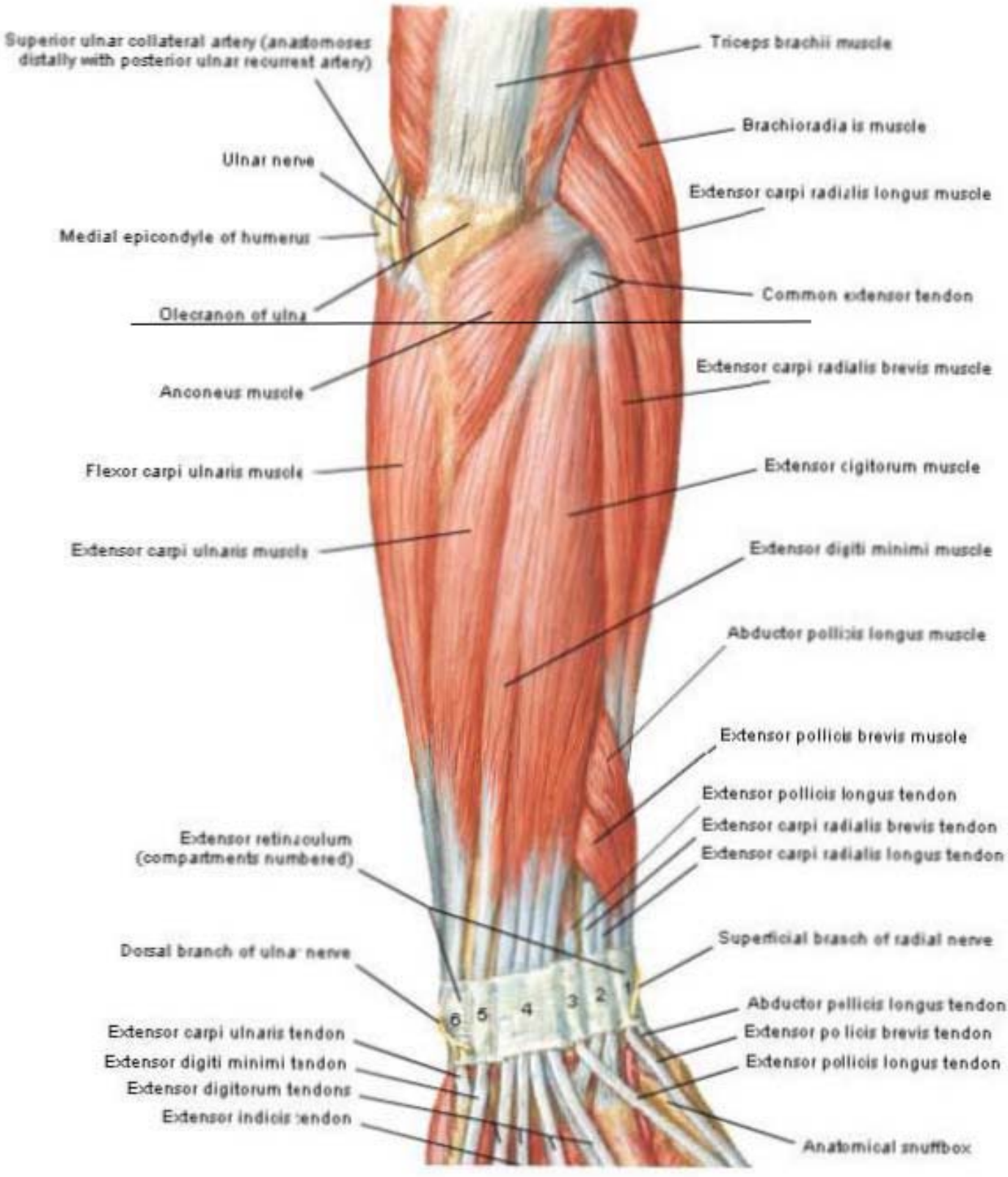

Figure 3.1 Posterior forearm muscles including wrist extensors. Modified from Netters Atlas of Human Anatomy (Netter, 2010).

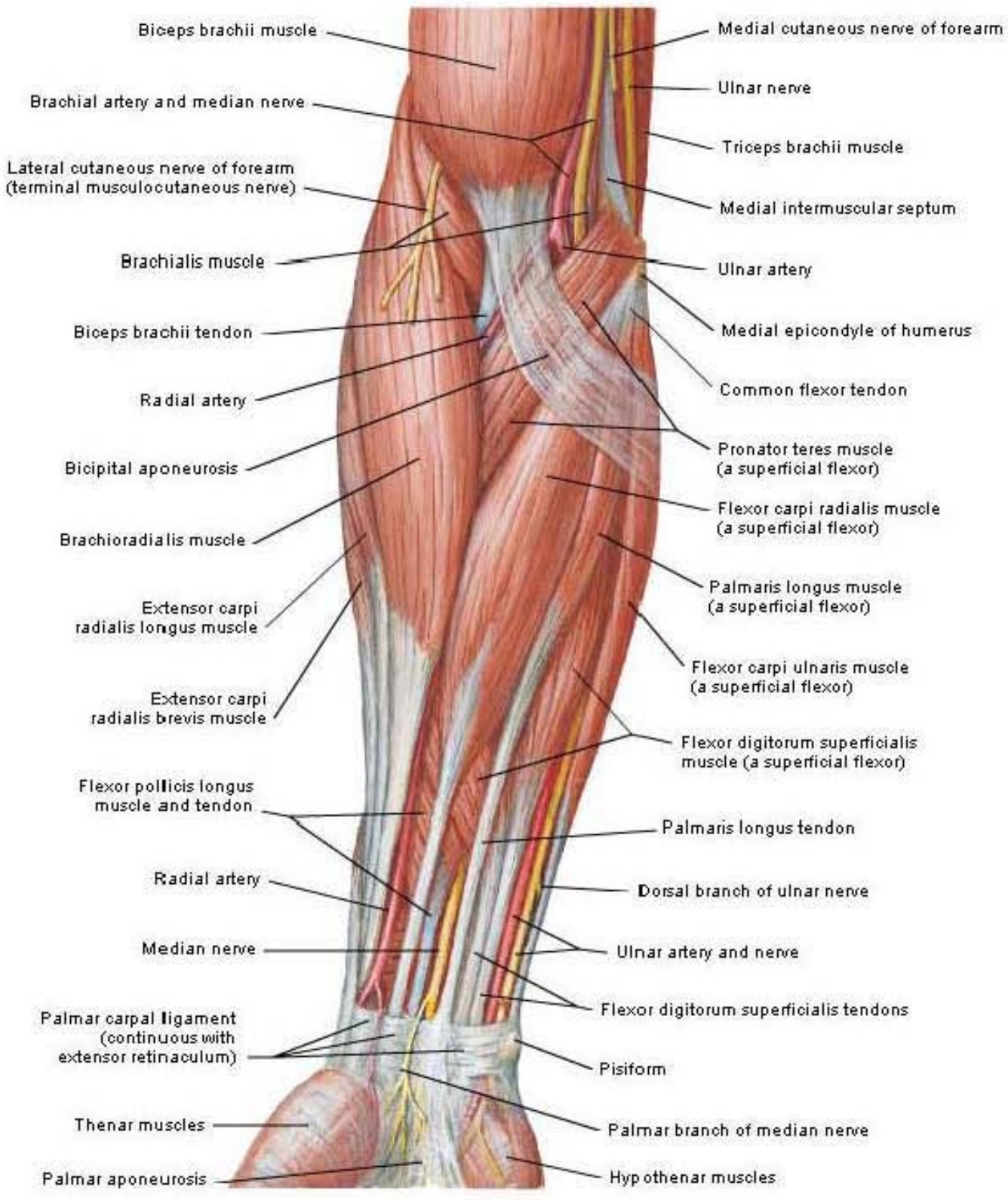

Figure 3.2 Anterior forearm muscles including wrist flexors. Modified from Netters Atlas of Human Anatomy (Netter, 2010).

The wrist joint typically has two degrees of freedom. That is rotation in the ulnar-radial direction (ulnar-radial deviation), and rotation in the flexion-extension direction; see Figure 3.3. Each of the primary wrist muscles produces a force about the wrist joint at a different angle. Hence for a pure rotation in any of the directions i.e., pure flexion, extension, ulnar deviation or radial deviation, there needs to be activation of more than one wrist muscle at the appropriate magnitude such that the desired resultant force vector (magnitude and direction) is achieved.

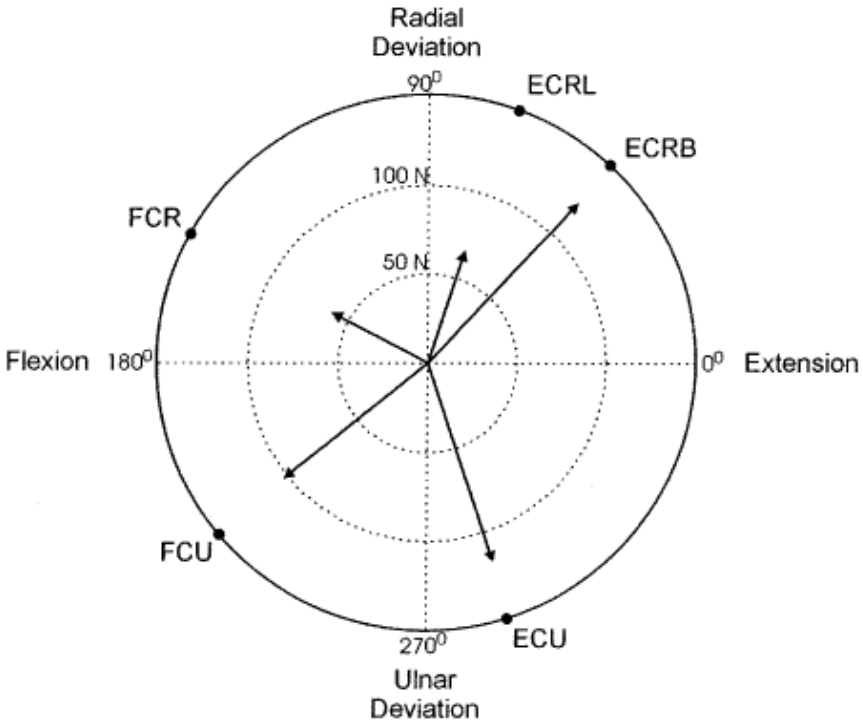

Figure 3.3 Vector representation of muscle action on the wrist joint. Adapted from Bawa et al. (2000).

3.1.2 Behavioural (motor precision) differences between wrist flexion and extension

Recently, Salonikidis et al. (2011) compared the steadiness of torque production at the wrist joint between the flexion and extension directions during an isometric torque compensation task. Visual feedback of the participants actual torque level and target torque level was provided on a monitor. The effect of varying target torque levels (5, 10, 20, 50, 75 and 100 % of MVC) as well as the effect of varying wrist angles (230, 210, 180, 150 and 130°) was also tested. To work out the steadiness of torque production, the coefficient of variation (CV) of the actual torque levels during the isometric task was calculated. The CV of a data stream

can be defined as: $CV = (Standard\ deviation)/Mean \times 100$ and is a measure of the amount of fluctuation in the data stream normalised by its mean. To analyse muscle activation characteristics, the EMG activity of one of the wrist flexor muscles (FCU) and one of the wrist extensor muscles (ED) was recorded and quantified as the integral of the EMG normalised to the maximal torque level EMG integral.

The main finding of the study of Salonikidis et al. (2011) was the significantly lower CV of torque during isometric wrist flexion as compared to extension, independent of torque level or joint angle (muscle length). As the CV of torque (measure of the fluctuation in torque) would be inversely related to motor precision, this result translates into wrist flexion having significantly higher motor precision as compared to wrist extension during isometric force production. Further, the participants also had higher maximal isometric torque levels for wrist flexion as compared to wrist extension. The coactivation of ED during wrist flexion was greater compared to the coactivation of FCU during wrist extension at 50 and 75 % of maximal torque, regardless of wrist angle.

Overall, muscle group type, contraction intensity, individual motor unit properties and behaviour of the population of motor units are all factors that could affect motor precision (Enoka et al., 2003). Salonikidis et al. attributed the higher motor precision of the wrist flexors mainly to their greater strength and greater daily use as compared to wrist extensors. It was estimated that the isometric contraction strength of wrist flexors is 40-60 % more than the extensors. It was also estimated that wrist flexors are used 2-3 times more than wrist extensors in daily life. These inherent and use induced factors were suggested to be associated with motor unit activation patterns that resulted in more precise force output for the wrist flexors as compared to the extensors. Particularly, larger and stronger muscles (wrist flexors) are theorised to have more motor units in general as compared to smaller and weaker ones (wrist extensors). A greater number of smaller motor units results in a higher resolution of force output (given smaller motor units are recruited before larger ones according to the size principle) and thus increased motor precision (Hamilton et al., 2004). Interestingly, an identical pattern had been reported earlier for the dorsi-plantar flexor sets, where plantar flexors (stronger and larger) performed with a lower CV than dorsi-flexors (weaker and smaller), despite similar task goals, visual feedback, and gross muscle activation between the muscles (Tracy, 2007). A difference in the transformation of the descending

input to motor output of the dorsi-plantar flexor sets was suggested as the reason for the motor precision differences.

Furthermore, the same discrepancy in motor precision exists when these two muscle groups (wrist flexors and extensors) are involved in more complex movements. Sports performance evaluation shows higher precision and faster learning of the forehand (predominantly involving flexors) compared to the backhand (predominantly involving extensors) in beginner's Tennis (Mavvidis et al., 2010). This suggests a possible trend in flexion and extension movements of the upper arm in general, with flexion movements being more accurate than extension.

Apart from the factors discussed by Salonikidis et al., differences in the interaction between the central and peripheral nervous systems, more particularly, the phenomenon of sensorimotor monitoring of muscles by the cortex could have also influenced the motor precision differences between wrist flexion and extension. Alternately, the precision differences could have influenced the sensorimotor monitoring levels of the muscles. Investigating such an interaction between the CNS and PNS (sensorimotor monitoring) is carried out in the research field of CMC; see section 3.2. Salonikidis et al.'s study (Salonikidis et al., 2011) neither measured cortical activity (EEG) nor CMC.

3.1.3 Neurophysiological differences between wrist flexion and extension

By using magnetic stimulation and constructing the corresponding peristimulus time histograms (PSTHs) of the activated motor units, it has been suggested that stronger monosynaptic corticospinal projections (see section 2.1.3.1) could exist to elbow flexor muscles as compared to elbow extensor muscles in humans (Palmer and Ashby, 1992) and primates (Phillips and Porter, 1964). This suggests greater direct facilitation of flexion compared to extension of the upper limb, however no conclusive differences between the wrist muscles specifically were found.

However, the results of a later study using electrical stimulation and PSTHs, suggest that wrist and finger extensors i.e. ECU and extensor indicis proprius respectively have denser corticospinal projections compared to wrist and finger flexors i.e. FCR and FDS (de Noordhout et al., 1999). This suggests greater relative involvement of the direct

monosynaptic corticospinal tract specific to wrist extensor control as compared to wrist flexor control.

Recently, Chye et al. (2010) compared the corticomotor excitability of a wrist flexor muscle (FCR) and a wrist extensor muscle (ECRL) during: active and passive, wrist flexion and extension tasks, by using transcranial magnetic stimulation and measuring the corresponding surface motor evoked potential (MEP) at the muscular level. While there was no difference in the excitability between the wrist extensor and flexor during passive movements, significantly greater corticomotor excitability was found for the wrist extensor muscle as compared to the wrist flexor muscle during active movements. This result agrees with the results of de Noordhout et al. (1999) suggesting stronger corticospinal projections to wrist extensors as compared to wrist flexors.

Further evidence of neurophysiological differences between wrist flexion and extension is also present. Output neurons controlling wrist extension fire at a higher rate than those controlling flexion in primates (Cheney and Fetz, 1980). The red nucleus of primates facilitates flexors of the fingers, this facilitation is absent for the extensors (Keifer and Houk, 1994). The basal ganglia of primates exert a greater inhibitory effect over wrist extensors than flexors (Mink and Thach, 1991; Keifer and Houk, 1994). Yu et al. (2000) found higher functional magnetic resonance imaging (fMRI) and movement-related cortical potential (MRCP) values for thumb extensors compared to flexors; while also suggesting a possible extrapolation of the results to the wrist level as well. Yu et al. (2000) attributed these differences to the higher activation needed to overcome the higher inhibition and lower facilitation of the thumb extensors.

Overall, these neurophysiological differences could influence the sensorimotor monitoring levels of the wrist flexors and extensors which can be gauged by CMC (covered in section 3.2).

3.1.4 Clinical differences between wrist flexion and extension

Faster motor recovery of flexion compared to extension has been reported in stroke patients (Lieberman, 1986; Duncan and Badke, 1987; Little and Massagli, 2007). Greater impairment of extensors compared to flexors has been reported in Parkinson's disease (Pfann et al., 2004). A recent study reported on the greater plasticity of the wrist flexors

compared to extensors after ischemic nerve block (Vallence et al., 2012). Overall, the clinical differences between wrist flexion and extension make studying the wrist joint a matter of importance. It would be of particular interest to obtain normative measures of CMC (covered in section 3.2) of the various wrist muscles as this would allow analysing their sensorimotor monitoring levels by the cortex.

3.2 Corticomuscular coherence (CMC)

CMC is the coupling of the oscillatory activity of the cortex and muscle. The subsequent subsections provide background (section 3.2.1) and an overview (section 3.2.2) of the process, as well as review its mediation (section 3.2.3), modulation (including motor precision and cognitive factors) (section 3.2.4) and functional roles (section 3.2.5).

3.2.1 Oscillatory neuronal activity

In the central nervous system, oscillatory activity has been measured over several areas of the cerebral cortex including the sensorimotor cortex (Pfurtscheller et al., 1996; Brown et al., 1998; Alegre et al., 2003). Both EEG (Pfurtscheller et al., 1996) and magnetoencephalography (MEG) (Salmelin and Hari, 1994) have been used successfully to measure this oscillatory activity over the sensorimotor cortex (see section 2.2 for EEG detection theory). Only the larger amplitude group oscillatory activity generated by the sum of individual neuronal oscillations from a neuronal ensemble can be measured by these surface measurement techniques. There are various mechanisms that are thought to produce the rhythmicity. One mechanism involves the inhibitory action of inhibitory interneurons (Pauluis et al., 1999). Inhibition of a group of neurons in a timely manner has the effect of producing oscillatory activity at a frequency which is determined by the time period of the inhibitions. Inhibition can also have the effect of resetting and thereby synchronising the on-going oscillatory activity of neurons. It has been shown that an increase in inhibition by administration of certain drugs increased beta activity over the sensorimotor cortex (Baker and Baker, 2003). Another mechanism that has been found to produce rhythmicity is related to gap junctional interactions between individual neurons. Gap junctional connections are electrical synapses that allow strong electrical coupling between neurons. Evidence of this kind of coupling producing beta oscillatory activity has been found in the layer V neurons of the motor cortex in the rat (Roopun et al., 2006).

Lastly, the intrinsic ability of neurons to fire at a particular frequency, 'rhythmogenesis' is a mechanism that can produce rhythmicity (Chen and Fetz, 2005).

3.2.1.1 Motor related cortical rhythms

The oscillations recorded over the sensorimotor cortex present themselves at certain distinct frequency ranges. Oscillatory activity at both the alpha (8-12 Hz) and beta frequency bands has been recorded from the sensorimotor cortex (Salmelin et al., 1995). Each frequency range has been shown to be reactive to certain tasks as well as to certain modes of a task. The oscillations in the alpha and beta band measured by EEG over the sensorimotor cortex react appreciably to certain motor perturbations (Salmelin et al., 1995; Pfurtscheller et al., 1996; Stancák Jr. and Pfurtscheller, 1996). Both alpha and beta oscillatory activity over the motor cortex is most prominent during the resting state or during isometric contraction of the contralateral limbs. However, it is suppressed during a dynamic movement (Stancák Jr. and Pfurtscheller, 1996). Further, this suppression can be caused by tactile stimuli, motor imagery of an action or even due to an observed movement (Pfurtscheller et al., 2005). The suppression actually starts 1-2 seconds before the execution of a dynamic movement. This phenomenon is called event related desynchronisation. It is thought to be caused by disinhibition of the motor cortex, as a step in the preparation for the movement. The alpha and beta oscillatory activities however increase substantially in magnitude about 1-2 seconds after the movement. This phenomenon is called event related synchronisation, or in the case of the beta oscillatory activity, the 'beta rebound' (Pfurtscheller et al., 1996). The beta activity recovery is however quicker (about 300ms quicker) and stronger than the alpha activity. The initial outlook on the functional role of the cortical beta oscillatory activity was limited and it was suggested that it merely functions as an 'idling' mechanism i.e. neuronal cells will fire at this frequency when they are not doing any particular task (Pfurtscheller et al., 1996). However according to more recent studies, cortical beta oscillations are suggested to represent the neural inertia of a task (Pogosyan et al., 2009; Engel and Fries, 2010). It was suggested that beta band oscillations may be involved in the maintenance of the existing sensorimotor or cognitive state, while compromising new movement.

Simultaneous recordings of local field potentials from spatially separated sites in awake behaving monkeys revealed an interesting pattern of oscillatory activity (Rubino et al.,

2006). It was found that oscillatory activity can organise into travelling waves across various areas of the cortex. The direction of wave travel tended to align along a major axis (anterior–posterior in primary motor cortex; medio-lateral in dorsal pre-motor cortex). The waves also encoded information about the cues guiding behaviour of the monkeys in both their amplitude and phase. This leads to the general idea that travelling oscillatory activity may be a medium for information transfer between various distant areas of the nervous system (Baker, 2007). Such type of communication has also been shown to occur between the central and peripheral nervous systems, in the form of CMC.

3.2.2 Overview of CMC

A little less than two decades ago, Conway et al. (1995) reported the first findings of coupling between rhythmic cortical activities measured using MEG and rhythmic muscular activities measured using EMG during low level isometric force production. This coupling was constrained to the beta frequency band. Later many other groups demonstrated this coupling between the cortex and the muscle using EEG and EMG respectively (Halliday et al., 1998; Kristeva et al., 2007; Witham et al., 2011).

At a particular frequency, the degree of this coupling (coherence) between the cortical signal and muscular signal can be mathematically calculated as a number between zero and one and is thus termed as corticomuscular coherence (CMC). Zero represents no correlation and one represents perfect correlation between the two signals. Particularly, the linear correlation between the cortical and muscular signals in the frequency domain is measured as the cross spectra of the two signals normalized by their auto spectra (Halliday, 1995). Figure 3.4 shows a typical CMC spectrum for an isometric contraction task taken from a prior study (Ushiyama et al., 2010).

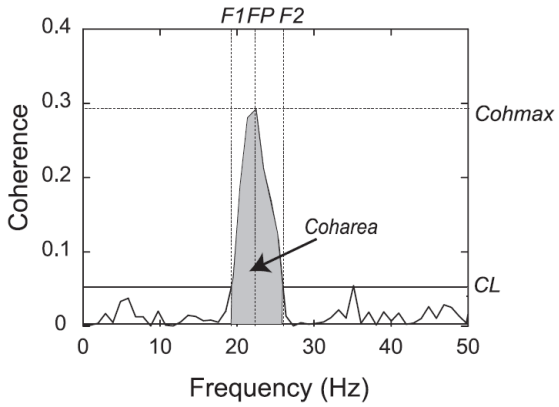

Figure 3.4 Typical CMC spectrum for an isometric contraction task. Adapted from Ushiyama et al. (2010).

CL was the confidence limit above which coherence was considered to be significant, FP was the frequency at which the peak coherence (Cohmax) occurred, F1 was the frequency at which the coherence curve fell below significance when traced backwards from FP, F2 was the frequency at which the coherence curve fell below significance as traced forwards from FP and Coharea was the significant coherence area acquired by integrating the coherence curve with respect to frequency with limits of F1 and F2.

3.2.3 Mediation of CMC

Figure 3.5 shows possible pathways through which CMC may arise. These consist of both the efferent (red) and afferent (blue) pathways.

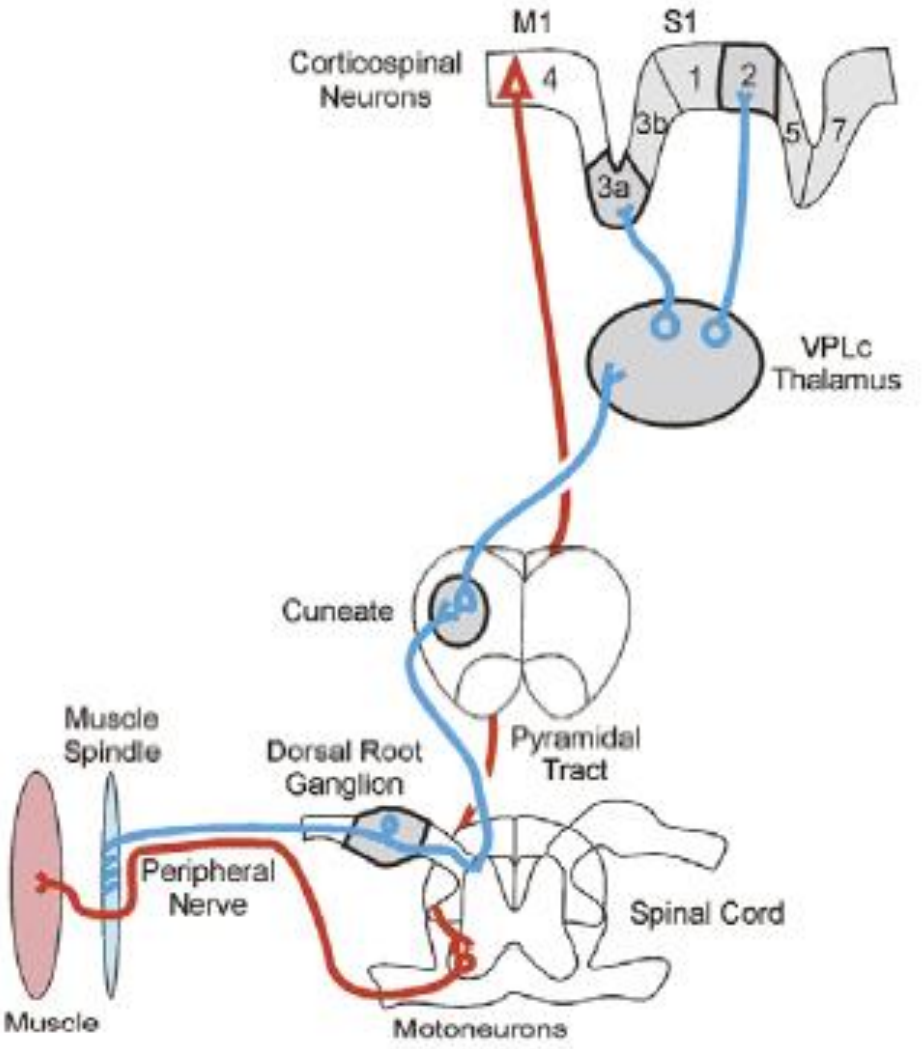

Figure 3.5 Efferent (RED) and afferent (BLUE) pathway involvement in muscle control. Adapted from Baker (2007).

3.2.3.1 Involvement of efferent pathways

Initial outlooks on CMC were that it is purely an efferent process (Salenius et al., 1997; Gross et al., 2000). The ability of the M1 motor neurons to produce oscillatory activity in the beta band was already demonstrated (Pfurtscheller et al., 1996). It was thus thought that these cortical oscillations merely transfer to the spinal alpha motor neurons via the corticospinal tract. The feature of the corticospinal tract that would facilitate this transmission is the existence of monosynaptic connections between some of its corticospinal neurons (originating from M1) and alpha LMNs (see background on the corticospinal tract; section 2.1.3.1). Such a process would mean that the phase differences between the cortical and muscle signals are linear with the frequency of the oscillations, given a constant conduction time from cortex to muscle. The phase difference in radians would then be given by [conduction delay] × [2π] × [frequency]. Then phase difference would be linearly related to frequency with a slope equal to [conduction delay] × [2π].

3.2.3.2 Involvement of afferent pathways

The linear relationship between phase and frequency was however only found in some studies (Salenius et al., 1997; Gross et al., 2000) and not in others (Halliday et al., 1998). In a later detailed study, the linear phase-frequency relationship was only found in some subjects and not in others (Riddle and Baker, 2005). Furthermore, it was found that the conduction delay worked out from the linear phase-frequency slope was ~10 ms; this was half the delay as compared to the standard delay from motor cortex to distal musculature of 20ms. Additionally, in Riddle and Baker's study (2005), the subject's arms were cooled in order to increase nerve conduction time (precise increase was measured by nerve stimulation). The slope of the phase-frequency relationship of CMC did increase after cooling. However, the slope resulted in a conduction time increase which was twice the amount to what was found using nerve stimulation. This was deemed to be possible due to the involvement of afferent pathways as well as efferent pathways that resulted in the final phase of CMC. The summation of efferent and afferent conduction times would form the total conduction time, which would be approximately double the conduction time calculated using nerve stimulation which takes into account just the efferent pathway. The absence of a linear phase-frequency relationship in some subjects as well as a discrepancy between the conduction times derived using the phase-frequency slopes and using

objective techniques such as nerve stimulation, lead authors to believe that CMC may not be solely mediated by efferent processes. Afferent processes were suggested to also mediate CMC.

There is also evidence from dorsal root recordings from monkeys to suggest involvement of afferent processes in CMC (Baker et al., 2006). The dorsal root discharge from muscle afferents (e.g. muscle spindles) was coherent with oscillations from the muscle. Thus sensory oscillations were found to encode efferent oscillatory information. In support of this a recent study (Witham et al., 2011) employed the technique of directed coherence (Granger Causality) to study the level of corticomuscular coupling. This technique provides a measure of the amount of influence one signal has on a second signal and vice versa. In the case of this study, it was found that in some subjects the EEG 'caused' the EMG (primarily efferent process) and in other subjects the EMG 'caused' the EEG (primarily afferent process). Thus overall there is sufficient evidence to believe that CMC may be a result of a feedback loop, involving the motor cortex, muscle and somatosensory cortex. This type of loop would explain the complex phase-frequency relationships found in the literature, as CMC is both a combination of efferent and afferent processes. To understand the functional role of CMC, various studies have investigated the factors that modulate it.

3.2.4 Modulation of CMC

3.2.4.1 Movement parameters

CMC is most prominent during static phases of a motor task; while CMC is abolished during dynamic movements as well as motor imagery (Baker et al., 1997). Significant CMC has been found in the 8-12 Hz (alpha), 15-30 Hz (beta) (Salenius and Hari, 2003) and 30-40Hz (gamma) bands (Salenius et al., 1996). Corticomuscular oscillation at around 10Hz (alpha) is believed to represent pulsatile communication between brain and muscle. CMC is prominent in the beta band for weak tonic contractions and therefore may represent a strategy for controlling submaximal force. CMC shifts to the gamma band for stronger contractions and therefore may represent strategy for controlling stronger muscle force production. It has also been found that there is a linear relationship between frequency of beta band CMC and % MVC (Chakarov et al., 2009); this relationship is absent in the gamma band.

3.2.4.2 Cortical oscillatory power

Diazepam falls under the group of drugs called Benzodiazepines which are known to enhance the effect of the neurotransmitter GABA. In a previous study, the subjects' EEG spectral power at 20 Hz (within the beta frequency range) significantly increased (~ doubled) after the administration of Diazepam (Baker and Baker, 2003). There was however no significant difference in the subjects' CMC levels at the 20Hz frequency before and after Diazepam administration. It was thus concluded that CMC is independent of the power of cortical sensorimotor oscillations. In a later study Carbamazepine (a drug that blocks frequency, use and voltage gated neuronal sodium channels) was administered to subjects and had the effect of enhancing beta range CMC although beta range EEG power was unaltered (Riddle et al., 2004). This further supported the disassociation between cortical oscillatory amplitude and CMC amplitude.

3.2.4.3 Motor precision

Kristeva et al. (2007) experimented on the pars indicis of the FDS muscle with the aim of clarifying the functional significance of beta CMC. They hypothesized that if beta CMC had a functional role, it would have a behavioural correlate. More specifically, they hypothesised the functional role of beta CMC would be related to the motor precision of the steady-state motor output during which beta CMC is most prominent.

Kristeva et al.'s experimental paradigm mainly consisted of isometric force compensation by the right index finger against a manipulandum for ~ 15 s at 4 % of the maximum voluntary contraction level, with visual feedback of the target and actual forces provided; i.e. the participants exerted a static force with their right index finger to keep a visual cursor within a target zone. Data (EEG, EMG and force) from the force compensation task was segmented into multiple 512 ms long segments. In order to work out the relation between CMC as well as beta EEG power and motor precision, each segment was grouped into either a "good" performance or "bad" performance group based on the mean square error (MSE) of the force signal of the segment. CMC and beta EEG power were then calculated for the "good" performance and "bad" performance groups. Similarly, in order to work out the relation between CMC and EEG beta power, each segment was grouped into either a "high" power or "low" power group based on the EEG beta spectral power of the segment. CMC was then calculated for the "high" power and "low" power groups.

The main finding was that beta CMC was significantly higher for the "good" performance group as compared to the "bad" performance group. Similarly, beta EEG spectral power was also significantly higher for "good" compared to "bad" performance. Further, it was found that beta CMC was significantly higher for the "high" power group compared to the "low" power group. Based on these findings, Kristeva et al. suggested that, higher beta-range cortical spectral power and increased CMC in the beta range improves motor performance during steady-state motor output. Overall, a direct relationship between beta CMC and motor precision is demonstrated in this study, and hence CMC was suggested to promote effective sensorimotor integration. However other studies appear to contradict this; see section 3.2.4.5 for information relating fatigue, CMC and motor precision. Further, it is yet to be studied whether this direct CMC – motor precision relationship would hold when comparing functionally different muscle groups such as the antagonistic wrist flexors and extensors (see section 3.1).

3.2.4.4 Training and muscle function

In a recent study it was shown that training of muscles affects their CMC levels (Ushiyama et al., 2010). This study compared CMC between untrained and trained (athletes) subjects. It was found that CMC levels were lower for trained subjects as compared to untrained subjects.

This same study also found inter-muscle variation between CMC. CMC levels were lower for proximal muscles as compared to distal muscles. Further, CMC levels were generally lower for upper limb muscles as compared to lower limb muscles. Thus muscle function (postural of fine movement) was suggested to modulate CMC. This study however did not simultaneously measure motor precision of the muscles along with their CMC to further analyse the functional properties of the muscles. Visual feedback of the EMG of the muscle was given to subjects, which had to be maintained at a target level during an isometric contraction of the muscle. Rather, providing visual feedback of force/torque signals that have to be isometrically compensated understandably allows the measure of motor precision and also allows for setting of higher precision constraints during isometric force compensation tasks (Kristeva et al., 2007; Salonikidis et al., 2011; Ushiyama, Katsu et al., 2011).

3.2.4.5 Fatigue

Multiple studies have analysed the effects of fatigue on CMC. The evidence is contradictory. Yang et al. (2009) show that CMC decreases after fatigue whereas a later study (Ushiyama, Katsu, et al., 2011) shows that CMC is enhanced post fatigue. The later study suggested that an attempted increase in the force production by the motor system after fatigue by greater synchronisation of motor units (increase in common drive) results in higher CMC. Furthermore, in the later study, along with enhanced CMC, higher beta-EMG discharge as well as higher force fluctuation (lower precision) was also found post fatigue as compared to pre fatigue. The authors suggested that CMC may be enhanced to increase force amplitude but at the cost of decreased motor precision. Therefore a possibly contradictory inverse relation between CMC and motor precision may seem apparent in the pre-post fatigue comparison scenario (see section 3.2.4.3 for information on CMC and motor precision).

3.2.4.6 Cognition

In an initial study (Kristeva-Feige et al., 2002) it was found that higher attention to the motor task resulted in higher beta CMC. Also, distraction of subjects while they carried out the motor task reduced CMC levels.

A later study compared the effects of the level of preparedness on CMC (Schoffelen et al., 2005). In this study, the "readiness to respond" or level of preparedness to a stimulus was altered by using variations in the experimental paradigm. It was found that 40-70 Hz (gamma) CMC was enhanced for a higher level of preparedness.

A recent study showed that CMC was higher during force compensation of a predictable force trajectory when compared to an unpredictable one (Mendez-Balbuena et al., 2013). Also, the predictable force tracking task was carried out with lower cortical resources as well as lower muscle activation. The authors thus suggested that successful anticipation results in increased CMC and a more stable motor state.

It may be possible that there are pre-existing factors that can influence the cognitive difficulty (or ease) associated with performing an isometric force compensation task when considering two different muscle sets (see section 3.1.2 and section 3.1.3 for such differences between wrist flexion and extension). Differences in difficulty may then result in subconscious alterations in attention e.g. higher attention given to a more difficult task

and/or level of preparedness e.g. higher level of preparedness for a more difficult task. Such alterations in attention (Kristeva-Feige et al., 2002) and level of preparedness (Schoffelen et al., 2005) may overall result in modulation of CMC. The influence of the level of perceived difficulty due to pre-existing factors on CMC has not been studied yet.

3.2.5 Proposed functional models of the CMC mechanism

While many research groups have tried to elucidate the exact functional role of CMC based on how it is modulated by certain parameters, it still remains unclear. One idea is that CMC acts to promote effective sensorimotor binding (Kristeva-Feige et al., 2002; Kristeva et al., 2007). As higher attention and higher precision was associated with increased beta CMC in these studies, it was suggested that neuronal oscillations and their coupling between the cortical and muscular levels, provide an effective means of communication between the sensory and motor systems. Attention may increase this communication, and once increased this may result in higher motor precision.

From this view point it was also likely that CMC acts as a recalibration mechanism after dynamic movement (disturbance in steady state). An initial study showed that the magnitude of CMC was inversely related to the compliance of the lever which the subjects pressed against until they reached the target force level which they had to maintain (Kilner et al., 2002). Later this theory was reconsidered when it was shown that it was actually the greater amount of digit displacement caused by the lower lever compliance before the maintenance of the target force that had caused the higher CMC (Riddle and Baker, 2006). The greater initial movement (displacement) was seen as a greater disturbance before the steady state force production and therefore there was a greater need for re-calibration by the motor system. The greater re-calibration meant higher CMC. A recent study (Omlor et al., 2011) also demonstrates a similar effect, where CMC is increased in tasks where there is greater uncertainty before the constant hold phase of a task. This again means a greater need for re-calibration and hence enhanced CMC.

Another research group proposed that CMC may act as a mechanism to promote the existing steady motor state (Gilbertson et al., 2005). This view point stems from findings in subjects whose reaction time in performing a cued movement was slower when their instantaneous CMC levels were higher. It was suggested that it takes longer for the motor

system to initiate a new movement with on-going oscillatory activity as the oscillations first have to be interrupted. A similar set of results was recently reported by Matsuya et al. (2013). Matsuya et al. found that the reaction time to performing a new ballistic movement from a prior sustained isometric contraction is higher; when the prior sustained contraction is associated with higher levels of beta CMC as well as higher levels of grouped beta EMG discharge. Matsuya et al. (2013) suggested, similarly to Gilbertson et al. (2005), that the generation of new movement is delayed with elevated levels of corticomuscular coupling, thus further supporting the idea that beta CMC functions to promote the existing steady motor state.

A recent attractive idea derived from the sensorimotor binding property of CMC is the analogy of CMC to a radar system. It has been suggested that the MI sends motor control commands to the muscle and also sends a copy of this command to the SI. Oscillations carrying skin and muscle spindle information (tension and length) then travel from muscle to SI in a feedback loop, where SI compares the motor command to the muscle spindle information and may correct for error by sending corrective information back to MI (Witham et al., 2011). Thus this "sensorimotor monitoring" of the muscles by the cortex would result in the coupling between the cortical and muscular activities, i.e. CMC.

4 EXPERIMENTAL APPARATUS

Section 4 covers the concept, design, construction, testing and calibration of the experimental apparatus that the objectives of the present study prompted (listed in section 1). Figure 4.1 shows a block diagram summary of the experimental apparatus. In the following subsections (section 4.1 – section 4.8) each of the subcomponents will be described. Their testing and calibration will then be described subsequently (section 4.9 – section 4.10).

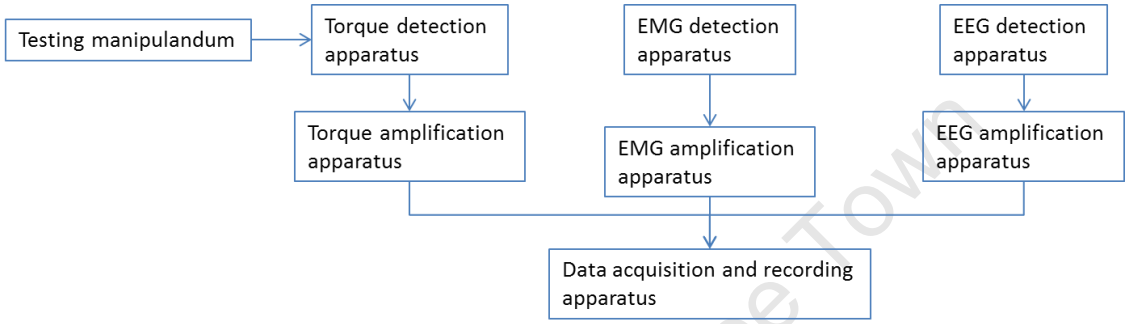

Figure 4.1 Block diagram summary of experimental apparatus.

Overall the objectives required testing neurophysiological, behavioural and perceptual variables between isometric wrist flexion and extension tasks. A testing manipulandum was built by the candidate to facilitate proper isometric flexion and extension of the wrist (section 4.1). To measure the behavioural variables, a torque measurement system was built by the candidate (section 4.2 and 4.3) which was integrated with the testing manipulandum. To measure the neurophysiological variables, an EMG measurement system (section 4.4 and section 4.5) and an EEG measurement system (section 4.6 and 4.7) were built to measure the muscular activity as well as the cortical activity respectively during isometric contractions. The EMG measurement system was built in entirety by the candidate. The conceptual stage of the EEG measurement system was carried out by the candidate in collaboration with a colleague while its construction was carried out by the colleague. Measuring the perceptual variable did not require any additional apparatus. To digitise and record data from each of the three measurement systems (torque, EMG and EEG), data acquisition (DAQ) hardware was setup by the candidate (section 4.8). The torque system was calibrated and tested by the candidate (section 4.9). The EMG and EEG systems were calibrated and tested by the candidate (section 4.10); the fundmental calibration hardware and software was provided by a colleague.

4.1 Testing manipulandum

The experiment required subjects to perform isometric wrist extension and flexion. A manipulandum was conceptualised and designed in SolidWorks for this purpose and was then constructed accordingly at the University mechanical workshop. Figure 4.2 is a picture of the assembly in SolidWorks. Figure 4.3 shows an isometric (left) and lateral (right) view of the final product that was used in the experiments.

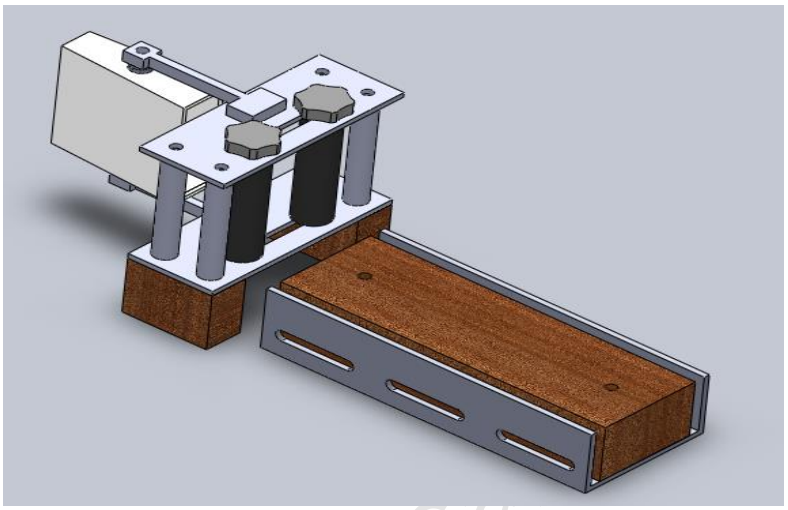

Figure 4.2 Design assembly of manipulandum in SolidWork.

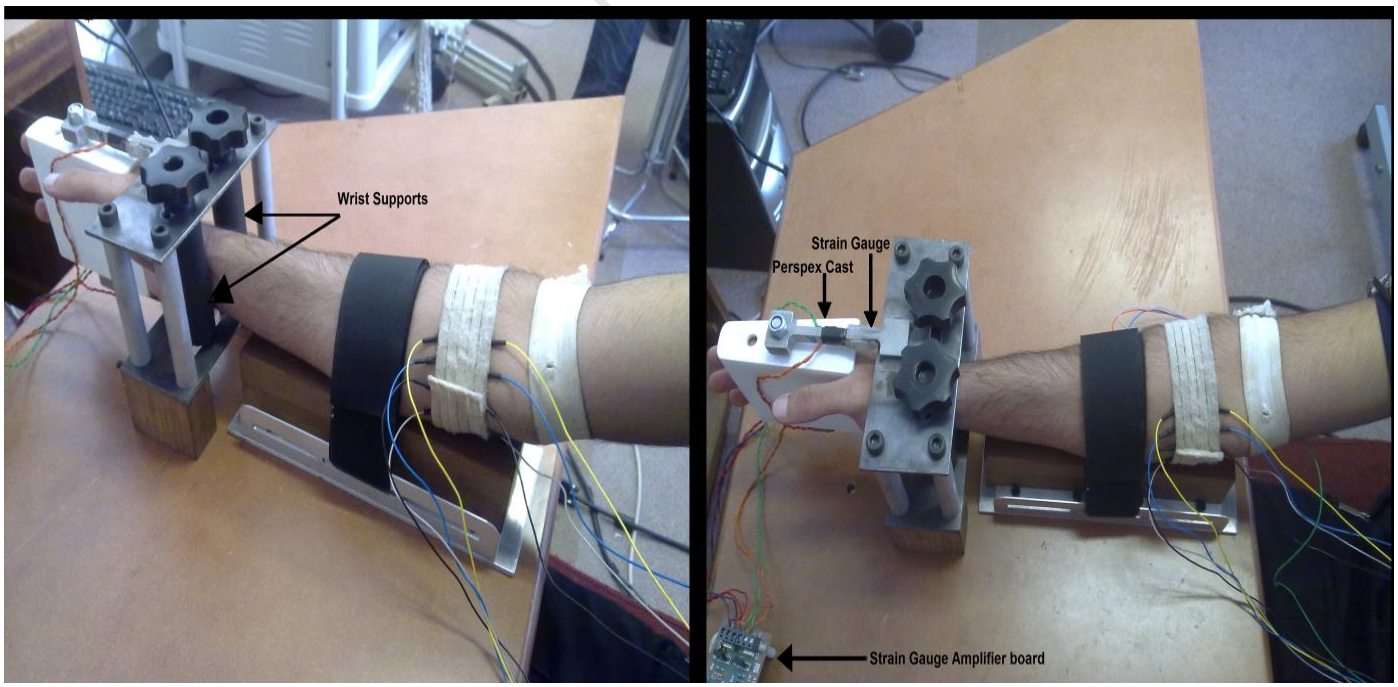

Figure 4.3 Isometric view (left) and lateral view (right) of constructed manipulandum based on the SolidWorks design that was used in the experiments. Visible features are the tapered cast to secure fingers, vertical bars to secure wrist, straps to support forearm and horizontal beams to resist as well as measure torque with the attached strain gauges.

The design of the manipulandum was based on the following considerations (section 4.1.1).

4.1.1 Wrist joint and its movements

The wrist joint is the adjoining point between the forearm and the hand. It has two degrees of freedom, i.e. in the flexion-extension directions and in the radial-ulnar directions (radial-ulnar deviation); see section 3.1.1. Torque about the wrist joint is produced by various muscles. Some muscles are dedicated wrist muscles. Other muscles, the digit flexors and extensors, are multi-function, i.e. they produce torque about the wrist joint by acting on the digits. But all the wrist extensor muscles produce torque in the extension direction and all flexors in the flexion direction. The design for the present study was aimed to match this property.

Two previous studies done on wrist flexion and extension (Lundbye-Jensen and Nielsen, 2008; Salonikidis et al., 2011) had utilised a manipulandum which was clasped by the fingers to perform wrist flexion and extension movements. However the first study's primary aim was not to compare between wrist flexion and extension and the second study did not involve measuring brain activity. Clasping of the manipulandum with the fingers will simultaneously activate the flexor compartment while performing an isometric wrist extension task. In order to avoid this, a slightly different approach was adopted in the design for the present study as can be seen in Figure 4.2 and Figure 4.3.

To eliminate movement of the fingers with respect to the hand or the need for clasping of any object with the fingers (Lundbye-Jensen and Nielsen, 2008; Salonikidis et al., 2011), a tapered cast was designed through which the hand would be inserted. The subjects were expected to apply a force against the cast by performing either an isometric wrist extension or flexion with the region of force application being at the level of the metacarpophalangeal joints; see Figure 4.4. This mechanism was aimed at ensuring that any force exerted on the cast from the isometric contractions would be unidirectional in the respective direction (flexion/extension). This was considered important as motor neurons are known to encode for direction of movement; see section 2.1.4.1. More importantly, it was aimed at ensuring that only the respective compartment of muscles would be activated for a particular movement. That is, during isometric wrist extension only the posterior forearm compartment would be activated and during isometric wrist flexion only the anterior

forearm compartment would be activated. It is also known that motor neurons controlling the posterior compartment synapse dorsal to the ones controlling the anterior compartment at the spinal cord. Therefore keeping the compartment of muscles activated during a task fixed was considered important.

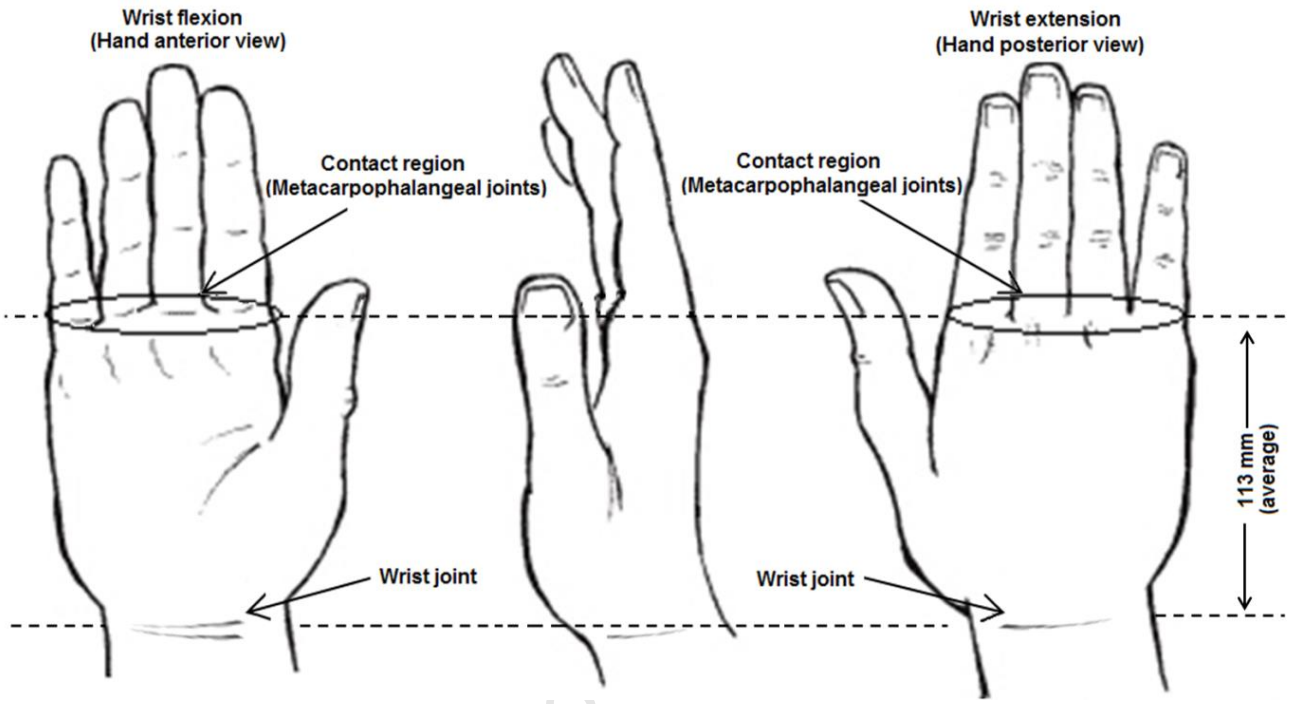

Figure 4.4 Force application regions on hand during isometric wrist flexion and extension.

One difficulty with such a design would be that subjects could "unintentionally" apply a force to the cast by using internal or external rotation of the shoulder instead of flexion or extension of the wrist respectively. To avoid this situation, two measures were taken. Firstly, a sports strap was provided so the forearm could be secured to the wooden platform using a double looping method to avoid any movement. Secondly and more importantly, two vertical bars[1] were provided which would secure the wrist joint between them. These bars were adjustable in the horizontal direction and therefore allowed tightening or loosening of their hold on the wrist. Any force exerted by external rotation of shoulder would therefore be nullified firstly by the forearm strap and secondly also by the right vertical bar. As for forces produced by internal rotation of the shoulder, these would be nullified again by the forearm strap and the left vertical bar. Overall, only the force due to torque produced about the wrist joint was aimed to be transferred on to the cast.

[1] Note the vertical bars were wrapped with foam rubber for comfort to the subject.

4.2 Torque detection apparatus

The next design consideration was to best measure the forces applied on the cast. The cast was mounted (fixed) between two horizontal steel (mild steel) bars; as can be seen in Figure 4.2 and Figure 4.3. Any force applied on the cast in either the flexion or extension direction would cause stresses on the steel bars causing them to bend (strain) in the respective direction. In order to detect these strains; strain gauges (steel, 120 Ω) were mounted on the bars; see Figure 4.3 (right). Four strain gauges were utilised in total, two on the top bar and two on the bottom i.e. with 1 gauge on either side of a bar. The thickness of the bars was another consideration. A bar too thick would result in reduced sensitivity of the strain gauges, a bar too thin and there would be the risk of permanent bending of the bars making them unusable. As maximum voluntary contraction was to be measured by the system, average MVC values of wrist flexion and extension from previous literature were used to decide on the thickness of the bars; see stress and strain calculations of steel bars (APPENDIX B) for a detailed explanation of this calculation.

4.3 Torque amplification apparatus

Using four strain gauges allowed for a full bridge strain gauge setup; see Figure 4.5 (left and middle).

Strain Gauge (SG)	Placement
1	Top beam right side
2	Top beam left side
3	Bottom beam left side
4	Bottom beam right side

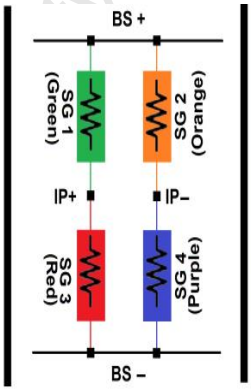

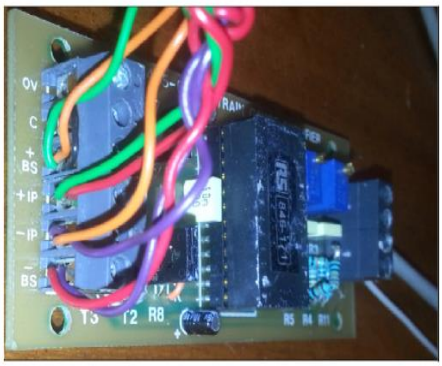

Figure 4.5 Strain gauge placement on manipulandum beams (left), full bridge strain gauge circuit setup (middle) and inputs to the commercial strain gauge amplifier (right).

The difference in signals from nodes on the full bridge, i.e. IP+ and IP- was amplified using a commercial strain gauge amplifier system (RS Components, Stock no. 435-692) with high common mode rejection ratio (CMRR) (> 120 dB), low voltage offset w.r.t. temperature (0.5µV/°C for input voltage and 20µV/°C for bridge supply voltage) and high precision resistors (1% tolerance and 50ppm/°C temperature coefficient); see Figure 4.5 (right) which

shows the amplifier and the corresponding inputs from the full bridge. The bridge supply voltage i.e. (BS+ - BS-) was set to 4.0 V. Too high a bridge supply voltage will increase sensitivity of the bridge but however result in higher currents passing through the strain gauges. The gain on the amplifier board was set by choosing appropriate resistor values on the amplifier circuit; gain = R1/R2 + 1. The gain was set to provide the best signal to noise ratio and also so that the output voltage does not exceed the rail limits when MVC torque is applied. The gain was set to 2701 by setting R1 = 270 kΩ and R2 = 100 Ω. See output voltage calculation (APPENDIX B) for a calculation of the theoretical output voltage based on the strain gauge configuration, bridge supply voltage, gain setting and force level.

4.4 EMG detection apparatus

There are four superficial muscles that act to flex the wrist i.e. FCR, PL, FDS and FCU; see section 3.1.1. Similarly there are four superficial muscles that act to extend the wrist i.e. ECRL, ECRB, ED and ECU; see section 3.1.1. It was decided to record bipolar EMG signals from all of these superficial muscles during wrist flexion and extension tasks; see EMG detection theory (section 2.3). The experimental methodology required recording 10 repetitions of isometric wrist flexion and 10 repetitions of isometric wrist extension; see experimental paradigm (section 5.2). It was also decided that these repetitions be carried out in alternate fashion (swapped between extension-flexion) to avoid bias due to the learning effect; see experimental paradigm (section 5.2). Thus it was decided to have dedicated bipolar electrode pairs for each of the 8 muscles (four flexors + four extensors). Thus on switching between tasks, there was no need to re-position the electrodes. Also this meant that the electrode positions would be consistent throughout the experiment avoiding bias due to electrode placement. Thus an 8 channel surface bipolar EMG detection system (16 recording electrodes + 1 active ground electrode) was designed; electrodes were cup type silver electrodes (Nihon Kohden, Japan, diameter = 10mm). The active ground electrode was decided to be placed over the lateral epicondyle of the wrist. The active ground electrode which is called the driven right leg (DRL) electrode serves to actively cancel common mode noise using the noise cancellation circuitry present on the amplifier boards (see section 4.5 for EMG amplification). Elefix paste (Nihon Kohden, Japan) was decided to be used to improve skin electrode contact. Elefix paste also serves to hold the

electrodes in place on the skin, however to further secure the electrodes in place; a forearm band that would be strapped over the electrodes was acquired.

Figure 4.6 shows the electrode setup used to detect EMG from the surface muscles of the forearm.

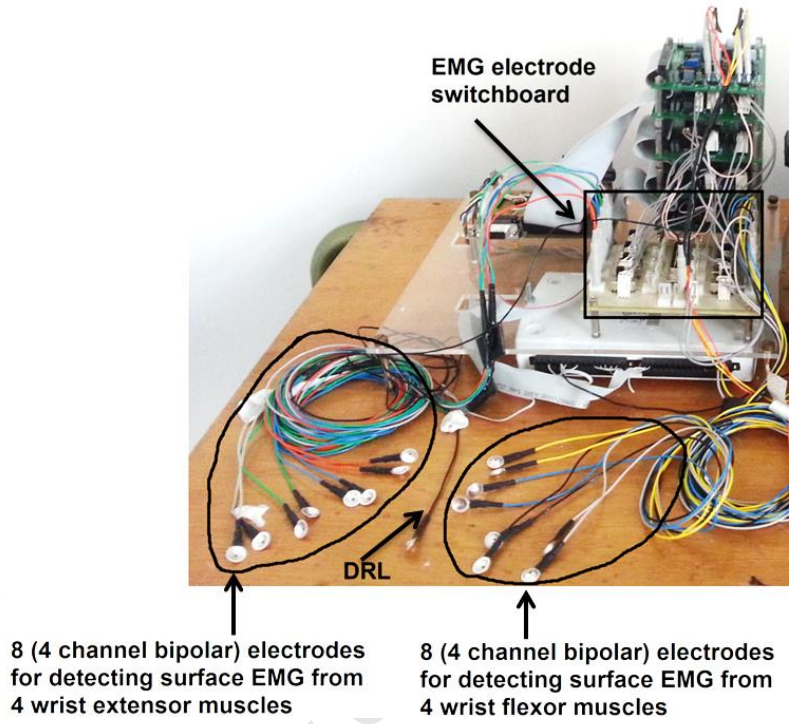

Figure 4.6 Electrode set for detection of flexor and extensor EMG.

4.5 EMG amplification apparatus

Figure 4.7 shows a summary diagram of the EMG amplification apparatus.

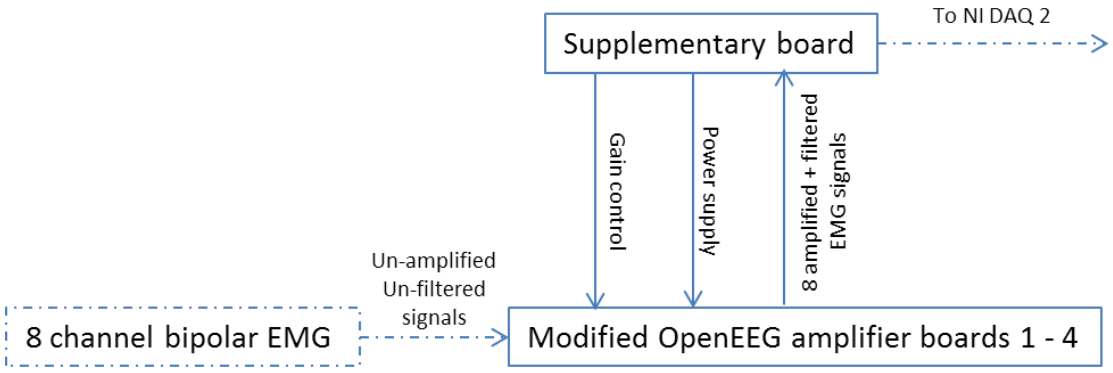

Figure 4.7 Summary of EMG amplification using modified OpenEEG amplifier boards and supplementary board.

Figure 4.8 is a picture showing the EMG amplification system.

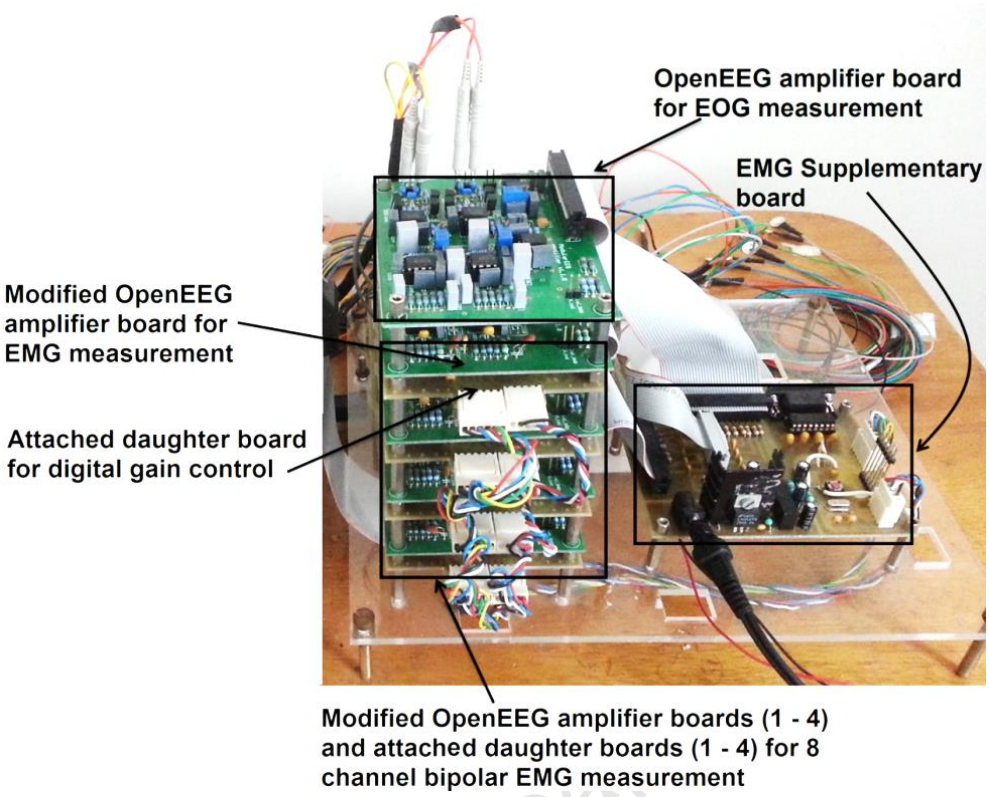

Figure 4.8 EMG amplification using modified (filter settings changed to match EMG) OpenEEG amplifier boards. Note, each amplifier board has two amplifier channels. Also visible is the supplementary board used to supply the amplifier boards with power, control their gain (using the attached daughter boards and micro-controller) as well as well as receive the amplified signals and communicate them to a data acquisition device.

For EMG amplification purposes it was decided to make use of OpenEEG amplifier boards (OpenEEG hardware [Internet], 2013); see Figure C.1 (APPENDIX C) for the circuit schematic of a single amplifier board. The OpenEEG amplifier board has a complementary board i.e. the OpenEEG digital board (OpenEEG hardware [Internet], 2013); see Figure C.2 (APPENDIX C) for the circuit schematic of a digital board. The digital board serves as a power supply to the OpenEEG amplifer boards, contains the last poles of the filter circuits which are primarily on the amplifier boards and ultimately communicates the amplified and filtered signals to a personal computer (PC) via the SCI port after digitizing them with the on-board microcontroller. Together the amplifier board (also called the analogue board) and digital board are called the ModularEEG amplifier. The OpenEEG amplifier boards are open source, cost effective and adequate for the purpose of this study. Each OpenEEG amplifier board can amplify up to two channels; therefore 4 amplifier boards were used to amplify signals from the 8 bipolar EMG electrode pairs (see section 4.4 on EMG detection apparatus). Each

channel has its own protection circuitry, amplifier circuitry, filter circuitry and noise cancellation circuitry (DRL) present on the board.

Figure 4.9 shows a simplified block diagram of one of the amplifier channels on the ModularEEG amplifier. Note the majority of this circuitry is on the amplifier board (only the last pole of the low-pass filter and the microcontroller are on the digital board).

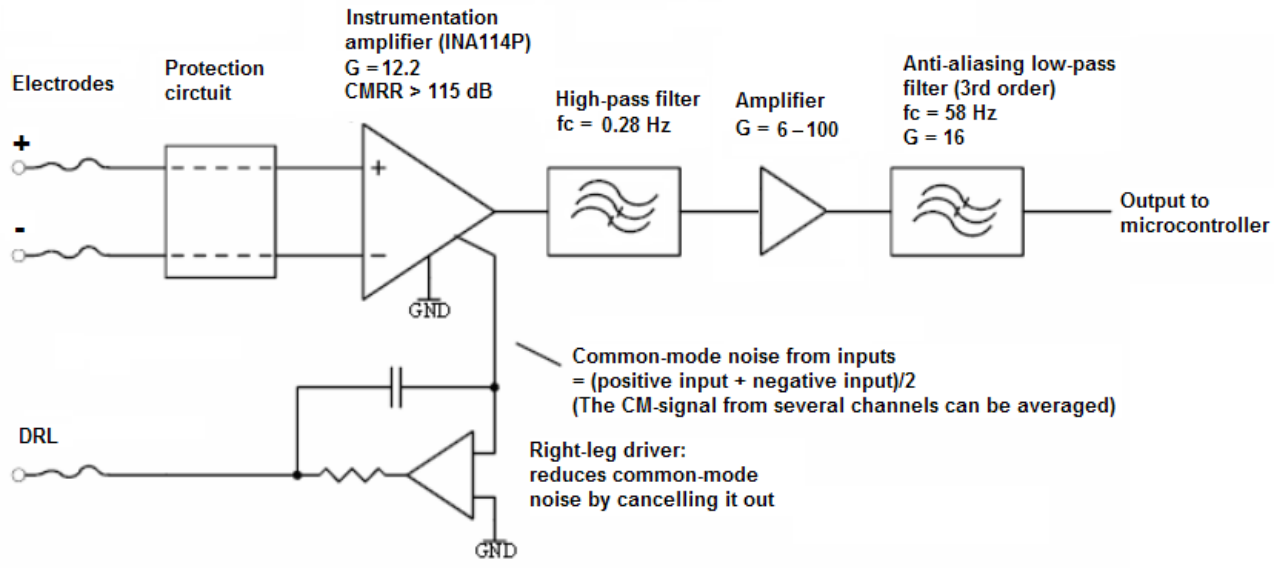

Figure 4.9 Simplified block diagram of one of the ModularEEG amplifier channels.

The bio-potential is picked up by the two (+ and -) electrodes. This signal is then passed through the protection circuitry (voltage and current limiter) which protects the rest of the circuit from electrostatic discharge (ESD) as well as protects the subject from failing circuitry. The signal is then pre-amplified (gain of 12.2) by a high quality instrumentation amplifier (INA114P). The INA114P has a high CMRR of 115 dB (minimum). Having a high CMRR is useful for cancelling noise (e.g. 50 Hz noise from the power lines) which will be "common" to both electrodes (+ and -). The INA114P also has a low offset voltage of 50 µV (maximum), low drift of 0.25 µV/°C (maximum) and a low input bias current of 2nA (maximum).

After pre-amplification, the signal is then passed through a second order high-pass filter which has a cut-off frequency (fc) of 0.28 Hz. The high-pass filter blocks DC; this is useful in cancelling any charge build-up on the electrode, which could result in "railing" of the subsequent amplifier circuitry. The signal is then amplified a second time using a standard

amplifier which has an adjustable gain (through a potentiometer) of 6-100. This gain is set to 40 as a default by the manufacturers. After this second stage of amplification the signal is then fed through a 3rd order low-pass "Besselworth" filter (mixture between Butterworth and Bessel) with fc of 58 Hz, rolloff of 19.2 dB/octave and also a gain of 16. The low-pass filter helps in reducing aliasing (high frequency signals appearing as low frequency signals due to low sampling rates during digitisation). The amplified and filtered signals are then passed to a microcontroller which digitizes them and communicates them to a PC via the SCI interface. The DRL electrode is an active ground electrode and reduces common-mode signals such as 50 Hz mains by cancelling them out using the right-leg driver circuitry. It replaces a ground electrode which older EEG designs use, and can attenuate mains hum up to 100 times more than the instrumentation amplifier can do by itself.

4.5.1 Modifications to the ModularEEG amplifier for EMG measurement

The ModularEEG amplifier is designed for EEG measurement i.e. high pass of 0.28 Hz and low pass of 58 Hz; see Figure C.3 and Figure C.4 (APPENDIX C) for the original filter circuit and its simulation in Microcap respectively. However useful EMG information can be detected at up to 500 Hz. Also movement artefacts are normally in the lower frequency range. Therefore the filter settings of the ModularEEG amplifier were modified to match the recommendations for EMG acquisition (Hermens et al., 1999; Merletti and Di Torino, 1999; Stegeman and Hermens, 2007). Accordingly, the high-pass filtering fc was changed from 0.28 Hz to 5 Hz and low-pass filtering fc was changed from 58 Hz to 500 Hz. This was carried out according to the following concept. In an electronic circuit with inductors and capacitors, the fc can be shifted from f1 to f2 by scaling all inductors (L) and capacitors (C) by an appropriate factor such that they have the same impedance (X) at f2 as they did have at f1 (Horowitz and Hill, 2006). Resistor values do not change. For a capacitor:

$$X = \frac{1}{2\pi f_1 C_{old}} = \frac{1}{2\pi f_2 C_{new}} \quad \textbf{Eq 1}$$

$$\frac{C_{new}}{C_{old}} = \frac{f_1}{f_2} \quad \textbf{Eq 2}$$

$$C_{new} = \frac{f_1}{f_2} C_{old} \quad \textbf{Eq 3}$$

Therefore, if the fc of a low-pass filter is required to be 10 times higher, then the capacitors must be made 10 times smaller in value. Due to these changes made in circuit

characteristics, the OpenEEG amplifier boards used for EMG measurement are referred to as “modified OpenEEG amplifier boards”. See Table 5 (APPENDIX C) for the list of changes made to the capacitors. See Figure C.5 and Figure C.6 (APPENDIX C) for the modified filter circuit and its simulation in Microcap respectively.

The SCI communication that the digital board carries out with the PC has limited speed capability when multiple signals are involved and when high sampling rates are required. Therefore a circuit similar to the digital board circuit (including the power supply circuitry and modified filter circuitry) was designed but with the ability to feed the amplified and filtered signals to modern universal serial bus (USB) DAQ hardware instead of to the SCI interface (this is called “circuit A” for further reference in this paragraph). The OpenEEG amplifier boards have a manual variable gain controller in the form of a potentiometer (adjustable resistor). It was required that the gain be digitally controlled so it can be standardised. It was decided to replace the existing potentiometers with digital potentiometers. An “AD5235” microchip (Analog Devices) was used as a digital potentiometer. The resistive range of the AD5235 matched the resistive range of the existing potentiometers. Thus each modified OpenEEG board was fitted with a daughter board consisting of the digital potentiometer chip which acted as a replacement for the existing analogue potentiometers; see Figure C.7 and Figure C.8 (APPENDIX C) for the circuit schematic and board layout of the daughter board respectively. A gain control circuit was designed to control the digital potentiometers (this is called “circuit B” for further reference in this paragraph). “Circuit B” was based around a microcontroller unit (MCU) which communicated with the digital potentiometers. A “PIC18F2520” (Microchip) was used as the MCU. The modified digital board circuit (“circuit A”) and gain controller circuit (“circuit B”) were integrated into 1 circuit that was made into a printed circuit board (PCB) i.e. the supplementary board that replaced the OpenEEG digital board; see Figure C.9 and Figure C.10 (APPENDIX C) for the circuit schematic and PCB layout of the EMG supplementary board respectively.

Serial peripheral interface (SPI) communication protocol was setup between the MCU and the digital potentiometers; see MCU code for digipot (APPENDIX D). The MCU was in turn controlled by the user via a PC using SCI with RS232 protocol via a graphical user interface (GUI) programmed in Matlab; see Figure 4.10 for a snapshot of the GUI as well as Matlab

code for digipot (APPENDIX D). The gains of all modified OpenEEG boards were standardised using the digipots, such that 15% MVC contraction would result in EMG signals which were of adequate quality and did not reach the amplifier board limits (or "rails"); see section 4.10 for exact gains.

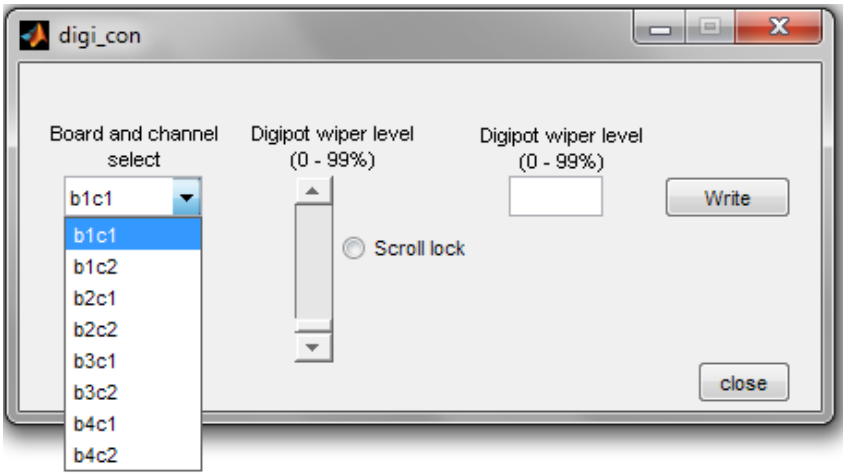

Figure 4.10 GUI to control digipot values. The GUI facilitates selection of the board and channel to be controlled and the selection of the digipot value in terms of % of the entire wiper range.

4.6 EEG detection apparatus

The present study aimed at measuring CMC of wrist flexors and extensors. This required simultaneously measuring EMG from the wrist muscles (covered in section 4.4) and EEG from the cortical areas related to the wrist; see EEG detection theory (section 2.2). Brodmann areas 3,1 and 2 represent the primary somatosensory cortex, area 4 represents the primary motor cortex and area 6 represents the premotor cortex (including the supplementary motor area); see section 2.1.4 and Brodmann areas (APPENDIX A). All of these cortical areas would be presumed to be involved in the CMC loop involved with wrist flexors and extensors (see Figure 3.5). The closest EEG 10-10 system locations for these sites are C3 and C4 for areas 1-5, and FC3 and FC4 for area 6. Further, according to the homunculus, the wrist area representation is closest to 10-10 locations C3 and C4. Based on this information, the electrode C3 was considered vital for detection of EEG related to right limb wrist flexion and extension.

The Laplacian transform is a mathematical technique that has been used in EEG studies to increase the spatial resolution or decrease the spatial blur of the EEG recordings at the scalp surface (Hjorth, 1975; Babiloni et al., 2001). The blurring is caused by the differences in the resistive properties of the cortex, skull and scalp. The Laplacian transform works by

estimating the orthogonal currents through the skull either entering ('sink') or exiting ('source') the scalp at each surface electrode site. The Laplacian transform also converts an EEG montage into a reference-free montage. It has been shown in previous studies (T. Mima and Hallett, 1999) that CMC derived from Laplacian transformed EEG and rectified EMG is enhanced. The Laplacian algorithm works better if the electrode of interest is surrounded by border electrodes.

Based on the wrist representation areas and the requirements for the Laplacian, a 16 channel monopolar EEG montage (with reference at Pz and DRL at FPz) following the international 10-10 spacing system was chosen for the present study; see Figure 4.11. Electrode C3 (electrode of interest) is surrounded by 4 neighbouring electrodes C1, C5, CP3 and FC3. Other electrodes are also included for further enhancement of the Laplacian algorithm. This includes mirror electrodes on the contralateral side (right hemisphere) to the side of interest (left hemisphere). An EEG Electro-cap (Electro-Cap International, Inc. or ECI) housing disc type tin electrodes (diameter = 12mm) was thus modified accordingly to match the chosen montage.

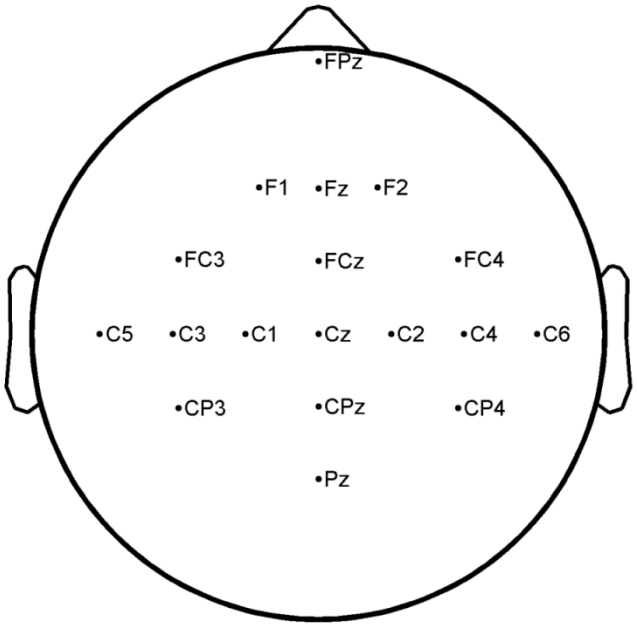

Figure 4.11 Chosen 16 channel EEG montage following international 10-10 system spacing for EEG detection of wrist control, with ground at Pz and DRL at FPz.

Figure 4.12 shows a picture of the 16 channel EEG electrode setup that was implemented for the present study along with two pairs of Electrooculogram (EOG) electrodes (horizontal and vertical) that were used to detect any ocular activity which might cause artefacts in the EEG.

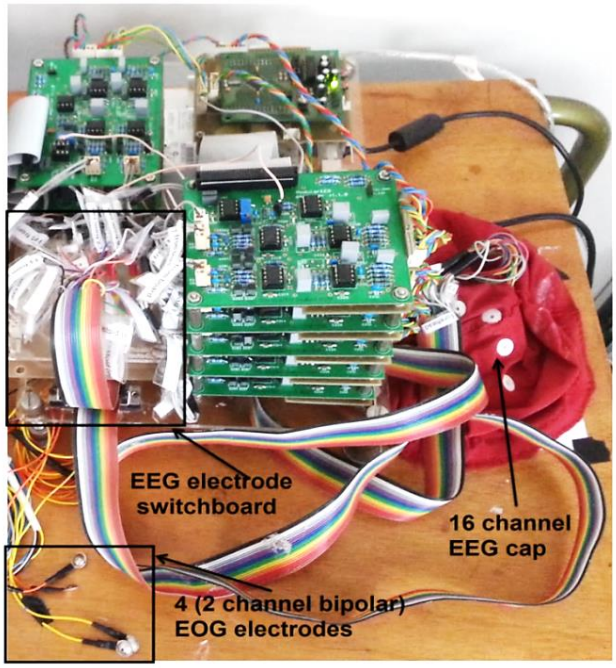

Figure 4.12 16 channel EEG electrode setup. Also can be seen are EOG electrodes for measuring horizontal and vertical EOG.

4.7 EEG amplification apparatus

Figure 4.13 shows a summary layout of the EEG amplification system.

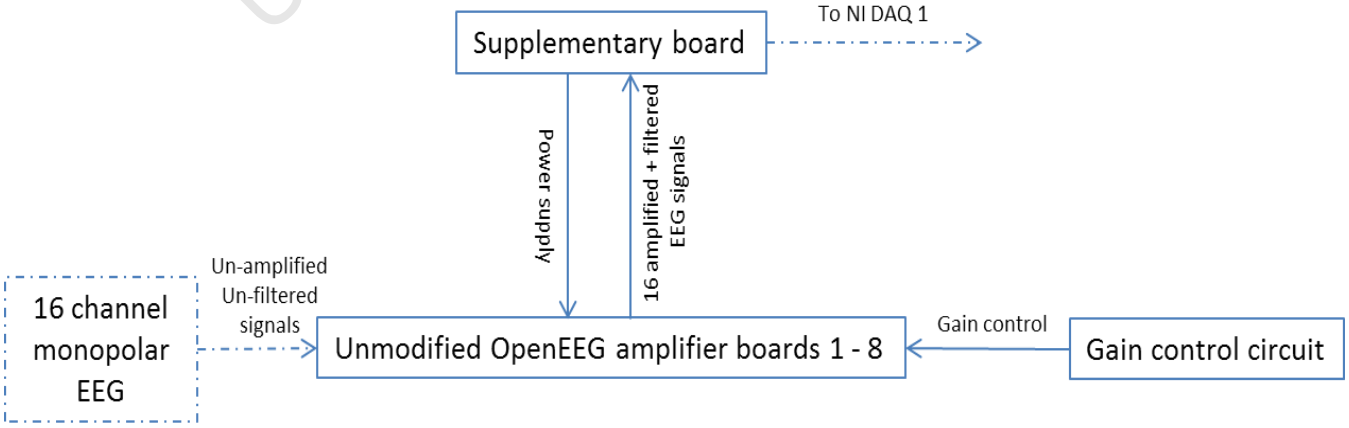

Figure 4.13 Summary of EEG amplification using OpenEEG amplifier boards.

Figure 4.14 shows the actual EEG amplification system used for the present study.

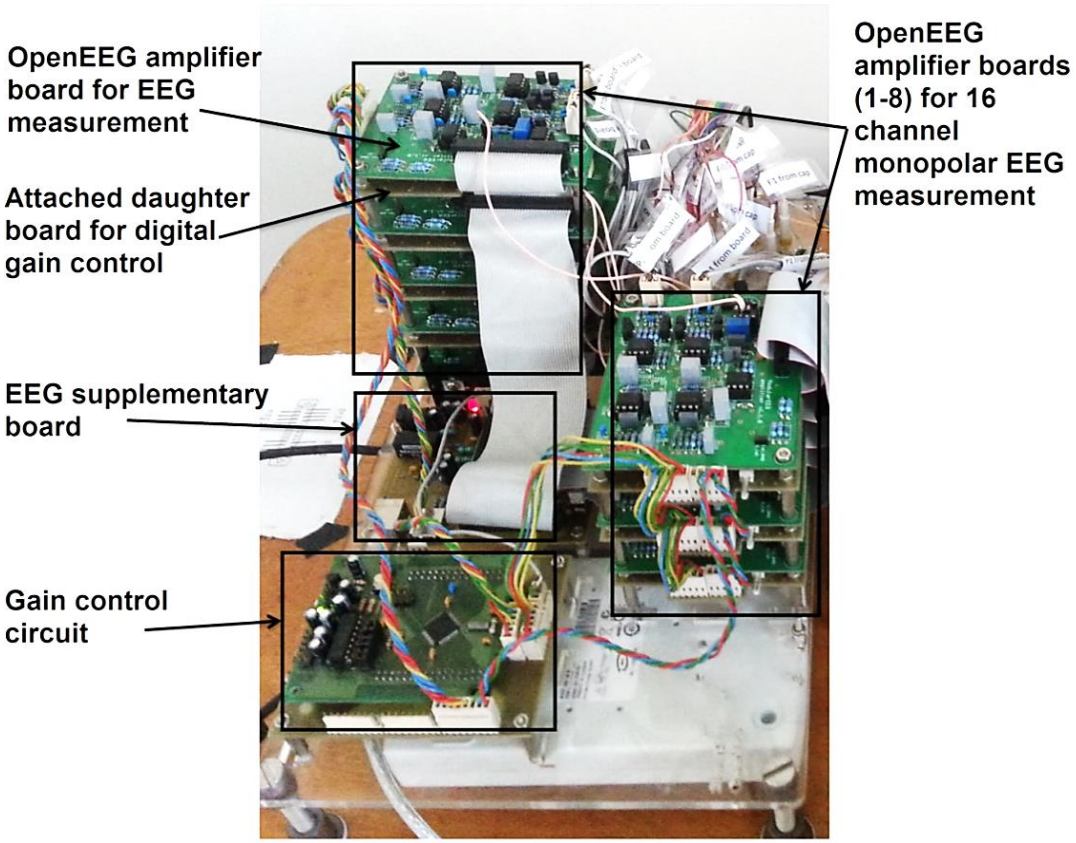

Figure 4.14 EEG amplification system consisting of 8 OpenEEG amplifier boards (16 channel monopolar EEG amplification) and the EEG supplementary board supplying power to the amplifier boards as well as receiving amplified signals from them. Also visible is the gain control circuit that controls the attached daughter boards (containing the digital potentiometers) that control the gain of the amplifier boards.

For the purposes of EEG amplification, 8 unmodified OpenEEG amplifier boards were used (see section 4.5 for information on OpenEEG amplifier boards, complimentary digital board and digital gain control). A similar supplementary board as the EMG system was designed for the purposes of power supply to the OpenEEG amplifier boards and output to the USB DAQ hardware i.e. a substitute for the OpenEEG digital board; see Figure C.11 and Figure C.12 (APPENDIX C) for schematic and PCB layout of the EEG supplementary board respectively. The gain controller circuit was built separately to the supplementary board and made use of a Freescale MCU (GT16). Note, as monopolar EEG was being recorded, all the negative (-) pins of the amplifier boards were tied to ground i.e. Pz electrode.

4.8 Data acquisition and recording apparatus

The National Instruments (i.e. NI) "NI6210" was decided upon as the DAQ hardware of choice. This device allows up to 16 analogue inputs. It has a very fast sampling rate (total of 250 KS/s). Also it has a very high resolution of 16 bits. Figure 4.15 shows a summary of the data acquisition process.

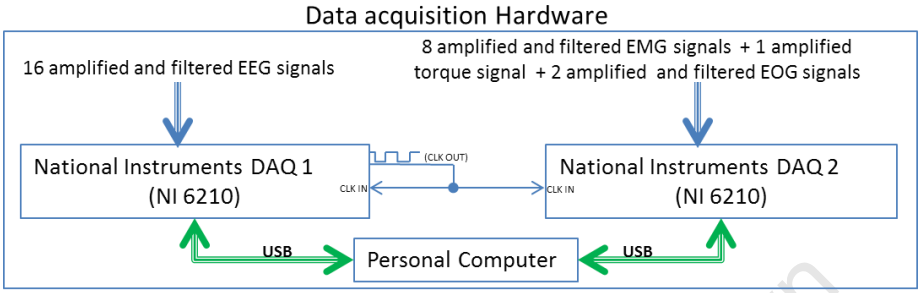

Figure 4.15 Summary of data acquisition hardware and synchronisation

Figure 4.16 shows the data acquisition using National Instruments data acquisition devices (NI DAQ 1 and NI DAQ 2).

Figure 4.16 Data acquisition using National Instruments data acquisition devices (NI DAQ 1 and NI DAQ 2).

NI DAQ1 (EEG signals) and NI DAQ2 (EMG, torque and EOG signals) had to be synchronised. This was firstly achieved in hardware and additionally in software. In hardware, one of the two DAQs, NI DAQ1, was made to produce a clock signal. This clock signal was fed to itself and also to NI DAQ2 through a physical wire. Both NI DAQs were setup to sample based on this common external clock signal instead of their independent internally generated clock signals. Next, to ensure that the two NI DAQs start acquisition on the same clock pulse, NI DAQ1 was made to produce a digital trigger which was fed to itself and also to NI DAQ2 through a physical wire; data acquisition on both DAQs was set to start on reception of the digital trigger. The clock and digital trigger lines are visible in Figure 4.16. In software, in order to additionally ensure that both DAQs start on the same clock pulse, both DAQs were included in the same 'sequential loop'.

4.9 Testing and calibrating of the torque system

See calibration of torque system (APPENDIX B) for tables and graphs of the calibration data for flexion and extension and a description of the process which is summarised below. For the estimation of MVC in terms of torque (Nm)[2], the torque system was calibrated by applying forces in both flexion and extension directions using a spring load at the average point of force application by the subjects (average distance between wrist pivot point and contact region); see Figure 4.17.

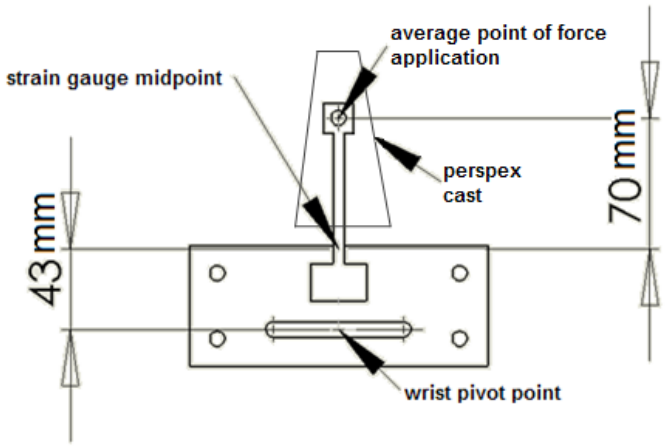

Figure 4.17 Calibration of strain gauge signals for estimation of MVC torque about wrist joint.

The torque system readings in volts acquired from NI DAQ 2 (Volts) were plotted against the respective forces applied using the spring load (Newtons) for both the extension and flexion directions. The slopes (gradients) of the lines of best fit of the Voltage vs Force plots were found. The slopes for extension and flexion i.e. VF_{ext} and VF_{flx} represented the torque system's voltage output per unit of force applied (V/N) at the average point of force application in the respective direction. VF_{ext} and VF_{flx} divided by the distance between the average point of force application and the wrist pivot point (0.113 m) gave the voltage per unit of torque at the wrist joint (V/Nm) for extension (VT_{ext}) and flexion (VT_{flx}). The calibration ratios VT_{ext} and VT_{flx} were found to be 0.499 V/Nm and 0.510 V/Nm respectively. For increasing the estimation accuracy of MVC, the distance of the subject's actual point of force application (contact region) w.r.t. the wrist was measured (D_{sub}), and the $VF_{flx/ext}$ adapted such that the subject's $VF_{ext/flx}$ i.e. $VF_{ext/flx,sub} = VF_{ext/flx} \times (D_{sub} - 0.113 + 0.07) / (0.07)$. Then $VT_{ext/flx,sub} = VF_{ext/flx,sub}/D_{sub}$.

[2] Note that calibration values were not used for the remaining behavioural variables i.e. PRECISION, Torque-low-PSD and Torqueβ-PSD, as these were based on normalised i.e. % MVC measures of Torque, i.e. voltage due to torque produced by the subject during the experiment scaled by voltage produced during MVC testing.

4.10 Testing and calibrating of the EEG and EMG systems

Figure 4.18 illustrates the steps taken in calibrating the EEG and EMG systems.

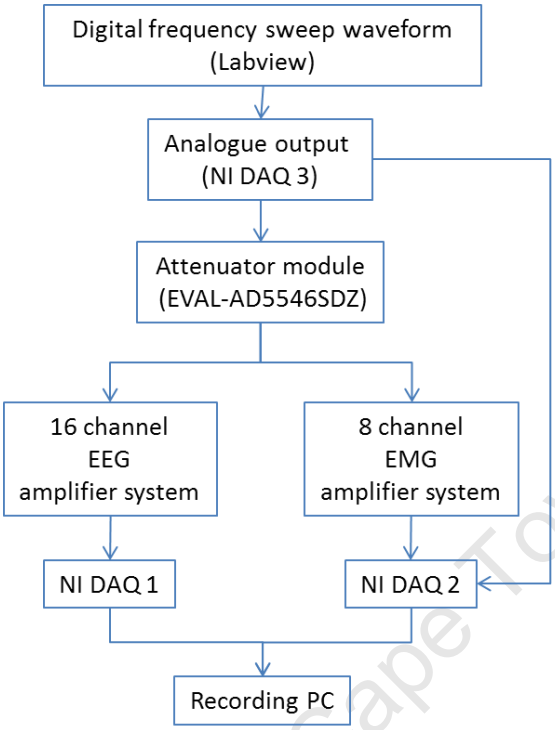

Figure 4.18 Block diagram of EEG-EMG system calibration.

A sinusoidal waveform of fixed amplitude but increasing frequency (frequency sweep) was first created in Labview. This was achieved using a function builder VI. The amplitude was set to 1V peak-to-peak and the frequency was swept through from 0.01 to 2000 Hz. This waveform was then output through the 'analogue out' port of an additional NI DAQ device (NI DAQ3). From the 'analogue out' port, the waveform was simultaneously sent to: 1) an 'analogue in' port of NI DAQ 2 and 2) the 'ref' pin of an attenuator module. The waveform at 1) was recorded in Labview on the recording PC.

The attenuator module is a pre-built evaluation board (EVAL-AD5546SDZ). The evaluation board is built around the AD5546 chip at its core. The AD5546 is a low power, high precision (16-bit) digital to analogue converter (DAC) chip. Thus the DAC chip can be used to attenuate a reference signal anywhere in the range of 0 to 1 times the reference signal with a resolution of (reference signal (V))/2^16. In this case the frequency sweep waveform at the 'ref' pin of the attenuator module was attenuated down from the original 1V peak-to-peak to 500uV peak-to-peak.

The attenuated analogue frequency sweep signal was then fanned out simultaneously to all EEG and EMG channels and was recorded after its amplification and filtering (unmodified and modified open EEG amplifier boards and corresponding supplementary boards) and digitisation (NI DAQ1 and NI DAQ2) by the recording PC. This recording was done simultaneously with the recording of the original frequency sweep waveform from NI DAQ 3. It was necessary that the original frequency sweep waveform was attenuated before feeding the amplifier boards such that it was similar to bio-potentials i.e. 500 uV peak-to-peak. Feeding in a signal of small amplitude was also important so that the amplified voltage would not be "railed" due to the high gains of the amplifier boards. The high precision of the DAC module allowed for accurate attenuation of the signal.

The amplified, filtered and digitized waveform signals (from the EEG and EMG systems) were then compared to the original waveform to work out the transfer function (gain and phase shift) of each EEG and EMG channel. This was achieved in Matlab using a function called "tfestimate" which accepts an input and output signal and estimates the system transfer function i.e. the gain and phase profiles of the system w.r.t. frequency. Note that the transfer function of the attenuator itself was worked out additionally prior to working out the transfer function of the EEG and EMG channels; see Figure 4.19. The transfer functions of the EEG and EMG channels were adjusted accordingly based on the transfer function of the attenuator module (mainly involved dividing the gains by the attenuator gain which was 0.0005).

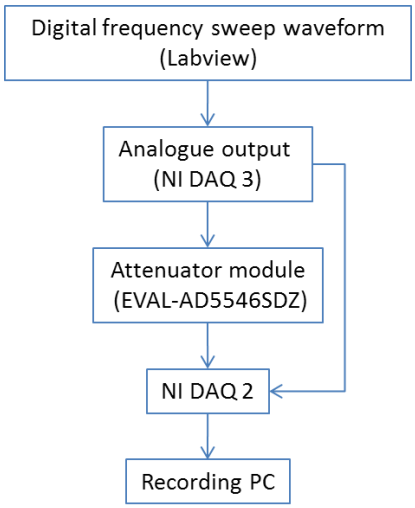

Figure 4.19 Block diagram of attenuator module calibration

Figure C.13 and Figure C.14 (APPENDIX C) show the EEG channels' gain and phase response plots (w.r.t. frequency) respectively after calibration. Figure C.15 and Figure C.16 (APPENDIX C) show the EMG channels' gain and phase response plots (w.r.t. frequency) respectively after calibration. Figure C.13 shows that the passband gain of the EEG channels was ~ 5000[3], the low -3 dB roll off (low fc) was at ~ 0.5 Hz[3] and the high -3 dB roll off (high fc) was at ~100 Hz[3]. Figure C.15 shows that the passband gain of the EMG channels was ~ 1800[3], the low -3 dB roll off (low fc) was at ~ 5 Hz[3] and the high -3 dB roll off (high fc) was at ~500 Hz[3]. The minor differences in the frequency response plots of the EEG channels can be due to component tolerances especially of the capacitors and resistors; similarly for the minor differences in the EMG channels' frequency response plots.

In general all the gains and roll-offs of both the EEG and EMG channels were adequate for the objectives of the present study. Note, the CMC variables, as well as normalised EEG and EMG powers measured in the present study are invariable to the absolute gains and phase shifts of the channels: - coherence (magnitude) is invariable to the absolute amplitude and phase difference between two signals but is rather dependent on the consistency of the ratio of their amplitudes and degree of their phase lock across a time series (Shaw, 1981; Guevara and Corsi-Cabrera, 1996); and normalising the EEG and EMG powers makes them invariable to the absolute amplitudes of the signals. Nevertheless, the exact phase vs frequency values of the EEG and EMG channels (Figure C.14 and Figure C.16) were considered a useful record for future work related to absolute phase (for example studying the delay between cortical and muscular activities) and directed coherence.

[3] Corrected from published value (Divekar et al., 2013).

5 EXPERIMENTAL METHODOLOGY

Section 5 describes the experiments carried out to test the objectives of the present study (listed in section 1). Particularly, details are given on the subjects tested on (section 5.1), experimental paradigm (section 5.2), data recording (section 5.3), data analysis (section 5.4) and statistical analysis (section 5.5).

5.1 Subjects

Fifteen healthy male right-handed subjects (23.5 ± 2.7 years of age), without any history of neurological disease participated in the study. The handedness was verified according to the Oldfield questionnaire (Oldfield, 1971). Subject participation followed approval by the university human ethics committee with written informed consent according to the declaration of Helsinki (World Medical Association, 2008).

5.2 Experimental paradigm

Figure 5.1 is a picture of a subject performing a typical isometric wrist flexion/extension task using visual feedback.

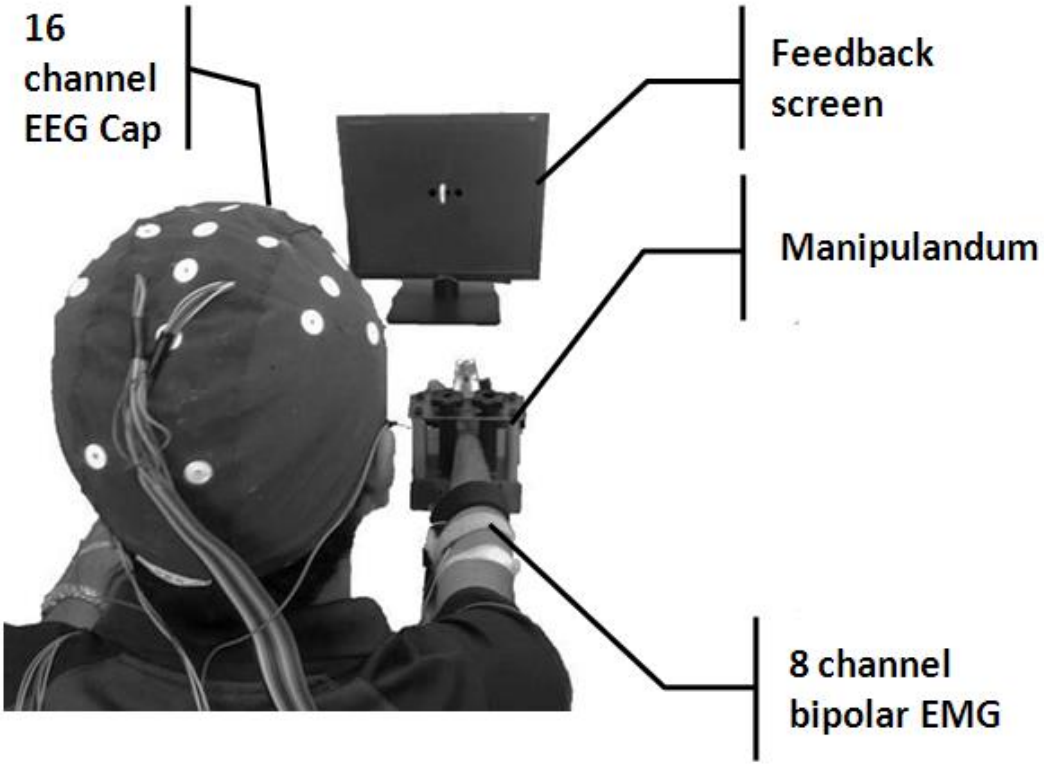

Figure 5.1 Subject performing isometric contraction task with visual feedback of % MVC torque levels. Adapted from candidate's publication (Divekar and John, 2013).

The Subjects were seated in a dimly lit room. The right forearm was rested on the wooden support and the right hand was inserted through the perspex splint of the testing manipulandum to prevent movement of the fingers relative to the hand; see section 4.1 for details on the testing manipulandum. The vertical bars of the testing manipulandum were used to secure the wrist between them. The wrist angle was thus maintained at 180°. The forearm was then strapped down to prevent any movement relative to the wrist. The forearm was positioned mid-way between pronation and supination to equalise the effect of gravity during extension and flexion. The Subjects were then prompted to either produce an isometric wrist extension (task 1) or flexion (task 2) against the perspex splint at a target torque (TT) of 15% MVC for 45 s. The region about the metacarpophalangeal joints was used by the subjects to impart force on the perspex cast during the isometric contractions; see Figure 4.4 (section 4.1.1). Visual feedback was provided of the actual torque (AT) as % MVC by a moving white needle indicator. The white needle indicator was to be kept coincident to a fixed black reference marker representing the TT; see Figure 5.1. To enforce high precision, additional boundary markers were placed at $15 \pm 1\%$ MVC creating an allowable window, which was not to be crossed ; see Figure 5.1. Indicator sensitivity was set such that an application of 1% MVC torque would result in a displacement of 10 mm in the corresponding direction (right or left, extension or flexion). The visual feedback described above was provided on a liquid crystal display (LCD) monitor placed at eye level, 1.5 m in front of the subject. Subjects were instructed to avoid any other movements and to fix their gaze on the visual feedback indicator avoiding blinking during the tasks.

Each task was repeated 10 times. Thus, a total of 20 data points (2 tasks x 10 repetitions at 45s each) were recorded for each subject; see data recording (section 5.3). A 30s break was allowed between repetitions to avoid fatigue. The sequence of the tasks was counter-balanced such that successive repetitions switched between the 2 tasks.

At the end of the experiment, subjects were asked to rate the perceived difficulty of the high precision flexion and extension tasks, using a scale of 1 to 5, where 1 = very easy, 2 = easy; 3 = moderate; 4 = difficult; 5 = very difficult. The subjects were instructed to base their judgement on the perceived difficulty associated with keeping the white indicator inside the allowable window.

Notes

1. The MVC for each subject for each task (extension, flexion) was measured prior to the experiments. Figure 5.2 shows the flow diagram of the Labview code used to carry out a single MVC measurement; see Figure E.1 and Figure E.2 (APPENDIX E) for the actual Labview code and front panel respectively. The maximum value from three such trials for each task was taken as the final MVC value.

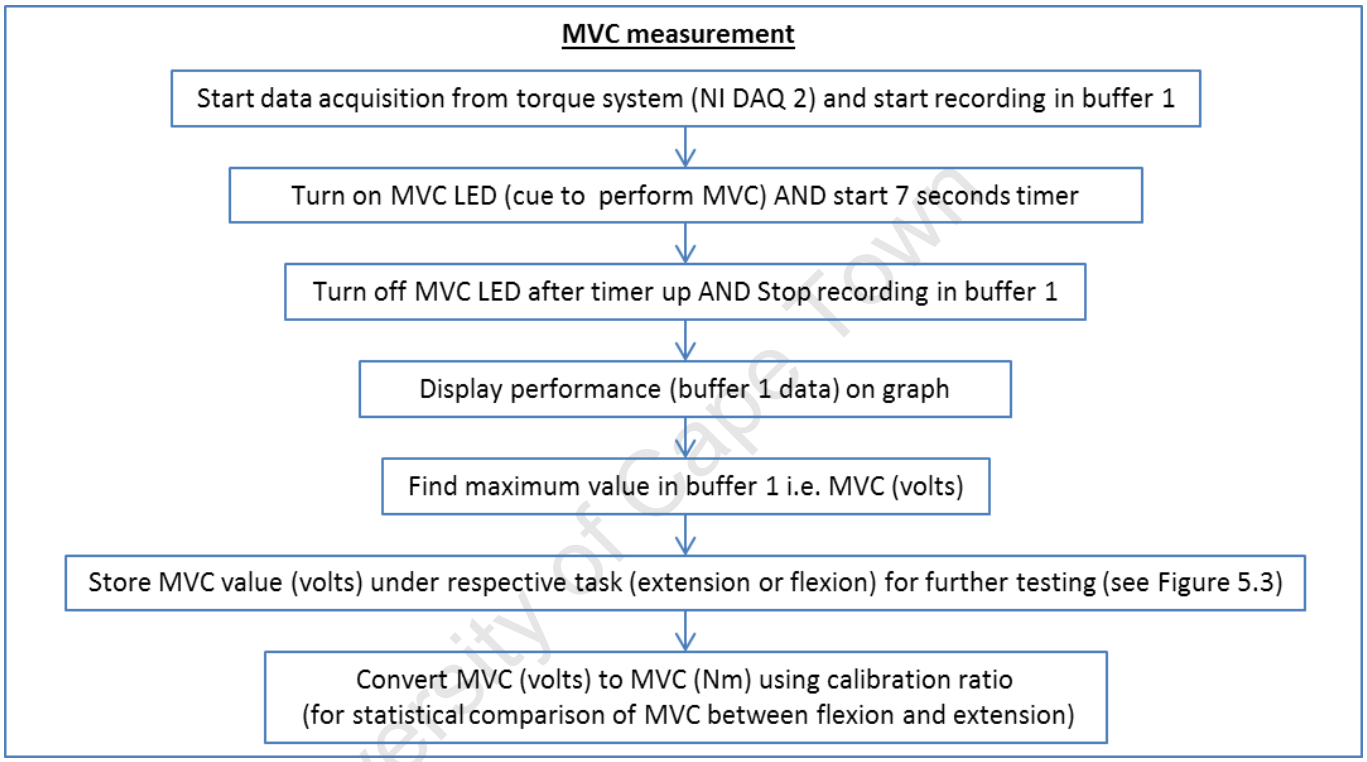

Figure 5.2 Flow diagram of MVC measurement in Labview.

2. Witte et al (2007) reported that beta range corticomuscular coupling is enhanced during isometric contraction at 16% MVC compared to a weaker 4% MVC. Accordingly, the target torque for the present study was chosen to be 15% MVC in an effort to enhance corticomuscular coupling for extension and flexion tasks and to increase the chances of finding any differences between these two tasks.

5.3 Data recording

During the tasks (task1, task2) described in the experimental paradigm section (section 5.2); EEG, EOG, EMG and Torque data were recorded using the experimental apparatus described in section 4 (see "summary" below) and also using Labview software (see Figure 5.3).

Summary:

1. EEG was detected using the 16 channel Electro-cap (Electro-Cap International, Inc. or ECI) with disc type tin electrodes (diameter = 12mm). Electrode spacing followed the international 10-10 system. The reference electrode was at Pz and the active ground electrode (DRL) was at FPz; see Figure 4.11 (section 4.6) for the 16-channel EEG 10-10 system montage that was used. The scalp was cleaned, slightly abraded, and ECI Electro-Gel was injected into the electrode holders to improve scalp-electrode conductivity such that all electrode impedances were under 3kΩ. Cup type silver electrodes (Nihon Kohden, Japan, diameter = 10mm) were placed to record both horizontal and vertical EOG, and injected with Elefix electrode paste (Nihon Kohden, Japan) to improve skin-electrode conductivity. The EEG and EOG signals were amplified with gains set to ~5000 and CMRR > 115 dB. The EEG and EOG signals were band-pass filtered in the range of 0.5 - 100 Hz using a "Besselworth" filter (blend between Butterworth and Bessel) with a roll-off of 19.2 dB/Octave.
2. Bipolar EMG was detected from the four wrist extensor muscles: - ECRL, ECRB, ED and ECU; and the four wrist flexor muscles: - FCR, PL, FDS and FCU; with cup type silver electrodes (Nihon Kohden, Japan, diameter = 10mm). The bipolar electrode pairs were positioned central to the respective muscle bellies following the appropriate identification of each muscle belly. The electrode pairs were aligned parallel to the respective muscle bellies with the two electrodes from each electrode pair separated by an inter electrode distance (IED) of 20 mm. The electrodes were injected with Elefix paste (Nihon Kohden, Japan) to improve skin-electrode conductivity, following appropriate skin preparation such that all electrode impedances were below 5kΩ. The electrodes were securely strapped to avoid movement. The EMG signals were amplified with gains set to ~1800 and CMRR > 115 dB. The EMG signals were band-pass filtered in the range of 5 - 500 Hz using a

"Besselworth" filter (blend between Butterworth and Bessel) with a roll-off of 19.2 dB/Octave.

3. Torque data was detected using strain gauges (mild steel foil, 5 mm, gain factor 2, 120 Ω) and amplified with a commercial strain gauge amplifier (G = 2701, CMMR > 120 dB).
4. All data was digitized at 1000 Hz and the resolution was 16 bits i.e. 60 nV for EEG and EOG, 170 nV for EMG and 610 µNm for Torque.

The summary of the steps undertaken in Labview software to acquire and record data are shown in Figure 5.3; see Figure E.3 and Figure E.4 (APPENDIX E) for actual Labview Code and examiners front panel respectively. All Data was stored then analysed offline (data analysis is described in the following section (section 5.4)).

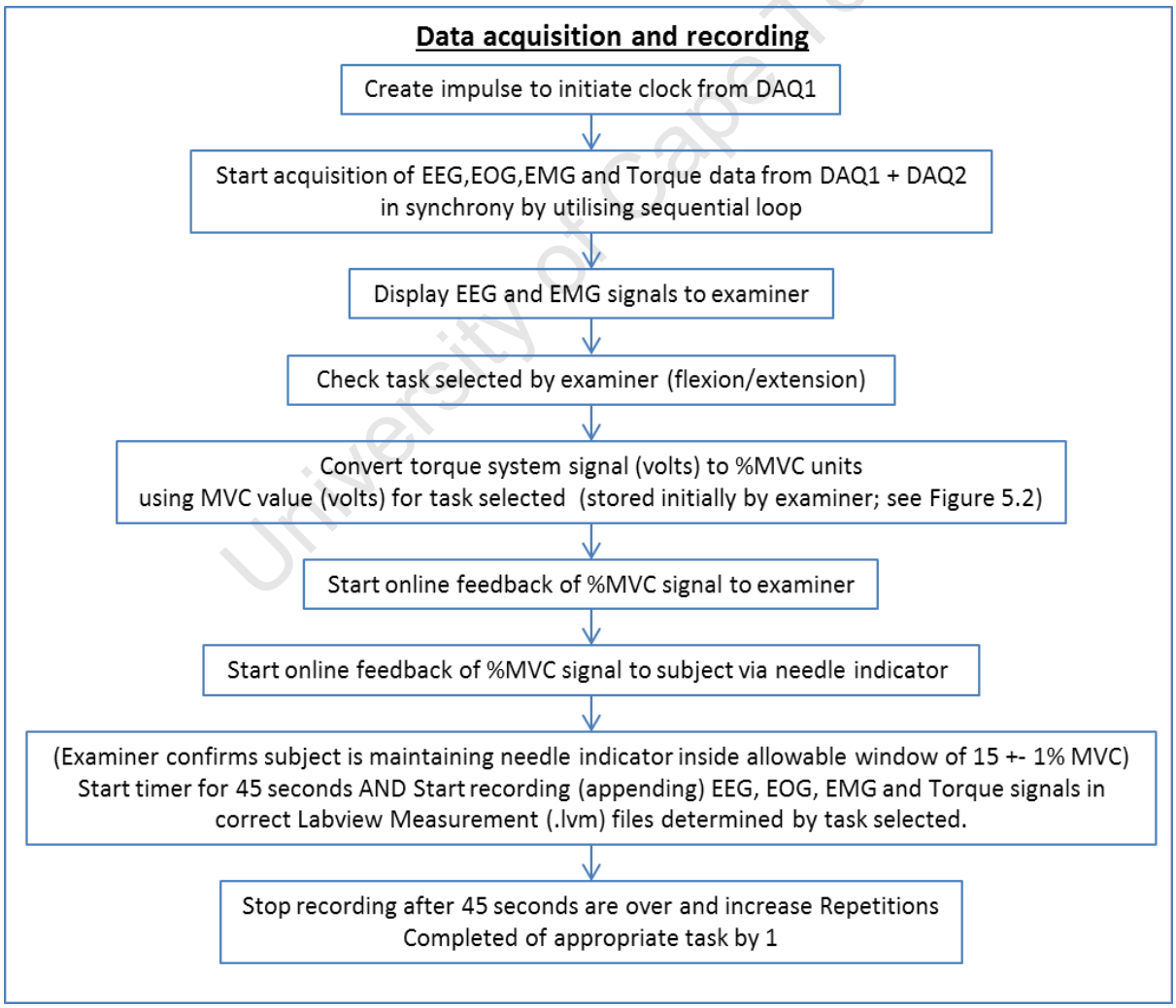

Figure 5.3 Flow diagram of data acquisition, recording and storage in Labview.

5.4 Data Analysis

Only data related to the constant hold phase was recorded and analysed, i.e. excluding the data related to the subject going from rest to 15% MVC. Further, EMG data related to only the agonist muscles for each task was analysed, i.e. EMG of the 4 wrist extensors for wrist extension (task1) and EMG of the 4 wrist flexors for wrist flexion (task2). The EMG signals were full wave rectified to enhance the temporal pattern of the grouped firing of motor units (Halliday, 1995; Halliday and Farmer, 2010). EEG voltage signals were derived as current source density (CSD) estimates using the spherical splines algorithm developed by Perrin et al. (1989) and implemented in MATLAB (Kayser and Tenke., 2006 a,b; Kayser, 2011). Continuous EEG and rectified EMG data from each 45s repetition was divided into 42 artefact-free segments of 1024 ms with no overlap (using a hamming window), allowing for a frequency resolution of 0.98 Hz.

The magnitude squared coherence Coh_{xy} between an EEG channel (x) and rectified EMG channel (y) with respect to frequency (f) was calculated using Welch's averaged periodogram method as follows:

$$\frac{|P \quad)|}{} \qquad \textbf{Eq 4}$$

Where $Coh_{xy}(f)$ is a number between 0 and 1 that indicates how well x corresponds to y at each frequency; $P_{xx}(f)$ and $P_{yy}(f)$ are the auto power spectral density (PSD) functions of the EEG and rectified EMG signal respectively, averaged over all (42) segments for a given frequency (f); and $P_{xy}(f)$ is the cross PSD function between the EEG and rectified EMG signal, averaged over all (42) segments. This was achieved in MATLAB using a function called "mscohere" (Park et al., 2009; Laine et al., 2012). Coherence was considered to be significant if $Coh_{xy}(f)$ was above the confidence level (CL) (Rosenberg et al., 1989):

$$\frac{}{} \qquad \textbf{Eq 5}$$

where N is the number of segments i.e. 42 and 'α' is the desired level of confidence. Coherence was considered to be significant over the upper 95% confidence limit. In the case of the present study, the CL is 0.07. Note that the stability of the coherence spectrum based on this CL was post-hoc verified by the non-significant variation of CMC_{MAX} (defined next) with repetition.

For each muscle (EMG channel), only the highest $Coh_{xy}(f)$ value i.e. $CMC_{MAX,}$ from the 16 EEG-EMG coherence spectra (as there are 16 EEG channels) was used for subsequent analyses; this process is similar to the method used by Witte et al (2007) and Johnson et al (2011). At CMC_{MAX}, the corresponding EEG channel was always one of the 5 contra-lateral motor region electrodes: FC3, C1, C3, C5, CP3; and the peak frequency (FP) was in the beta (15–35 Hz) band. In addition, when CMC_{MAX} was greater than the CL, the frequencies where the coherence curve first met the CL when traced backward from FP (F1), and where the coherence curve first met the CL when traced forward from FP (F2) were found, facilitating an estimate of the frequency width (FW) of significant coherence:

$$\mathrm{FW} = \mathrm{F2} - \mathrm{F1} \qquad \textbf{Eq 6}$$

The significant Coherence area (CMC_{AREA}) was also calculated according to:

$$\mathrm{CMC_{AREA}} = \int_{\mathrm{F1}}^{\mathrm{F2}} Coh_{XY}(\mathrm{f})\mathrm{df} \qquad \textbf{Eq 7}$$

In a recent study (Ushiyama, Suzuki, et al., 2011), a direct relationship between beta CMC and normalised EEG and EMG beta powers was reported. To investigate the same in the present study, the ratio of the integral of the auto PSD function within the beta band (15-35 Hz) to that of the entire frequency range (3-500 Hz) for both EEG (EEGβ-PSD) and EMG (EMGβ-PSD) was calculated. The PSD functions of the EEG and EMG signals were calculated using a function in MATLAB called “pwelch”, which uses Welch’s estimation method. Then:

$$\mathrm{EEG\beta{-}PSD} = \frac{\int_{15}^{35} \mathrm{P_{xx}(f)df}}{\int_{3}^{500} \mathrm{P_{xx}(f)df}} \qquad \textbf{Eq 8}$$

$$\mathrm{EMG\beta{-}PSD} = \frac{\int_{15}^{35} \mathrm{P_{yy}(f)df}}{\int_{3}^{500} \mathrm{P_{yy}(f)df}} \qquad \textbf{Eq 9}$$

In the same manner, the normalised EEG alpha band power (EEGα-PSD) was calculated to examine the mu rhythm and possibly subject attention levels. Then:

$$\mathrm{EEG\alpha{-}PSD} = \frac{\int_{8}^{12} P_{xx}(f)df}{\int_{3}^{500} P_{xx}(f)df} \qquad \textbf{Eq 10}$$

Note, EEGβ-PSD and EEGα-PSD were calculated w.r.t. each muscle at the EEG electrode with CMC_{MAX}.

Normalisation is necessary to account for the inter-subject variation in EEG and EMG oscillatory activity levels as well as to account for variations in electrode-skin impedances which may differ across subjects as well as across trials. Normalisation also compensates for any constant gain differences of the amplifier boards.

The Mean Squared Error (MSE) of motor output was calculated as follows:

$$\mathrm{MSE} = \sum_{i=1}^{N} \frac{(\mathrm{TT} - \mathrm{AT}_i)^2}{N} \qquad \textbf{Eq 11}$$

Where i is the sample point; N is the number of sample points in a repetition (42 x 1024); TT is the target torque (as target % MVC level i.e. 15 %) and AT_i is the actual torque (as actual % MVC level) at the i^{th} sample. Precision for each repetition was then calculated as the inverse of MSE:

$$\mathrm{PRECISION} = \frac{1}{\mathrm{MSE}} \qquad \textbf{Eq 12}$$

The major frequency component of torque fluctuation that contributes to differences in precision is the low frequency band (0.1-5Hz). These changes were examined by taking the integral of the auto PSD function of the actual torque signal (as % MVC) between 0.1-5Hz (Torque-low-PSD) (Ushiyama, Katsu, et al., 2011). Since significant EEG-EMG coherence (CMC) was observed in the beta band, the changes in the same frequency band of the actual torque signal (as % MVC) were also examined by determining the integral of the auto-PSD function of the actual torque signal between 15-35Hz (Torqueβ-PSD) (Ushiyama, Katsu, et al., 2011). The torque PSD functions were calculated using "pwelch" in MATLAB. Then:

$$\mathrm{Torque{-}low{-}PSD} = \int_{0.1}^{5} \mathrm{P_{AT}(f)df} \qquad \textbf{Eq 13}$$

$$\mathrm{Torque\beta{-}PSD} = \int_{15}^{35} \mathrm{P_{AT}(f)df} \qquad \textbf{Eq 14}$$

Where P_{AT} is the auto PSD function of the actual torque (AT) measured as % MVC.

Overall, a total of 1200 (15 subjects×10 repetitions× 8 Muscles) observations of CMC_{MAX}, FP, FW, $CMC_{AREA,}$ EEGβ-PSD, EEGα-PSD, EMGβ-PSD, 300 (15 subjects × 10 repetitions × 2 Tasks) observations of PRECISION, Torque-low-PSD, Torqueβ-PSD and 30 (15 subjects × 2 Tasks) observations of MVC and perceived difficulty ratings were thus gathered for statistical analysis.

5.5 Statistical Analysis

The following statistical methodology was formulated after extensive consultation with the University's statistician and is essentially aimed at comparing the acquired observed variables between wrist extension (task 1) and wrist flexion (task 2) tasks.

A repeated measures multilevel mixed effects linear regression analysis was carried out to test the effect of 'Muscle' ('Task' being explicit in the muscle tested) on observed variables: - CMC_{MAX}, FP, FW, $CMC_{AREA,}$ EEGβ-PSD, EEGα-PSD, EMGβ-PSD; and the effect of 'Task' on observed variables: - PRECISION, Torque-low-PSD, Torqueβ-PSD.

To test the effect of 'Muscle' ('Task' being explicit in the muscle tested), Muscle, Repetition and the Muscle*Repetition interaction were set as fixed effects (independent variables – IVs). As there are eight muscles, eight separate regression analyses were thus carried out, where each time a different muscle was used as the reference. To account for the correlation structure inherent in the data due to multiple testing on subject (muscle 1-8) and within muscle (repetitions 1-10), 'subject' and 'muscle within subject' were set as additional specific random effects to improve the model fit.

Similarly to test the effect of 'Task', Task, Repetition and the Task*Repetition interaction were set as fixed effects (independent variables – IVs). The task of extension was set as the reference. To account for the correlation structure inherent in the data due to multiple testing on subject (task 1-2) and within task (repetitions 1-10), 'subject' and 'task within subject' were set as additional specific random effects to improve the model fit.

After the initial model setup (all fixed effects initially included in model), any non-significant fixed effect variable was removed one at a time and the model was rechecked for improvement in goodness of fit (Aikaikes Information Criterion, Bayesian IC, Likelihood ratio test). This procedure was repeated until all the remaining factors were significant or the goodness of fit became worse after removal of a factor, in which case it was restored. Examination of the residuals for the final model indicated that the underlying assumptions of the model were not violated. Note, CMC_{MAX} data was normalised by applying the arc hyperbolic tangent transformation (Rosenberg et al., 1989) prior to statistical analysis; and for other observed variables that deviated from a normal distribution, a natural log (Ln) transform was applied and the residual diagnostics carefully examined to ensure validity of

the model. Linear regression was the preferred method over the simpler and more common ANOVA, due to data not being entirely normally distributed, even after transformation, and also due to its superiority over ANOVA in a repeated measures within subject design (Gueorguieva and Krystal, 2004).

A paired samples t-test was conducted to compare normal (Shapiro-Wilk, 0.210) MVC data in wrist flexion and extension task conditions within-subjects.

A Wilcoxon matched-pairs signed rank test was conducted to compare perceived difficulty ratings in wrist flexion and extension task conditions within-subjects.

6 RESULTS

Section 6 presents the results of the experiments that were carried out to test the objectives of the present study. Section 6.1 presents the qualitative results and section 6.2 presents the quantitative results.

6.1 Qualitative Results

Figure 6.1 illustrates typical examples of raw EEG, raw EMG and Torque waveforms, their PSDs and finally EEG-EMG coherence (CMC), in wrist flexion and extension tasks.

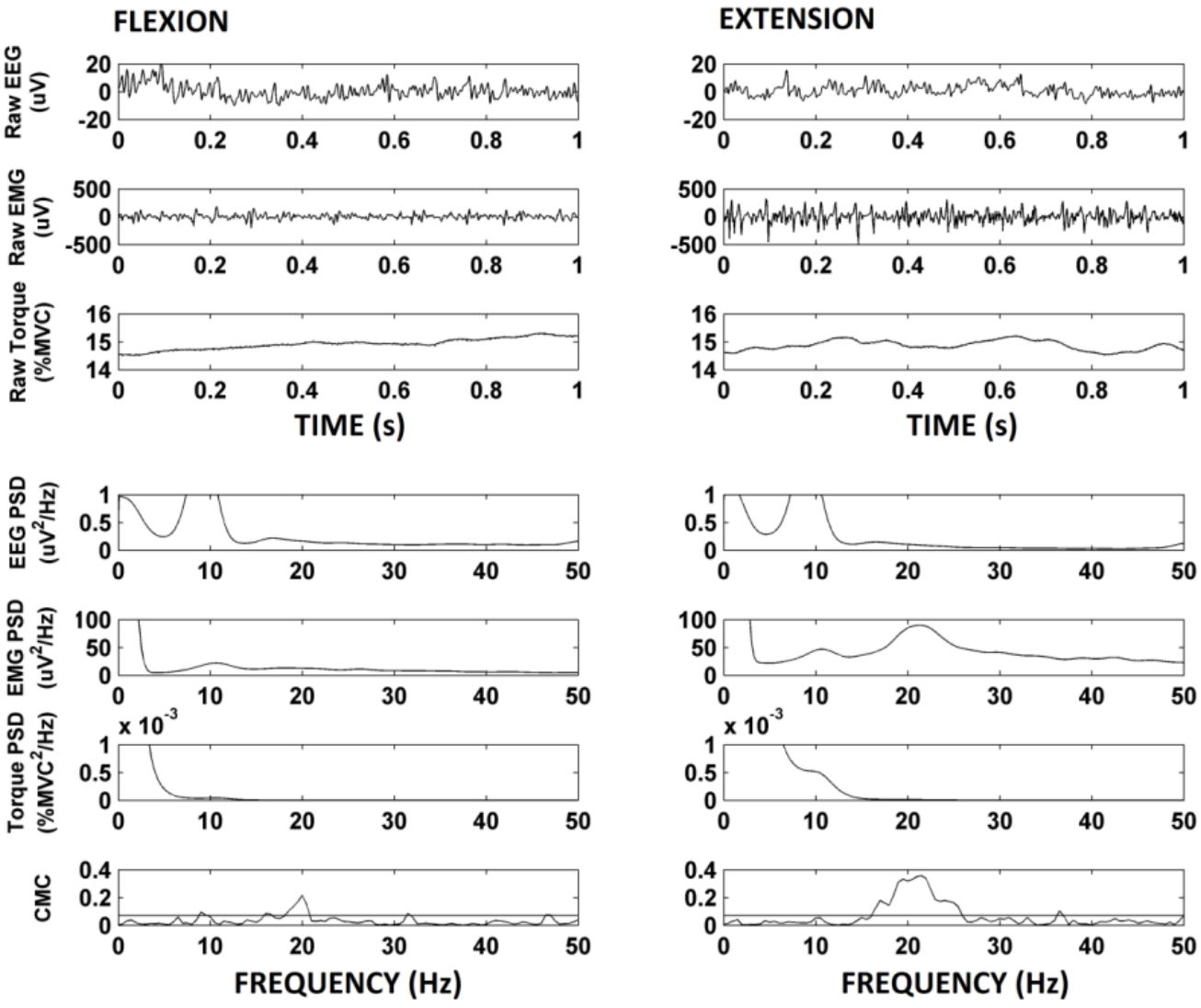

Figure 6.1 Wrist flexion and extension comparisons between typical raw EEG, EMG and torque signals, their power spectral density functions and EEG-EMG coherence (CMC) spectra, during sustained isometric contraction at 15% of MVC. In the coherence spectra, the estimated confidence limit (CL) is shown by the horizontal dashed lines at 0.07. Adapted from candidate's publication (Divekar and John, 2013).

From the raw EEG waveforms and also the EEG PSD waveforms, there do not seem to be any apparent differences in the amplitudes of EEG fluctuation between flexion and extension tasks, at any particular frequency band. It may be observed that the EEG PSD for both flexion and extension tasks was predominated by alpha oscillatory activity.

From the raw EMG waveforms and also the rectified EMG PSD waveforms, it can be observed that the amplitude of EMG fluctuation was greater in extension compared to flexion. This difference is especially apparent in the beta band, where a distinct peak in the rectified EMG PSD for extension can be seen, whereas such a peak is not clear in the flexion rectified EMG PSD.

From the raw Torque waveforms and also the Torque PSD waveforms, it can be observed that the amplitude of torque fluctuation was greater in extension compared to flexion. This difference is especially apparent in the lower frequency (<5Hz) band, as well as the beta band.

Finally, a clearly higher peak can be seen in the CMC spectrum for extension as compared to the peak in flexion. For both tasks (flexion and extension), the peaks in the CMC spectra can be seen to be constrained to the beta band. It may also be observed that for extension, the specific frequency at which the peak in the CMC spectrum occurs seems to match the frequency at which the peak in the corresponding rectified EMG PSD occurred.

Figure 6.2 illustrates typical single repetition topographical plots of peak CMC values across all EEG channels for extensors and flexors; and the corresponding CMC frequency spectrum of the EEG-EMG channel pair with the highest peak CMC (CMC_{MAX}).

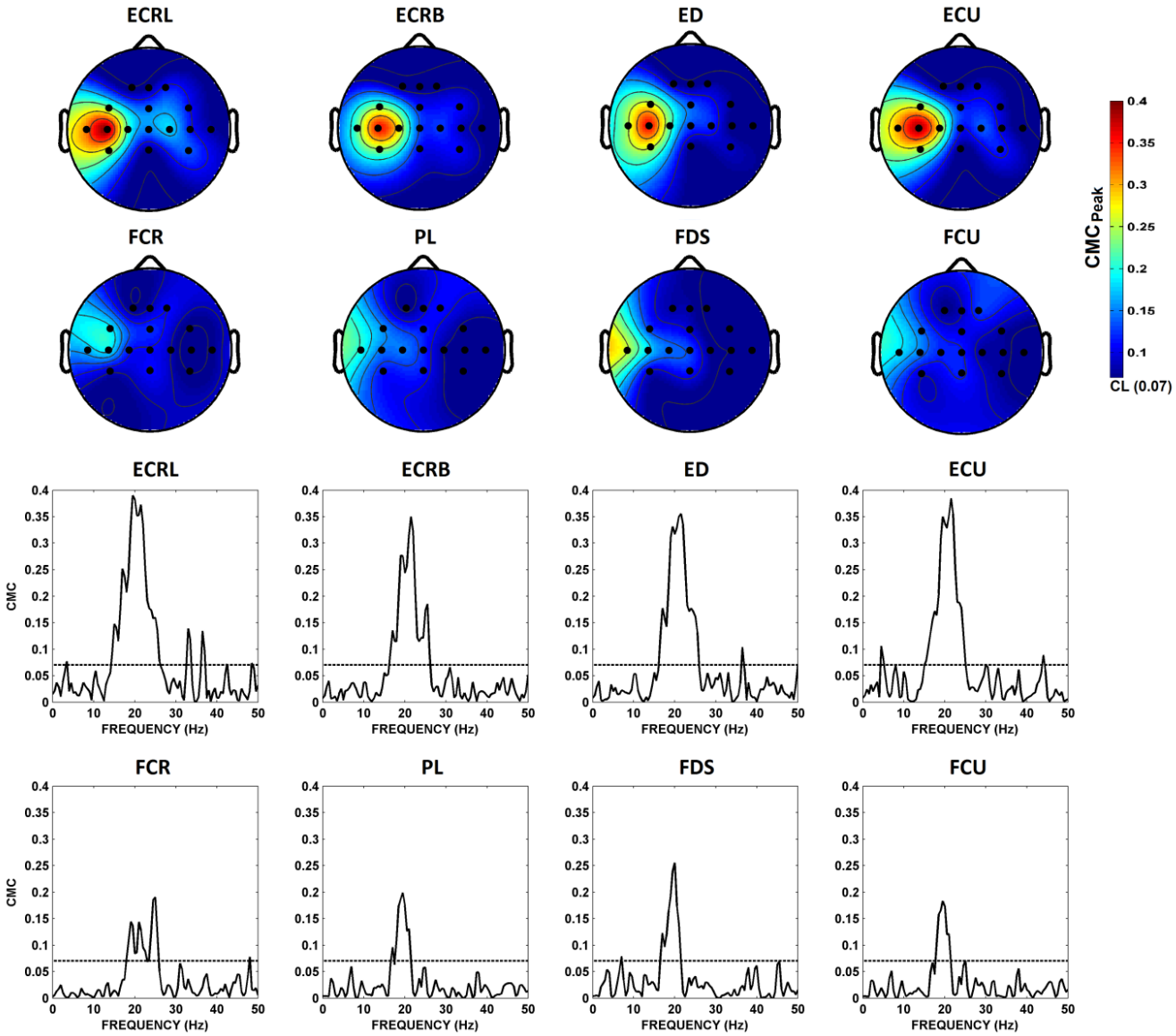

Figure 6.2 Typical single repetition topographical plots of peak CMC values across all EEG channels for extensors and flexors, and the corresponding CMC frequency spectrum of the EEG-EMG channel pair with the highest peak CMC (CMC_{MAX}). Adapted from candidate's publication (Divekar and John, 2013).

It is evident that for every muscle, CMC_{MAX} was primarily obtained from one of the EEG electrodes representing the contra-lateral sensorimotor area, and its peak frequency was primarily restricted to the beta band. Overall higher CMC_{MAX} values are apparent for extensor muscles compared to flexor muscles. From the topographical plots, CMC_{MAX} values can be seen to be restricted to the contra-lateral sensorimotor cortex, whereas their peak frequencies restricted to the beta-band as can be seen in their spectra below. Note that the dotted line on the CMC spectra represents the computed CL i.e. 0.07, thus all CMC_{MAX} values were above the CL.

6.2 Quantitative Results

Section 6.2 contains the results of the statistical comparisons of the neurophysiological, behavioural and perceptual variables between wrist flexion and extension. All group data are represented as (means (M) ± standard derivation (SD)); and significance of a factor conforms to $p<0.05$.

6.2.1 Neurophysiological variables

6.2.1.1 CMC_{MAX} comparisons between flexors and extensors

CMC_{MAX} was significantly lower for any flexor (FCR (0.15 ± 0.08); PL (0.16 ± 0.08); FDS (0.16 ± 0.09); FCU (0.16 ± 0.08)) muscle compared to an extensor (ECRL (0.20 ± 0.10); ECRB (0.20 ± 0.09); ED (0.19 ± 0.10); ECU (0.19 ± 0.10)), and was not significantly different among the synergists i.e. within the extensors and flexors; see Figure 6.3. Repetition and its interaction with muscles were not significant.

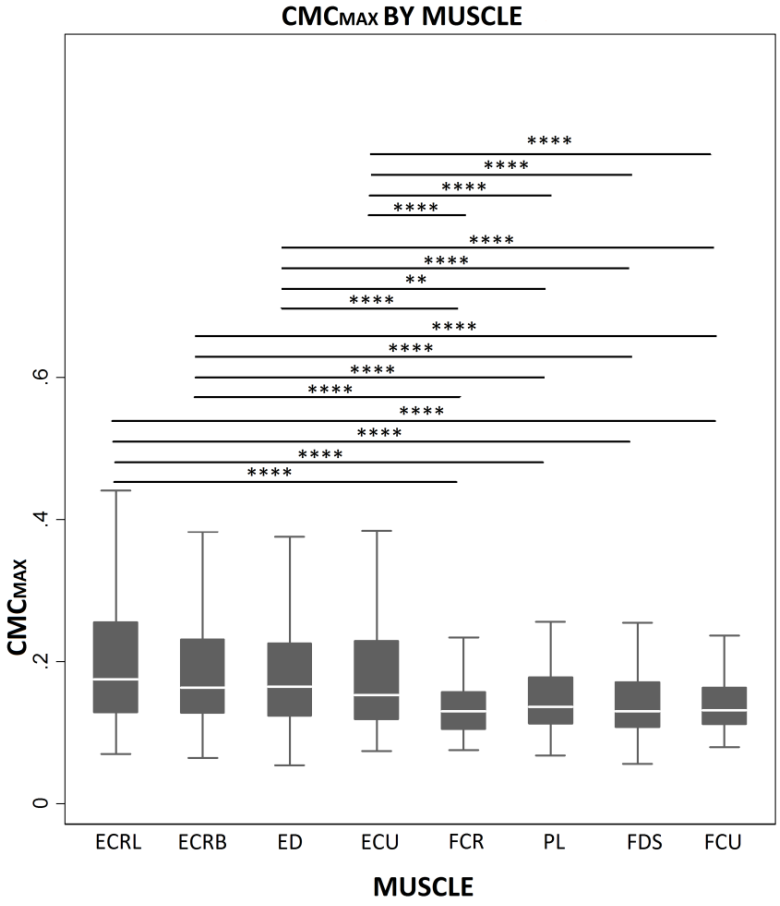

Figure 6.3 CMC_{MAX} comparisons between wrist muscles ('task' explicit in muscle tested). Lower CMC_{MAX} is evident for flexors compared to extensors. Significant differences denoted by: * ($p < 0.05$), ** ($p < 0.01$), * ($p < 0.001$),**** ($p < 0.0001$). Adapted from candidate's publication (Divekar and John, 2013).**

6.2.1.2 Peak frequency of CMC (FP) comparisons between flexors and extensors

FP was significantly lower for any flexor (FCR (25.1 ± 5.4 Hz); PL (24.3 ± 5.6 Hz); FDS (24.5 ± 5.8 Hz); FCU (25.2 ± 5.6 Hz)) muscle compared to an extensor (ECRL (26.5 ± 5.7 Hz); ECRB (26.5 ± 5.8 Hz); ED (26.1 ± 5.7 Hz); ECU (26.1 ± 6.1 Hz)), except when comparing FCR-ED, FCU-ED, FCR-ECU and FCU-ECU where there was no significant difference. FP was not significantly different among the synergists i.e. within the extensors and flexors; see Figure 6.4. Repetition and its interaction with muscles were not significant.

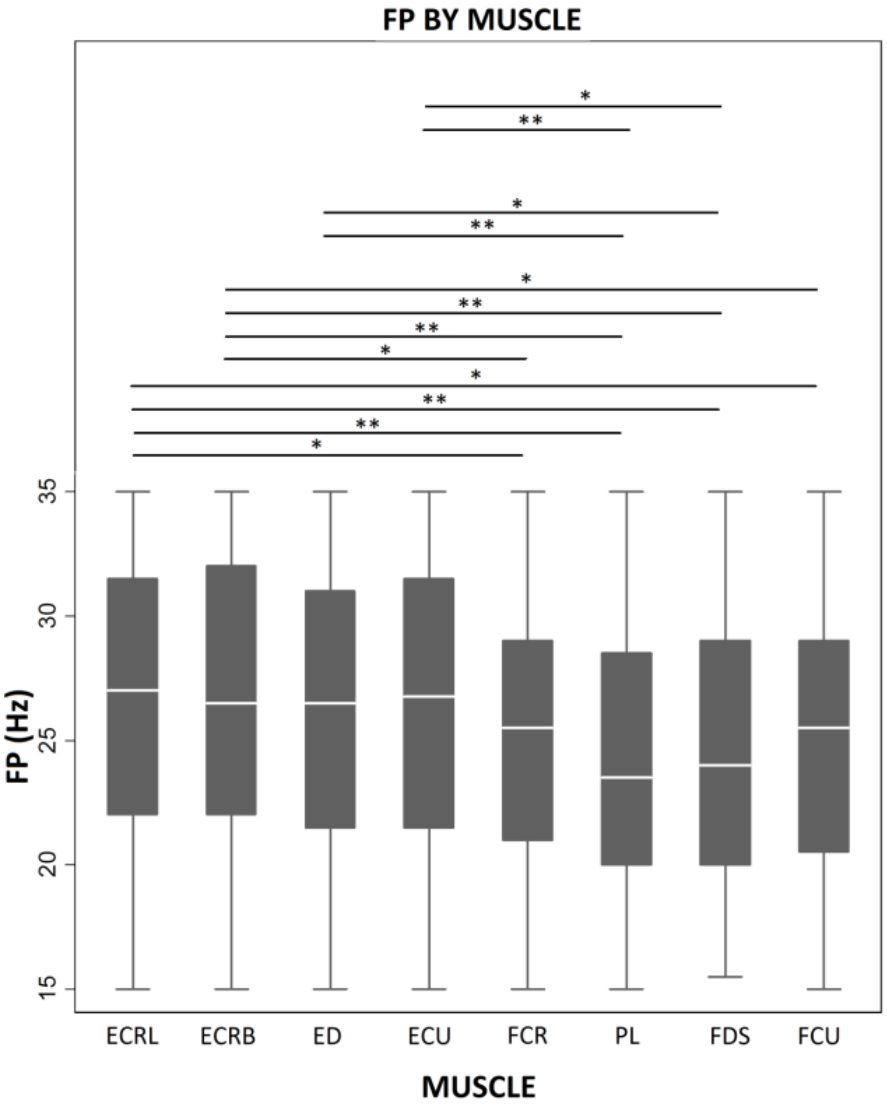

Figure 6.4 FP comparisons between wrist muscles ('task' explicit in muscle tested). Lower FP is evident for flexors compared to extensors. Significant differences denoted by: * (P < 0.05), ** (P < 0.01), * (P < 0.001),**** (P < 0.0001). Adapted from candidate's publication (Divekar and John, 2013).**

6.2.1.3 Significant CMC frequency width (FW) comparisons between flexors and extensors

FW was significantly lower for any flexor (FCR (2.62 ± 3.17 Hz); PL (2.93 ± 3.35 Hz); FDS (3.06 ± 3.96 Hz); FCU (3.01 ± 3.87 Hz)) muscle compared to an extensor (ECRL (4.84 ± 5.14 Hz); ECRB (4.55 ± 5.22 Hz); ED (4.43 ± 5.22 Hz); ECU (4.76 ± 5.70 Hz)). FW was not significantly different among the synergists i.e. within the extensors and flexors; see Figure 6.5. Repetition and its interaction with muscles were not significant.

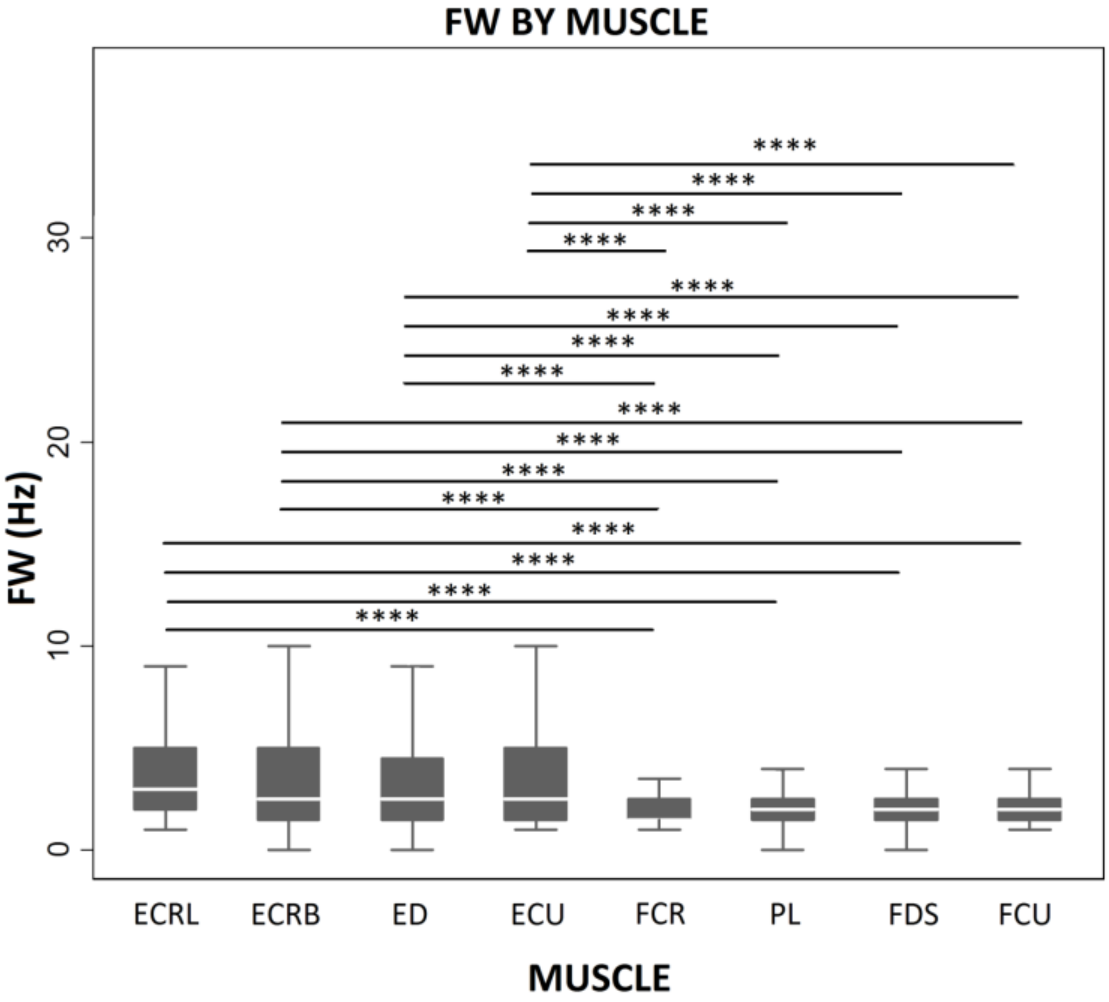

Figure 6.5 FW comparisons between wrist muscles ('task' explicit in muscle tested). Lower FW is evident for flexors compared to extensors. Significant differences denoted by: * (P < 0.05), ** (P < 0.01), * (P < 0.001),**** (P < 0.0001). Adapted from candidate's publication (Divekar and John, 2013).**

6.2.1.4 Significant CMC area (CMC_{AREA}) comparisons between flexors and extensors

CMC_{AREA} was significantly lower for any flexor (FCR (M=0.37, SD=0.69); PL (M=0.42, SD=0.69); FDS (M=0.45, SD=0.86); FCU (M=0.43, SD=0.84)) muscle compared to an extensor (ECRL (M=0.82, SD=1.16); ECRB (M=0.76, SD=1.20); ED (M=0.75, SD=1.26); ECU (M=0.82, SD=1.42)). CMC_{AREA} was not significantly different among the synergists i.e. within the extensors and flexors; see Figure 6.6. Repetition and its interaction with muscles were not significant.

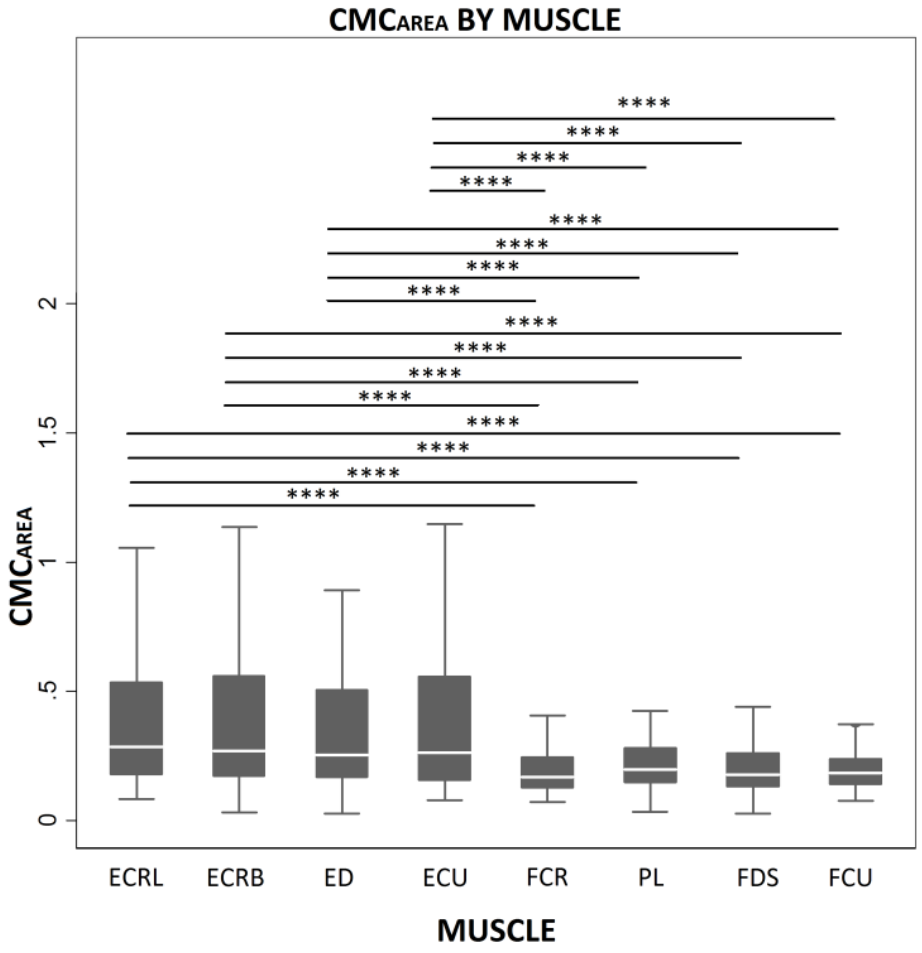

Figure 6.6 CMC_{AREA} comparisons between wrist muscles ('task' explicit in muscle tested). Lower CMC_{AREA} is evident for flexors compared to extensors. Significant differences denoted by: * (P < 0.05), ** (P < 0.01), * (P < 0.001),**** (P < 0.0001).**

6.2.1.5 Normalised EEG alpha power (EEGα-PSD) comparisons between flexors and extensors

EEGα-PSD was NOT significantly different for any flexor (FCR (M=0.32, SD=0.16); PL (M=0.32, SD=0.16); FDS (M=0.33, SD=0.16); FCU (M=0.33, SD=0.16)) muscle[4] compared to an extensor (ECRL (M=0.33, SD=0.16); ECRB (M=0.34, SD=0.16); ED (M=0.33, SD=0.16); ECU (M=0.33, SD=0.16)). EEGα-PSD was not significantly different among the synergists i.e. within the extensors and flexors; see Figure 6.7. EEGα-PSD was significantly ($p<0.0001$) different for repetition of muscle specific task with a 1% increase for every unit of repetition regardless of muscle. The interaction of repetition with muscle was not significant.

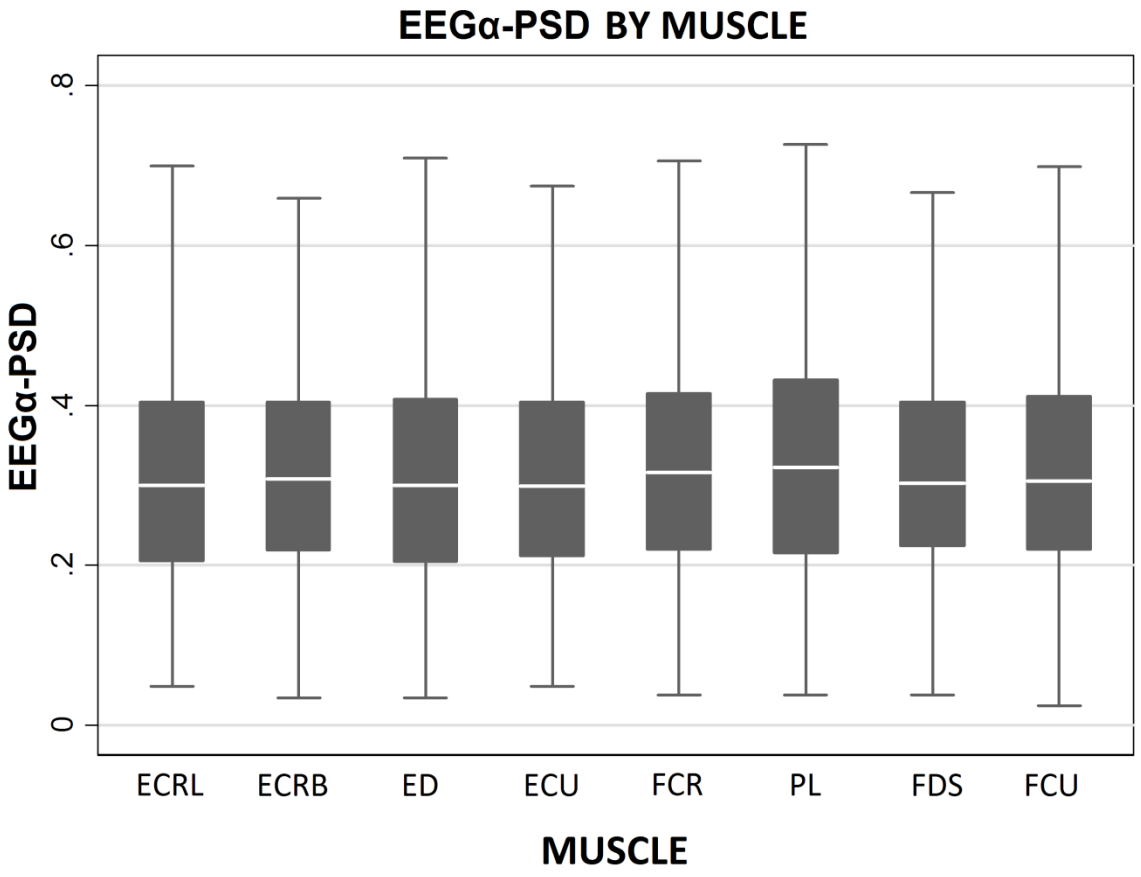

Figure 6.7 EEGα-PSD comparisons between wrist muscles[4] (task, wrist flexion/extension explicit in muscle tested). No significant differnces are evident when comparing w.r.t. any two muscles[4].

[4] Note that EEGα-PSD was calculated w.r.t. each muscle at the EEG electrode with CMC_{MAX}; see Data Analysis (section 5.4).

6.2.1.6 Normalised EEG beta power (EEGβ-PSD) comparisons between flexors and extensors

EEGβ-PSD was NOT significantly different for any flexor (FCR (M=0.13, SD=0.05); PL (M=0.13, SD=0.05); FDS (M=0.13, SD=0.05); FCU (M=0.13, SD=0.05)) muscle[5] compared to an extensor (ECRL (M=0.13, SD=0.05); ECRB (M=0.13, SD=0.05); ED (M=0.13, SD=0.05); ECU (M=0.13, SD=0.05)). EEGβ-PSD was not significantly different among the synergists i.e. within the extensors and flexors; see Figure 6.8. Repetition and its interaction with muscles were not significant.

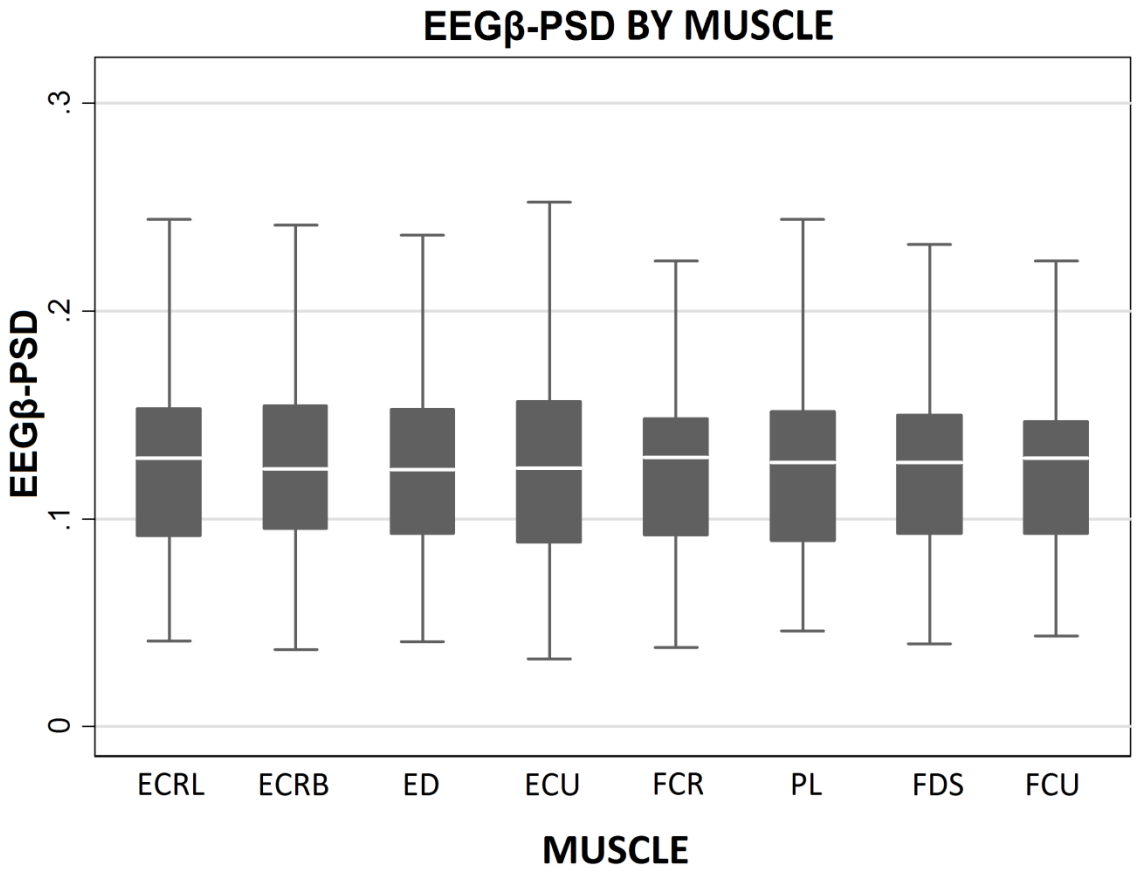

Figure 6.8 EEGβ-PSD comparisons between wrist muscles[5] ('task' explicit in muscle tested) . No significant differnces are evident when comparing w.r.t. any two muscles[5].

[5] Note that EEGβ-PSD was calculated w.r.t. each muscle at the EEG electrode with CMC_{MAX}; see Data Analysis (section 5.4).

6.2.1.7 Normalised EMG beta power (EMGβ-PSD) comparisons between flexors and extensors

EMGβ-PSD was significantly lower for any flexor (FCR (0.15 ± 0.03); PL (0.15 ± 0.04); FDS (0.16 ± 0.03); FCU (0.16 ± 0.03)) muscle compared to extensor ECRL (0.18 ± 0.05); and was significantly lower for flexors FCR and PL compared to extensors ECRB (0.17 ± 0.04) and ED (0.17 ± 0.05). There was no significant difference between any flexor muscle and extensor ECU (0.16 ± 0.05). Also there was no significant difference among the synergists i.e. within the extensors and flexors; see Figure 6.9. Repetition and its interaction with muscles were not significant.

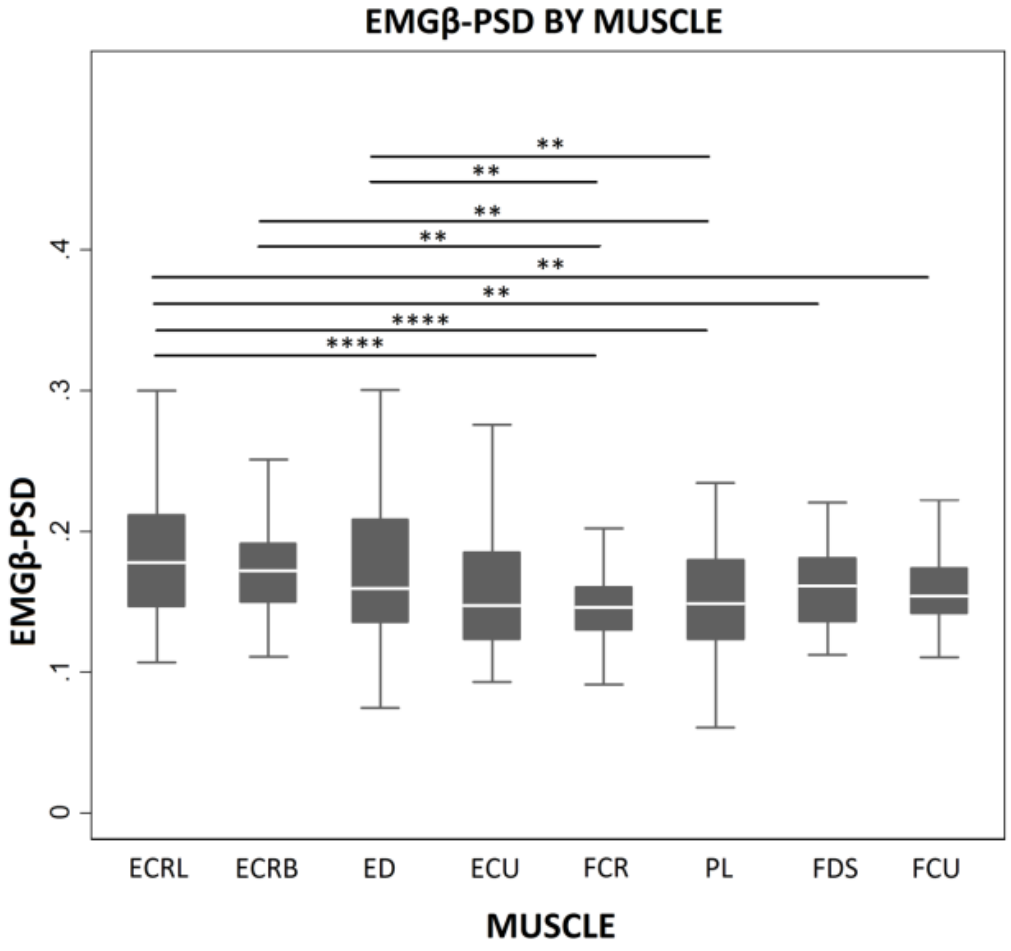

Figure 6.9 EMGβ-PSD comparisons between wrist muscles ('task' explicit in muscle tested). Lower EMGβ-PSD is evident for flexors compared to extensors. Significant differences denoted by: * (P < 0.05), ** (P < 0.01), * (P < 0.001),**** (P < 0.0001). Adapted from candidate's publication (Divekar and John, 2013).**

6.2.2 Behavioural variables

6.2.2.1 Maximum voluntary contraction (MVC) torque comparison between flexion and extension

MVC torque was significantly higher for wrist flexion (14.7 ± 2.1 Nm) compared to extension (8.7 ± 2.7 Nm); see Figure 6.10.

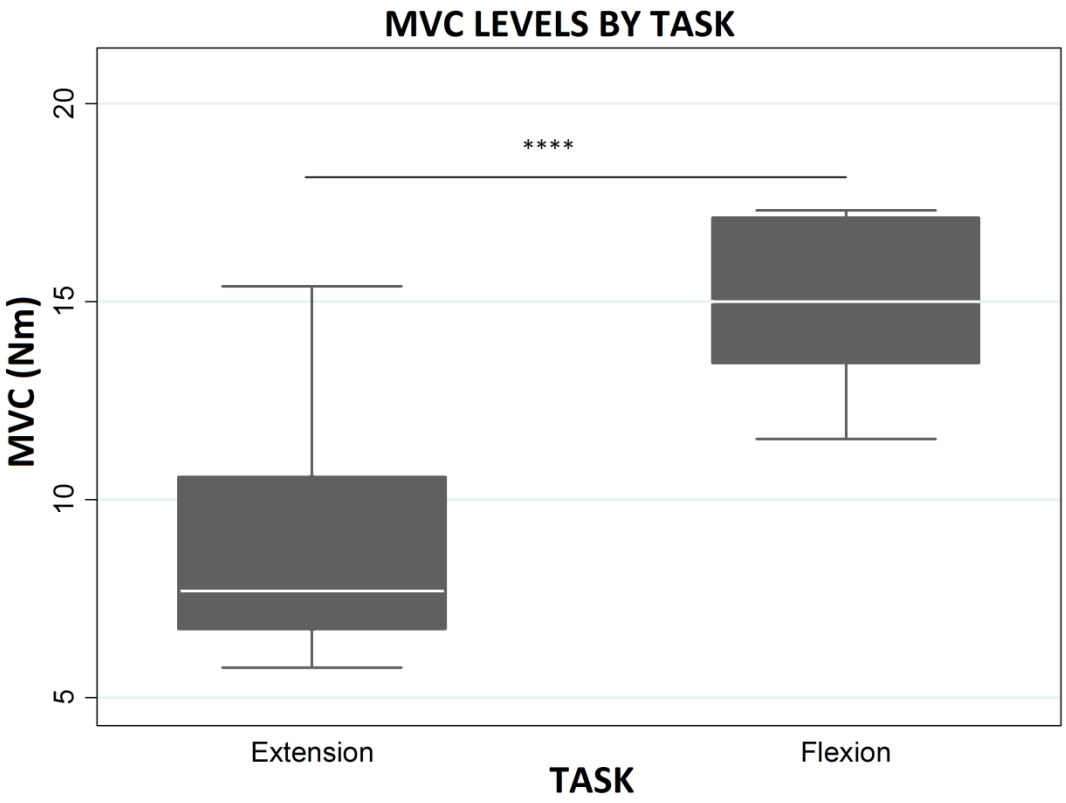

Figure 6.10 MVC level comparison between wrist flexion and extension tasks. Higher MVC is evident for flexion compared to extension. Significant difference denoted by: **(p<0.0001). Adapted from candidate's publication (Divekar and John, 2013).**

6.2.2.2 Motor precision (PRECISION) comparison between flexion and extension

Precision was significantly higher for wrist flexion (15.9 ± 12.2) compared to extension (4.9 ± 3.8) task conditions; see Figure 6.11. Precision was significantly (p=0.03) different with Repetition, with a 2% decrease with every unit of repetition regardless of task. The interaction between task and repetition was non-significant.

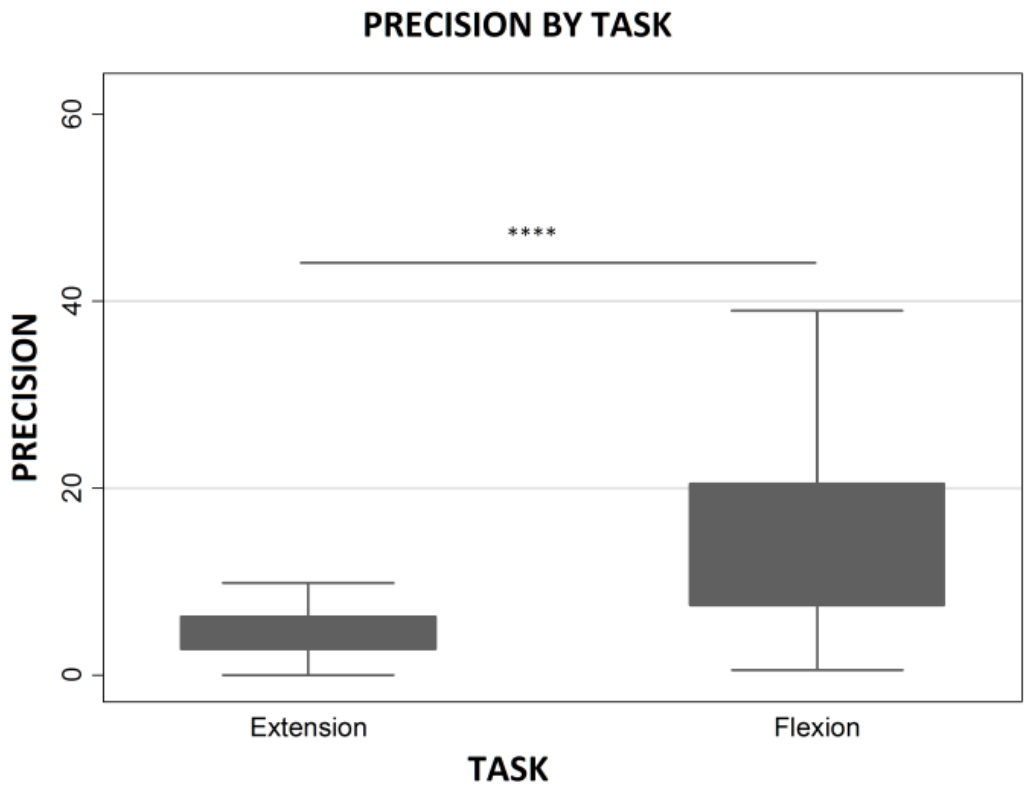

Figure 6.11 PRECISION comparison between wrist flexion and extension tasks. Higher PRECISION is evident for flexion compared to extension. Significant difference denoted by: ** (p<0.0001). Adapted from candidate's publication (Divekar and John, 2013).**

6.2.2.3 Low-Frequency torque fluctuation (Torque-low-PSD) comparison between flexion and extension

Torque-low-PSD was significantly lower in wrist flexion (0.10 ± 0.15 $\%MVC^2$) compared to extension (0.48 ± 1.58 $\%MVC^2$) task conditions; see Figure 6.12. Torque-low-PSD was significantly ($p<0.01$) different with Repetition, with a 3% increase with every unit of repetition regardless of task. Interaction of task and repetition was not significant.

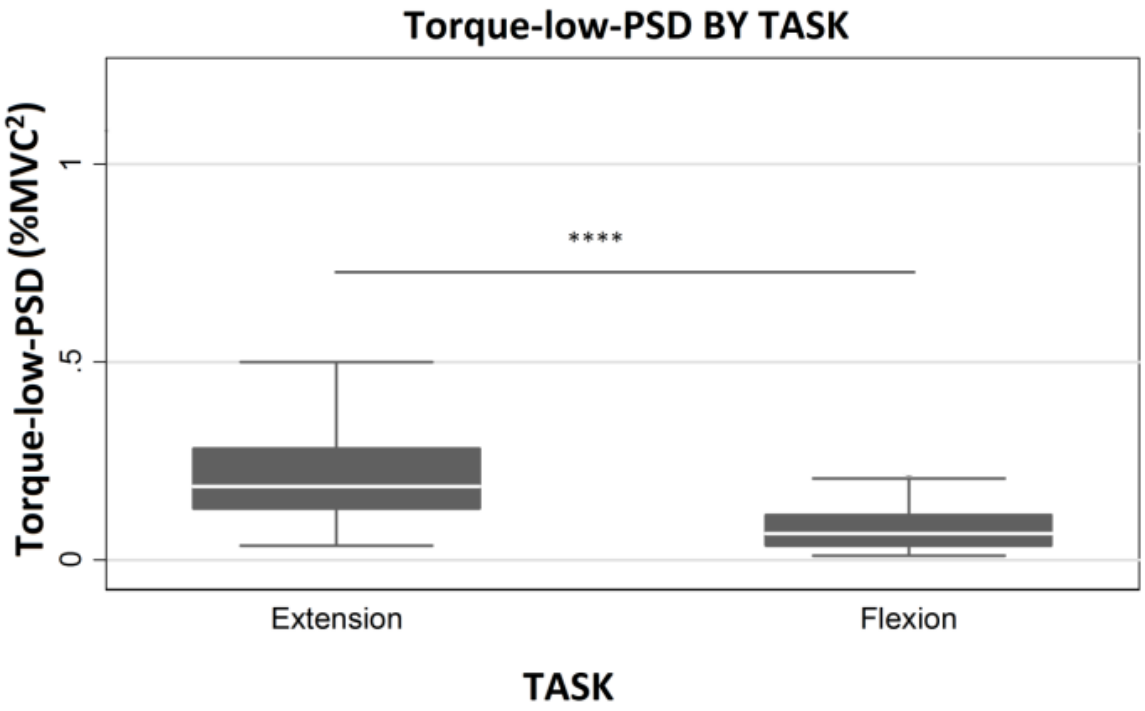

Figure 6.12 Torque power at lower (<5Hz) frequency band (Torque-low-PSD) comparison between wrist extension and flexion tasks. Lower Torque-low-PSD is evident for flexion compared to extension. Significant difference denoted by: ** ($p<0.0001$). Adapted from candidate's publication (Divekar and John, 2013).**

6.2.2.4 Beta band torque fluctuation (Torqueβ-PSD) comparison between flexion and extension

Torqueβ-PSD was significantly lower in wrist flexion ($4.0E^{-5} \pm 5.0E^{-5}$ $\%MVC^2$) compared to extension ($1.4E^{-4} \pm 2.1E^{-4}$ $\%MVC^2$) task conditions; see Figure 6.13. Repetition and its interaction with task were not significant.

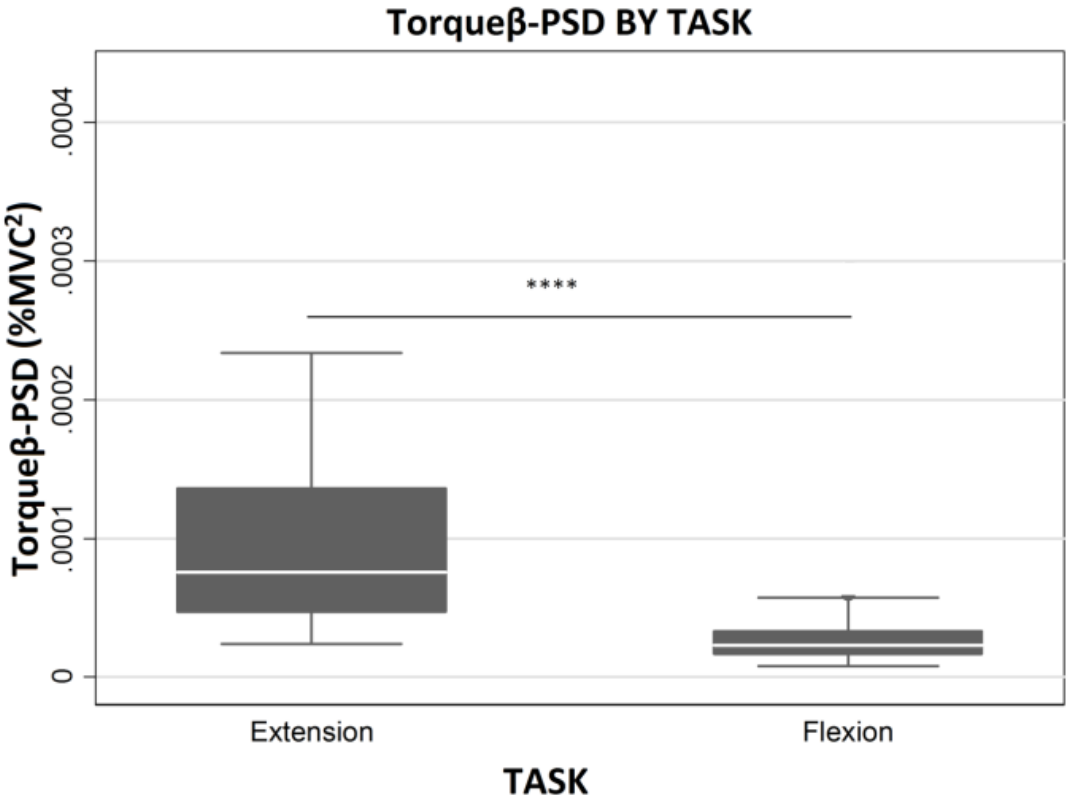

Figure 6.13 Torque power at beta (15-35 Hz) frequency band (Torqueβ-PSD) comparison between wrist extension and flexion tasks. Lower Torqueβ-PSD is evident for flexion compared to extension. Significant difference denoted by: ** ($p<0.0001$). Adapted from candidate's publication (Divekar and John, 2013).**

6.2.3 Perceptual variable

6.2.3.1 Perceived difficulty rating comparison between flexion and extension

Perceived difficulty ratings were significantly lower for the wrist flexion task (2.1 ± 0.6) as compared to the wrist extension task (3.9 ± 0.8); see Figure 6.14.

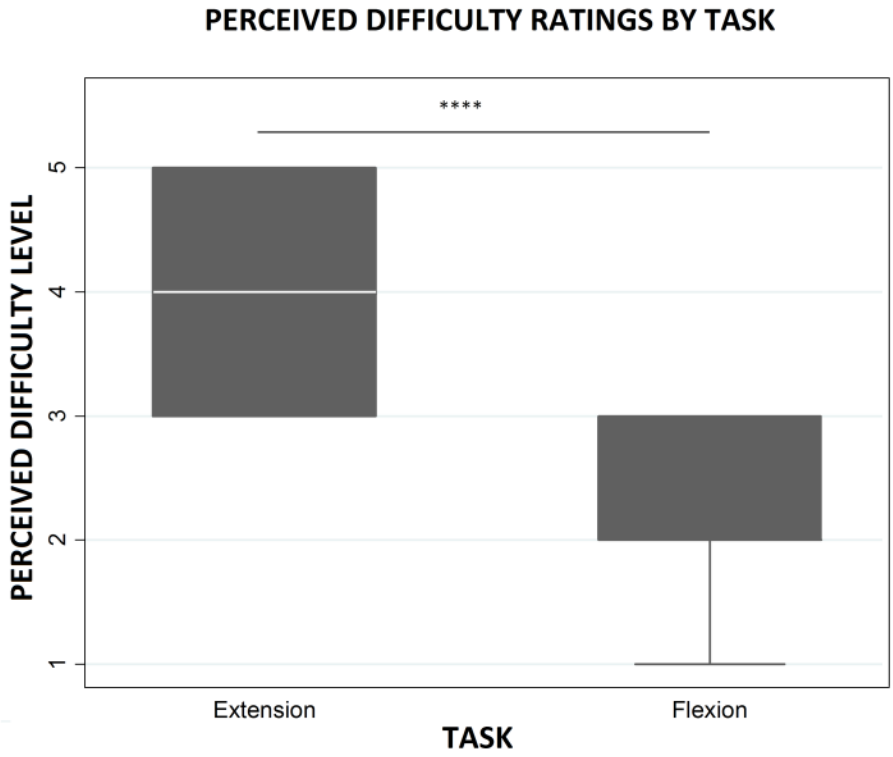

Figure 6.14 Perceived difficulty rating comparison between wrist flexion and extension tasks. Lower perceived difficulty ratings are evident for wrist flexion compared to extension. Significant difference denoted by: ** (p<0.0001). Adapted from candidate's publication (Divekar and John, 2013).**

7 DISCUSSION

The first main finding of this study is the lower beta CMC levels for wrist flexors as compared to wrist extensors when comparing high-precision isometric wrist flexion and extension tasks: - peak beta CMC levels (CMC_{MAX}), frequency range of significant CMC levels about the peak (FW) as well as the integral of significant CMC levels (CMC_{AREA}) were all significantly lower for the wrist flexors when compared to the extensors. Following from the first main finding, the second main finding is the inverse relationship between beta CMC and motor precision; as wrist flexion was performed with significantly higher motor precision (PRECISION) compared to wrist extension as was expected from prior literature. When considering that the proposed functional roles of beta CMC in prior literature relate it to effecting higher motor output stability through improved sensorimotor integration (Baker, 2007; Kristeva et al., 2007; Witham et al., 2011), the results of the present study seem to be contradictory and disprove the initial hypothesis of a direct relationship between beta CMC and motor precision when comparing wrist flexion and extension.

Various factors can potentially influence beta CMC levels and/or motor precision and may have caused the inversion of the beta CMC motor precision relationship; these differences are explored in section 7.1 and include the effect of perceived difficulty. In section 7.2, the pattern of common drive to synergistic muscles is discussed. The discussion ends with the clinical relevance of the present study mentioned in section 7.3.

7.1 Potential factors related to CMC and/or motor precision

7.1.1 Cortical (M1, S1, SMA) representation of muscles and EEG power

The ability of the scalp surface electrodes to successfully record the oscillatory electrical activity of the cortical neurons which are controlling (M1) and/or monitoring (S1) the wrist muscles depends on factors such as neuronal location, depth and orientation relative to the recording site. Little difference is expected between the locations and depths of cortical neurons related to wrist extensors and flexors as both sets of muscles are of the same joint (Cheyne et al., 1991; Hluštík et al., 2001). Regarding the orientation of the neuronal dipoles, EEG is shown to be able to detect both tangential as well as radial sources (Nunez, 1989; Handy, 2005) while MEG can measure only radial sources. Although orientation would alter EEG amplitude, coherence measures are unaffected by absolute amplitudes of the signals

(Baker and Baker, 2003; Riddle et al., 2004). In fact, there was no significant difference in normalised EEG powers (EEGα-PSD, EEGβ-PSD) between wrist extension and flexion in the present study. Although EEGα-PSD increased significantly, albeit slightly (+1%) with repetition, this may be attributed to the subjects performing the tasks with slightly reduced attention as the experiment progressed.

Previous findings (Yue et al., 2000), using the fMRI imaging technique, indicated higher CNS activation volumes, globally as well as in the SMA, contralateral motor cortex (MC) and cerebellum, for the thumb extensor compared to the flexor. In addition, EEG-derived MRCP levels (SMA, contralateral MC) were higher for the extensor. These findings were attributed to higher brain activation needed to compensate for the greater inhibition and lower facilitation of the extensors compared to flexors, with a possible extrapolation of results to the elbow ***as well as wrist levels***.

The fMRI-BOLD technique which measures blood oxygen levels of an area is presumably positively related to the firing rate of the underlying neurons among other factors (Singh, 2012). Further, in the present study the CMC peak frequency (FP) was higher for extensors compared to flexors (Figure 6.4), suggesting that cortical neurons controlling wrist extensors fire at a higher rate than those controlling flexors. Using computer simulations, neuronal firing rate was in turn demonstrated to be positively related to CMC levels due to an increase in the signal:noise ratio between the PSPs and axonal firing of neurons at higher firing rates (Baker et al., 2003); possibly explaining the higher CMC for wrist extensors compared to flexors in the present study.

7.1.2 Thalamus and basal ganglia

See section 2.1.5 for basic information on the role of the basal ganglia and thalamus in motor control.The thalamus is deemed to be one of the structures responsible for the generation and or modulation of the oscillatory activity measured by EEG at the cortical level (Herrero et al., 2002; Baker and Baker, 2003). The thalamus is also a relay centre sub-serving both sensory and motor mechanisms. It is thus possible that it plays a key role in the process of sensorimotor binding tagged by CMC. Even though the wrist extensors and flexors are anatomically close (both exert force about the wrist joint), they are functionally different. It is likely that this differentiation also exists at the thalamic level, where greater

sensorimotor monitoring may have been effected for the wrist extensors, resulting in their greater CMC levels, as was found in this study.

Similarly, the basal ganglia also have a regulatory influence on the cortex, as they provide information for both automatic and voluntary motor responses to the pyramidal system (Herrero et al., 2002). The basal ganglia have also been proposed as one of the likely structures responsible for modulating the beta oscillatory activity at the cortical level (Brown and Marsden, 1998; Brown, 2000), which is postulated to drive the oscillatory activity at the muscular level. It is thus possible that the variance found in the present study between flexor-extensor beta CMC levels (extensors having higher beta CMC), may also have been prompted at the level of the basal ganglia. Such neurophysiological differences at the basal ganglia between wrist flexors and extensors, have been reported in prior literature, for example, cells in the monkey basal ganglia (globus pallidus pars interna) have been reported to exert a greater inhibitory effect on wrist extensors than on wrist flexors (Mink and Thach, 1991).

7.1.3 Cortico-spinal projection density

See section 2.1.3.1 for information on the corticospinal pathway and its role in motor control. CMC is proposed to be mediated via the fast corticospinal pathways; hence the density of monosynaptic corticospinal projections to a muscle would reflect on the relative involvement of this direct pathway in motor control, denser projections signifying greater relative involvement and possibly higher resulting CMC levels. Palmer and Ashby (1992), using magnetic stimulation, concluded that there were denser projections to distal musculature of the upper limb compared to proximal, as well as to biceps (elbow flexors) compared to triceps (elbow extensors), but did not find conclusive differences between wrist extensors and flexors.

However, in a later study using electrical stimulation, it was reported that wrist and finger extensors have denser corticospinal projections compared to flexors (de Noordhout et al., 1999). Furthermore, a recent study analysing motor evoked potentials (MEPs) reports wrist extensors have greater corticomotor excitability compared to wrist flexors (Chye et al., 2010). These results support the findings of higher CMC for wrist extensors in this study, as

they suggest greater relative involvement of the direct monosynaptic corticospinal tract in wrist extensor control.

However it is not clear how this trend would result in reduced precision for the wrist extensors as greater involvement of the direct corticospinal tract would suggest greater fine motor control and hence high motor precision. One explanation could be related to the 6-13 Hz (~ 10 Hz) oscillatory activity that has been recorded at M1, cerebellum as well as the reticular formations in monkeys (Williams et al., 2010). Using accelerometer records and coherence analysis, such oscillatory activity has been shown to be the main exponent of tremor that was found in healthy adults during slow movements, and hence also would be responsible for impairing motor precision (Williams et al., 2010). A few models of spinal cord circuits are suggested that cancel-out and/or block this ~ 10 Hz activity from reaching the LMNs, thereby explaining why tremor is not a persistent feature of the motor system but rather occasionally observed. The lower motor precision for extension found in the present study could thus be due to a combination of: increased transmission of the M1 originating ~ 10 Hz deleterious oscillatory activity to the LMNs due to an increased use of the direct corticospinal tract (evidenced by the higher CMC of extensors compared to flexors); and the reduced action of the spinal circuits that counter this deleterious activity in extensors as compared to flexors.

7.1.4 Renshaw Cells

See section 2.1.2.3 for basic information on the role of Renshaw cells in motor control. Renshaw cells are spinal interneurons that serve to regulate motor output, by inhibiting the oscillatory activity of the same alpha motor neurons that they receive excitatory input from. Thus stronger recurrent inhibition by Renshaw cells has an effect of reducing CMC (Williams and Baker, 2009). Differences in the strength of recurrent inhibition by Renshaw cells have been reported for distal versus proximal muscles of the upper limb (Katz et al., 1993). However recurrent inhibition by Renshaw cells for the antagonistic wrist muscle groups present a different scenario. For example Renshaw cells of wrist extensors not only inhibit themselves, but also inhibit their antagonist flexor groups, and vice versa, where the flexor coupled Renshaw cells inhibit the flexors as well as the antagonistic extensors (Aymard et al., 1997). This has an effect of levelling the Renshaw component of inhibition across these

antagonistic muscle groups, eliminating the bias in inhibition to any one set of muscles, and therefore does not explain the CMC differences between these muscle groups.

7.1.5 Muscle spindle density

See section 2.1.1.2 for information on the role of muscle spindles in motor control. CMC is influenced by oscillatory activity in both efferent and afferent pathways (Witham et al., 2011). As part of the afferent pathway, higher muscle spindle density would imply stronger oscillatory feedback to the sensorimotor cortex from the periphery with a resultant increase in CMC. The radial wrist extensors (ECRB and ECRL) have lower spindle densities than the flexors, while the digit and ulnar extensors (ED and ECU) have higher (Banks, 2006). Therefore muscle spindle density differences between wrist extensors and flexors do not explain the findings of the present study and therefore cannot be the reason for lower CMC in all wrist flexors (Figure 6.3 and Figure 6.6) compared to extensors.

However, this anatomical difference may not be a limiting one, as reported by Witham et al. (2011) who found inter-subject variance between the level of CMC arising from differences in the relative contributions from the descending (motor) and ascending (sensory) signals, depending on factors such as the strategy used for force control. In support of this finding, Chapman et al. (1987) also show that the level of feedback from afferents can also be modulated, via the descending command, thereby suggesting that overall higher sensory feedback may have been effected for the extensors (regardless of muscle spindle density differences) in an attempt to increase the extension precision level, ultimately resulting in higher CMC.

Conversely, it is plausible that torque fluctuation (motor precision) and CMC influence each other in tandem. Baker et al. (2006) found significant beta band coherence between single afferent Iα (muscle spindle) spike trains and EMG, suggesting that muscle spindle discharge encodes oscillations in EMG activity, essentially forming a peripheral feedback loop. Furthermore, the sensitivity of spindles is dynamically controlled by γ motor neurons. In line with this theory, the results of the present study showing higher EMGβ-PSD for the extensors, associated with higher Torqueβ-PSD (lower precision) for extension, would also be associated with higher gains via the γ motor neurons, possibly enhancing the cortico-

muscular phase synchrony, resulting in higher beta CMC for the extensors as was found in the present study.

7.1.6 Motor functional suitability of flexors – muscle size, strength and motor-units

Ushiyama et al. (2010) reported that upper limb proximal muscles which are more suited for postural control had lower CMC than the distal ones that are more suited to manipulative actions; suggesting that functional suitability of a muscle has an influence on CMC. Flexors of the upper limb (including wrist flexors) act primarily anti-gravity (e.g. lifting of objects), whereas the corresponding extensors are primarily pro-gravity. In the lower limb, anti-gravity muscles are known to be more suited for isometric torque maintenance compared to pro-gravity ones. Extrapolation to the upper limb, suggests that the anti-gravity wrist flexors were more functionally suited to the isometric contraction task than their antagonist extensors. Furthermore, a muscle's functional suitability for high precision tasks may also be predicted by considering its relative size and strength, as Hamilton et al. (2004) showed that, larger and stronger muscles are steadier than smaller and weaker ones; as they have a comparatively higher number of motor units recruited for a given % MVC, decreasing the CV of output force. Wrist flexors, as reported by Salonikidis et al (2011), are larger, stronger and steadier, further supporting their higher functional suitability over extensors. If CMC is the product of the complimentary 'test pulse' mechanism used to effect efficient sensorimotor monitoring of the peripheral system (Baker, 2007; Witham et al., 2011); then it is likely that more functionally suited muscles, being inherently steadier, require less sensorimotor monitoring for stabilisation; explaining the lower CMC for the flexors.

The present study CMC findings for the equally distal intra-limb wrist muscles are not generalizable to all inter-muscle comparisons. For example, despite Ushiyama et al. (2010) reporting lower CMC for the larger and stronger arm muscles compared to the weaker and smaller hand muscles i.e. upper limb proximal vs. distal, they also reported higher CMC in general for the larger and stronger lower limb muscles compared to smaller and weaker upper limb muscles.

7.1.7 Long-term usage adaptations

Salonikidis et al. (2011) estimated that wrist flexors are used relatively more frequently compared to extensors in everyday work, e.g. for lifting and holding on to objects, possibly leading to their greater adaptation to isometric force maintenance tasks. Evidence from brain activity studies as measured by cerebral blood flow (Seitz et al., 1990) and fMRI (Büchel et al., 1999), showed decreased activity in various areas of the cortex after extensive learning of motor tasks. Furthermore, daily-use induced technique improvements are associated with an independency in the motor unit firing rate, lower motor unit synchronization and substantially lower common oscillatory input from the sensorimotor cortex, especially in the beta (15-35Hz) band (Semmler and Nordstrom, 1998; Semmler et al., 2004). This suggests that as the CNS adapts to make control more automatic, less cortical resources as well as less resource synchronisation are required. For the more adapted wrist flexors, it is likely that the reduced oscillatory drive from the sensorimotor cortex combined with the consequent reduction in motor unit synchronisation at the peripheral level; resulted in their lower beta cortico-muscular coupling (CMC_{MAX}, CMC_{AREA}) levels as well as lower normalised EMG beta power (EMGβ-PSD) levels as found in the present study.

The present study thus suggests a possible reduction in flexor CMC, due to their greater adaptation compared to the extensors, as a result of a natural bias in inter-muscle usage levels during ordinary day-to-day activities; similarly, a reduction in CMC due to adaptation after specialised training of a particular muscle set in athletes, has been reported by Ushiyama et al. (2010).

7.1.8 Fatigue

Yang et al (2009) reported lower precision and CMC in severe fatigue compared to minimal fatigue, whereas, Ushiyama, Katsu et al. (2011) reported lower precision but higher CMC in post-fatigue compared to pre-fatigue conditions. Although in the present study, PRECISION was found to decrease slightly (2%) with repetition, matched by a corresponding slight (3%) increase in Torque-low-PSD, this would not be attributable to fatigue, as the changes, although significant are very small and may be a result of a slight decrease in attention as the experiment progressed, possibly indicated by the small (1%) increase in EEGα-PSD.

Furthermore, no significant changes in CMC_{MAX}, FW and CMC_{AREA} levels were found with repetition.

7.1.9 EMG beta discharge

Computer simulations (Yao et al., 2000) demonstrate that with motor-unit recruitment and discharge rates kept constant; increasing the number of synchronised motor units increased the magnitude of force fluctuation i.e. decreased precision, without increasing the average force levels. This also resulted in a significant increase in the measurable surface EMG power. These simulations, match the present study's experimental results of lower motor precision, higher torque fluctuation (Torque-low-PSD, Torqueβ-PSD) and higher EMGβ-PSD in extensors as compared to flexors. It therefore seems that beta band CMC (CMC_{MAX}, CMC_{AREA}) positively influences beta oscillatory activity in EMG (EMGβ-PSD). The direct relationship between EMGβ-PSD and CMC_{MAX} (with FP being always in the beta band) found in the present study has been reported before (Ushiyama, Katsu, et al., 2011; Ushiyama, Suzuki, et al., 2011).

Therefore in the present study, the lower EMGβ-PSD for flexors (possibly linked to their lower beta CMC) may partially explain their higher precision levels, as it would result in their correspondingly lower torque fluctuations in the beta band (Torqueβ-PSD). More important however is the predominant lower frequency (<5Hz) torque component (Torque-low-PSD) as can be seen in the torque spectrum profiles (Figure 6.1) which responds in the same manner as Torqueβ-PSD in the tasks. There is a suggested relationship between Torqueβ-PSD and Torque-low-PSD (Ushiyama, Katsu et al., 2011); however the practical mechanism that could underlie this is unclear. Therefore it cannot be concluded that higher beta CMC reduces overall motor precision by increasing overall torque fluctuation in the muscle via increased beta EMG discharge.

7.1.10 Perceived difficulty

Acquired in the present study were perceived difficulty ratings of the experimental tasks (wrist flexion, wrist extension) from subjects, which were based on the difficulty associated with being able to maintain the actual torque within the 15 ± 1% MVC allowable window. Perceived difficulty is a perceptual variable that may be influenced by any of the central, peripheral as well as adaptive factors. Lower perceived difficulty ratings were reported for

the wrist flexion task, which was carried out at higher precision levels compared to extension. Thus perceived difficulty was found to be directly related to CMC, EMG and torque power variables but inversely related to precision.

It is plausible that in the context of maintaining high precision (as in the present study), performing a perceptually more difficult task, such as wrist extension, which is hypothetically inherently less steady than flexion, would induce an increase in the relative engagement of precision enhancing mechanisms as a compensatory measure. Such mechanisms may involve an increase in the relative involvement of the direct corticospinal tract to facilitate finer motor control, and also an increase in the gains of somatosensory afferents via the peripheral tracts to facilitate better feedback of muscle tension (gauged by Golgi tendon organs) and muscle length variation (gauged by muscle spindles); ultimately resulting in increased CMC.

This may have been the likely situation in the studies of Kristeva et al. (2007), and Ushiyama, Katsu et al. (2011), where opposite precision vs CMC relationships were found. In the intra-task scenario of Kristeva et al. (2007), it would be more difficult to maintain higher precision compared to lower precision given constant task conditions; whereas in the pre-post fatigue task comparisons of Ushiyama, Katsu et al. (2011), it would be more difficult to maintain high precision, post fatigue, as compared to pre fatigue. In both studies the more difficult task was associated with higher CMC levels. In the intra-task fatiguing scenario of Yang et al. (2009), the experimental protocol is peculiar, as it emphasised maintenance of high force 'amplitudes' (above 90% of target force level), with little emphasis on high force 'precision'. Therefore the relationship between CMC and perceived task difficulty with respect to maintenance of high precision, in the case of Yang et al. (2009), is unclear.

7.2 Synchrony in motor control among the synergists

No significant differences were found in CMC_{MAX}, CMC_{AREA} and related variables (FP, FW) within the synergists for wrist flexion or extension. I.e. there was no significant difference in these variables within the extensors for extension, and within the flexors for flexion; see Figures 6.3 – 6.6. Although discrepancies exist within synergists in their corticospinal projection densities, muscle spindle densities as well as muscle mass etc, this results pattern is likely to be attributable to the uniform sensorimotor monitoring of all the synergistic

muscles by the cortex for force production in a particular direction (flexion or extension). The wrist flexion and extension isometric force compensation tasks carried out in the present study, require co-contraction of all synergists, as also explained by a force vector diagram of this process (Bawa et al., 2000); see section 3.1.1. Thus the synergists would require an equal share of sensorimotor monitoring by the cortex to sustain the direction and magnitude of the final resultant force vector. It is likely that that this may be facilitated by a common descending 'test pulse' (Witham et al., 2011) that is used to monitor all muscles in the synergistic group in parallel. This may be confirmed by testing for equal CMC phase lag values between the synergistic muscles, however this requires additional analyses.

7.3 Clinical relevance

In the context of Stroke recovery and Parkinson's disease rehabilitation, it could be speculated that extensive prior training involving wrist extensor movements, would in the short term result in lower associated CMC and perceived difficulty levels. More importantly, in the long term, particularly if applied early to groups with a high risk of Stroke or Parkinson's disease, it is possible that such extensor training would influence long term adaptation and may ultimately partially reduce the extensor motor deficits of those diseases. Furthermore, Lundbye and Nielsen (2008) brought forward the recovery tracking ability of CMC; as significantly reduced CMC levels, post hand and wrist immobilisation, subsequently returned to pre-immobilisation levels following a week of recovery time. Future rehabilitation programmes may thus incorporate CMC as an additional recovery tracking measure in Stroke and Parkinson's patients, and the present study may serve as a normative source reference in such a clinical setting, particularly at the wrist joint.

8 CONCLUSIONS

8.1 General conclusions

Wrist flexion was performed with significantly higher motor precision compared to wrist extension; agreeing with the study of Salonikidis et al. (2011). It was established that wrist flexors have significantly lower beta CMC levels (CMC_{MAX} and CMC_{AREA}) compared to wrist extensors during high precision isometric contraction, and implies an inverse beta CMC – motor precision relationship. Better functional suitability and long term adaptation of the flexors to isometric force production appear to be the main reasons for this inversion. Further, there was an observed direct co-variation between beta CMC, EMGβ-PSD and torque fluctuation (inversely related to precision); similar to the study of Ushiyama, Katsu et al. (2011). That is, higher beta CMC seems to be associated with higher EMGβ-PSD and lower motor precision. Additionally, it was established that isometric wrist flexion is performed with lower perceived difficulty compared to extension. It may be thus possible that that CMC levels may be directly correlated to the relative perceived difficulty levels experienced by the subjects in maintaining high motor precision during isometric contraction tasks. Perceived difficulty may have been enhanced for wrist extension due to its hypothetically inherent lower level of motor precision compared to flexion, and knowing that task performance can be gauged by the subject through the fluctuation of the visual indicator.

The following point is still unclear. Kristeva et al. (2007) suggest a direct beta CMC – motor precision relationship, whereas the present study and the study by Ushiyama, Katsu et al. (2011) suggest an inverse relationship. However, due to some experimental differences (see Section 8.2.1), it is not possible to conclusively say that higher beta CMC causes lower motor precision without additional analyses or experiments (see Section 8.3).

8.2 Limitations

8.2.1 Generalizability of the CMC - motor precision relationship

The study by Ushiyama, Katsu et al. (2011) was based on a single agonist muscle performing two different (pre/post fatigue) isometric force maintenance tasks (i.e. between-task, within-muscle). The experimental protocol in the present study, while being non-fatiguing

was based on different muscles performing two different (isometric wrist extension/flexion) tasks (i.e. between-task, between-muscle). Since both studies showed an inversion of the beta CMC – motor precision relationship, this was not necessarily solely due to the effect of fatigue. The Kristeva et al. study (2007) showing a direct beta CMC – motor precision relationship, was based on a single agonist muscle performing a single isometric force maintenance task (i.e. within-task, within-muscle). Thus muscle factors as well as task factors could have influenced the beta CMC – motor precision relationship in the present study when compared to the Kristeva etl al. (2007) study. Therefore the differences in experimental design of the 3 studies affect the generalizability of the relationship between CMC and precision.

Further, whilst the direct co-variation between beta CMC, EMGβ-PSD and torque fluctuation found in this study and the study of Ushiyama, Katsu et al. (2011) may support the findings of the inverse beta CMC - precision relationships (Ushiyama, Katsu, et al., 2011; Divekar and John, 2013), it does not however explain the direct relationship found in the within-task within-muscle study of Kristeva et al. (2007). However, whilst Kristeva et al. (2007) reported measures of beta CMC, subsequent variables in the sequence i.e. beta EMG and band separated (beta and low-frequency) torque fluctuations were not reported. Therefore additional analyses or experiments done on the data set of the present study, would clarify these relationships (see section 8.3).

In addition to agonist action, isometric movements are known to be also associated with antagonist co-contraction, a phenomenon that has been shown to co-vary with motor precision (Baratta et al., 1988; Gardner-Morse and Stokes, 1998; Burnett et al., 2000; Gribble et al., 2003), as well as with the precision demand of the isometric task (Osu et al., 2004; L. P. J. Selen et al., 2006; L. Selen et al., 2006; Lametti et al., 2007). As such, a study of the relationship between CMC and precision should include recordings of antagonist processes along with agonist. Yet, antagonist CMC has been a key omission, since virtually every study has focused solely on CMC measures of the agonists. Only Hansen et al. (2002) have reported CMC of both co-contracting agonist and antagonist muscles in order to study antagonistic coupling at the ankle joint; however they did not report a corresponding precision outcome. Furthermore, their subjects performed deliberate co-contraction of the

agonist-antagonist muscles, a method that was referred to as “un-natural”. Virtually every muscle has its antagonist, and although most CMC studies have not measured the EMG and hence CMC from the antagonist, this is not to say that antagonist activity did not occur in these studies. It has been indicated in EMG only studies; that agonist-antagonist co-contraction is a common phenomenon occurring during isometric contraction tasks. Since antagonist data was also recorded (but not analysed) in the present study, additional analyses would clarify the role of the antagonist.

8.2.2 Crosstalk EMG (Antagonists, Multiple Synergists)

As wrist flexion and extension is performed using multiple synergistic muscles (and multiple antagonistic muscles, considering agonist-antagonist co-contraction), there is the possibility of cross-talk in the EMG recordings. However even in the single agonist muscle study of Kristeva et al. (2007) there would still be the potential of an active antagonist, therefore antagonist cross-talk would still be a problem, in this study. Antagonist cross-talk would have been enhanced by the “un-natural” experiment of Hansen et al. (2002) which required deliberate co-contraction of the agonist-antagonist muscles, but this enhancement was avoided in the present study as subjects were instructed to either contract their flexors (during flexion) or extensors (during extension).

The agonist flexor group had significantly lower CMC_{MAX}, FW and CMC_{AREA} compared to the agonist extensor group in the present study, and these flexor-extensor comparisons are not affected by cross-talk because these were between-task comparisons (see Figures 6.3 - 6.6). However the within-task synergist comparisons could be influenced by inter-synergist cross-talk, but could also be compatible with synergists behaving similarly to each other which is known to be the case in the wrist joint. Therefore the only CMC uncertainty is whether the flexor and extensor groups could be analysed down to the level of individual muscles within the same group.

To reduce the effect of synergistic cross-talk, some research groups have focused on movements that are primarily performed by a single muscle, for example dorsiflexion primarily (60 %) performed by the tibialis anterior muscle (Ushiyama, Suzuki, et al., 2011). However, even in these studies, there is still the question of cross-talk from the antagonist muscle (even though the antagonist was not recorded) during natural co-contraction; for

example, the gastrocnemius muscle is the antagonist to the tibialis anterior that may co-contract and result in cross-talk.

Thus the only remaining potential criticism of the present study would be the choice of movement selected, as there are multiple synergists for wrist flexion and similarly multiple synergists for wrist extension. However, the studies of the wrist joint are very important clinically and it has been shown that wrist extensors are more impaired than wrist flexors during Parkinson's disease and after Stroke. Thus co-synergist action cannot be completely avoided, if the wrist joint is to be studied. Nevertheless, if CMC is studied but not specific to the wrist joint, this present study may be replicated using muscles with fewer synergists, for example comparisons between the antagonistic dorsi-plantar flexor movements would reduce but not eliminate (since tibialis anterior only accounts for 60% of force leaving the remaining 40% to be produced by synergists) the co-contracting synergist issue.

8.2.3 Crosstalk EEG

Due to the low spatial resolution of EEG for example compared to MEG; cross-talk from cortical areas representing co-contracting muscles is another limitation of this study. However this limitation is equally applicable to all experiments of movements involving contraction (whether co-contracting synergists or antagonists) of more than one muscle. Therefore even if a study ignores the co-contracting muscles, those muscle actions would still have an influence on the corresponding EEG, since both synergist and antagonist cortical areas would be close to each other.

8.3 Future Work

Future work (currently in preparation) to elucidate the relationship between CMC and precision should be carried out by examining the co-variation in beta CMC, EMGβ-PSD and torque fluctuation in the within-task within-muscle scenario of Kristeva et al. (2007). Further, the examination should be inclusive of co-contracting antagonist variables and thereby also examine the yet to be studied relationship between antagonist CMC and motor precision. Thus overall, compare variables: beta CMC, beta EMG, beta torque fluctuation and low-frequency torque fluctuation between high-precision (HP) and low-precision (LP) periods within wrist flexion and extension tasks (within-task, within-muscle), in agonists and co-contracting antagonists alike. As Kristeva et al. (2007) also found a relation between beta

EEG and precision, this variable should also be additionally compared between HP and LP. Such a study would more conclusively resolve the relationship between CMC and motor precision, and the corresponding co-varying variables.

REFFERENCES

Alegre M, Labarga A, Gurtubay I, Iriarte J, Malanda A, Artieda J. Movement-related changes in cortical oscillatory activity in ballistic, sustained and negative movements. Exp Brain Res. 2003 Jan 1;148(1):17–25.

Aymard C, Decchi B, Katz R, Lafitte C, Pénicaud A, Raoul S, et al. Recurrent inhibition between motor nuclei innervating opposing wrist muscles in the human upper limb. J Physiol. 1997;499(Pt 1):267–82.

Babiloni F, Cincotti F, Carducci F, Rossini PM, Babiloni C. Spatial enhancement of EEG data by surface Laplacian estimation: the use of magnetic resonance imaging-based head models. Clinical neurophysiology : official journal of the International Federation of Clinical Neurophysiology. 2001 May 1;112(5):724–7.

Baker MR, Baker SN. The effect of diazepam on motor cortical oscillations and corticomuscular coherence studied in man. J Physiol. 2003;546(3):931–42.

Baker SN. Oscillatory interactions between sensorimotor cortex and the periphery. Curr Opin Neurobiol. 2007 Dec;17(6):649–55.

Baker SN, Chiu M, Fetz EE. Afferent Encoding of Central Oscillations in the Monkey Arm. J Neurophysiol. 2006 Jun;95(6):3904 –3910.

Baker SN, Olivier E, Lemon RN. Coherent oscillations in monkey motor cortex and hand muscle EMG show task-dependent modulation. J Physiol. 1997 May 1;501(1):225–41.

Banks R. An allometric analysis of the number of muscle spindles in mammalian skeletal muscles. J Anat. 2006;208(6):753–68.

Baratta R, Solomonow M, Zhou BH, Letson D, Chuinard R, D'Ambrosia R. Muscular Coactivation The Role of the Antagonist Musculature in Maintaining Knee Stability. Am J Sports Med. 1988 Mar 1;16(2):113–22.

Basmajian JV. Muscles Alive: Their Functions Revealed by Electromyography. Williams & Wilkins; 1974.

Bawa P, Chalmers GR, Jones KE, Søgaard K, Walsh ML. Control of the wrist joint in humans. Eur J Appl Physiol. 2000 Oct 7;83(2):116–27.

Brown P. Cortical drives to human muscle: the Piper and related rhythms. Progress in Neurobiology. 2000 Jan;60(1):97–108.

Brown P, Marsden C. What do the basal ganglia do? The Lancet. 1998 Jun 13;351(9118):1801–4.

Brown P, Salenius S, Rothwell JC, Hari R. Cortical Correlate of the Piper Rhythm in Humans. J Neurophysiol. 1998 Dec 1;80(6):2911 –2917.

Büchel C, Coull JT, Friston KJ. The Predictive Value of Changes in Effective Connectivity for Human Learning. Science. 1999 Mar 5;283(5407):1538 –1541.

Burnett RA, Laidlaw DH, Enoka RM. Coactivation of the antagonist muscle does not covary with steadiness in old adults. J Appl Physiol. 2000 Jul 1;89(1):61–71.

Chakarov V, Naranjo JR, Schulte-Monting J, Omlor W, Huethe F, Kristeva R. Beta-Range EEG-EMG Coherence With Isometric Compensation for Increasing Modulated Low-Level Forces. J Neurophysiol. 2009 May 20;102(2):1115–20.

Chapman CE, Bushnell MC, Miron D, Duncan GH, Lund JP. Sensory perception during movement in man. Exp Brain Res. 1987 Nov;68(3):516–24.

Chen D, Fetz EE. Characteristic Membrane Potential Trajectories in Primate Sensorimotor Cortex Neurons Recorded In Vivo. J Neurophysiol. 2005 Oct 1;94(4):2713–25.

Cheney PD, Fetz EE. Functional classes of primate corticomotoneuronal cells and their relation to active force. J Neurophysiol. 1980;44(4):773–91.

Cheyne D, Kristeva R, Deecke L. Homuncular organization of human motor cortex as indicated by neuromagnetic recordings. Neurosci Lett. 1991 Jan 14;122(1):17–20.

Chye L, Nosaka K, Murray L, Edwards D, Thickbroom G. Corticomotor excitability of wrist flexor and extensor muscles during active and passive movement. Human Movement Science. 2010 Aug;29(4):494–501.

Conway BA, Halliday DM, Farmer SF, Shahani U, Maas P, Weir AI, et al. Synchronization between motor cortex and spinal motoneuronal pool during the performance of a maintained motor task in man. J Physiol. 1995;489(Pt 3):917–24.

Daube JR, Rubin DI. Clinical Neurophysiology. Oxford University Press; 2009.

Divekar NV, John LR. Neurophysiological, behavioural and perceptual differences between wrist flexion and extension related to sensorimotor monitoring as shown by corticomuscular coherence. Clin Neurophysiol. 2013 Jan;124(1):136–47.

Duncan P, Badke M. The recovery of motor control. Stroke Rehab. Year Book Medical Pub; 1987.

Engel AK, Fries P. Beta-band oscillations — signalling the status quo? Curr Opin Neurobiol. 2010 Apr;20(2):156–65.

Enoka RM, Christou EA, Hunter SK, Kornatz KW, Semmler JG, Taylor AM, et al. Mechanisms that contribute to differences in motor performance between young and old adults. Journal of Electromyography and Kinesiology. 2003 Feb;13(1):1–12.

Farina D, Negro F, Jiang N. Identification of common synaptic inputs to motor neurons from the rectified electromyogram. J Physiol. 2013 May 15;591(10):2403–18.

Gardner-Morse MG, Stokes IAF. The Effects of Abdominal Muscle Coactivation on Lumbar Spine Stability. Spine [Internet]. 1998;23(1). Available from: http://journals.lww.com/spinejournal/Fulltext/1998/01010/The_Effects_of_Abdominal_Muscle_Coactivation_on.19.aspx

Gathercole SE. Cognitive approaches to the development of short-term memory. Trends in Cognitive Sciences. 1999 Nov 1;3(11):410–9.

Gilbertson T, Lalo E, Doyle L, Di Lazzaro V, Cioni B, Brown P. Existing Motor State Is Favored at the Expense of New Movement during 13-35 Hz Oscillatory Synchrony in the Human Corticospinal System. J Neurosci. 2005;25(34):7771 –7779.

Gribble PL, Mullin LI, Cothros N, Mattar A. Role of Cocontraction in Arm Movement Accuracy. J Neurophysiol. 2003 May 1;89(5):2396 –2405.

Gross J, Tass PA, Salenius S, Hari R, Freund H-J, Schnitzler A. Cortico-muscular synchronization during isometric muscle contraction in humans as revealed by magnetoencephalography. J Physiol. 2000 Sep 1;527(3):623–31.

Gueorguieva R, Krystal JH. Move over ANOVA: progress in analyzing repeated-measures data and its reflection in papers published in the Archives of General Psychiatry. Arch Gen Psychiatry. 2004;61(3):310–7.

Guevara MA, Corsi-Cabrera M. EEG coherence or EEG correlation? Int J Psychophysiol. 1996 Oct;23(3):145–53.

Guyton AC, Hall J. Textbook of Medical Physiology. 11th ed. Elsevier; 2006.

Halliday D. A framework for the analysis of mixed time series/point process data—Theory and application to the study of physiological tremor, single motor unit discharges and electromyograms. Prog Biophys Mol Biol. 1995;64(2-3):237–78.

Halliday DM, Conway BA, Farmer SF, Rosenberg JR. Using electroencephalography to study functional coupling between cortical activity and electromyograms during voluntary contractions in humans. Neurosci Lett. 1998;241(1):5–8.

Halliday DM, Farmer SF. On the Need for Rectification of Surface EMG. J Neurophysiol. 2010 Jun 1;103(6):3547–3547.

Hamilton AF de C, Jones KE, Wolpert DM. The scaling of motor noise with muscle strength and motor unit number in humans. Exp Brain Res. 2004 Aug 1;157(4):417–30.

Handy TC. Event-Related Potentials: A Methods Handbook. MIT Press; 2005.

Hansen S, Hansen N, Christensen L, Petersen N, Nielsen J. Coupling of antagonistic ankle muscles during co-contraction in humans. Exp Brain Res. 2002;146(3):282–92.

Hermens HJ, Freriks B, Merletti R, Stegeman D, Blok J, Rau G, et al. European recommendations for surface electromyography [Internet]. Roessingh Research and

Development The Netherlands; 1999 [cited 2013 Aug 19]. Available from: http://www.seniam.org/pdf/contents8.PDF

Herrero M-T, Barcia C, Navarro J. Functional anatomy of thalamus and basal ganglia. Child's Nervous System. 2002;18(8):386–404.

Hjorth B. An on-line transformation of EEG scalp potentials into orthogonal source derivations. Electroenceph clin Neurophysiol. 1975 Nov;39(5):526–30.

Hluštík P, Solodkin A, Gullapalli RP, Noll DC, Small SL. Somatotopy in Human Primary Motor and Somatosensory Hand Representations Revisited. Cereb Cortex. 2001 Apr 1;11(4):312 –321.

Horowitz P, Hill W. The Art of Electronics. Cambridge University Press; 2006.

Johnson AN, Wheaton LA, Shinohara M. Attenuation of corticomuscular coherence with additional motor or non-motor task. Clin Neurophysiol. 2011;122(2):356–63.

Kaiser D. Brodmann Montage [Internet]. 2013. Available from: http://www.skiltopo.com/papers/BrodmannMontageKaiser-v2.pdf

Katz R, Mazzocchio R, Penicaud A, Rossi A. Distribution of recurrent inhibition in the human upper limb. Acta Physiol. 1993;149(2):183–98.

Kayser J. CSD Toolbox - Current Source Density (CSD) and Surface Potential (SP) interpolation using spherical splines [Internet]. 2011 [cited 2012 Jan 21]. Available from: http://psychophysiology.cpmc.columbia.edu/Software/CSDtoolbox/

Kayser J, Tenke CE. Principal components analysis of Laplacian waveforms as a generic method for identifying ERP generator patterns: I. Evaluation with auditory oddball tasks. Clin Neurophysiol. 2006;117(2):348–68.

Kayser J, Tenke CE. Principal components analysis of Laplacian waveforms as a generic method for identifying ERP generator patterns: II. Adequacy of low-density estimates. Clin Neurophysiol. 2006;117(2):369–80.

Keifer J, Houk J. Motor function of the cerebellorubrospinal system. Physiol Rev. 1994;74(3):509–42.

Kilner JM, Alonso-Alonso M, Fisher R, Lemon RN. Modulation of synchrony between single motor units during precision grip tasks in humans. J Physiol. 2002 Jun 1;541(3):937–48.

Knierim J. Neuroscience Online Text Book [Internet]. Motor Units and Muscle Receptors (Section 3, Chapter 1) Neuroscience Online: An Electronic Textbook for the Neurosciences | Department of Neurobiology and Anatomy - The University of Texas Medical School at Houston. 2013 [cited 2013 Mar 4]. Available from: http://neuroscience.uth.tmc.edu/s3/chapter01.html

Kristeva R, Patino L, Omlor W. Beta-range cortical motor spectral power and corticomuscular coherence as a mechanism for effective corticospinal interaction during steady-state motor output. Neuroimage. 2007;36(3):785–92.

Kristeva-Feige R, Fritsch C, Timmer J, Lücking CH. Effects of attention and precision of exerted force on beta range EEG-EMG synchronization during a maintained motor contraction task. Clin Neurophysiol. 2002;113(1):124–31.

Kumar S, Mital A. Electromyography in Ergonomics. Taylor & Francis; 1996.

Laine CM, Nickerson LA, Bailey EF. Cortical entrainment of human hypoglossal motor unit activities. J Neurophysiol. 2012 Jan 1;107(1):493–9.

Lametti DR, Houle G, Ostry DJ. Control of Movement Variability and the Regulation of Limb Impedance. J Neurophysiol. 2007 Dec 1;98(6):3516 –3524.

Lieberman J. Hemiplegia: Rehabilitation of upper extremity. Stroke Rehab. Butterworths, Boston; 1986. p. 95–117.

Little J, Massagli T. Spasticity and associated abnormalities of muscle tone. Rehabilitation medicine principles and practice. 3rd ed. Lippincott-Raven; 2007. p. 997–1013.

Lundbye-Jensen J, Nielsen JB. Central nervous adaptations following 1 wk of wrist and hand immobilization. J Appl Physiol. 2008 May 1;105(1):139–51.

Matsuya R, Ushiyama J, Ushiba J. Prolonged reaction time during episodes of elevated β-band corticomuscular coupling and associated oscillatory muscle activity. J Appl Physiol. 2013 Apr 1;114(7):896–904.

Mavvidis A, Stamboulis A, Dimitiou V, Giampanidoy A. Differences in forehand and backhand performance in young tennis players. Stud Phys cult tour. 2010;17(4):315–9.

Mendez-Balbuena I, Naranjo JR, Wang X, Andrykiewicz A, Huethe F, Schulte-Mönting J, et al. The strength of the corticospinal coherence depends on the predictability of modulated isometric forces. J Neurophysiol. 2013 Mar 15;109(6):1579–88.

Merletti R, Di Torino P. Standards for reporting EMG data. J Electromyogr Kinesiol. 1999;9(1):3–4.

Mima Tatsuya, Hallett M. Electroencephalographic analysis of cortico-muscular coherence: reference effect, volume conduction and generator mechanism. Clin Neurophysiol. 1999 Nov 1;110(11):1892–9.

Mima T., Hallett M. Corticomuscular coherence: a review. Clin Neurophysiol. 1999;16(6):501.

Mink JW, Thach WT. Basal ganglia motor control. III. Pallidal ablation: normal reaction time, muscle cocontraction, and slow movement. J Neurophysiol. 1991 Feb 1;65(2):330 –351.

Netter FH. Atlas of Human Anatomy. Elsevier Health Sciences; 2010.

De Noordhout AM, Rapisarda G, Bogacz D, Gérard P, De Pasqua V, Pennisi G, et al. Corticomotoneuronal synaptic connections in normal man. Brain. 1999 Jul 1;122(7):1327 –1340.

Nunez P. Estimation of large scale neocortical source activity with EEG surface Laplacians. Brain Topogr. 1989 Sep 1;2(1-2):141–54.

Oldfield R. The assessment and analysis of handedness: The Edinburgh inventory. Neuropsychologia. 1971;9(1):97–113.

Omlor W, Patino L, Mendez-Balbuena I, Schulte-Mönting J, Kristeva R. Corticospinal Beta-Range Coherence Is Highly Dependent on the Pre-stationary Motor State. J Neurosci. 2011 Jun 1;31(22):8037–45.

Osu R, Kamimura N, Iwasaki H, Nakano E, Harris CM, Wada Y, et al. Optimal Impedance Control for Task Achievement in the Presence of Signal-Dependent Noise. J Neurophysiol. 2004;92(2):1199 –1215.

Palmer E, Ashby P. Corticospinal projections to upper limb motoneurones in humans. J Physiol. 1992;448(1):397–412.

Park H, Kim JS, Paek SH, Jeon BS, Lee JY, Chung CK. Cortico-muscular coherence increases with tremor improvement after deep brain stimulation in Parkinson's disease. NeuroReport [Internet]. 2009;20(16). Available from: http://journals.lww.com/neuroreport/Fulltext/2009/10280/Cortico_muscular_coherence_increases_with_tremor.10.aspx

Pauluis Q, Baker S, Olivier E. Emergent Oscillations in a Realistic Network: The Role of Inhibition and the Effect of the Spatiotemporal Distribution of the Input. J Comput Neurosci. 1999 Jan 1;6(1):27–48.

Perrin F, Pernier J, Bertrand O, Echallier J. Spherical splines for scalp potential and current density mapping. Electroenceph clin Neurophysiol. 1989;72(2):184–7.

Pfann KD, Comella CL, Corcos DM, Brandabur M, Robichaud JA. Greater impairment of extension movements as compared to flexion movements in Parkinson's disease. Exp Brain Res. 2004 May 1;156(2):240–54.

Pfurtscheller G, Neuper C, Brunner C, da Silva FL. Beta rebound after different types of motor imagery in man. Neurosci Lett. 2005 Apr 22;378(3):156–9.

Pfurtscheller G, Stancák Jr. A, Neuper C. Post-movement beta synchronization. A correlate of an idling motor area? Electroenceph clin Neurophysiol. 1996 Apr;98(4):281–93.

Phillips C, Porter R. The Pyramidal Projection to Motoneurones of Some Muscle Groups of the Baboon's Forelimb. Physiology of spinal neurons. Elsevier; 1964.

Pogosyan A, Gaynor LD, Eusebio A, Brown P. Boosting Cortical Activity at Beta-Band Frequencies Slows Movement in Humans. Current Biology. 2009 Oct 13;19(19):1637–41.

Riddle C, Baker S. Digit displacement, not object compliance, underlies task dependent modulations in human corticomuscular coherence. Neuroimage. 2006 Nov;33(2):618–27.

Riddle CN, Baker MR, Baker SN. The effect of carbamazepine on human corticomuscular coherence. Neuroimage. 2004;22(1):333–40.

Riddle CN, Baker SN. Manipulation of peripheral neural feedback loops alters human corticomuscular coherence. J Physiol. 2005 Jul 1;566(2):625–39.

Riddle CN, Baker SN. Convergence of Pyramidal and Medial Brain Stem Descending Pathways Onto Macaque Cervical Spinal Interneurons. J Neurophysiol. 2010 May 1;103(5):2821–32.

Riddle CN, Edgley SA, Baker SN. Direct and Indirect Connections with Upper Limb Motoneurons from the Primate Reticulospinal Tract. J Neurosci. 2009 Apr 15;29(15):4993–9.

Roopun AK, Middleton SJ, Cunningham MO, LeBeau FEN, Bibbig A, Whittington MA, et al. A beta2-frequency (20–30 Hz) oscillation in nonsynaptic networks of somatosensory cortex. Proceedings of the National Academy of Sciences. 2006 Oct 17;103(42):15646–50.

Rosenberg JR, Amjad AM, Breeze P, Brillinger DR, Halliday DM. The Fourier approach to the identification of functional coupling between neuronal spike trains. Prog Biophys Mol Biol. 1989;53(1):1–31.

Rubino D, Robbins KA, Hatsopoulos NG. Propagating waves mediate information transfer in the motor cortex. Nat Neurosci. 2006 Dec;9(12):1549–57.

Sabate M, Llanos C, Enriquez E, Rodriguez M. Mu rhythm, visual processing and motor control. Clin Neurophysiol. 2012 Mar;123(3):550–7.

Salenius S, Hari R. Synchronous cortical oscillatory activity during motor action. Curr Opin Neurobiol. 2003 Dec;13(6):678–84.

Salenius S, Portin K, Kajola M, Salmelin R, Hari R. Cortical Control of Human Motoneuron Firing During Isometric Contraction. J Neurophysiol. 1997 Jun 1;77(6):3401–5.

Salenius S, Salmelin R, Neuper C, Pfurtscheller G, Hari R. Human cortical 40 Hz rhythm is closely related to EMG rhythmicity. Neurosci Lett. 1996 Aug 2;213(2):75–8.

Salmelin R, Hámáaláinen M, Kajola M, Hari R. Functional Segregation of Movement-Related Rhythmic Activity in the Human Brain. NeuroImage. 1995 Dec;2(4):237–43.

Salmelin R, Hari R. Spatiotemporal characteristics of sensorimotor neuromagnetic rhythms related to thumb movement. Neuroscience. 1994 May;60(2):537–50.

Salonikidis K, Amiridis I, Oxyzoglou N, Giagazoglou P, Akrivopoulou G. Wrist Flexors are Steadier than Extensors. Int J Sports Med. 2011;32(10):754–60.

Schoffelen J-M, Oostenveld R, Fries P. Neuronal Coherence as a Mechanism of Effective Corticospinal Interaction. Science. 2005 Apr 1;308(5718):111–3.

Seitz RJ, Roland PE, Bohm C, Greitz T. Motor learning in man: A positron emission tomographic study. Neuroreport. 1990;1(1):57–60.

Selen L, Beek P, van Dieën J. Impedance is modulated to meet accuracy demands during goal-directed arm movements. Exp Brain Res. 2006;172(1):129–38.

Selen LPJ, van Dieën JH, Beek PJ. Impedance Modulation and Feedback Corrections in Tracking Targets of Variable Size and Frequency. J Neurophysiol. 2006 Nov 1;96(5):2750 –2759.

Semmler JG, Nordstrom MA. Motor unit discharge and force tremor in skill-and strength-trained individuals. Exp Brain Res. 1998;119(1):27–38.

Semmler JG, Sale MV, Meyer FG, Nordstrom MA. Motor-Unit Coherence and Its Relation With Synchrony Are Influenced by Training. J Neurophysiol. 2004 Dec 1;92(6):3320 – 3331.

Shaw JC. An introduction to the coherence function and its use in EEG signal analysis. J Med Eng Technol. 1981 Jan 1;5(6):279–88.

Stancák Jr. A, Pfurtscheller G. Event-related desynchronisation of central beta-rhythms during brisk and slow self-paced finger movements of dominant and nondominant hand. Cognitive Brain Research. 1996 Oct;4(3):171–83.

Stegeman D, Hermens H. Standards for surface electromyography: The European project Surface EMG for non-invasive assessment of muscles (SENIAM). Línea). Disponible en: http://www. med. uni-jena. de/motorik/pdf/stegeman. pdf [Consultado en agosto de 2008] [Internet]. 2007 [cited 2013 Aug 19]; Available from: http://www.med.uni-jena.de/motorik/pdf/stegeman.pdf

Tracy BL. Force control is impaired in the ankle plantarflexors of elderly adults. Eur J Appl Physiol. 2007 Aug 15;101(5):629–36.

University of Michigan. The Human Brain [Internet]. The Human Brain. 2013. Available from: http://www.umich.edu/~cogneuro/jpg/Brodmann.html

University of Wisconsin-Madison. Motor Systems [Internet]. Motor Systems. 2009. Available from: http://www.neuroanatomy.wisc.edu/coursebook/motor1.pdf

Ushiyama J, Katsu M, Masakado Y, Kimura A, Liu M, Ushiba J. Muscle fatigue-induced enhancement of corticomuscular coherence following sustained submaximal

isometric contraction of the tibialis anterior muscle. J Appl Physiol. 2011;110(5):1233–40.

Ushiyama J, Suzuki T, Masakado Y, Hase K, Kimura A, Liu M, et al. Between-subject variance in the magnitude of corticomuscular coherence during tonic isometric contraction of the tibialis anterior muscle in healthy young adults. J Neurophysiol. 2011;106(3):1379 –1388.

Ushiyama J, Takahashi Y, Ushiba J. Muscle dependency of corticomuscular coherence in upper and lower limb muscles and training-related alterations in ballet dancers and weightlifters. J Appl Physiol. 2010;109(4):1086–95.

Vallence AM, Hammond GR, Reilly KT. Increase in flexor but not extensor corticospinal motor outputs following ischemic nerve block. J Neurophysiol. 2012;107(12):3417–27.

Williams ER, Baker SN. Renshaw Cell Recurrent Inhibition Improves Physiological Tremor by Reducing Corticomuscular Coupling at 10 Hz. J Neurosci. 2009 May 20;29(20):6616 – 6624.

Williams ER, Soteropoulos DS, Baker SN. Spinal interneuron circuits reduce approximately 10-Hz movement discontinuities by phase cancellation. Proceedings of the National Academy of Sciences. 2010 Jun 15;107(24):11098–103.

Witham CL, Riddle CN, Baker MR, Baker SN. Contributions of descending and ascending pathways to corticomuscular coherence in humans. J Physiol. 2011;589(15):3789–800.

Witte M, Patino L, Andrykiewicz A, Hepp-Reymond M, Kristeva R. Modulation of human corticomuscular beta-range coherence with low-level static forces. Eur J Neurosci. 2007 Dec 1;26(12):3564–70.

World Medical Association. WMA Declaration of Helsinki - Ethical Principles for Medical Research Involving Human Subjects [Internet]. 2008 [cited 2012 Jan 20]. Available from: http://www.wma.net/en/30publications/10policies/b3/

Yang Q, Fang Y, Sun C-K, Siemionow V, Ranganathan VK, Khoshknabi D, et al. Weakening of functional corticomuscular coupling during muscle fatigue. Brain Res. 2009 Jan 23;1250(0):101–12.

Yao W, Fuglevand RJ, Enoka RM. Motor-unit synchronization increases EMG amplitude and decreases force steadiness of simulated contractions. J Neurophysiol. 2000;83(1):441–52.

Yue GH, Liu JZ, Siemionow V, Ranganathan VK, Ng TC, Sahgal V. Brain activation during human finger extension and flexion movements. Brain Res. 2000;856(1-2):291–300.

OpenEEG hardware [Internet]. 2013 [cited 2013 Mar 5]. Available from: http://openeeg.sourceforge.net/doc/hw/

APPENDICES

APPENDIX A BRODMANN AREAS

Brodmann areas were laid out by the German anatomist Korbinian Brodmann, who studied the cytoarchitectural organization of the human cortex. Since then they have been refined, and renamed. Figure A.1 shows the Brodmann areas relative to the frontal, parietal, temporal and occipital lobes of the human cerebral cortex.

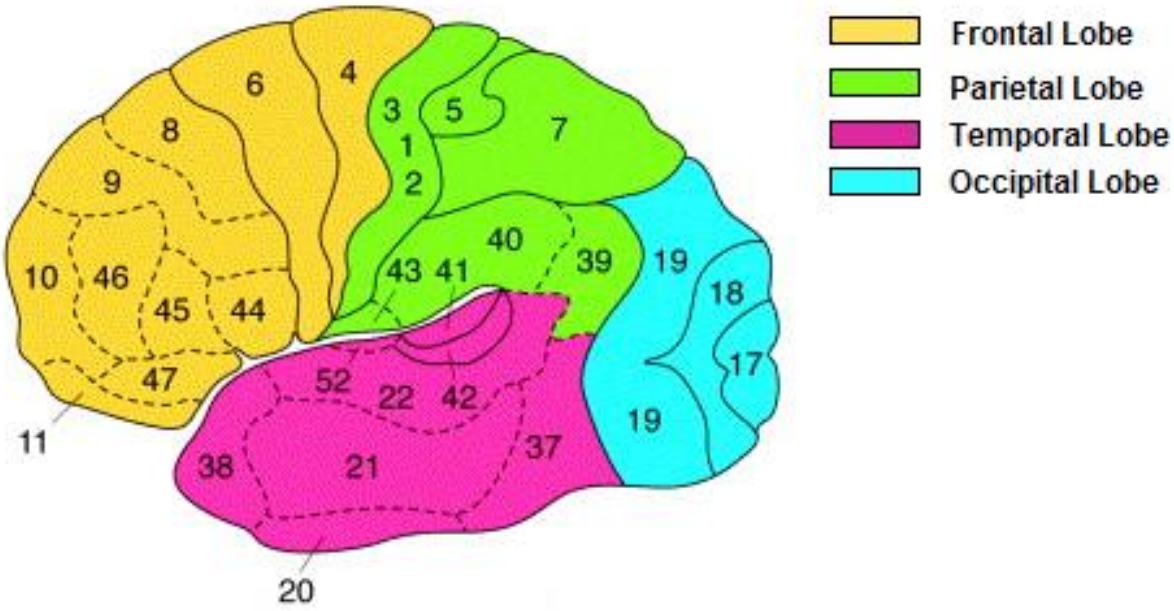

Figure A.1 Brodmann areas. Adapted from Gathercole (Gathercole, 1999).

Table 1 lists some important functional divisions of the cerebral cortex, i.e. vision, audition, body sensation and motor, and their corresponding Brodmann areas; while Table 2 lists all the Broadmann areas and their corresponding closest 10-10 EEG electrode positions.

Table 1 Brain functions related to Brodmann areas. Adapted from University of Michigan online (University of Michigan, 2013).

Function	Brodmann Area
Vision	
Primary	17
Secondary	18,19,20,21,37
Audition	
Primary	41
Secondary	22, 42
Body Sensation	
Primary	1,2,3
Secondary	5,7
Tertiary	7, 22, 37, 39, 40
Motor	
Primary	4
Secondary	6
Tertiary	9, 10, 11, 45, 46, 47
Eye movement	8
Speech	44

Table 2 Closest 10-10 Electrode position to the center of each Brodmann area in the Brodmann montage. Adapted from Kaiser (Kaiser, 2013).

Brodmann Area	Closest 10-10 electrode	Closest 10-10 electrode	Brodmann Area	Closest 10-10 electrode	Closest 10-10 electrode
ba01	C3	C4	ba21	T7	T8
ba02	C3	C4	ba22	T7	T8
ba03	C3	C4	ba23	Pz	Pz
ba04	C3	C4	ba24	F1	F2
ba05	C1	CP2	ba31	Pz	Pz
ba06	FC3	FC4	ba32	F1	AFz
ba07	P1	P2	ba37	P7	P8
ba08	F1	F2	ba38	FT9	FT10
ba09	AF3	AF4	ba39	P5	P6
ba10	FP1	FP2	ba40	CP3	CP4
ba11	AF7	FPz	ba41	C5	T8
ba17	O1	O2	ba42	T7	C6
ba18	O1	O2	BROCA	F5	
ba19	PO7	PO4	ba44		FC6
ba20	FT9	FT10	ba45		F8
			ba46	AF7	F6
			ba47	F7	F8

APPENDIX B TORQUE SYSTEM

Stress and strain calculations of steel bars

The cantilever beams on which the strain gauges are placed resist the torque produced by the wrist. It is important that the dimensions of the beams are such that the stress placed on them at maximum voluntary contraction does not exceed their elastic limit. It is also important that the beams bend sufficiently to effectively measure the torque produced by the wrist i.e. they are sensitive enough. According to a previous study (Lundbye-Jensen and Nielsen, 2008) the average MVC for wrist flexion was 16 Nm and for wrist extension was 8 Nm. As the dimensions of the beams are symmetric in the flexion-extension direction, it was assumed that the beam should be able to handle the higher (flexion) MVC between extension and flexion i.e. 16 Nm. It was assumed that the MVC of any subject would not be 1.5 times higher than the average MVC i.e. 16 Nm $\times$ 1.5 = 24 Nm.

Figure B.1 shows the force application regions (contact regions) on the hand during isometric wrist flexion and extension against the perspex cast. Figure B.2 shows the dimensions of the testing rig including the perspex cast and beams, while Figure B.3 shows the dimensions of a single beam in particular. It was decided that the length (L) of the effective beam should be 0.07 m (70 mm) i.e. the distance between the average point of force application and the strain gauges. This was so that the average point of force application would be at the end of the beam if the wrist pivot point is considered to be at 0 mm and the average length between the wrist pivot point and the contact region on the hand is 113 mm, then 113 mm – 43 mm (distance from wrist pivot to strain gauges) = 70 mm (length of beam). It was decided that the breadth (b) of the beam should be 0.01 m (enough to place the strain gauges). The next step was to work out the height (h) the beam should have in order to have sensitivity to torque whilst still remaining in the elastic limits. Every material has a limit to how much stress it can handle before its deformation is termed as plastic (non-elastic); and is termed it's yield strength. It was thus decided to make the height of the beam in such a way that at MVC, the beam would be at 50% of its yield strength. The yield strength of mild steel is 248 MPa. So 50% of this is 124 MPa.

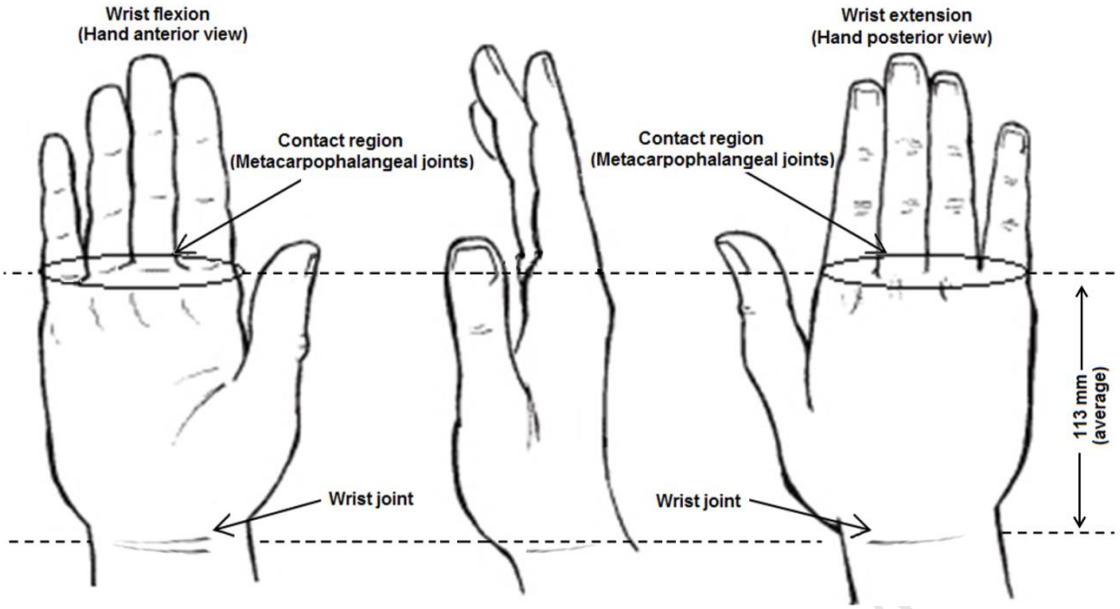

Figure B.1 Force application regions on hand during isometric wrist flexion and extension.

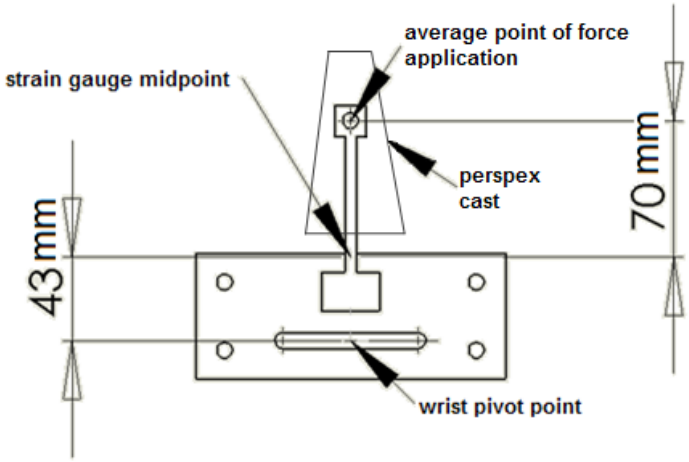

Figure B.2 Top view of testing manipulandum, including dimensions.

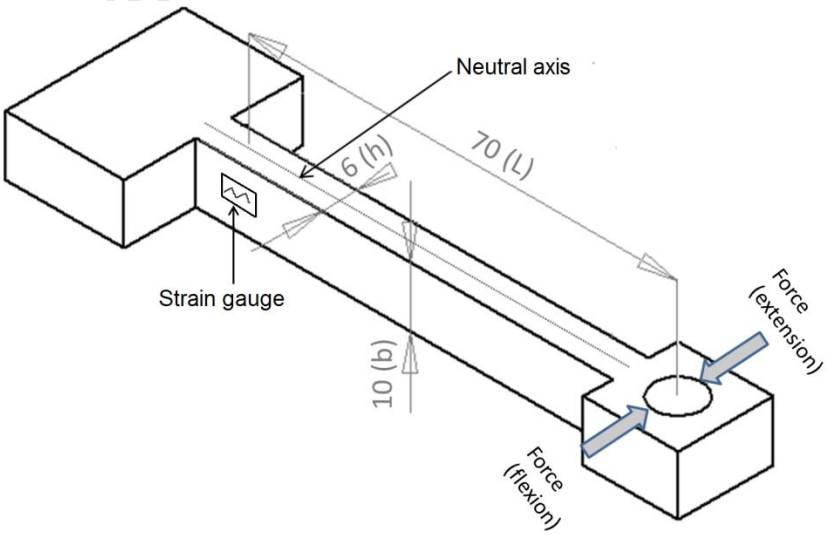

Figure B.3 Isometric view of a single mild steel beam including dimensions (in mm).

The equation for working out the stress (σ) at a cantilever beam due to a bending moment (M) is as follows:

$$\sigma = \frac{My}{I} \qquad \textbf{Eq B.1}$$

The bending moment (torque) on a beam due to a point force is:

$$M = WL \qquad \textbf{Eq B.2}$$

Where W is the force applied and L is the distance to the point force. In the case of this experiment the force applied will be as a result of the torque produced about the wrist. If 24 Nm is considered to be the MVC torque then, this should produce a point force of 24 Nm / (0.07m + 0.043m) = 212.4 N at the average point of force application. As there are two beams sharing this force, each beam would be subjected to a force of 212.4 N / 2 = 106.2 N. This force in turn would produce a moment of 106.2 N × 0.07 m = 7.43 Nm on the cantilever beam at the location of the strain gauges, i.e. M = 7.43 Nm.

Y is the distance from the neutral axis (no stress) to the surface where the strain gauges are placed (maximum stress). For a rectangular beam the neutral axis is halfway between the two sides of the beam, i.e. y = h/2.

I is the moment of inertia of the beam about the bending axis. The higher the moment of inertia, the lower the stress the beam will experience for a given moment. For a rectangular beam:

$$I = \frac{bh^3}{12} \qquad \textbf{Eq B.3}$$

Therefore with beam height (h) being the only unknown left, Eq B.1 becomes:

$124\ \mathrm{MPa} = (7.43\ \times h/2)/((0.01\ \times h\text{^}3)/12).$

This resolves to h being 0.006 m i.e. 6 mm. This was the height chosen for the cantilever beams.

Strain (ε) in a material is proportional to stress using the following equation:

$$\varepsilon = \frac{\sigma}{E} \qquad \textbf{Eq B.4}$$

E is the Young's Modulus of the material. E for mild steel is 210000 MPa. Therefore strain at the strain gauges at MVC will be 124 MPa / 210000 MPa = 590 microstrain. This is well within the limits of the strain gauges which are ± 3000 microstrain.

Output voltage calculation

A full bridge strain gauge system was implemented, with a gauge on each side of a cantilever beam. For a full bridge system:

Eq B.5

Where V_o is the output voltage, V_s is the bridge supply voltage, G_s is the gain factor of the strain gauges (2.0 for the gauges used), G_a is the amplification and ε is the strain. The bridge supply voltage was set to 4.0 V. Too high a bridge voltage will increase sensitivity of the bridge but however result in a higher current passing through the strain gauges. The gain (G_a) on the amplifier circuit was set to 2701. With this configuration, for a typical average flexion MVC torque of 16 Nm, resulting in 393.33 microstrain (590 microstrain / 24 Nm 16 Nm), a theoretical V_o of 4.0V 2.0 2701 393.33 E-6 = 8.49 V would be achieved.

Calibration of the torque system

For the estimation of MVC in terms of torque (Nm)[6], a full calibration of the torque system was done using a spring load (known force output) applied at the average point of force application.

Calibration for wrist extension direction

Table 3 shows the calibration data for the extension direction using the spring load and Figure B.4 shows the scatter plot of Voltage vs Force along with the best fit line through the points.

Table 3 Calibration data for extension direction.

Mass (kg)	Force (N)	Trial 1 (V)	Trial 2 (V)	Average (V)
1	9.81	0.77	0.81	0.79
2	19.62	1.28	1.29	1.29
3	29.43	1.89	1.94	1.91
4	39.24	2.50	2.42	2.46
5	49.05	2.98	2.90	2.94
6	58.86	3.45	3.49	3.47
7	68.67	4.11	4.03	4.07

[6] Note that calibration values were not used for the remaining behavioural variables i.e. PRECISION, Torque-low-PSD and Torqueβ-PSD, as these were based on normalised i.e. % MVC measures of Torque, i.e. voltage of torque produced by the subject during the experiment scaled by voltage produced during MVC.

8	78.48	4.60	4.52	4.56
9	88.29	5.24	5.08	5.16
10	98.1	5.72	5.73	5.73
11	107.91	6.20	6.24	6.22
12	117.72	6.74	6.67	6.71
13	127.53	7.23	7.17	7.20
14	137.34	7.69	7.68	7.69
15	147.15	8.17	8.19	8.18
16	156.96	8.64	8.69	8.67
17	166.77	9.16	9.15	9.15
18	176.58	9.65	9.64	9.65

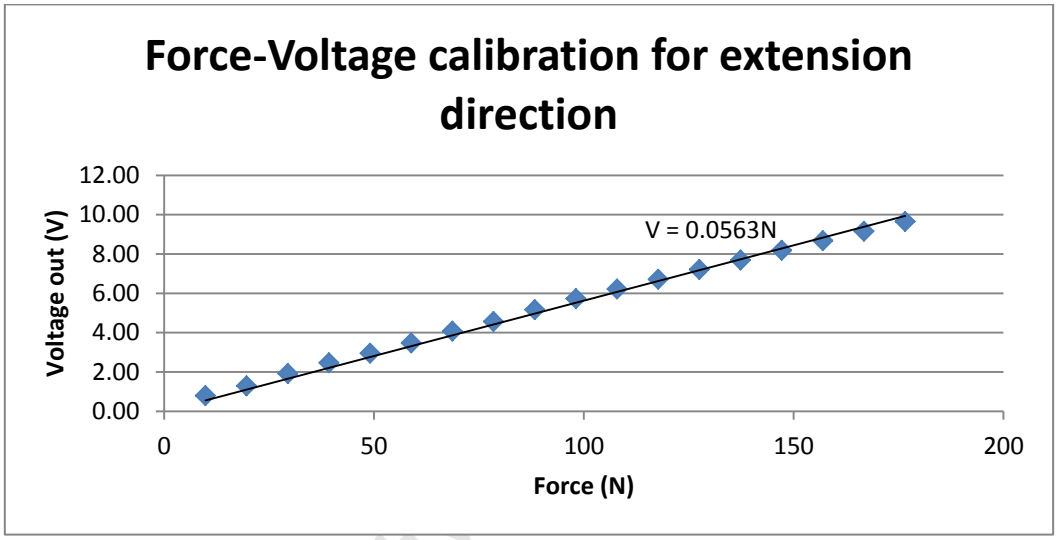

Figure B.4 Voltage vs Force calibration line for extension.

The Voltage vs Force scaling for the wrist extension direction (VF_{ext}) was thus 0.0563 V/N i.e. 0.0563 V for 1 N of force applied at the average point of force application.

Thus the Voltage vs Torque scaling for the wrist extension direction (VT_{ext}) was 0.0564 V/N / 0.113 m = 0.499 V/Nm i.e. 0.499 V for 1 Nm of torque applied in the wrist extension direction by a subject with a distance of 0.113 m between his wrist and contact region.

For increasing the estimation accuracy, the actual distance between the subject's wrist and contact region was measured (D_{sub}), and the VF_{ext} adapted such that the subject's VF_{ext} i.e. $VF_{ext,sub} = VF_{ext} \times (D_{sub} - 0.113 + 0.07) / (0.07)$.

Then the subject's VT_{ext} i.e. $VT_{ext,sub} = VF_{ext,sub} / D_{sub}$.

The voltage readings (V) during the actual MVC testing were divided by $VT_{ext,sub}$ (V/Nm) to get the MVC torque applied at the wrist joint in Newton metres (Nm).

Calibration for wrist flexion direction

Table 4 shows the calibration data for the flexion direction using the spring load and Figure B.5 shows the scatter plot of Voltage vs Force along with the best fit line through the points.

Table 4 Calibration data for flexion direction.

Mass (kg)	Force (N)	Trial 1 (V)	Trial 2 (V)	Average (V)
1	9.81	0.71	0.75	0.73
2	19.62	1.28	1.29	1.29
3	29.43	1.82	1.87	1.85
4	39.24	2.43	2.41	2.42
5	49.05	2.89	2.90	2.90
6	58.86	3.46	3.48	3.47
7	68.67	4.01	4.05	4.03
8	78.48	4.67	4.69	4.68
9	88.29	5.08	5.00	5.04
10	98.1	5.65	5.64	5.65
11	107.91	6.40	6.43	6.41
12	117.72	6.69	6.89	6.79
13	127.53	7.47	7.48	7.48
14	137.34	8.02	8.04	8.03
15	147.15	8.41	8.49	8.45
16	156.96	8.93	8.95	8.94
17	166.77	9.52	9.43	9.48
18	176.58	9.88	9.89	9.89

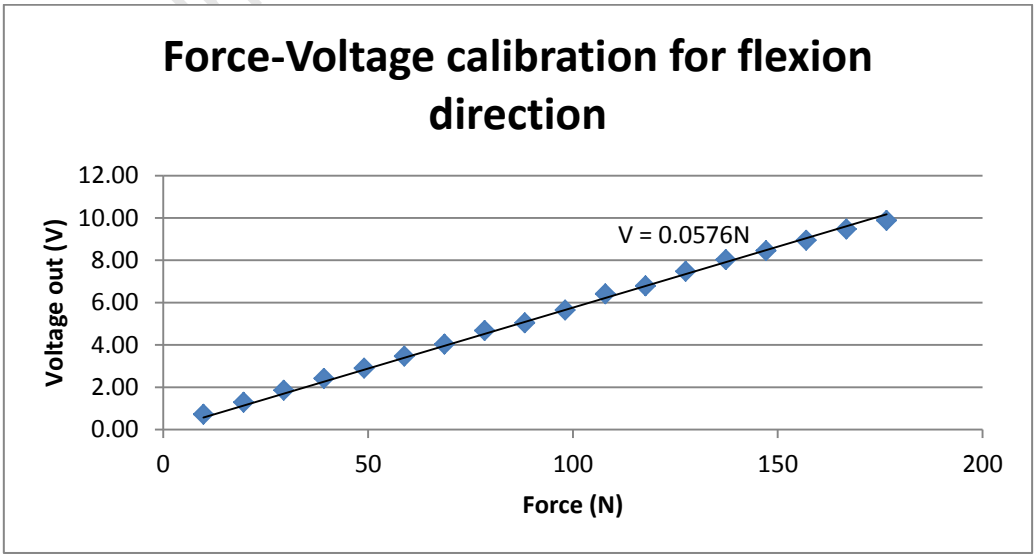

Figure B.5 Voltage vs Force calibration line for flexion.

The Voltage vs Force scaling for the wrist flexion direction (VF_{flx}) was thus 0.0576 V/N i.e. 0.0576 V for 1 N of force applied at the average point of force application.

Thus the Voltage vs Torque scaling for wrist flexion direction (VT_{flx}) was 0.0576 V/N / 0.113 m = 0.510 V/Nm i.e. 0.510 V for 1 Nm of torque applied in the wrist flexion direction by a subject with a distance of 0.113 m between his wrist and contact region.

For increasing the estimation accuracy, similarly to the wrist extension direction, VF_{flx} was adapted according to the actual distance between the subject's wrist and contact region (D_{sub}) such that the subject's VF_{flx} i.e. $VF_{flx,sub} = VF_{flx} \times (D_{sub} - 0.113 + 0.07) / (0.07)$.

Then the subject's VT_{flx} i.e. $VT_{flx,sub} = VF_{flx,sub} / D_{sub}$.

The voltage readings (V) during the actual MVC testing were divided by $VT_{flx,sub}$ (V/Nm) to get the MVC torque applied at the wrist joint in Newton metres (Nm).

APPENDIX C EMG AND EEG SYSTEM CIRCUITRY

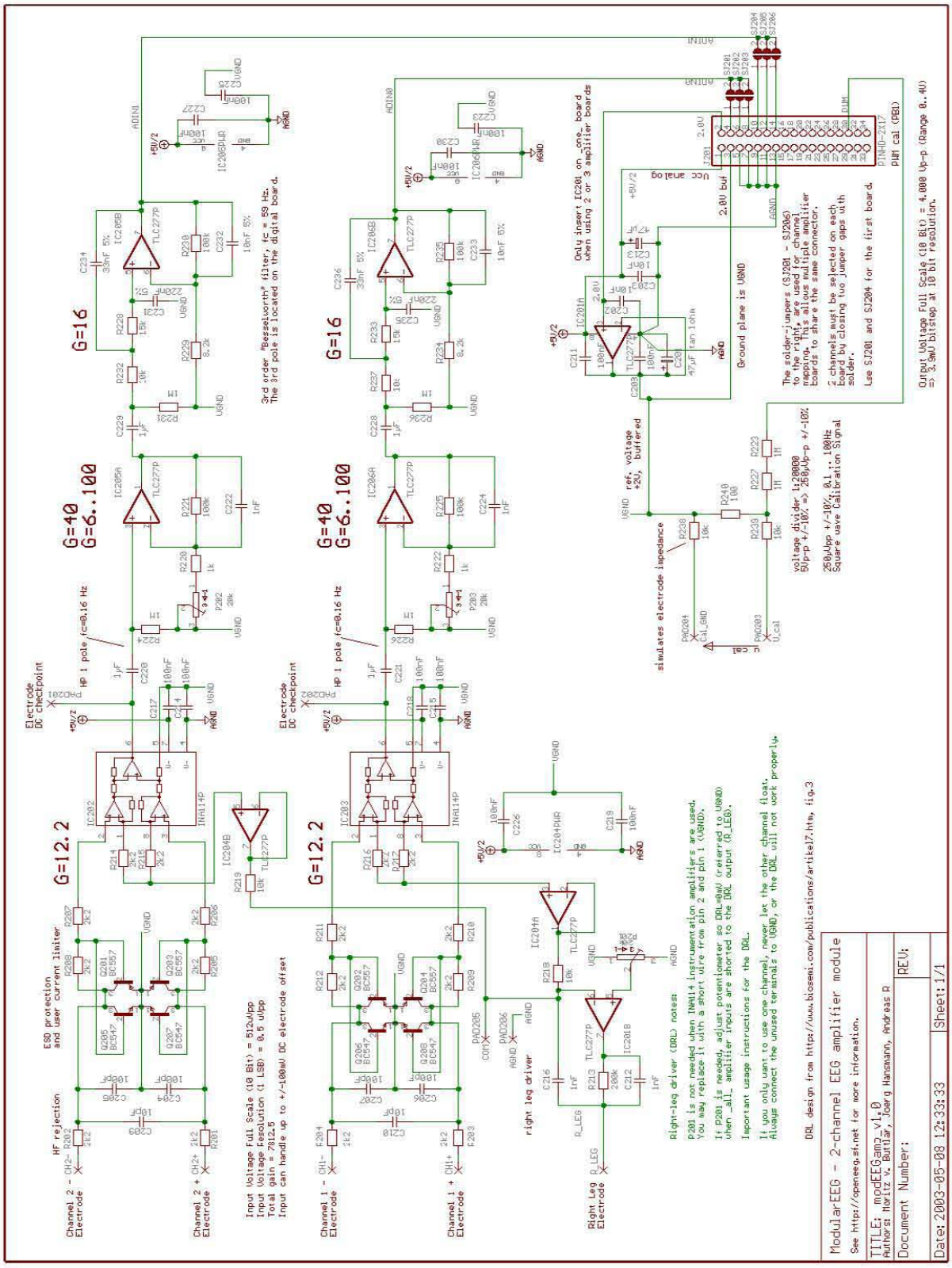

Figure C.1 OpenEEG amplifier board schematic. The protection circuitry, filtering stages, gain stages and active ground i.e. driven right leg (DRL) circuitry can be seen. Each board has two channels.

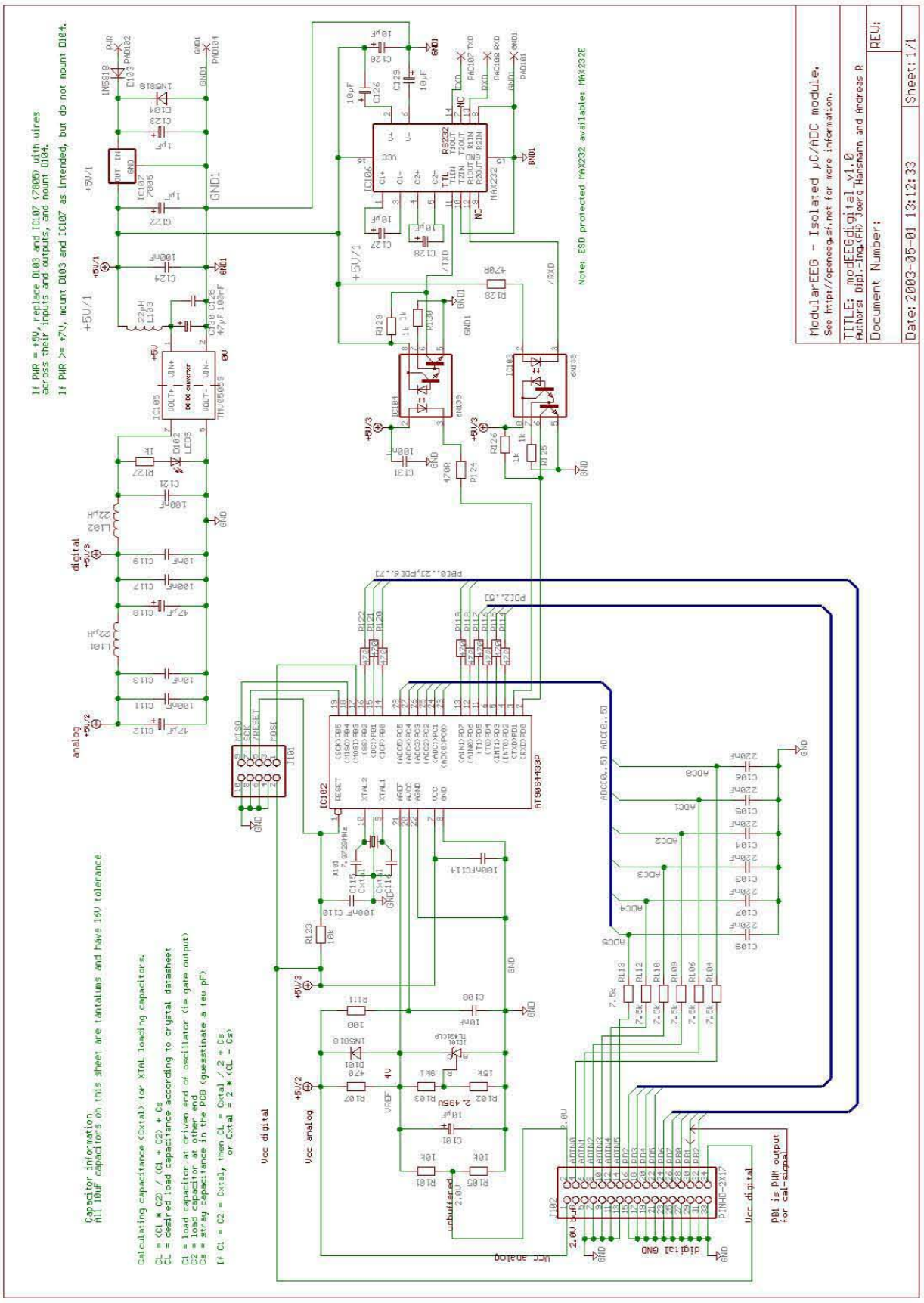

Figure C.2 OpenEEG digital board schematic. The filter circuitry, microcontroller and serial communication circuitry can be seen.

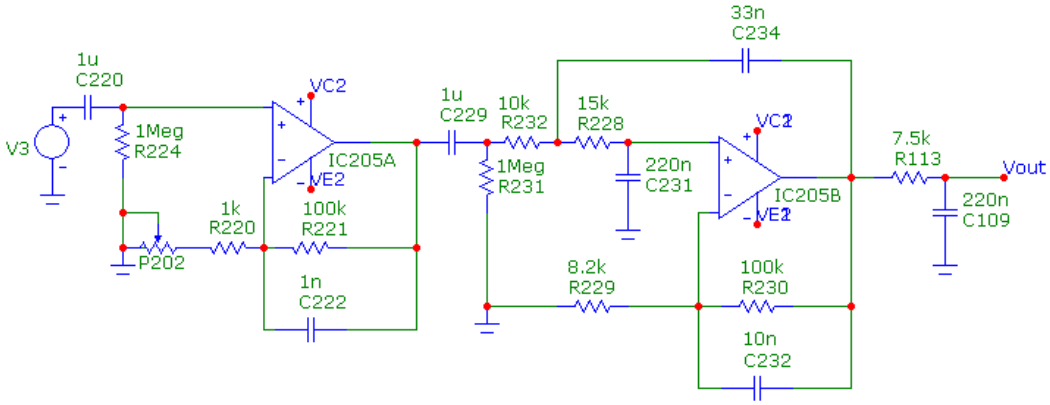

Figure C.3 Original OpenEEG filter circuit: - combined filtering on the amplifier board, including the last pole which is on the digital board. This filter circuit was used for measuring EEG i.e. kept unchanged.

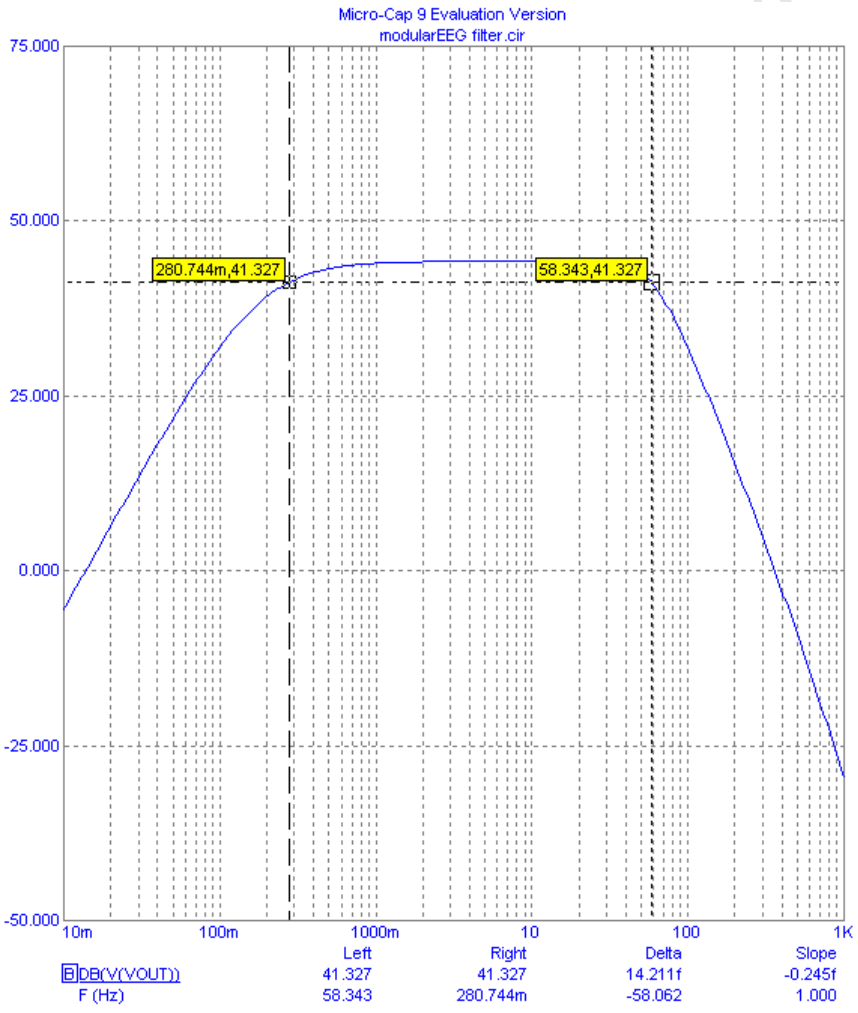

Figure C.4 The simulated bode plot of the original OpenEEG filter circuit. A high pass cut-off frequency of 281 mHz and a low pass cut-off frequency of 58 Hz can be seen.

Table 5 Old and new capacitor values for modifying the ModularEEG filter settings for EMG measurement.
***Note that C103 – C109 are on the digital board.**

Filter	Capacitor	Old Value (nF)	New Value (nF)	E12 Value (nF)
High Pass	C220 & C221	1000	56.2	57
	C229 & C228	1000	56.2	57
Low Pass	C231 & C235	220	25.67	22
	C232 & C233	10	1.17	1
	C234 & C236	33	3.85	3.3
	C103 – C109 *	220	25.67	22

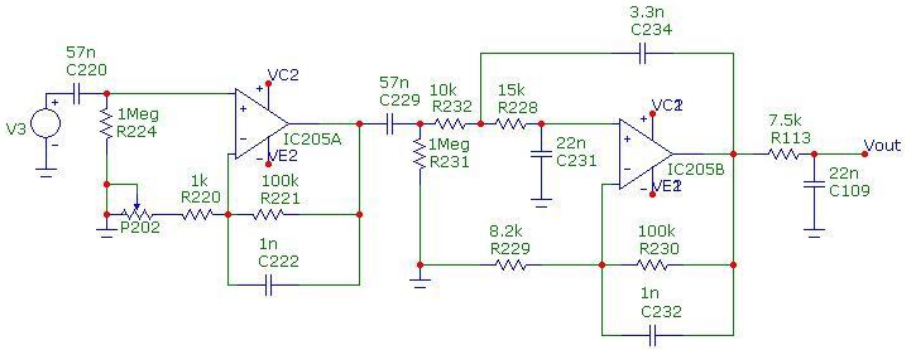

Figure C.5 Modified OpenEEG filter circuit. The capacitors were changed to increase the high pass cut-off frequency as well as the low pass cut-off frequency to match the EMG frequency range.

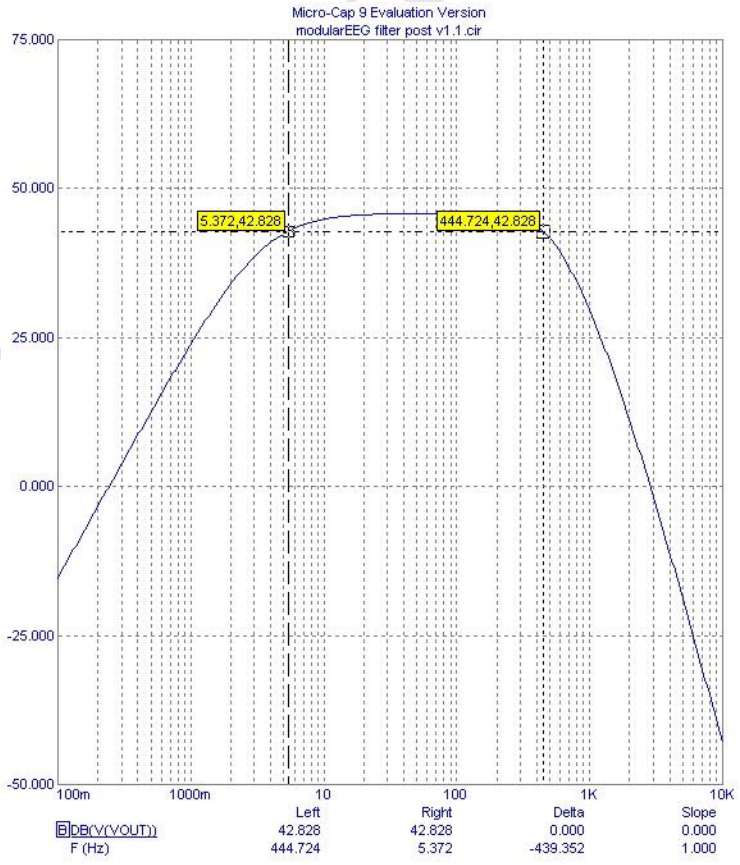

Figure C.6 The simulated bode plot of the modified OpenEEG filter circuit. A high pass cut-off frequency of 5 Hz and a low pass cut-off frequency of 445 Hz can be seen.

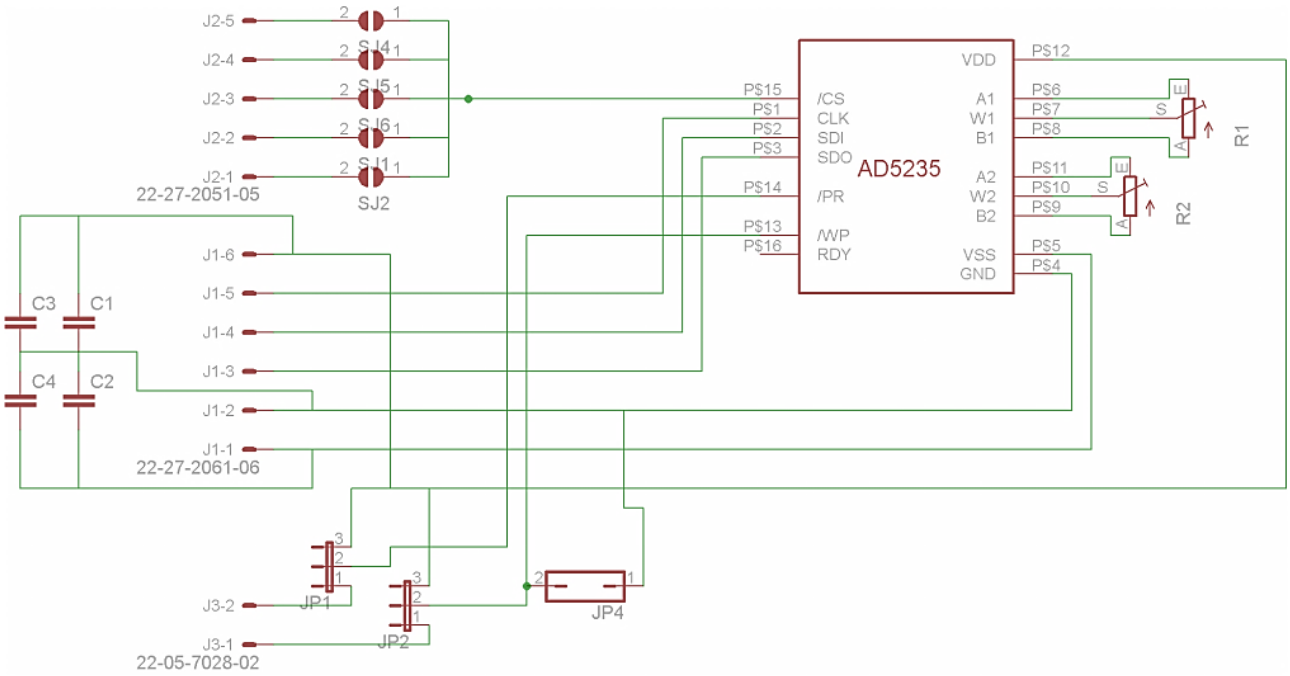

Figure C.7 Schematic of gain daughter board.

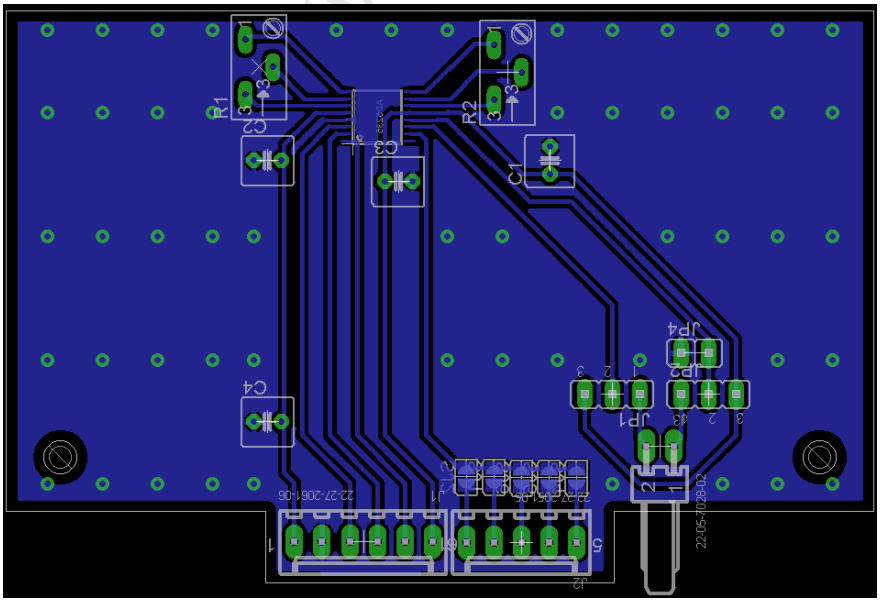

Figure C.8 PCB layout of gain daughter board.

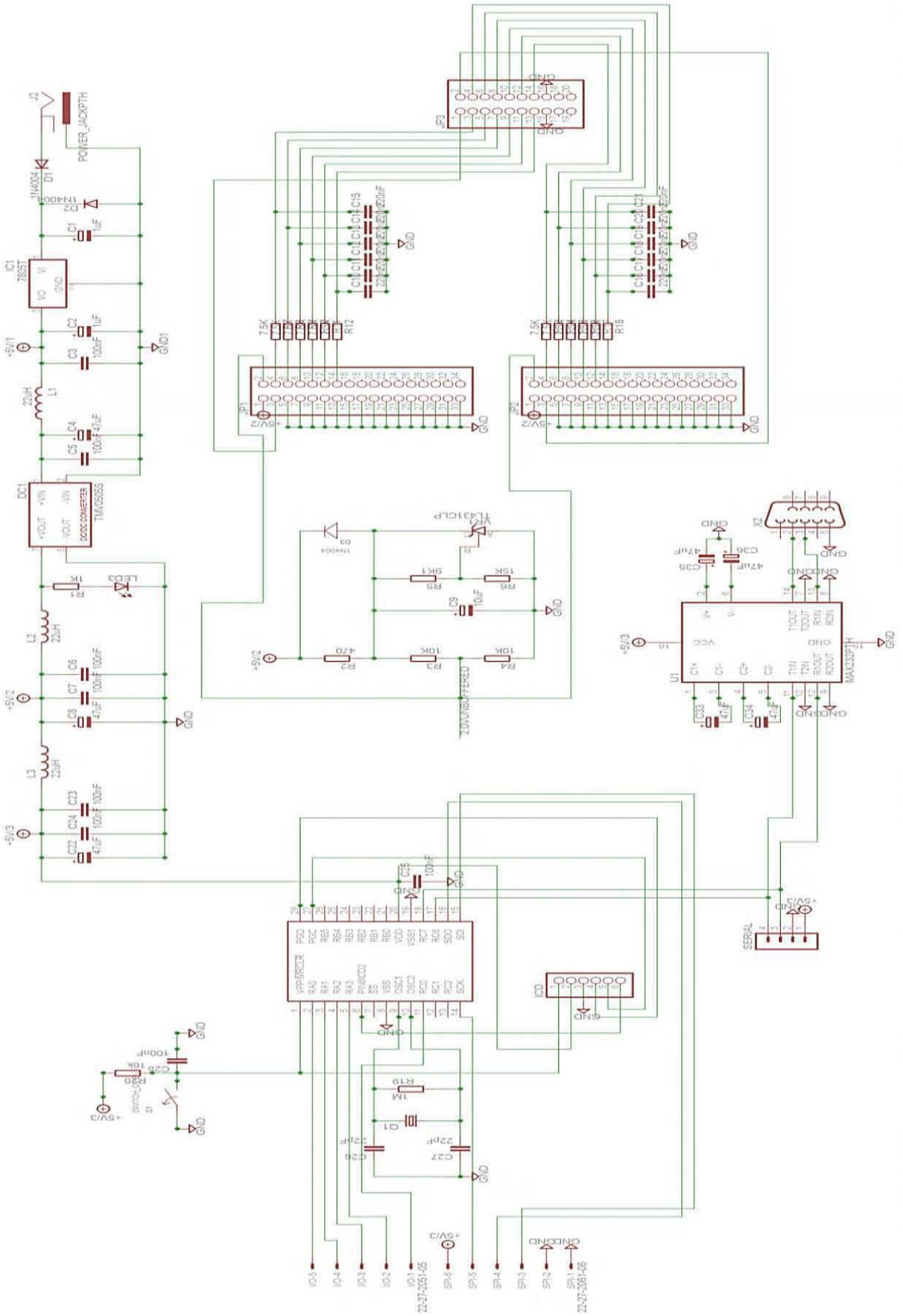

Figure C.9 Schematic of EMG supplementary board.

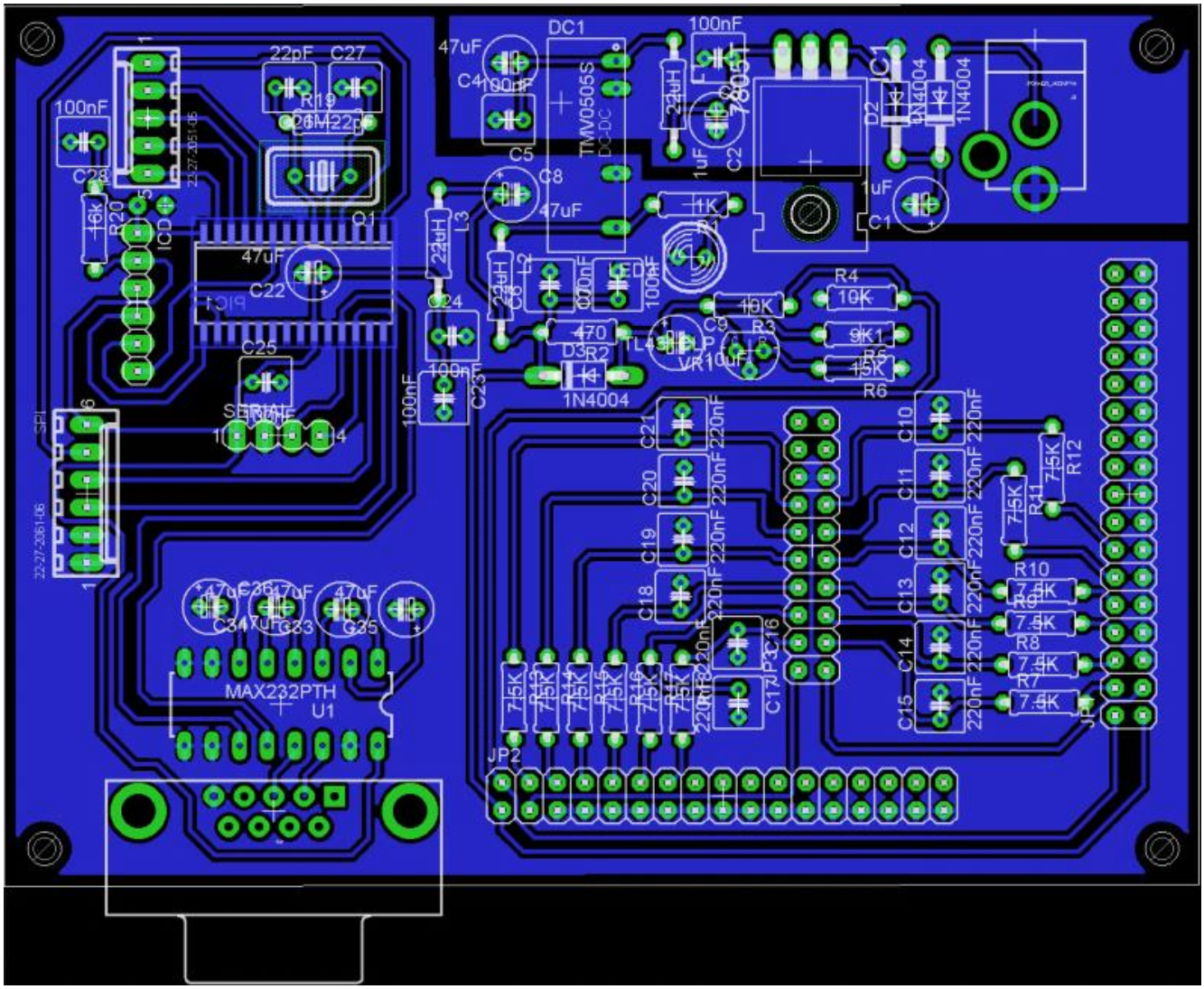

Figure C.10 PCB layout of EMG supplementary board.

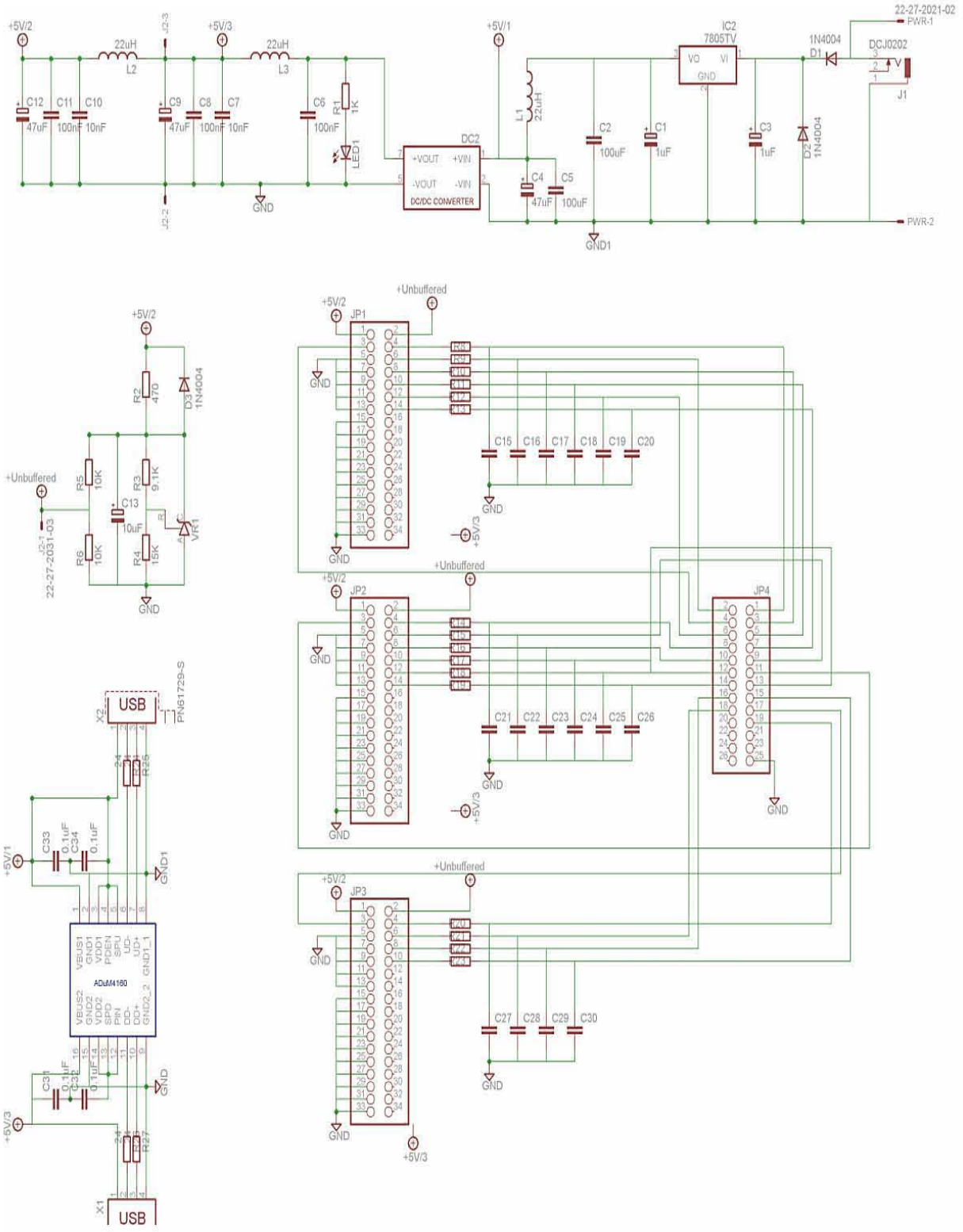

Figure C.11 Schematic of EEG supplementary board.

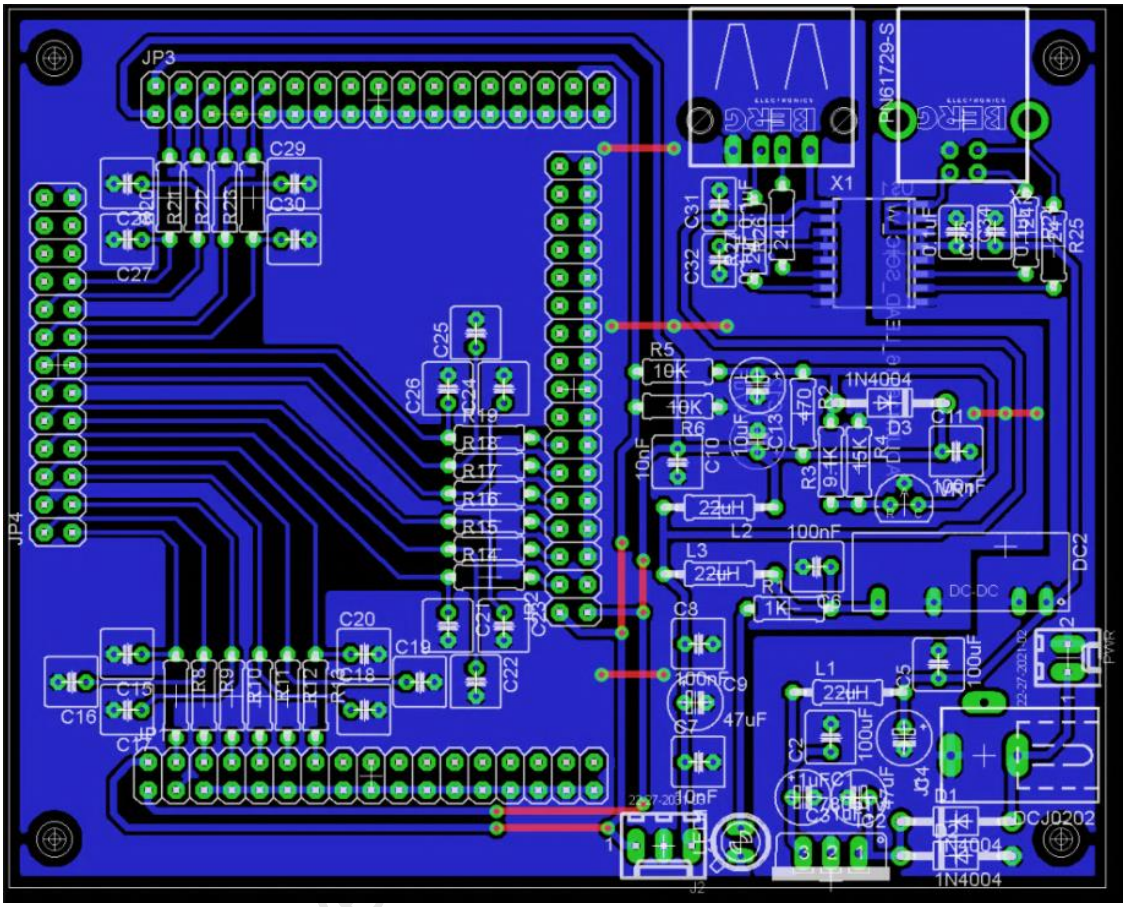

Figure C.12 PCB layout of EEG supplementary board.

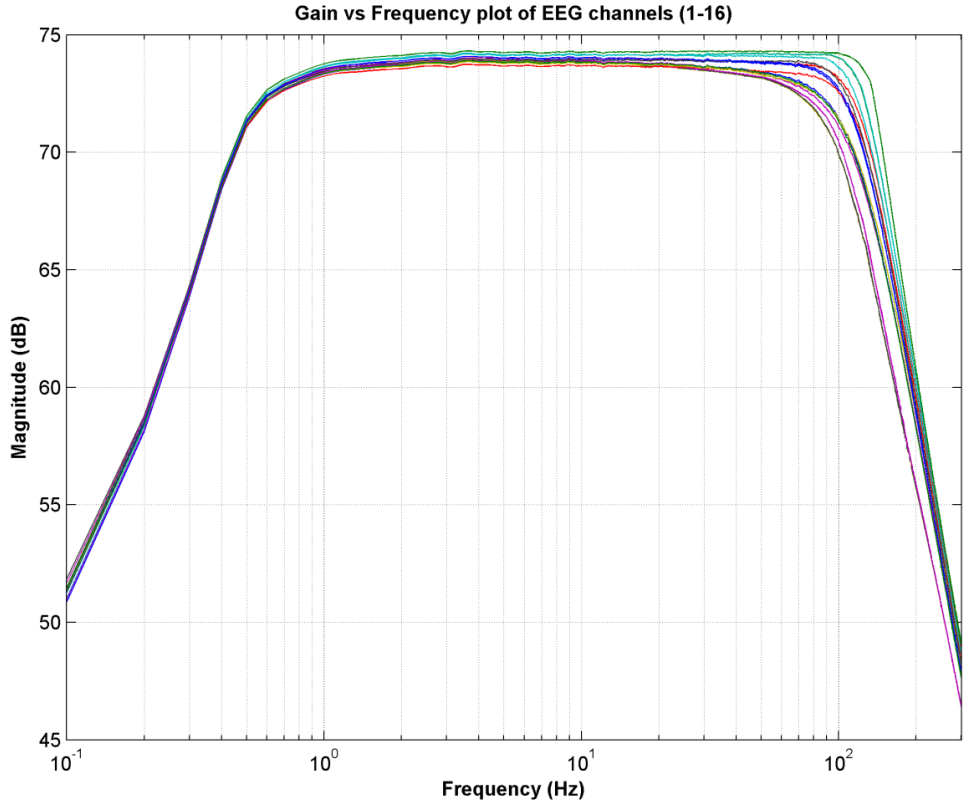

Figure C.13 EEG channels magnitude plot.

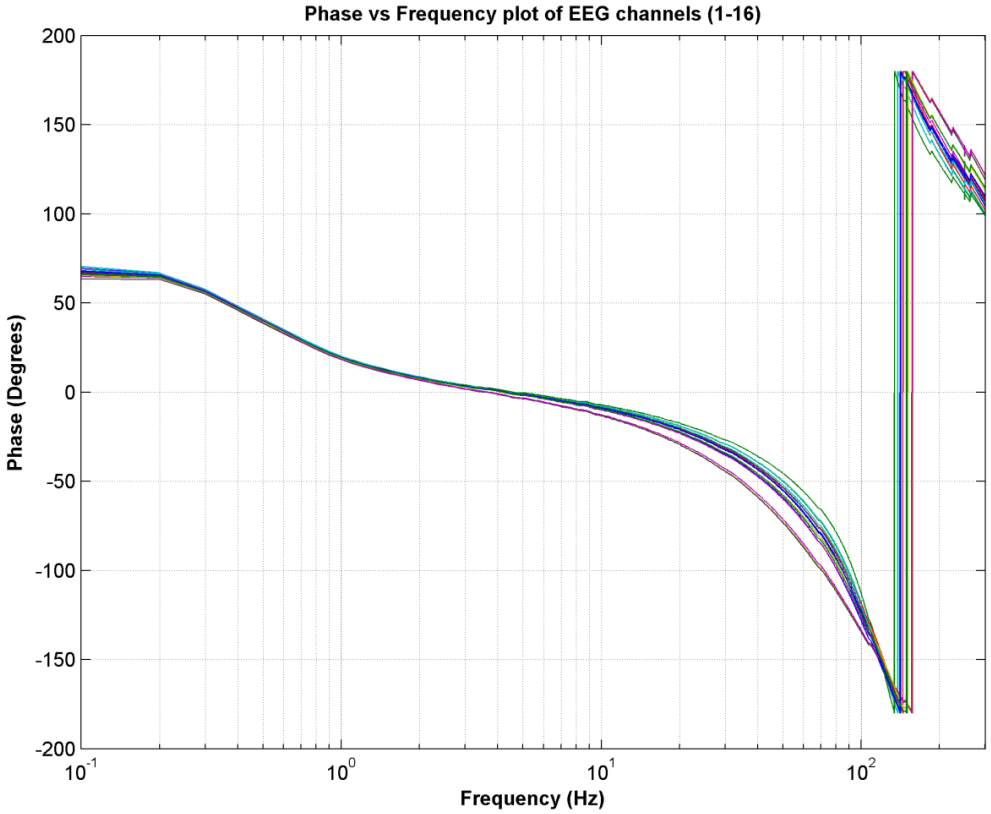

Figure C.14 EEG channels phase plot.

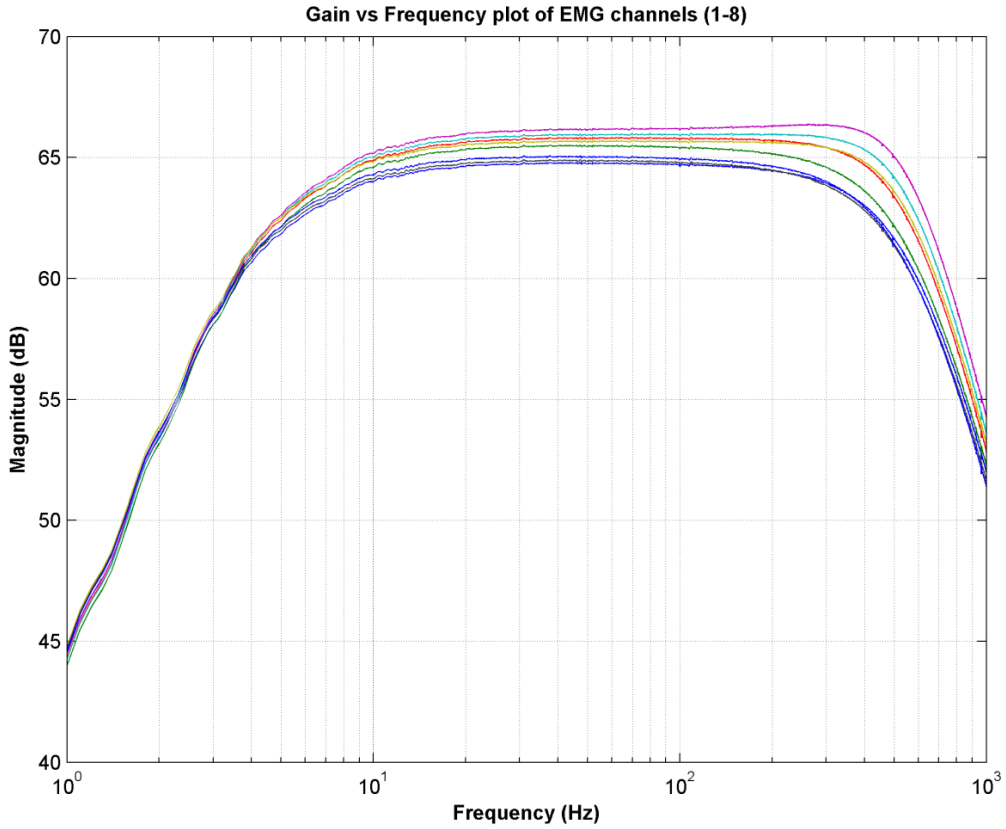

Figure C.15 EMG channels magnitude plot.

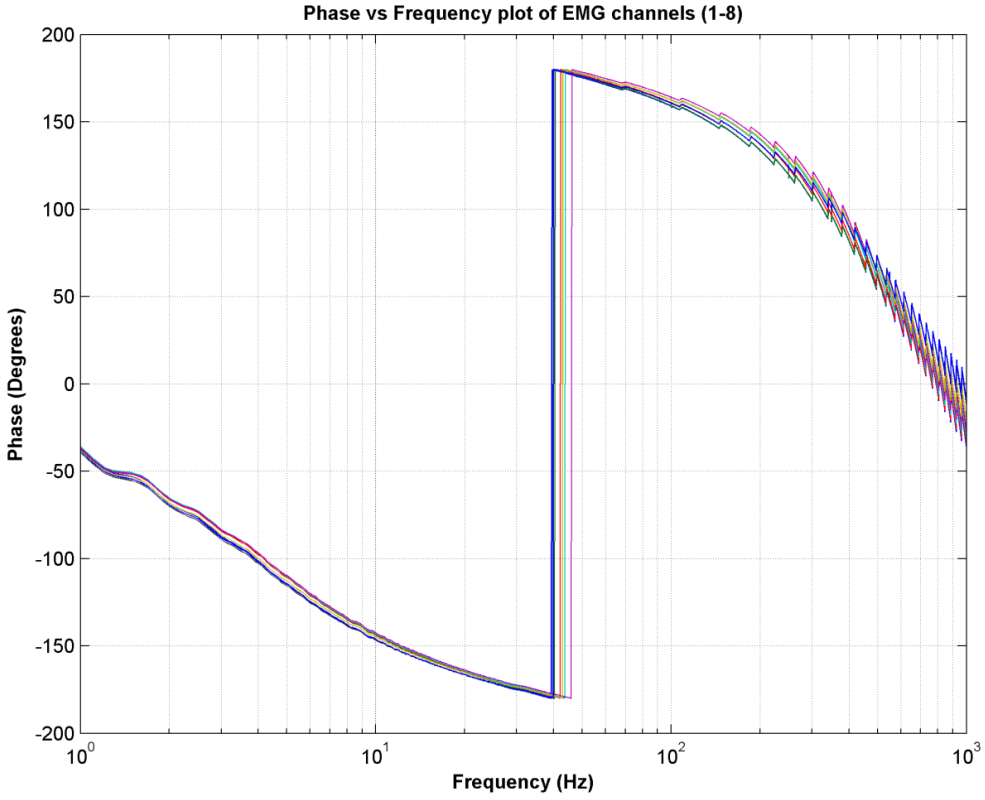

Figure C.16 EMG channels phase plot.

APPENDIX D DIGIPOT CONTROL SOFTWARE

MCU code

The following is the code that was programmed onto the MCU. The MCU communicates with the PC via SCI and also communicates with the digipot via SPI.

```
% Digipot control with PIC2035 using SPI and serial communication with PC
% Author : Nikhil Divekar, University of Cape Town, Electroencephalography
% Lab

#include <p18cxxx.h> // header file for pic family
#pragma config WDT = OFF // turn off watchdog timer

static unsigned char count;
static unsigned char v11; static unsigned char v12; static unsigned char
v21; static unsigned char v22;
static unsigned char v31; static unsigned char v32; static unsigned char
t1; static unsigned char t2;
static unsigned char t3; static unsigned char board;

void main(void);
void isr_sci (void);

// FUNCTION Prototypes for SCI
void scisetup(void);

// FUNCTION Prototypes for SPI
void spisetup(void);
void SPI_enable(void);
void SPI_disable(void);
void write2pots1(unsigned char var1, unsigned char var2, unsigned char
var3);
void write2pots2(unsigned char var1, unsigned char var2, unsigned char
var3);
void write2pots3(unsigned char var1, unsigned char var2, unsigned char
var3);
void write2pots4(unsigned char var1, unsigned char var2, unsigned char
var3);
void write_byte(unsigned char byte);
void check_wcol(unsigned char byte);
```

```
void delay(void);
void delay2(void);

// VARIABLE Definitions for SCI

#define RX TRISCbits.TRISC7
#define TX TRISCbits.TRISC6

#define TX9 TXSTAbits.TX9
#define TXEN TXSTAbits.TXEN
#define SYNC TXSTAbits.SYNC
#define BRGH TXSTAbits.BRGH
#define TRMT TXSTAbits.TRMT
#define TXIE PIE1bits.TXIE
#define TXIF PIR1bits.TXIF

#define SPEN RCSTAbits.SPEN
#define RX9 RCSTAbits.RX9
#define CREN RCSTAbits.CREN
#define FERR RCSTAbits.FERR
#define OERR RCSTAbits.OERR
#define RCIE PIE1bits.RCIE
#define RCIF PIR1bits.RCIF


#define RCIDL BAUDCONbits.RCIDL
#define RXDTP BAUDCONbits.RXDTP
#define TXCKP BAUDCONbits.TXCKP
#define BRG16 BAUDCONbits.BRG16
#define WUE BAUDCONbits.WUE
#define ABDEN BAUDCONbits.ABDEN

// VARIABLE Definitions for SPI

#define SCK_set_dir TRISCbits.TRISC3 // direction for clock pin
#define SDO_set_dir TRISCbits.TRISC5 // direction for SDO pin
#define SPI_CS_set_dir1 TRISAbits.TRISA0 // direction for CS pin
#define SPI_CS_set_dir2 TRISAbits.TRISA1 // direction for CS pin
#define SPI_CS_set_dir3 TRISAbits.TRISA2 // direction for CS pin
#define SPI_CS_set_dir4 TRISAbits.TRISA3 // direction for CS pin
```

```
#define SPI_CS1 LATAbits.LATA0 // control for CS pin
#define SPI_CS2 LATAbits.LATA1 // control for CS pin
#define SPI_CS3 LATAbits.LATA2 // control for CS pin
#define SPI_CS4 LATAbits.LATA3 // control for CS pin
#define wcol SSPCON1bits.WCOL // write collision bit
#define bf SSPSTATbits.BF // buffer full bit
#define SCK_con LATCbits.LATC3 // control for CS pin
#define SDO_con LATCbits.LATC5 // control for CS pin

//*************************************************

#define GIE INTCONbits.GIE //global interrupts enable
#define PEIE INTCONbits.PEIE //peripheral interrupts enable

#define IPEN RCONbits.IPEN // interrupt priority

#pragma code rx_interrupt = 0x8 // pic18 high interrupt vector address
void rx_int (void) // handler
{
 _asm goto isr_sci _endasm // makes it go to interrupt handler code
}
#pragma code // returns compiler to default code section

void main(void)
{

//setup serial port
scisetup();

//setup spi port
spisetup();

SPI_enable(); // enables SPI after setup completed

count = 0;

while(1) // wait in loop forever OR till serial (SCI) interrupt occurs
// due to received data which will then run handler
// ''void rx_int (void)''. If successful it will make count = 7.
{
if (count == 7) // check if count = 7 or if expected bytes have
```

```
// been received
{
switch(board) // switch case depending on board selected (1-4).
// 'board' is acquired from interrupt handler ''rx_int''
{
case 1: write2pots1(t1,t2,t3); // if board '1' is selected by user
// carry out appropriate function 'write2pots'1'. t1, t2 and t3 are
// acquired from interrupt handler rx_int.
break;
case 2: write2pots2(t1,t2,t3); // if board '2' is selected by user
// carry out appropriate function 'write2pots'2'.t1, t2 and t3 are
// acquired from interrupt handler rx_int.
break;
case 3: write2pots3(t1,t2,t3); // if board '3' is selected by user
// carry out appropriate function 'write2pots'3'.t1, t2 and t3 are
// acquired from interrupt handler rx_int.
break;
case 4: write2pots4(t1,t2,t3); // if board '4' is selected by user
// carry out appropriate function 'write2pots'4'.t1, t2 and t3 are
// acquired from interrupt handler rx_int.
break;
}
count = 0; // reset count so that next write can be detected by
//interrupt handler rx_int
}
}
}

void write2pots1(unsigned char var1, unsigned char var2, unsigned char
var3)
{
SPI_CS1 = 1; // make sure chip select line is high to begin with
delay2(); // small delay
SPI_CS1 = 0; // pull down chip select line so bytes can be send
write_byte(var1); // write 1st byte
write_byte(var2); //write 2nd byte
write_byte(var3); // write 3rd byte
delay(); // small delay
SPI_CS1 = 1; // pull chip select line high as per chip protocol
SPI_CS1 = 0; // pull chip select line low as per chip protocol
SPI_CS1 = 1; // pull chip select line high again as per chip protocol
```

```
while(!TRMT);
TXREG = 1; // give feedback to PC that write was done to board 1
}

void write2pots2(unsigned char var1, unsigned char var2, unsigned char
var3)
{
SPI_CS2 = 1;
delay2();
SPI_CS2 = 0;
write_byte(var1); // write 1st byte
write_byte(var2); //write 2nd byte
write_byte(var3); // write 3rd byte
delay();
SPI_CS2 = 1;
SPI_CS2 = 0;
SPI_CS2 = 1;
while(!TRMT);
TXREG = 2; // give feedback to PC that write was done to board 2
}

void write2pots3(unsigned char var1, unsigned char var2, unsigned char
var3)
{
SPI_CS3 = 1;
delay2();
SPI_CS3 = 0;
write_byte(var1); // write 1st byte
write_byte(var2); //write 2nd byte
write_byte(var3); // write 3rd byte
delay();
SPI_CS3 = 1;
SPI_CS3 = 0;
SPI_CS3 = 1;
while(!TRMT);
TXREG = 3; // give feedback to PC that write was done to board 3
}

void write2pots4(unsigned char var1, unsigned char var2, unsigned char
var3)
{
```

```
SPI_CS4 = 1;
delay2();
SPI_CS4 = 0;
write_byte(var1); // write 1st byte
write_byte(var2); //write 2nd byte
write_byte(var3); // write 3rd byte
delay();
SPI_CS4 = 1;
SPI_CS4 = 0;
SPI_CS4 = 1;
while(!TRMT);
TXREG = 4; // give feedback to PC that write was done to board 4
}

void write_byte(unsigned char byte)
{
unsigned char TempVariable;
//while(!bf); // wait till buffer empty
TempVariable = SSPBUF; // Reads from SSPBUF, ensures BF bit is clear before
check_wcol(byte); // checks if there has been a write collision
SSPBUF = byte; // send byte
}

void check_wcol(unsigned char byte)
{
if (wcol == 1) // if write collosion has occured
{
wcol = 0; // clear the flag
write_byte(byte); // go back to write_byte code and send it
// the byte to be written
}
}

void spisetup(void)
{
// set SCK and SDO as outputs
SCK_set_dir = 0;
SDO_set_dir = 0;
// set chip select pin as output
SPI_CS_set_dir1 = 0;
SPI_CS_set_dir2 = 0;
```

```
SPI_CS_set_dir3 = 0;
SPI_CS_set_dir4 = 0;
// set sample bit to sample at middle of transmission
SSPSTATbits.SMP = 1;
// set transmission to occur at shift from active to idle clock state
SSPSTATbits.CKE = 1;
// set idle state of clock to low level
SSPCON1bits.CKP = 0;
// set clock frequency to Fosc/16
SSPCON1bits.SSPM3 = 0;
SSPCON1bits.SSPM2 = 0;
SSPCON1bits.SSPM1 = 0;
SSPCON1bits.SSPM0 = 1;
}

void SPI_enable(void)
{
SSPCON1bits.SSPEN = 1; //enable SPI
}

void SPI_disable(void)
{
SSPCON1bits.SSPEN = 0; //disable SPI
}

void scisetup(void)
{
RX = 1; // sets direction of RX
TX = 1; // sets direction of TX
SPEN = 1; // enables Serial Port
// setup baud rate settings
SYNC = 0;
BRGH = 0;
BRG16 = 0;
// write to SPBRG and SPBRGH registers for 19200Hz with 20Mhz oscillator
SPBRGH = 0x00;
SPBRG = 0x0F;

SYNC = 0; // set to Asynchronous mode
TXIF = 0;
TXIE = 0; // transmit interrupts not requried
```

```
RCIF = 0;
RCIE = 1; // receive interrupts required
IPEN = 0; // interrupt priority not required
TX9 = 0; // set to 8 bit operation
RX9 = 0; // set to 8 bit operation
TXEN = 1; // enable transmission
CREN = 1; // enable reception
WUE = 1; // set to continuously monitor rx pin

GIE = 1;
PEIE = 1;
}


void delay(void) // delay routine very small delay
{
unsigned int i;
for (i = 0; i < 1 ; i++)
;
}

void delay2(void) // delay routine small delay
{
unsigned int i;
for (i = 0; i < 10000 ; i++);
}

#pragma interrupt isr_sci //defines isr_sci as high interrupt
void isr_sci (void) // code for interrupt handler
{
unsigned char a1; unsigned char add; unsigned char v3; unsigned char a4;
RCIF == 0;

switch(count)
{
case 0:
a1 = RCREG; // take in variable from receive register
add = a1 >> 4; // extract address (code for halfbyte)
v11 = a1 << 4; // extract half byte
if (add == 1) // code for this halfbyte should be 1
{
```

```
count = count + 1; // first halfbyte has come successfully
}
break;

case 1:
a1 = RCREG; // take in variable from receive register
add = a1 >> 4; // extract address (code for halfbyte)
v12 = a1 << 4; // extract halfbyte
v12 = v12 >> 4; // shift halfbyte 4 bits down as this is 2nd halfbyte
t1 = v11 + v12; // add two halfbytes to make databyte1
if (add == 2) // code for this halfbyte should be 2
{
count = count + 1; // second halfbyte has come successfully
}
break;

case 2:
a1 = RCREG; // take in variable from receive register
add = a1 >> 4; // extract address (code for halfbyte)
v21 = a1 << 4; // extract half byte
if (add == 3) // code for this halfbyte should be 3
{
count = count + 1; //third halfbyte has come successfully
}
break;

case 3:
a1 = RCREG; // take in variable from receive register
add = a1 >> 4; // extract address (code for halfbyte)
v22 = a1 << 4; // extract halfbyte
v22 = v22 >> 4; // shift halfbyte 4 bits down as this is 2nd halfbyte
t2 = v21 + v22; // add two halfbytes to make databyte2
if (add == 4) // code for this halfbyte should be 4
{
count = count + 1; //fourth halfbyte has come successfully
}
break;

case 4:
a1 = RCREG; // take in variable from receive register
add = a1 >> 4; // extract address (code for halfbyte)
```

```
v31 = a1 << 4; // extract half byte
if (add == 5) // code for this halfbyte should be 5
{
count = count + 1; //fifth halfbyte has come successfully
}
break;

case 5:
a1 = RCREG; // take in variable from receive register
add = a1 >> 4; // extract address (code for halfbyte)
v32 = a1 << 4; // extract halfbyte
v32 = v32 >> 4; // shift halfbyte 4 bits down as this is 2nd halfbyte
t3 = v31 + v32; // add two halfbytes to make databyte3
if (add == 6) // code for this halfbyte should be 6
{
count = count + 1; //sixth halfbyte has come successfully
}
break;

case 6:
a1 = RCREG; // take in variable from receive register
add = a1 >> 4; // extract address (code for halfbyte)
board = a1 << 4; // extract halfbyte
board = board >> 4; // shift halfbyte 4 bits down as this is only halfbyte
(boardsel)
if (add == 7) // code for this halfbyte should be 7
{
count = count + 1; // count should now be 7 (all halfbytes have arrived)
}
break;

}
}
```

Matlab code

The following is the code that was used to create and operate the GUI in Matlab to facilitate communication with the MCU that in turn was programmed to control the digipots on the EMG amplifier boards.

```
% Digipot gain control GUI
% Author : Nikhil Divekar, University of Cape Town, Electroencephalography
% Lab

function varargout = digi_con(varargin)
% DIGI_CON M-file for digi_con.fig
%      DIGI_CON, by itself, creates a new DIGI_CON or raises the existing
%      singleton*.
%
%      H = DIGI_CON returns the handle to a new DIGI_CON or the handle to
%      the existing singleton*.
%
%      DIGI_CON('CALLBACK',hObject,eventData,handles,...) calls the local
%          function named CALLBACK in DIGI_CON.M with the given input
arguments.
%
%       DIGI_CON('Property','Value',...) creates a new DIGI_CON or raises
the
%       existing singleton*.  Starting from the left, property value pairs
are
%      applied to the GUI before digi_con_OpeningFcn gets called.  An
%          unrecognized property name or invalid value makes property
application
%      stop.  All inputs are passed to digi_con_OpeningFcn via varargin.
%
%      *See GUI Options on GUIDE's Tools menu.  Choose "GUI allows only one
%      instance to run (singleton)".
%
% See also: GUIDE, GUIDATA, GUIHANDLES

% Edit the above text to modify the response to help digi_con

% Last Modified by GUIDE v2.5 12-Apr-2013 12:51:49
```

```
% Begin initialization code - DO NOT EDIT
gui_Singleton = 1;
gui_State = struct('gui_Name',       mfilename, ...
                   'gui_Singleton',  gui_Singleton, ...
                   'gui_OpeningFcn', @digi_con_OpeningFcn, ...
                   'gui_OutputFcn',  @digi_con_OutputFcn, ...
                   'gui_LayoutFcn',  [] , ...
                   'gui_Callback',   []);
if nargin && ischar(varargin{1})
    gui_State.gui_Callback = str2func(varargin{1});
end

if nargout
    [varargout{1:nargout}] = gui_mainfcn(gui_State, varargin{:});
else
    gui_mainfcn(gui_State, varargin{:});
end
% End initialization code - DO NOT EDIT



% --- Executes just before digi_con is made visible.
function digi_con_OpeningFcn(hObject, eventdata, handles, varargin)
% This function has no output args, see OutputFcn.
% hObject    handle to figure
% eventdata  reserved - to be defined in a future version of MATLAB
% handles    structure with handles and user data (see GUIDATA)
% varargin   command line arguments to digi_con (see VARARGIN)

% Choose default command line output for digi_con
handles.output = hObject;
% Update handles structure

handles.pot_val = []; % variable for storing the digipot value to be sotred
handles.board_sel = []; % variable to select board to control (1-4)
handles.potnum = []; % variable to select digipot on board (1st or 2nd)

set(handles.val_box,'String','50');
set(handles.slider,'Value',50);
```

```
handles.s1                                                              =
serial('COM7','BaudRate',19200,'DataBits',8,'StopBits',1,'Timeout',0.04); %
initiate serial comm to appropriate proerties

handles.s1.OutputBufferSize = 1; % set buffer size

fopen(handles.s1); % open the serial port

guidata(hObject, handles);

% UIWAIT makes digi_con wait for user response (see UIRESUME)
% uiwait(handles.figure1);

% --- Outputs from this function are returned to the command line.
function varargout = digi_con_OutputFcn(hObject, eventdata, handles)
% varargout  cell array for returning output args (see VARARGOUT);
% hObject    handle to figure
% eventdata  reserved - to be defined in a future version of MATLAB
% handles    structure with handles and user data (see GUIDATA)

% Get default command line output from handles structure
varargout{1} = handles.output;

% --- Executes on selection change in pop_menu.
function pop_menu_Callback(hObject, eventdata, handles)
% hObject    handle to pop_menu (see GCBO)
% eventdata  reserved - to be defined in a future version of MATLAB
% handles    structure with handles and user data (see GUIDATA)

% Hints: contents = get(hObject,'String') returns pop_menu contents as cell
array
%        contents{get(hObject,'Value')} returns selected item from pop_menu

% --- Executes during object creation, after setting all properties.
function pop_menu_CreateFcn(hObject, eventdata, handles)
% hObject    handle to pop_menu (see GCBO)
% eventdata  reserved - to be defined in a future version of MATLAB
% handles    empty - handles not created until after all CreateFcns called
```

```
% Hint: popupmenu controls usually have a white background on Windows.
%       See ISPC and COMPUTER.
if          ispc          &&          isequal(get(hObject,'BackgroundColor'),
get(0,'defaultUicontrolBackgroundColor'))
    set(hObject,'BackgroundColor','white');
end

function val_box_Callback(hObject, eventdata, handles)
% hObject    handle to val_box (see GCBO)
% eventdata  reserved - to be defined in a future version of MATLAB
% handles    structure with handles and user data (see GUIDATA)

% Hints: get(hObject,'String') returns contents of val_box as text
%        str2double(get(hObject,'String')) returns contents of val_box as a
double
    val = str2double(get(hObject,'String')); % retrieve value from text box
and store in val

    if ((val <= 99)&&(val >= 0)) % check if entered value is within range
    set(handles.slider,'Value',val); % match slider value with text box
value
    end
    guidata(hObject,handles);

% --- Executes during object creation, after setting all properties.
function val_box_CreateFcn(hObject, eventdata, handles)
% hObject    handle to val_box (see GCBO)
% eventdata  reserved - to be defined in a future version of MATLAB
% handles    empty - handles not created until after all CreateFcns called

% Hint: edit controls usually have a white background on Windows.
%       See ISPC and COMPUTER.
if          ispc          &&          isequal(get(hObject,'BackgroundColor'),
get(0,'defaultUicontrolBackgroundColor'))
    set(hObject,'BackgroundColor','white');
end

% --- Executes on slider movement.
function slider_Callback(hObject, eventdata, handles)
```

```
% hObject    handle to slider (see GCBO)
% eventdata  reserved - to be defined in a future version of MATLAB
% handles    structure with handles and user data (see GUIDATA)

% Hints: get(hObject,'Value') returns position of slider
%          get(hObject,'Min') and get(hObject,'Max') to determine range of
slider
val = get(hObject,'Value'); % get current value of slider
str = num2str(val); %convert number into string
set(handles.val_box,'String',str); % display value of slider in text box

val2 = get(handles.Scroll_select,'value'); % check if scroll option is on
(checked to send data with every change of slider without clicking on write
button
if val2 == 1 % if it is on
    send_data(hObject,handles) % carry out send data function after each
change in slider (user will be able to write data without clicking on Write
button
end

guidata(hObject,handles);

% --- Executes during object creation, after setting all properties.
function slider_CreateFcn(hObject, eventdata, handles)
% hObject    handle to slider (see GCBO)
% eventdata  reserved - to be defined in a future version of MATLAB
% handles    empty - handles not created until after all CreateFcns called

% Hint: slider controls usually have a light gray background.
if                                  isequal(get(hObject,'BackgroundColor'),
get(0,'defaultUicontrolBackgroundColor'))
    set(hObject,'BackgroundColor',[.9 .9 .9]);
end



% --- Executes on button press in Write_button.
function Write_button_Callback(hObject, eventdata, handles)
% hObject    handle to Write_button (see GCBO)
% eventdata  reserved - to be defined in a future version of MATLAB
% handles    structure with handles and user data (see GUIDATA)
```

```
send_data(hObject,handles); % clicking this button will go to the send data
function.

function send_data(hObject,handles)

board_sel = []; % board select variable (which one of the 4 boards does the
user want to control gain for)
potnum = []; % digipot select variable (which one of the 2 digipots on the
selected board does the user want to control)
potval = []; % digipot value set variable (percentage from 0 to 99 percent
initially, converted to a byte form later to represent a number between 0
to 1024 depending on the percentage)

channel = get(handles.pop_menu,'Value'); % check which board and channel
combination (1-8) is selected from gui drop down list
    if (channel == 1);
    board_sel = [0 0 0 1]; % set board selected to 1
    potnum = 0; % set pot selected to 0 (1st pot)
    elseif (channel == 2)
    board_sel = [0 0 0 1]; % set board selected to 1
    potnum = 1; % set pot selected to 1 (2nd pot)
    elseif (channel == 3)
    board_sel = [0 0 1 0]; % set board selected to 2
    potnum = 0;% set pot selected to 0 (1st pot)
    elseif (channel == 4)
    board_sel = [0 0 1 0];% set board selected to 2
    potnum = 1;% set pot selected to 1 (2nd pot)
    elseif (channel == 5)
    board_sel = [0 0 1 1];% set board selected to 3
    potnum = 0;% set pot selected to 0 (1st pot)
    elseif (channel == 6)
    board_sel = [0 0 1 1];% set board selected to 3
    potnum = 1;% set pot selected to 1 (2nd pot)
    elseif (channel == 7)
    board_sel = [0 1 0 0];% set board selected to 4
    potnum = 0;% set pot selected to 0 (1st pot)
    elseif (channel == 8)
    board_sel = [0 1 0 0];% set board selected to 4
    potnum = 1;% set pot selected to 1 (2nd pot)
    end
```

```
potval = str2double(get(handles.val_box,'String')); % check the value that
the user has selected to be written to the digipot (given as a percentage
of the full range of the digipot)

s1 = handles.s1; % sci setup handle

databyte1 = []; % byte for command and address to digipot
databyte2 = []; % 1st byte for value to digipot
databyte3 = []; % 2nd byte for value to digipot
% note databytes 1-3 is the standard protocol of communication to the chip
from its
% datasheet

var = [];
var2 = [];

databyte1(1,1:7) = [1 0 1 1 0 0 0]; % command for writing to the RDAC
register of digopot
databyte1(1,8) = potnum; % bit to select the pot to write to
databyte4 = board_sel; % halfbyte for representing which board should be
written to

putval = dec2binvec(1024*potval./100,16); % convert the percentage the user
selected as a number between 0 and 1023 (digopot accepts programmable range
from 0-1023 which is a 10 bit number),
% then convert that number two 2 bytes binary number

var2 = putval;

for k = 1:16
putval(1,(17-k)) = var2(1,k); %dec2binvec makes a vector in reverse (LSB
first), so it is converted to make it MSB first.
end

databyte2(1,1:8) = putval(1,1:8); % store first 8 bits as byte two
databyte3(1,1:8) = putval(1,9:16); % store last 8 bits as byte three

%--------encoding bytes----------------------------
```

```
% As a way to control for errors in byte transmission, each byte is coded
% with an address. Each byte is broken down into two, e.g. databyte1 will
% be broken down into databyte11 and databyte12. The first four bits of the
% split bytes are coded with an address (1-7) as there will be 7 such bytes
% that will be trasmitted in total. The MCU is asked to check whether the
% bytes are received in the correct order and only processes data if this
% is so. The mcu will respond if the correct order is received.

databyte11(1,5:8) = databyte1(1,1:4); % first half of databyte1 stored in
databyte11
databyte12(1,5:8) = databyte1(1,5:8); % second half of databyte1 stored in
databyte12
databyte11(1,1:4) = [0 0 0 1]; % databyte11 is coded with 1 (0 0 0 1), as
it is the first byte to be transmitted
databyte12(1,1:4) = [0 0 1 0]; % databyte12 is coded with 2 (0 0 1 0), as
it is the second byte to be transmitted

databyte21(1,5:8) = databyte2(1,1:4);
databyte22(1,5:8) = databyte2(1,5:8);
databyte21(1,1:4) = [0 0 1 1];
databyte22(1,1:4) = [0 1 0 0];
databyte31(1,5:8) = databyte3(1,1:4);
databyte32(1,5:8) = databyte3(1,5:8);
databyte31(1,1:4) = [0 1 0 1];
databyte32(1,1:4) = [0 1 1 0];

t1 = databyte4; % databyte 4 is actually set as a 4 bit byte (represents
boards selected 1-4)

databyte4(1,1:4) = [0 1 1 1]; % coded with 7 (0 1 1 1) as it is the 7th and
last byte to be transmitted.
databyte4(1,5:8) = t1;
%--------------------------------------
databyte11 = num2str(databyte11); % convert bytes to string. This is a work
around to convert them to decimal for before transmission (bin2dec requires
string input)
databyte12 = num2str(databyte12);
databyte21 = num2str(databyte21);
databyte22 = num2str(databyte22);
databyte31 = num2str(databyte31);
```

```
databyte32 = num2str(databyte32);
databyte4 = num2str(databyte4);

databyte11 = bin2dec(databyte11); % convert bytes to decimal for
transmission through serial comm.
databyte12 = bin2dec(databyte12);
databyte21 = bin2dec(databyte21);
databyte22 = bin2dec(databyte22);
databyte31 = bin2dec(databyte31);
databyte32 = bin2dec(databyte32);
databyte4 = bin2dec(databyte4);

fwrite(s1,databyte11); % transmit bytes though serial comm to MCU
fwrite(s1,databyte12);
fwrite(s1,databyte21);
fwrite(s1,databyte22);
fwrite(s1,databyte31);
fwrite(s1,databyte32);
fwrite(s1,databyte4);
fread(s1) % check response from MCU (should acknowledge successful
transmission sequence)

guidata(hObject,handles);

% --- Executes on button press in close.
function close_Callback(hObject, eventdata, handles)
% hObject    handle to close (see GCBO)
% eventdata  reserved - to be defined in a future version of MATLAB
% handles    structure with handles and user data (see GUIDATA)
s1 = handles.s1;
fclose(s1); % close the serial port to release resource
close();

% --- Executes on button press in Scroll_select.
function Scroll_select_Callback(hObject, eventdata, handles)
% hObject    handle to Scroll_select (see GCBO)
% eventdata  reserved - to be defined in a future version of MATLAB
% handles    structure with handles and user data (see GUIDATA)

% Hint: get(hObject,'Value') returns toggle state of Scroll_select
```

APPENDIX E LABVIEW CODES AND FRONT PANELS

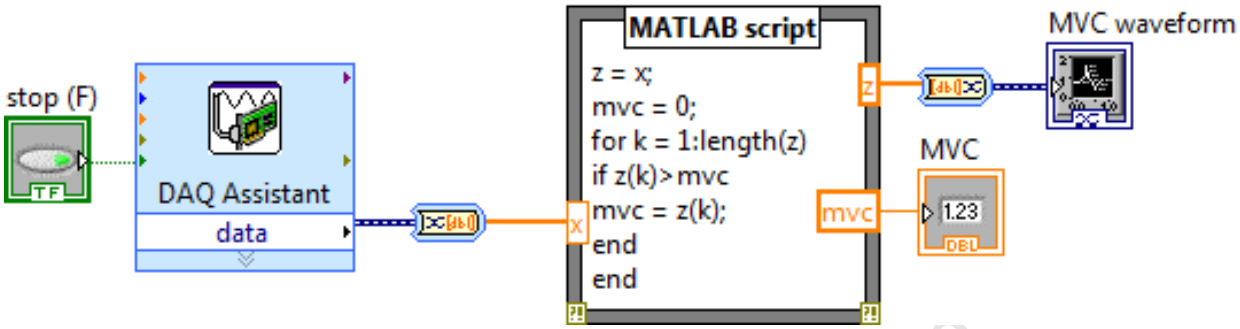

Figure E.1 Labview code for MVC measurement.

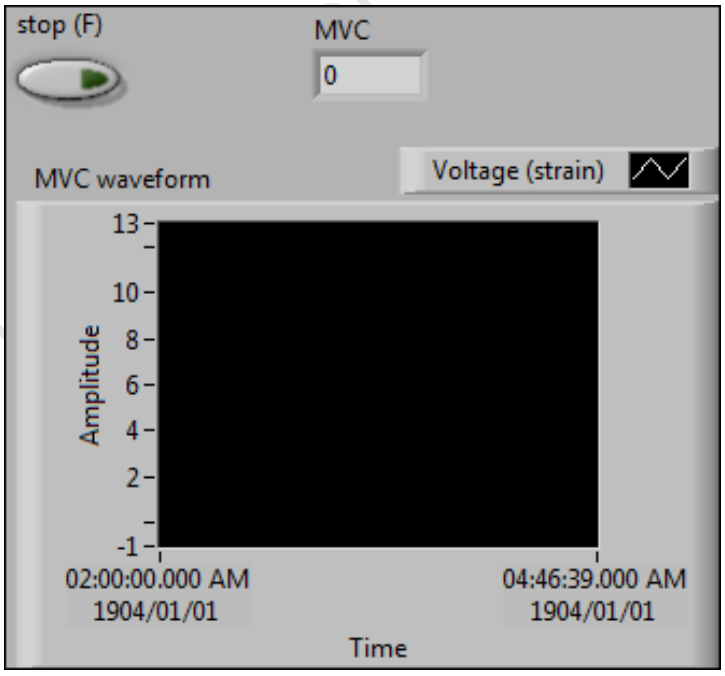

Figure E.2 Labview front panel for MVC measurement.

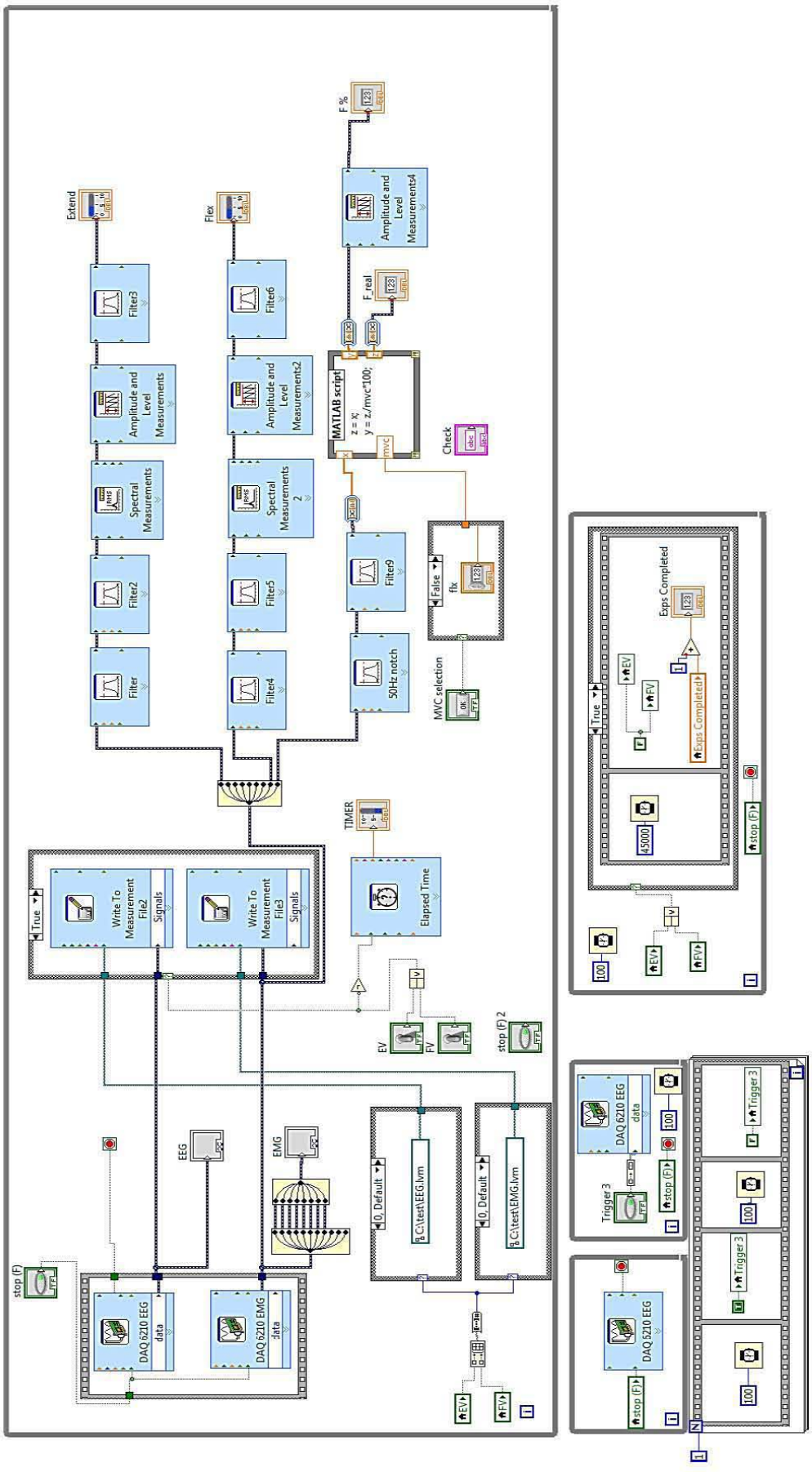

Figure E.3 Labview code for testing routine.

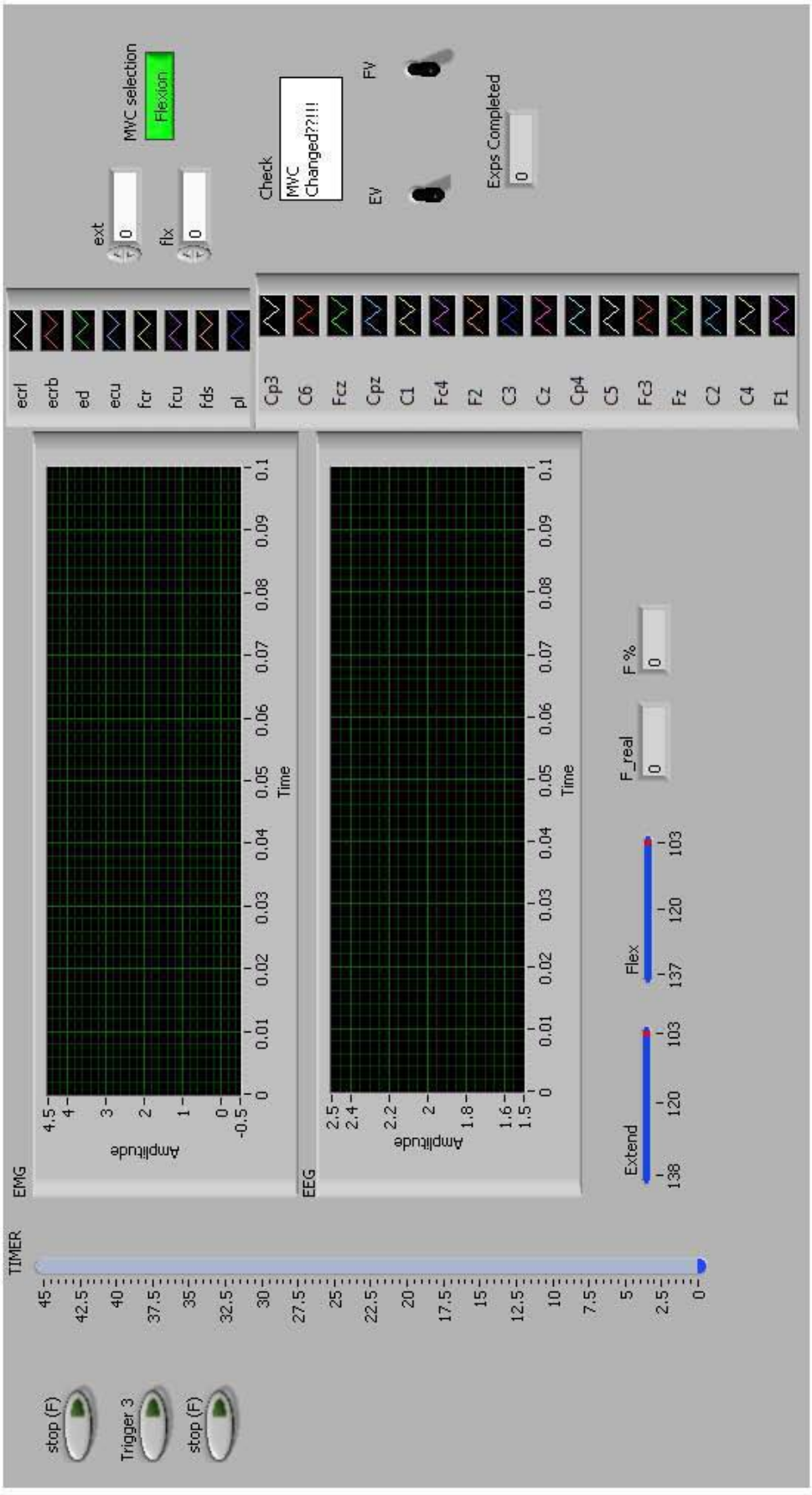

Figure E.4 Labview front panel (GUI) for testing routine.

Clinical Neurophysiology 124 (2013) 136–147

Contents lists available at SciVerse ScienceDirect

Clinical Neurophysiology

journal homepage: www.elsevier.com/locate/clinph

Neurophysiological, behavioural and perceptual differences between wrist flexion and extension related to sensorimotor monitoring as shown by corticomuscular coherence

Nikhil V. Divekar *, Lester R. John

MRC/UCT Medical Imaging Research Unit, Division of Biomedical Engineering, Department of Human Biology, University of Cape Town, Faculty of Health Sciences, Anzio Rd, Observatory, 7925 Cape Town, South Africa

See Editorial, pages 5–7

ARTICLE INFO

Article history:
Available online 5 September 2012

Keywords:
Corticomuscular coherence
Wrist flexion
Wrist extension
Precision
Perceived difficulty

HIGHLIGHTS

- Our inter-antagonistic corticomuscular coherence (CMC) comparison between wrist flexors and extensors accentuates an inverse relationship between CMC and precision, as opposed to the direct relationship found in a previous intra-muscle study.
- Functional suitability, long term usage adaptation and lower perceived difficulty of wrist flexion may explain this inverse relationship.
- We add to the debate around the contradictory literature relating CMC and precision by positing the confounding effect of perceived difficulty.

ABSTRACT

Objective: To investigate the effects of neurophysiological, behavioural and perceptual differences between wrist flexion and extension movements, on their corticomuscular coherence (CMC) levels.
Methods: CMC was calculated between simultaneously recorded electroencephalography (EEG) and electromyography (EMG) measures from fifteen healthy subjects who performed 10 repetitions of alternating isometric wrist flexion and extension tasks at 15% of their maximum voluntary contraction (MVC) torque levels. Task precision was calculated from torque recordings. Subjects rated the perceived difficulty levels for both tasks.
Results: Flexors had significantly lower; peak beta CMC, peak frequency, frequency width, normalised EMG beta power, torque fluctuation (<5 Hz and beta band) and perceived difficulty ratings; but higher MVC and precision compared to extensors. EEG alpha and beta powers were non-different between flexion and extension.
Conclusions: An inverse relationship between CMC and motor precision was found in our inter-muscle study, contrary to the direct relationship found in a prior intra-muscle study. Functional suitability, long term usage adaptation and lower perceived difficulty of wrist flexion may explain the results.
Significance: We extend the CMC literature to include the clinically different, antagonistic wrist flexors and extensors and add to the debate relating CMC and motor precision by positing the confounding effect of perceived difficulty.

1. Introduction

The antagonistic wrist flexor–extensor muscle sets are distinctive as present evidence reveals that there are neurophysiological, behavioural as well as clinical differences associated with their

* Corresponding author. Tel.: +27 214066235; fax: +27 214487226.
E-mail addresses: Nikhil.Divekar@uct.ac.za (N.V. Divekar), Lester.John@uct.ac.za (L.R. John).

1388-2457/$36.00 © 2012 International Federation of Clinical Neurophysiology. Published by Elsevier Ireland Ltd. All rights reserved.
http://dx.doi.org/10.1016/j.clinph.2012.07.019

motor functionality. There is sufficient evidence in humans (Palmer and Ashby, 1992; Yue et al., 2000; Vallence et al., 2012) as well as primates (Phillips and Porter, 1964; Cheney and Fetz, 1980; Mink and Thach, 1991; Keifer and Houk, 1994) to suggest that overall, upper limb flexors are more facilitated compared to extensors. This tendency is supported by the behavioural differences found by Salonikidis et al. (2011), who reported higher precision (lower coefficient of variation of force) for isometric wrist flexion compared to wrist extension; as well as Mavvidis et al. (2010) who reported faster learning and higher accuracy of forehand strokes (primarily involving flexors) compared to backhand strokes (primarily involving extensors) in Tennis. Furthermore, clinical observations have been reported such as faster motor recovery of wrist flexion compared to extension in stroke patients (Lieberman, 1986; Duncan and Badke, 1987; Little and Massagli, 2007) and greater impairment of wrist extensors in Parkinson's disease (Pfann et al., 2004).

Electrophysiological changes related to motor control can be investigated at the central and peripheral levels of the nervous systems, by using the non-invasive electroencephalogram (EEG) and the electromyogram (EMG), either independently, or in conjunction, in the form of corticomuscular coherence (CMC). CMC measures the degree of synchronisation between the oscillatory activity of the sensorimotor cortex (measured by EEG) and muscle (measured by EMG), and is prevalent in the beta band for weak to moderate isometric contractions (Halliday et al., 1998; Kristeva-Feige et al., 2002). However, this primarily phase sensitive process is deemed to be independent of other movement related amplitude changes observed in the EEG beta band (Baker and Baker, 2003; Riddle et al., 2004). In Baker's study, 20 Hz EEG power over the sensorimotor cortex doubled after administration of diazepam but no significant change in CMC was reported; conversely in Riddle's study, after administration of carbamazepine, a significant increase (89%) in beta band CMC was reported with no associated significant increase in 20 Hz EEG power. The functional role of CMC is still not fully understood; although proposed theories associate it with promoting of the existing steady motor state (Gilbertson et al., 2005); and facilitation of efficient sensorimotor monitoring of the peripheral system (Baker, 2007). CMC therefore appears to indicate an independent efferent phase adjustment process that operates in parallel with fundamental motor control processes, for the purpose of monitoring the state of the muscle through subsequent phase-synchronised afferent feedback (Witham et al., 2011). These proposed functional roles seem to match the results of Kristeva et al. (2007), who reported a direct relationship between beta CMC and motor precision, in a study involving a single muscle, where the higher precision periods had significantly higher CMC as well as EEG beta band spectral power compared to the lower precision periods.

The direct relationship between motor precision and CMC found by Kristeva et al. (2007), whilst being true for a single muscle (motor unit pool), may not necessarily hold true for comparisons between different muscle sets with varying neurophysiological properties e.g. wrist flexors-extensors. Indeed, inter-muscle CMC comparisons have been studied in the past, for example, between the upper limb vs lower limb and between proximal and distal musculature (Ushiyama et al., 2010). However, no study has investigated the relationship between motor precision and CMC of the equally distal, antagonistic, wrist flexors and extensors. We hypothesise that an inverse motor precision vs CMC relationship may exist between wrist flexors and extensors; i.e. isometric wrist flexion would be carried out at higher motor precision levels, but with lower flexor CMC levels, due to a reduced need for their sensorimotor monitoring by the cortex for stabilisation, as they are better facilitated and possibly better adapted to isometric force production compared to extensors.

We therefore aim to compare CMC (peak CMC, peak frequency, peak frequency width), as well as associated variables related to cortical activity (normalised EEG alpha and beta powers), muscle activity (normalised EMG beta power) and behaviour (motor precision) between wrist flexion and extension tasks in a high precision experiment, in order to explore this inter-muscle precision vs CMC relationship. Additionally, we will investigate any possible correlation between perception (task perceived difficulty) and beta-CMC, as we theorise that wrist flexion would be performed with greater ease (less perceived difficulty) than extension. This CMC comparison between the antagonistic wrist muscles may help to improve our overall understanding of the functional role of EEG–EMG synchronisation and also provide insight into the underlying causes of the functional differences (clinical and normative) reported between wrist flexors and extensors.

2. Methods

2.1. Subjects

Fifteen healthy male right-handed subjects (23.5 ± 2.7 years), without any history of neurological disease, participated in the study. The handedness was verified according to the Oldfield questionnaire (Oldfield, 1971). Subject participation followed approval by the university human ethics committee with written informed consent according to the declaration of Helsinki (World Medical Association, 2008).

2.2. Experimental paradigm

Subjects were seated in a dimly lit room. The right forearm was rested on a wooden support and the right hand was inserted through a perspex splint to prevent movement of the fingers relative to the hand (Fig. 1A). The wrist angle was thus maintained at 180°. The forearm was then strapped down to prevent any movement relative to the wrist. The forearm was positioned mid-way between pronation and supination to equalise the effect of gravity during extension and flexion. The MVC for each task (extension, flexion) was measured as torque about the wrist joint prior to the experiments. During a task, subjects were prompted to either hold a wrist extension (task 1) or flexion (task 2) at a target Torque (TT) of 15% MVC for 45 s. This was achieved by providing visual feedback of the actual Torque (AT) represented by a moving white indicator which was to be kept coincident to a fixed black reference marker representing the TT. To enforce high precision, additional boundary markers were placed at 15 ± 1% MVC creating an allowable window, which was not to be crossed. Indicator sensitivity was set such that an application of 1% MVC torque would result in a displacement of 10 mm in the corresponding direction (right or left, extension or flexion). The visual feedback described above

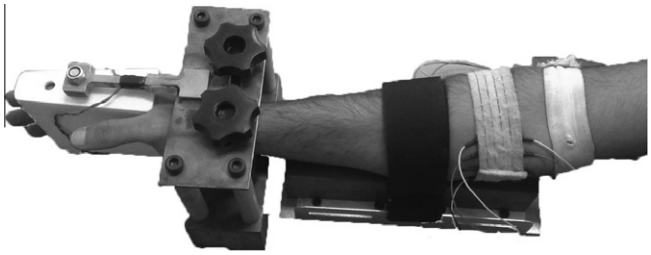

Fig. 1A. Subject carrying out isometric force maintenance task. The forearm is strapped to restrict movement; the hand is inserted into a splint to restrict finger movement with respect to the palm. Bipolar EMG electrodes are placed over corresponding flexor and extensor muscle bellies.

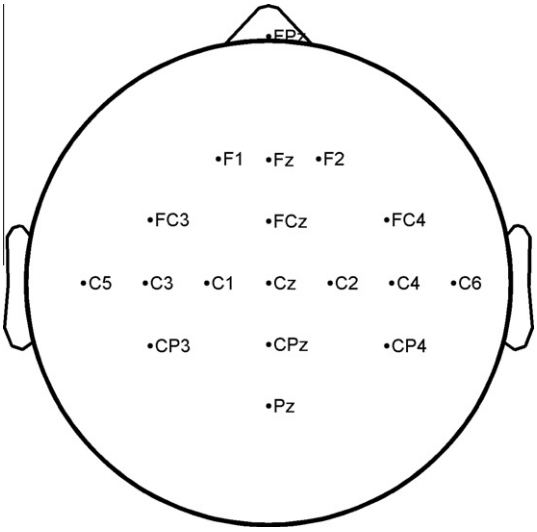

Fig. 1B. EEG measurement electrode positions. Electrode montage was chosen to best represent the sensorimotor areas of the wrist, and follows the standard 10–20 international system.

was provided on a monitor placed at eye level, 1.5 m in front of the subject. A total of 20 data points (2 tasks × 10 repetitions at 45 s each) were recorded for each subject. A 30 s break was allowed between repetitions to avoid fatigue. The sequence of the tasks was counter-balanced such that successive repetitions switched between the 2 tasks. To ensure that only isometric data was recorded, the recording was only started after the subject had managed to bring the indicator inside the allowable window. Subjects were instructed to avoid any other movements and to fix their gaze on the visual feedback indicator during the task. Data outside of the precision window was discarded.

2.3. Data acquisition

EEG, EMG and Electro-oculogram (EOG) data were recorded using bio-amplifiers with gains of 10000 for EEG and EOG and 3600 for EMG, filtered in the range of 0.1–200 Hz for EEG and EOG and 5–200 Hz for EMG. Torque data was recorded using strain gauges (mild steel foil, 5 mm, GF 2, 120 Ω) connected to a commercial strain gauge amplifier (CMMR > 120 dB, closed loop gain 3–60000). All data was digitized at 1000 Hz and the resolution was 16 bits i.e. 30 nV for EEG and EOG and 85 nV for EMG. Data was stored and analysed offline.

EEG was recorded using a 16 channel Electro-cap (Electro-Cap International Inc., or ECI) with tin electrodes (diameter = 12 mm) with the reference electrode placed at Pz and an active ground electrode at FPz (Fig. 1B). The scalp was cleaned, slightly abraded, and ECI Electro-Gel was injected into the electrode holders such that all electrode impedances were under 3 kΩ. Silver cup electrodes (Nihon Kohden, Japan, diameter = 10 mm) were placed to record both horizontal and vertical EOG, and injected with Elefix (Nihon Kohden, Japan) electrode paste.

Bipolar EMG was recorded from four wrist flexor muscles – Flexor Carpi Radialis (FCR), Palmaris Longus (PL), Flexor Digitorum Superficialis (FDS) and Flexor Carpi Ulnaris (FCU); and four wrist extensor muscles – Extensor Carpi Radialis Longus (ECRL), Extensor Carpi Radialis Brevis (ECRB), Extensor Digitorum (ED) and Extensor Carpi Ulnaris (ECU); with silver cup electrodes (Nihon Kohden, Japan, diameter = 10 mm) which were injected with Elefix paste, following appropriate skin preparation such that all electrode impedances were below 5 kΩ. Prior to the experiment, the flexion and extension torques were first recorded at MVC. Witte et al (2007) reported that beta range corticomuscular coupling is enhanced during isometric torque production at 16% MVC compared to a weaker 4% MVC. We accordingly chose our target torque to be 15% MVC in an effort to enhance corticomuscular coupling for extension and flexion tasks and to increase the chances of finding any differences between these two tasks. During the experiment

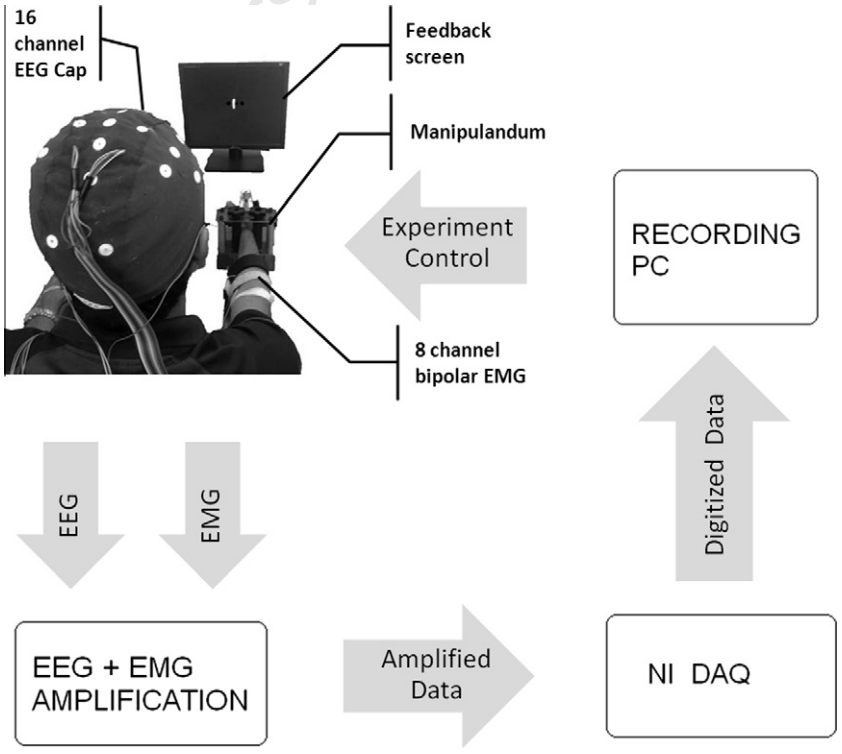

Fig. 1C. Block diagram of the overall system. % MVC visual feedback, manipulandum, EEG and EMG recording, digitization and storage are illustrated.

the wrist torques were then scaled to their respective MVCs, and displayed in real time using Labview (National Instruments, USA) on an LCD computer monitor (Fig. 1C).

At the end of the experiment, subjects were asked to rate perceived difficulty of the high precision flexion and extension tasks, using a scale of 1–5, where 1 = very easy, 2 = easy; 3 = moderate; 4 = difficult; 5 = very difficult.

2.4. Data analysis

Only data relating to the constant hold phase were analysed, i.e. excluding the data related to the subject going from rest to 15% MVC. The EMG signals were rectified. EEG voltage signals were derived as current source density (CSD) estimates using the spherical splines algorithm developed by Perrin et al. (1989) and implemented in MATLAB (Kayser and Tenke, 2006a,b; Kayser, 2011). Continuous EEG and EMG data from each 45 s repetition was divided into 42 artefact-free segments of 1024 ms with no overlap, allowing for a frequency resolution of 0.98 Hz.

Spectral Power SP_C for each EEG or EMG channel C was calculated:

$$SP_C(f) = \frac{1}{N}\sum_{i=1}^{N} C_i(f)C_i^*(f) \quad (1)$$

where C_i is the Fourier transformed channel C for a segment number ($i = 1 \ldots N$) and '*' represents the complex conjugate. The number of segments (N) was 42.

Coherence between an EEG channel ($c1$) and EMG channel ($c2$) was calculated as follows:

$$Coh_{C1C2}(f) = \frac{|S_{c1,c2}(f)|^2}{|Sp_{c1}(f)| \times |SP_{c2}(f)|} \quad (2)$$

Where $SP_{c1}(f)$ and $SP_{c2}(f)$ are the spectral powers of EEG channel ($c1$) and EMG channel ($c2$) respectively. $S_{c1,c2}(f)$ is the cross-spectrum of c1and $c2$ respectively, calculated using Eq. (3) as:

$$S_{c1,c2}(f) = \frac{1}{N}\sum_{i=1}^{N} C1_i C2_i^*(f) \quad (3)$$

For each task, CMC was calculated between every EEG and EMG channel, i.e. 16 EEG channels and 4 (synergist muscles) EMG channels.

Coherence is considered to be significant if the resulting value lies above the confidence level (CL) (Rosenberg et al., 1989) i.e.

$$CL = 1 - (1-\alpha)^{\frac{1}{n-1}} \quad (4)$$

where n is the number of segments i.e. 42 and alpha, 'α', is the desired level of confidence. We considered coherence to be significant over the upper 95% confidence limit. In our case the confidence limit is 0.07. Note that the stability of the CMC spectrum based on this confidence limit (CL) was post-hoc verified by the non-significant variation of CMC_{MAX} (defined below) with repetition.

For each muscle (EMG channel), only the highest CMC value (CMC_{MAX}) from the 16 EEG–EMG coherence spectra, was used for subsequent analyses; this process is similar to the method used by Witte et al (2007) and Johnson et al (2011). At CMC_{MAX}, the corresponding EEG channel was always one of the 5 contra-lateral motor region electrodes: FC3, C1, C3, C5, CP3; and the peak frequency (FP) was in the beta (15–35 Hz) band.

In addition, when CMC_{MAX} was greater than the CL, the frequencies where the coherence curve first met the CL when traced backward from FP (F1), and where the coherence curve first met the CL when traced forward from FP (F2) were found, facilitating an estimate of the frequency width (FW) of significant coherence, F2–F1.

In a recent study (Ushiyama et al., 2011b), a direct relationship between beta-CMC and normalised EEG and EMG beta powers was reported. To investigate the same in our study, we similarly calculated the ratio of the sum of the auto power spectral density within the beta band (15–35 Hz) to that of the entire frequency range (3–500 Hz) for both EEG (EEGβ-PSD) and EMG (EMGβ-PSD). In the same manner, we additionally calculated normalised EEG alpha (8–12 Hz) band power (EEGα-PSD) to examine the mu rhythm and possibly subject attention levels. Note, EEGβ-PSD and EEGα-PSD were calculated for each muscle at the EEG electrode with CMC_{MAX}. Normalisation is necessary to account for the inter-subject variation in EEG and EMG oscillatory activity levels as well as to account for variations in electrode-skin impedances which may differ across subjects as well as across trials.

The Mean Squared Error (MSE) of motor output was calculated for the flexion and extension tasks for each repetition:

$$MSE_k = \sum_{i=1}^{N} \frac{(TT - ATi)^2}{N} \quad (5)$$

where k is the repetition number; i is the sample point, N is the number of sample points (42×1024). TT is the target torque i.e. 15% MVC and ATi is the actual measured torque (as %MVC) for the ith sample.

Precision for each repetition was then calculated as the inverse of MSE:

$$PRECISION_K = \frac{1}{MSE_K} \quad (6)$$

The major frequency component of torque fluctuation that contributes to differences in precision is the low frequency band (0.1–5 Hz). We examined these changes by taking the sum of the auto-PSD function of the actual torque signal (as %MVC) between 0.1–5 Hz (Torque-low-PSD). Since significant EEG–EMG coherence was observed in the beta band, the changes in the same frequency band of the torque signal were also examined by determining the sum of the auto-PSD function of the actual torque signal (as %MVC) between 15–35 Hz (Torqueβ-PSD).

A total of 1200 (15 subjects × 10 repetitions × 8 muscles) observations of CMC_{MAX}, FP, FW, EEGβ-PSD, EEGα-PSD, EMGβ-PSD and 300 (15 subjects × 10 repetitions × 2 tasks) observations of Precision, Torque-low-PSD and Torqueβ-PSD were thus gathered for statistical analysis.

2.5. Statistical analysis

A repeated measures multilevel mixed effects linear regression analysis was carried out to test the effect of 'muscle' on observed variables – CMC_{MAX}, FP, FW, EEGβ-PSD, EEGα-PSD EMGβ-PSD; and the effect of 'task' on observed variables – Precision, Torque-low-PSD, Torqueβ-PSD.

To test the effect of 'Muscle' (task being explicit in the muscle tested), Muscle, Repetition and the Muscle × Repetition interaction were set as fixed effects (independent variables – IVs). As there are eight muscles, eight separate regression analyses were thus carried out, where each time a different muscle was used as the reference. To account for the correlation structure inherent in the data due to multiple testing on subject (muscle 1–8) and within muscle (repetitions 1–10), 'subject' and 'muscle within subject' were set as additional specific random effects to improve the model fit.

Similarly to test the effect of 'Task', Task, Repetition and the Task × Repetition interaction were set as fixed effects (independent variables – IVs). The task of extension was set as the reference. To account for the correlation structure inherent in the data due to multiple testing on subject (task 1–2) and within task (repetitions 1–10), 'subject' and 'task within subject' were set as additional specific random effects to improve the model fit.

After the initial model setup (all fixed effects initially included in model), any non-significant fixed effect variable was removed

one at a time and the model was rechecked for improvement in goodness of fit (Aikaikes Information Criterion, Bayesian IC, Likelihood ratio test). This procedure was repeated until all the remaining factors were significant or the goodness of fit became worse after removal of a factor, in which case it was restored. Examination of the residuals for the final model indicated that the underlying assumptions of the model were not violated. Note, CMC_{MAX} data was normalised by applying the arc hyperbolic tangent transformation (Rosenberg et al., 1989) prior to statistical analysis; and for other observed variables that deviated from a normal distribution, a natural log (Ln) transform was applied and the residual diagnostics carefully examined to ensure validity of the model. Linear regression was the preferred method over the simpler and more common ANOVA, due to data not being entirely normally distributed, even after transformation, and also due to its superiority in a repeated measures design (Gueorguieva and Krystal, 2004).

A paired samples *t*-test was conducted to compare normal (Shapiro-Wilk, 0.210) MVC data in wrist flexion and extension task conditions within-subjects.

A Wilcoxon matched-pairs signed rank test was conducted to compare perceived difficulty ratings in wrist flexion and extension task conditions within-subjects.

3. Results

All group data are represented as (means ± standard derivations); and significance of a factor conforms to $P < 0.05$.

Fig. 2 illustrates typical examples of raw EEG, raw EMG and Torque waveforms, their PSDs and finally EEG–EMG coherence (CMC), in flexion and extension tasks. Differences in the amplitudes of EEG fluctuation were not apparent between flexion and extension tasks, at any particular frequency band. It is evident that the amplitude of EMG fluctuation was greater in extension compared to flexion, particularly in the beta band, and was also associated with greater torque fluctuation in the beta (15–35 Hz) band as well as the lower frequency (<5 Hz) band for the extension task. The maximum CMC, which was restricted to the beta band, was higher in extension compared to flexion.

Fig. 3 illustrates typical single repetition topographical plots (Delorme and Makeig, 2004) of peak CMC values across all EEG channels for extensors and flexors; and the corresponding CMC frequency spectrum of the EEG–EMG channel pair with the highest peak CMC (CMC_{MAX}). It is evident that for every muscle, CMC_{MAX} was primarily obtained from one of the EEG electrodes representing the contra-lateral sensorimotor area, and its peak frequency was primarily restricted to the beta band. Overall higher CMC_{MAX} values are apparent for extensor muscles compared to flexor muscles.

CMC_{MAX} was significantly lower for any flexor (FCR (0.15 ± 0.08); PL (0.16 ± 0.08); FDS (0.16 ± 0.09); FCU (0.16 ± 0.08)) muscle compared to an extensor (ECRL (0.20 ± 0.10); ECRB (0.20 ± 0.09); ED (0.19 ± 0.10); ECU (0.19 ± 0.10)). CMC_{MAX} was not significantly different among the synergists i.e. within the extensors and flexors. See Fig. 4A. Repetition and its interaction with muscles were not significant.

FP was significantly lower for any flexor (FCR (25.1 ± 5.4 Hz); PL (24.3 ± 5.6 Hz); FDS (24.5 ± 5.8 Hz); FCU (25.2 ± 5.6 Hz)) muscle compared to an extensor (ECRL (26.5 ± 5.7 Hz); ECRB (26.5 ± 5.8 Hz); ED (26.1 ± 5.7 Hz); ECU (26.1 ± 6.1 Hz)), except when comparing FCR-ED, FCU-ED, FCR-ECU and FCU-ECU where there was no significant difference. FP was not significantly different among the synergists i.e. within the extensors and flexors. See Fig. 4B. Repetition and its interaction with muscles were not significant.

FW was significantly lower for any flexor (FCR (2.62 ± 3.17 Hz); PL (2.93 ± 3.35 Hz); FDS (3.06 ± 3.96 Hz); FCU (3.01 ± 3.87 Hz)) muscle compared to an extensor (ECRL (4.84 ± 5.14 Hz); ECRB (4.55 ± 5.22 Hz); ED (4.43 ± 5.22 Hz); ECU (4.76 ± 5.70 Hz)). FW was not significantly different among the synergists i.e. within the extensors and flexors. See Fig. 4C. Repetition and its interaction with muscles were not significant.

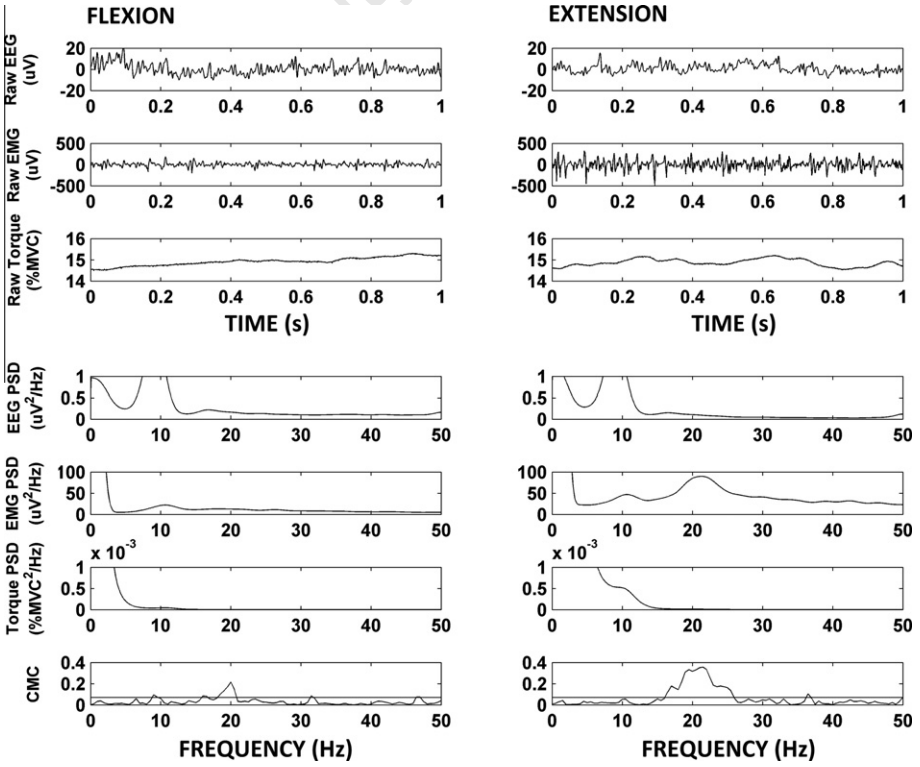

Fig. 2. Flexion and extension comparisons between typical raw EEG, EMG and torque signals, their power spectral density functions and EEG–EMG coherence (CMC) spectra, during sustained isometric contraction at 15% of MVC. In the coherence spectra, the estimated confidence limit (CL) is shown by the horizontal dashed lines at 0.07.

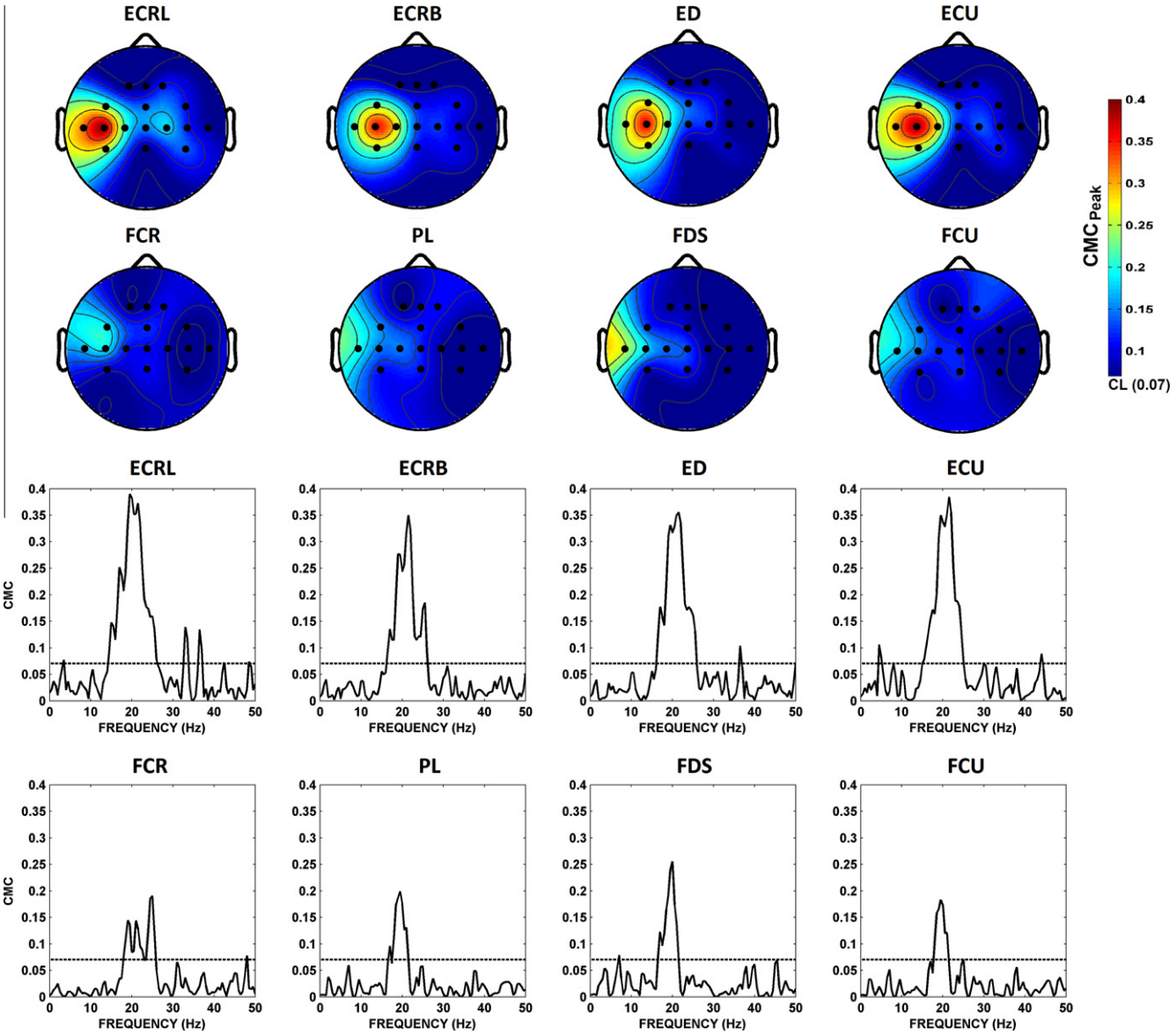

Fig. 3. Typical single repetition topographical plots of peak CMC values across all EEG channels for extensors and flexors, and the corresponding CMC frequency spectrum of the EEG–EMG channel pair with the highest peak CMC (CMC_{MAX}). From the topographical plots, CMC_{MAX} values can be seen to be restricted to the contra-lateral sensorimotor cortex, whereas their peak frequencies restricted to the beta-band as can be seen in their spectra below. Note that the dotted line on the CMC spectra represents the computed confidence level (CL) i.e. 0.07, thus all CMC_{MAX} values were above the CL.

EEGα-PSD was not significantly different between muscles. EEGα-PSD was significantly ($P < 0.0001$) different for repetition of muscle specific task with a 1% increase for every unit of repetition regardless of muscle. The interaction of repetition with muscle was not significant.

EEGβ-PSD was not significantly different between muscles. Repetition and its interaction with muscles were not significant.

EMGβ-PSD was significantly lower for any flexor (FCR (0.15 ± 0.03); PL (0.15 ± 0.04); FDS (0.16 ± 0.03) and FCU (0.16 ± 0.03)) compared to ECRL (0.18 ± 0.05); and was significantly lower for FCR and PL compared to ECRB (0.17 ± 0.04) and ED (0.17 ± 0.05). There was no significant difference between any flexor and ECU (0.16 ± 0.05). Also there was no significant difference among the synergists i.e. within the extensors and flexors. See Fig. 5. Repetition and its interaction with muscles were not significant.

MVC torque was significantly higher for wrist flexion (14.7 ± 2.1 Nm) compared to extension (8.7 ± 2.7 Nm). See Fig. 6A.

Precision was significantly higher for wrist flexion (15.9 ± 12.2) compared to extension (4.9 ± 3.8) task conditions. See Fig. 6B. Precision was significantly ($P = 0.03$) different with Repetition, with a 2% decrease with every unit of repetition regardless of task. The interaction between task and repetition was non-significant.

Torque-low-PSD was significantly lower in wrist flexion (0.10 ± 0.15%MVC^2) compared to extension (0.48 ± 1.58%MVC^2) task conditions. See Fig. 6C. Torque-low-PSD was significantly ($P < 0.01$) different with Repetition, with a 3% increase with every unit of repetition regardless of task. Interaction of task and repetition was not significant.

Torqueβ-PSD was significantly lower in wrist flexion ($4.0E^{-5}$ ± $5.0E^{-5}$%MVC^2) compared to extension ($1.4E^{-4}$ ± $2.1E^{-4}$%MVC^2) task conditions. See Fig. 6D. Repetition and its interaction with task were not significant.

Perceived difficulty ratings were significantly lower for the wrist flexion task (2.1 ± 0.6) as compared to the wrist extension task (3.9 ± 0.8). See Fig. 6E.

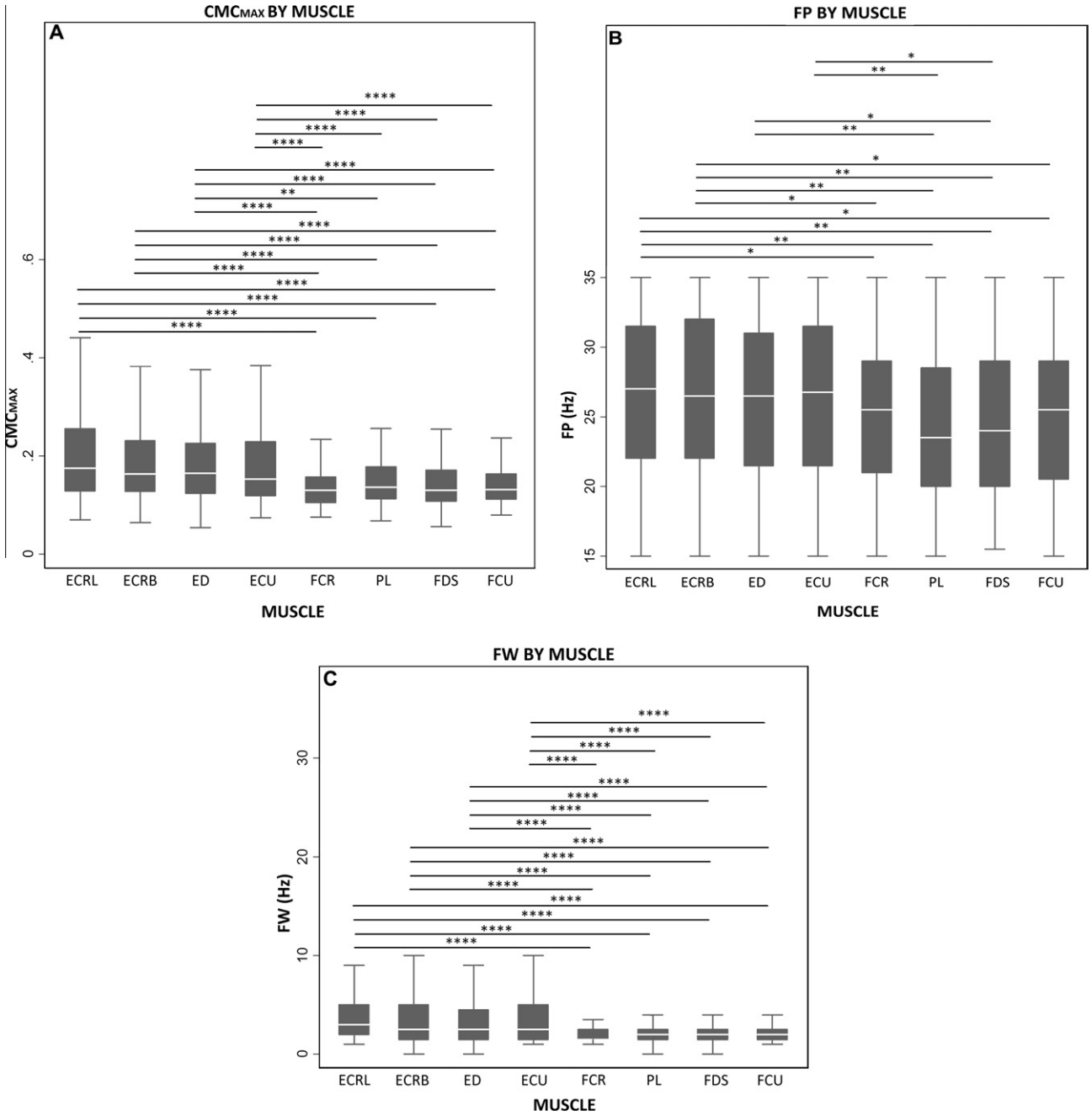

Fig. 4. (A–C) CMC_{MAX}, FP and FW comparisons between wrist flexors and extensors. Significant differences between extensors and flexors denoted by: *($P < 0.05$), **($P < 0.01$), ***($P < 0.001$), ****($P < 0.0001$).

4. Discussion

The main finding of this study is the inverse relationship between beta CMC and motor precision when comparing the antagonistic wrist flexion and extension tasks; i.e. peak beta CMC (CMC_{MAX}) as well as Frequency Width (FW) were significantly lower for the wrist flexors compared to extensors, although wrist flexion was performed with significantly higher precision compared to extension. When considering that the proposed functional roles of beta CMC in prior literature relate it to effecting higher motor output stability through improved sensorimotor integration (Baker, 2007; Kristeva et al., 2007; Witham et al., 2011), our results are contradictory. However, various neurophysiological, as well as perceptual (as found in our study) differences exist between the antagonistic wrist flexor–extensor muscles, and corresponding flexion-extension tasks, that may have influenced the beta CMC levels. We explore these differences to help explain our results and consequently further extend our understanding of the motor precision vs CMC relationship.

4.1. Neurophysiological factors related to flexor-extensor CMC differences

4.1.1. EEG power and cortical (M1, S1, SMA) representation of muscles

The ability of the scalp surface electrodes to successfully record the oscillatory electrical activity of the cortical neurons which are controlling (M1) and/or monitoring (S1) the wrist muscles depends on factors such as neuronal location, depth and orientation relative

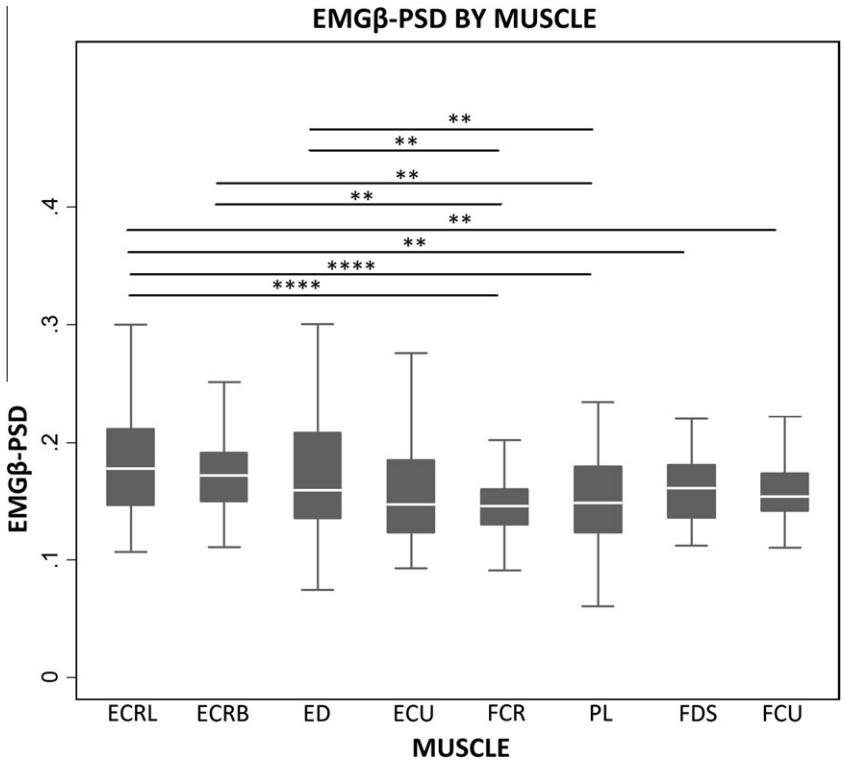

Fig. 5. EMGβ-PSD comparisons between wrist flexors and extensors. Lower EMGβ-PSD is evident for flexors compared to extensors. Significant differences between extensors and flexors denoted by: $^{*}(P < 0.05)$, $^{**}(P < 0.01)$, $^{***}(P < 0.001)$, $^{****}(P < 0.0001)$. Significant intra-group differences (within extensors, flexors) denoted by: $^{\#}(P < 0.05)$, $^{\#\#}(P < 0.01)$, $^{\#\#\#}(P < 0.001)$, $^{\#\#\#\#}(P < 0.0001)$.

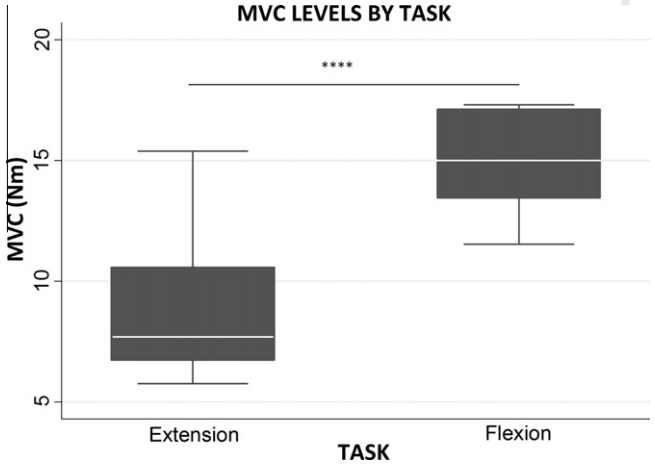

Fig. 6A. MVC Levels for flexors and extensors. Results showing MVC levels of subjects were significantly higher for flexion than for extension. Significant difference denoted by: $^{****}(P < 0.0001)$.

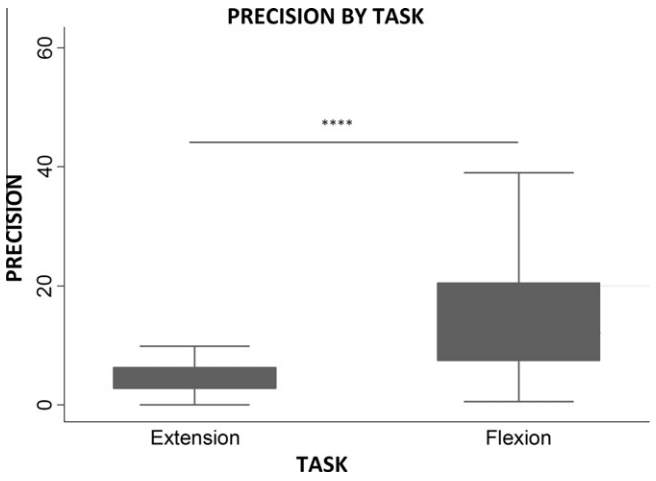

Fig. 6B. Precision comparisons between flexion and extension tasks. Higher precision is evident for flexion compared to extension. Significant difference denoted by: $^{****}(P < 0.0001)$.

to the recording site. Little difference is expected between the locations and depths of cortical neurons related to wrist extensors and flexors as both sets of muscles are of the same joint (Cheyne et al., 1991; Hluštík et al., 2001). But, although unlikely, a significant bias in neuronal orientation between flexors and extensors may affect the CSD derived EEG, as CSD estimates are sensitive only to normal currents. However there was no significant difference in normalised EEG powers (EEGα-PSD, EEGβ-PSD) between wrist extension and flexion in our study. Furthermore, EEG power has been suggested to be independent of CMC (Baker and Baker, 2003; Riddle et al., 2004). Although EEGα-PSD increased significantly, albeit slightly (+1%) with repetition, this may be attributed to the subjects performing the tasks with slightly reduced attention as the experiment progressed. Since there are no apparent differences in the scalp EEG representations of wrist flexion and extension, it does not explain the differences in CMC.

Previous findings (Yue et al., 2000), using the fMRI imaging technique, indicated higher CNS activation volumes, globally as well as in the supplementary motor area (SMA), contralateral motor cortex (MC) and cerebellum, for the thumb extensor compared to the flexor. In addition, EEG-derived MRCP levels (SMA, contralateral MC) were higher for the extensor. These findings were attributed to higher brain activation needed to compensate for the

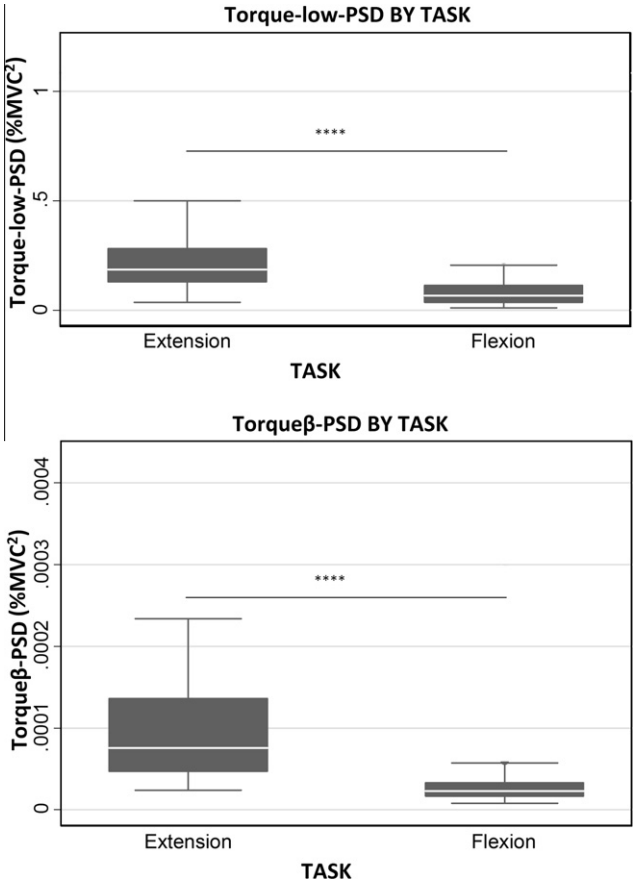

Fig. 6. (C and D) Torque powers at lower (<5 Hz) frequency band (Torque-low-PSD) and beta (15–35 Hz) frequency band (Torqueβ-PSD) compared between wrist extension and flexion tasks. Significantly lower Torque-low-PSD and Torqueβ-PSD are evident for flexion compared to extension. Significant difference denoted by: ****($P < 0.0001$).

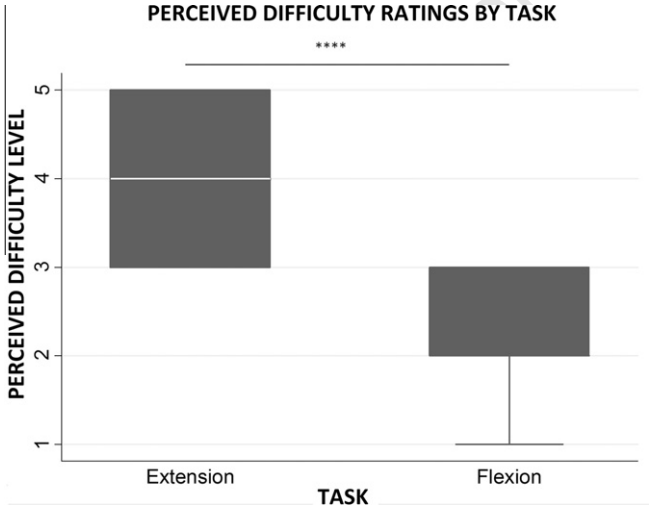

Fig. 6E. Perceived difficulty ratings of tasks compared between wrist flexion and extension. Results showing lower perceived difficulty for wrist flexion compared to extension. Significant difference denoted by: ****($P < 0.0001$).

greater inhibition and lower facilitation of the extensors compared to flexors, with a possible extrapolation of results to the elbow as well as wrist levels. However, as previously indicated, specifically in the contralateral MC, motor process activity levels are reported (albeit in experimental studies confined to beta EEG) to be independent of the phase synchronisation tagged by CMC. Thus it is unlikely that greater activity in the contralateral MC could have directly contributed to the higher wrist extensor CMC observed in our study.

4.1.2. Thalamus and basal ganglia

The thalamus is deemed to be one of the structures responsible for the generation and or modulation of the oscillatory activity measured by EEG at the cortical level (Herrero et al., 2002; Baker and Baker, 2003). The thalamus is also a relay centre sub-serving both sensory and motor mechanisms. It is thus possible that it plays a key role in the process of sensorimotor binding tagged by CMC. Even though the wrist extensors and flexors are anatomically close (both control the wrist joint), they are functionally different. It is likely that this differentiation also exists at the thalamic level, where greater sensorimotor monitoring may have been effected for the wrist extensors, resulting in their greater CMC levels, as was found in our study.

Similarly, the basal ganglia also have a regulatory influence on the cortex, as they provide information for both automatic and voluntary motor responses to the pyramidal system (Herrero et al., 2002). The basal ganglia have also been proposed as one of the likely structures responsible for modulating the beta oscillatory activity at the cortical level (Brown and Marsden, 1998; Brown, 2000), which is postulated to drive the oscillatory activity at the muscular level. It is thus possible that the variance found in our study between flexor-extensor beta-CMC levels (extensors having higher beta-CMC), may also have been prompted at the level of the basal ganglia. Such neurophysiological differences at the basal ganglia between wrist flexors and extensors, have been reported in prior literature, for example, cells in the monkey basal ganglia (globus pallidus pars interna) have been reported to exert a greater inhibitory effect on wrist extensors than on wrist flexors (Mink and Thach, 1991).

4.1.3. Cortico-spinal projection density

CMC is proposed to be mediated via the fast corticospinal pathways; hence the density of monosynaptic corticospinal projections to a muscle would reflect on the relative involvement of this direct pathway in motor control, denser projections signifying greater relative involvement and possibly higher resulting CMC levels. Palmer and Ashby (1992), using magnetic stimulation, concluded that there were denser projections to distal musculature of the upper limb compared to proximal, as well as to biceps (elbow flexors) compared to triceps (elbow extensors), but did not find conclusive differences between wrist extensors and flexors. However, in a later study using electrical stimulation, it was reported that wrist and finger extensors have denser projections compared to flexors (de Noordhout et al., 1999). These results support our findings of higher CMC for wrist extensors, as they suggest greater relative involvement of the direct monosynaptic corticospinal tract in wrist extensor control.

4.1.4. Renshaw cells

Renshaw cells are spinal interneurons that serve to regulate motor output, by inhibiting the oscillatory activity of the same alpha motor neurons that they receive excitatory input from. Thus stronger recurrent inhibition by Renshaw cells has an effect of reducing CMC (Williams and Baker, 2009). Differences in the strength of recurrent inhibition by Renshaw cells have been reported for distal versus proximal muscles of the upper limb (Katz et al., 1993). However recurrent inhibition by Renshaw cells for the antagonistic wrist muscle groups presents a different scenario. For example Renshaw cells of wrist extensors not only inhibit

themselves, but also inhibit their antagonist flexor groups, and vice versa, where the flexor coupled Reshaw cells inhibit the flexors as well as the antagonistic extensors (Aymard et al., 1997). This has an effect of levelling the Renshaw component of inhibition across these antagonistic muscle groups, eliminating the bias in inhibition between them and thus does not explain the observed differences between their CMC levels.

4.1.5. Muscle spindle density

CMC is influenced by oscillatory activity in both efferent and afferent pathways (Witham et al., 2011). As part of the afferent pathway, higher muscle spindle density would imply stronger oscillatory feedback to the sensorimotor cortex from the periphery with a resultant increase in CMC. The radial wrist extensors (ECRB and ECRL) have lower spindle densities than the flexors, while the digit and ulnar extensors (ED and ECU) have higher (Banks, 2006). Therefore spindle density differences between wrist extensors and flexors do not explain our findings and therefore cannot be the reason for lower CMC in all wrist flexors (Fig. 4a).

However, this anatomical difference may not be a limiting one, as reported by Witham et al. (2011) who found inter-subject variance between the level of CMC arising from differences in the relative contributions from the descending (motor) and ascending (sensory) signals, depending on factors such as the strategy used for torque control. In support of this finding, Chapman et al. (1987) also show that the level of feedback from afferents can also be modulated, via the descending command, thereby suggesting that overall higher sensory feedback may have been effected for the extensors (regardless of muscle spindle density differences) in an attempt to increase the extension precision level, ultimately resulting in higher CMC.

Conversely, it is plausible that torque fluctuation (precision) and CMC influence each other in tandem. Baker et al. (Baker et al., 2006) found significant beta band coherence between single afferent Ia (muscle spindle) spike trains and EMG, suggesting that muscle spindle discharge encodes oscillations in EMG activity, essentially forming a peripheral feedback loop. Furthermore, the sensitivity of spindles is dynamically controlled by γ motor neurons. In line with this theory, our results showing higher EMGβ-PSD for the extensors, associated with higher Torqueβ-PSD (lower precision) for extension, would also be associated with higher gains via the γ motor neurons, possibly enhancing the cortico-muscular phase synchrony, resulting in higher beta CMC for the extensors as found in our study.

4.1.6. Motor functional suitability of flexors – muscle size, strength and motor-units

Ushiyama et al. (2010) reported that upper limb distal muscles which are more suited for postural control had lower CMC than the proximal ones that are more suited to manipulative actions; suggesting that functional suitability of a muscle has an influence on CMC. Flexors of the upper limb (including wrist flexors) act primarily anti-gravity (e.g. lifting of objects), whereas the corresponding extensors are primarily pro-gravity. In the lower limb, anti-gravity muscles are known to be more suited for isometric torque maintenance compared to pro-gravity ones. Extrapolation to the upper limb, suggests that the anti-gravity wrist flexors were more functionally suited to the isometric contraction task than their antagonist extensors. Furthermore, a muscle's functional suitability for high precision tasks may also be predicted by considering its relative size and strength, as Hamilton et al. (2004) showed that, larger and stronger muscles are steadier than smaller and weaker ones; as they have a comparatively higher number of motor units recruited for a given %MVC, decreasing the CV of output torque. Wrist flexors, as reported by Salonikidis et al. (2011), are larger, stronger and steadier, further supporting their higher functional suitability over extensors. If CMC is the product of the complimentary 'test pulse' mechanism used to effect efficient sensorimotor monitoring of the peripheral system (Baker, 2007; Witham et al., 2011); then it is likely that more functionally suited muscles, being inherently steadier, require less sensorimotor monitoring for stabilisation; explaining the lower CMC for the flexors.

Our CMC findings for the equally distal intra-limb wrist muscles are however not generalizable to all inter-muscle comparisons. For example, despite Ushiyama et al. (2010) reporting lower CMC for the larger and stronger arm muscles compared to the weaker and smaller hand muscles i.e. upper limb proximal vs. distal, they also reported higher CMC in general for the larger and stronger lower limb muscles compared to smaller and weaker upper limb muscles.

4.1.7. Long-term usage adaptations

Salonikidis et al. (2011) estimated that wrist flexors are used relatively more frequently compared to extensors in everyday work, e.g. for lifting and holding on to objects, possibly leading to their greater adaptation to isometric force maintenance tasks. Evidence from brain activity studies as measured by cerebral blood flow (Seitz et al., 1990) and fMRI (Büchel et al., 1999), showed decreased activity in various areas of the cortex after extensive learning of motor tasks. Furthermore, daily-use induced technique improvements are associated with an independency in the motor unit firing rate, lower motor unit synchronization and substantially lower common oscillatory input from the sensorimotor cortex, especially in the beta (15–35 Hz) band (Semmler and Nordstrom, 1998; Semmler et al., 2004). This suggests that as the CNS adapts to make motor control more automatic, less cortical resources as well as less resource synchronisation are required. For the more adapted wrist flexors, it is likely that the reduced oscillatory drive from the sensorimotor cortex combined with the consequent reduction in motor unit synchronisation at the peripheral level; resulted in their lower beta cortico-muscular coupling (CMC_{MAX}) levels as well as lower EMG beta power (EMGβ-PSD) levels as found in our study.

Our study suggests a possible reduction in flexor CMC, due to their greater adaptation compared to the extensors, as a result of a natural bias in inter-muscle usage levels during ordinary day-to-day activities; similarly, a reduction in CMC due to adaptation after specialised training of a particular muscle set in athletes, has been reported by Ushiyama et al. (2010).

4.1.8. Synchrony in motor control among the synergists

We found no significant difference in CMC_{MAX} and related variables (FP, FW) within the synergists for wrist flexion or extension i.e. there was no significant difference in these variables within the extensors for extension, and within the flexors for flexion. See Fig. 4(A–C). Although discrepancies exist within synergists in their corticospinal projection densities, muscle spindle densities as well as muscle mass etc, we attribute this null result to the uniform sensorimotor monitoring of all the synergistic muscles by the cortex for force production in a particular direction (flexion or extension). The isometric wrist flexion and extension tasks used in this study, with the forearm oriented mid-way between pronation and supination requires co-contraction of all synergists, as also explained by a force vector diagram of this process (Bawa et al., 2000). Thus the synergists require an equal share of sensorimotor monitoring to sustain the direction and strength of the final resultant vector. We suspect that this may be facilitated by a common descending 'test pulse' (Witham et al., 2011) that is used to monitor all muscles in the synergistic group in parallel. This may be confirmed by testing for equal CMC phase lag values between the synergistic muscles, however this requires additional analyses.

4.2. Behavioural (precision) and perceptual (perceived difficulty) factors related to flexor-extensor CMC differences

We found an inverse CMC vs Precision relationship in this inter-muscle study, however it is apparent that this relationship is not generalizable, as Kristeva et al. (2007) experimenting on a single muscle, showed that periods of higher precision were associated with higher CMC, thus signifying a direct CMC vs Precision relationship. This discrepancy between precision and CMC also extends to fatigue studies done on CMC. Yang et al. (2009) reported lower precision and CMC in severe fatigue compared to minimal fatigue, whereas, Ushiyama et al. (2011a) reported lower precision but higher CMC in post-fatigue compared to pre-fatigue conditions. As a note, although we found Precision to decrease slightly (2%) with repetition, matched by a corresponding slight (3%) increase in Torque-low-PSD, we don't attribute this to fatigue, as the changes, although significant are very small and may be a result of a slight decrease in attention as the experiment progressed, possibly indicated by the small (1%) increase in EEGα-PSD. Furthermore, we found no significant change in CMC_{MAX} and FW levels with repetition.

Computer simulations (Yao et al., 2000) demonstrate that with motor-unit recruitment and discharge rates kept constant; increasing the number of synchronised motor units increased the magnitude of force fluctuation i.e. decreased precision, without increasing the average force levels. This also resulted in a significant increase in the measurable surface EMG power. These simulations, match our experimental results of higher torque fluctuation (Torque-low-PSD, Torqueβ-PSD) and higher EMGβ-PSD in extensors. It therefore seems that beta band CMC (CMC_{MAX}) positively influences beta oscillatory activity in EMG (EMGβ-PSD). The direct relationship between EMGβ-PSD and CMC_{MAX} (with FP being always in the beta band) found in our study has already been reported by Ushiyama et al. (2011a,b). The lower EMGβ-PSD for flexors in our study may partially explain their higher precision levels, as it would result in correspondingly lower torque fluctuations in the beta band (Torqueβ-PSD). More important is the predominant lower frequency (<5 Hz) torque component (Torque-low-PSD) as can be seen in the torque spectrum profiles (Fig. 2) which responds in the same manner as Torqueβ-PSD in our tasks. There is a suggested relationship between Torqueβ-PSD and Torque-low-PSD; however the practical mechanism that could underlie this is unclear.

In this study we additionally gathered perceived difficulty ratings of the experimental tasks (wrist flexion, wrist extension) from subjects, which were based on the ease with which they were able to maintain the Target Torque within the 15 ± 1% MVC window. Perceived difficulty is a perceptual variable that may be influenced by any of the central, peripheral as well as adaptive factors. Lower perceived difficulty ratings were reported for the wrist flexion task, which was carried out at higher precision levels compared to extension. Thus perceived difficulty was found to be directly related to CMC, EMG and torque power variables but inversely related to precision. We suggest that in the context of maintaining high precision (as in our study), performing a perceptually more difficult task, such as wrist extension, which is inherently less steady than flexion, would possibly induce an increase in the relative engagement of precision enhancing mechanisms as a compensatory measure. Such mechanisms may involve an increase in the relative involvement of the direct corticospinal tract to facilitate finer motor control, and also an increase in the gains of somatosensory afferents via the peripheral tracts to facilitate better feedback of muscle tension (gauged by Golgi Tendon Organs) and muscle length variation (gauged by muscle spindles); ultimately resulting in increased CMC. This may have been the likely situation in the studies of Kristeva et al. (2007) and Ushiyama et al. (2011a), where opposite precision vs CMC relationships were found. In the intra-task scenario of Kristeva et al. (2007), it would be more difficult to maintain higher precision compared to lower precision given constant task conditions; whereas in the pre-post fatigue task comparisons of Ushiyama et al. (2011a), it would be more difficult to maintain high precision, post fatigue, as compared to pre fatigue. In both studies the more difficult task was associated with higher CMC levels. In the intra-task fatiguing scenario of Yang et al. (2009), the experimental protocol is peculiar, as it emphasised maintenance of high force 'amplitudes' (above 90% of target force level), with little emphasis on high force 'precision'. Therefore the relationship between CMC and perceived task difficulty with respect to maintenance of high precision, in this case, is unclear.

5. Conclusions and clinical relevance

Our normative study has established that the generally better facilitated and clinically less compromised wrist flexors have significantly lower peak beta-CMC (CMC_{MAX}) levels compared to wrist extensors during high precision isometric tasks. Better functional suitability and long term adaptation of the flexors to isometric force production appear to be the main reasons for this difference. Consequently, flexion is performed with higher precision and lower perceived difficulty compared to extension. Our results thus reveal an inverse inter-muscle relationship between CMC and motor precision, opposite to the direct relationship found in a prior intra-muscle study (Kristeva et al., 2007). Accordingly we suggest that CMC levels may be directly correlated to the relative perceived difficulty levels experienced by the subjects in maintaining high motor precision during isometric contraction tasks.

In the context of Stroke recovery and Parkinson's disease rehabilitation, we speculate that extensive prior training involving wrist extensor movements, would in the short term result in lower CMC and perceived difficulty of wrist extensor movements. More importantly, in the long term, particularly if applied early to groups with a high risk of Stroke or Parkinson's disease, it is possible that such extensor training would influence long term adaptation and may ultimately partially reduce the extensor motor deficits of those diseases. Furthermore, Lundbye-Jensen and Nielsen (2008) brought forward the recovery tracking ability of CMC; as significantly reduced CMC levels, post hand and wrist immobilisation, subsequently returned to pre-immobilisation levels following a week of recovery time. Future rehabilitation programmes may thus incorporate CMC as an additional recovery tracking measure in Stroke and Parkinson's patients, and our study may serve as a normative source reference in such a clinical setting, particularly at the wrist joint.

Acknowledgements

We thank the National Reseach Fund (NRF) of South Africa for funding this study in part; S. Stoeckigt for the design of the electroencephalography system; L. Webb and J. Joseph for assistance with data recording; K. Mauff (Statistical Department, University of Cape Town) for statistical support and C. Harris for technical support in construction of the manipulandum.

References

Aymard C, Decchi B, Katz R, Lafitte C, Pénicaud A, Raoul S, et al. Recurrent inhibition between motor nuclei innervating opposing wrist muscles in the human upper limb. J Physiol. 1997;499:267–82.

Baker MR, Baker SN. The effect of diazepam on motor cortical oscillations and corticomuscular coherence studied in man. J Physiol. 2003;546:931–42.

Baker SN. Oscillatory interactions between sensorimotor cortex and the periphery. Curr Opin Neurobiol. 2007;17:649–55.

Baker SN, Chiu M, Fetz EE. Afferent Encoding of Central Oscillations in the Monkey Arm. J Neurophysiol. 2006;95:3904–10.

Banks R. An allometric analysis of the number of muscle spindles in mammalian skeletal muscles. J Anat. 2006;208:753–68.
Bawa P, Chalmers GR, Jones KE, Søgaard K, Walsh ML. Control of the wrist joint in humans. Eur J Appl Physiol. 2000;83:116–27.
Brown P. Cortical drives to human muscle: the Piper and related rhythms. Progress in Neurobiology. 2000;60:97–108.
Brown P, Marsden C. What do the basal ganglia do? The Lancet. 1998;351:1801–4.
Büchel C, Coull JT, Friston KJ. The Predictive Value of Changes in Effective Connectivity for Human Learning. Science. 1999;283:1538–41.
Chapman CE, Bushnell MC, Miron D, Duncan GH, Lund JP. Sensory perception during movement in man. Exp Brain Res. 1987;68:516–24.
Cheney PD, Fetz EE. Functional classes of primate corticomotoneuronal cells and their relation to active force. J Neurophysiol. 1980;44:773–91.
Cheyne D, Kristeva R, Deecke L. Homuncular organization of human motor cortex as indicated by neuromagnetic recordings. Neurosci Lett. 1991;122:17–20.
Duncan PW, Badke MB. Stroke *Rehabilitation:* The recovery of motor control. Chicago: Year Book Medical Publishers; 1987.
Delorme A, Makeig S. EEGLAB: an open source toolbox for analysis of single-trial EEG dynamics including independent component analysis. J Neurosci Methods. 2004;134:9–21.
Gilbertson T, Lalo E, Doyle L, Di Lazzaro V, Cioni B, Brown P. Existing Motor State Is Favored at the Expense of New Movement during 13–35 Hz Oscillatory Synchrony in the Human Corticospinal System. J Neurosci. 2005;25:7771–9.
Gueorguieva R, Krystal JH. Move over ANOVA: progress in analyzing repeated-measures data and its reflection in papers published in the Archives of General Psychiatry. Arch Gen Psychiatry. 2004;61:310–7.
Halliday DM, Conway BA, Farmer SF, Rosenberg JR. Using electroencephalography to study functional coupling between cortical activity and electromyograms during voluntary contractions in humans. Neurosci Lett. 1998;241:5–8.
Hamilton AFde C, Jones KE, Wolpert DM. The scaling of motor noise with muscle strength and motor unit number in humans. Exp Brain Res. 2004;157:417–30.
Herrero M-T, Barcia C, Navarro J. Functional anatomy of thalamus and basal ganglia. Child's Nervous System. 2002;18:386–404.
Hluštík P, Solodkin A, Gullapalli RP, Noll DC, Small SL. Somatotopy in Human Primary Motor and Somatosensory Hand Representations Revisited. Cereb Cortex. 2001;11:312–21.
Johnson AN, Wheaton LA, Shinohara M. Attenuation of corticomuscular coherence with additional motor or non-motor task. Clin Neurophysiol. 2011;122:356–63.
Katz R, Mazzocchio R, Penicaud A, Rossi A. Distribution of recurrent inhibition in the human upper limb. Acta Physiol. 1993;149:183–98.
Kayser J. CSD Toolbox – Current Source Density (CSD) and Surface Potential (SP) interpolation using spherical splines [Internet]. 2011 [cited 2012 Jan 21]. Available from: <http://psychophysiology.cpmc.columbia.edu/Software/CSDtoolbox/>.
Kayser J, Tenke CE. Principal components analysis of Laplacian waveforms as a generic method for identifying ERP generator patterns: I. Evaluation with auditory oddball tasks. Clin Neurophysiol. 2006a;117:348–68.
Kayser J, Tenke CE. Principal components analysis of Laplacian waveforms as a generic method for identifying ERP generator patterns: II. Adequacy of low-density estimates. Clin Neurophysiol. 2006b;117:369–80.
Keifer J, Houk J. Motor function of the cerebellorubrospinal system. Physiol Rev. 1994;74:509–42.
Kristeva R, Patino L, Omlor W. Beta-range cortical motor spectral power and corticomuscular coherence as a mechanism for effective corticospinal interaction during steady-state motor output. Neuroimage. 2007;36:785–92.
Kristeva-Feige R, Fritsch C, Timmer J, Lücking CH. Effects of attention and precision of exerted force on beta range EEG-EMG synchronization during a maintained motor contraction task. Clin Neurophysiol. 2002;113:124–31.
Lieberman J. Hemiplegia: rehabilitation of upper extremity. Boston: Butterworths; 1986. Stroke Rehab. p. 95–117.
Little J, Massagli T. Spasticity and associated abnormalities of muscle tone Rehabilitation medicine principles and practice. 3rd ed. Lippincott-Raven; 2007. p. 997–1013.
Lundbye-Jensen J, Nielsen JB. Central nervous adaptations following 1 wk of wrist and hand immobilization. J Appl Physiol. 2008;105:139–51.
Mavvidis A, Stamboulis A, Dimitiou V, Giampanidoy A. Differences in forehand and backhand performance in young tennis players. Stud Phys cult tour. 2010;17:315–9.
Mink JW, Thach WT. Basal ganglia motor control. III. Pallidal ablation: normal reaction time, muscle cocontraction, and slow movement. J Neurophysiol. 1991;65:330–51.
de Noordhout AM, Rapisarda G, Bogacz D, Gérard P, De Pasqua V, Pennisi G, et al. Corticomotoneuronal synaptic connections in normal man. Brain. 1999;122:1327–40.
Oldfield R. The assessment and analysis of handedness: The Edinburgh inventory. Neuropsychologia. 1971;9:97–113.
Palmer E, Ashby P. Corticospinal projections to upper limb motoneurones in humans. J Physiol. 1992;448:397–412.
Perrin F, Pernier J, Bertrand O, Echallier J. Spherical splines for scalp potential and current density mapping. Electroenceph clin Neurophysiol. 1989;72:184–7.
Pfann KD, Comella CL, Corcos DM, Brandabur M, Robichaud JA. Greater impairment of extension movements as compared to flexion movements in Parkinson's disease. Exp Brain Res. 2004;156:240–54.
Phillips C, Porter R. The Pyramidal Projection to Motoneurones of Some Muscle Groups of the Baboon's Forelimb. Physiology of spinal neurons: Elsevier; 1964.
Riddle CN, Baker MR, Baker SN. The effect of carbamazepine on human corticomuscular coherence. Neuroimage. 2004;22:333–40.
Rosenberg JR, Amjad AM, Breeze P, Brillinger DR, Halliday DM. The Fourier approach to the identification of functional coupling between neuronal spike trains. Prog Biophys Mol Biol. 1989;53:1–31.
Salonikidis K, Amiridis I, Oxyzoglou N, Giagazoglou P, Akrivopoulou G. Wrist Flexors are Steadier than Extensors. Int J Sports Med. 2011;32:754–60.
Seitz RJ, Roland PE, Bohm C, Greitz T. Motor learning in man: A positron emission tomographic study. Neuroreport. 1990;1:57–60.
Semmler JG, Nordstrom MA. Motor unit discharge and force tremor in skill-and strength-trained individuals. Exp Brain Res. 1998;119:27–38.
Semmler JG, Sale MV, Meyer FG, Nordstrom MA. Motor-Unit Coherence and Its Relation With Synchrony Are Influenced by Training. J Neurophysiol. 2004;92:3320–31.
Ushiyama J, Katsu M, Masakado Y, Kimura A, Liu M, Ushiba J. Muscle fatigue-induced enhancement of corticomuscular coherence following sustained submaximal isometric contraction of the tibialis anterior muscle. J Appl Physiol. 2011a;110:1233–40.
Ushiyama J, Suzuki T, Masakado Y, Hase K, Kimura A, Liu M, et al. Between-subject variance in the magnitude of corticomuscular coherence during tonic isometric contraction of the tibialis anterior muscle in healthy young adults. J Neurophysiol. 2011b;106:1379–88.
Ushiyama J, Takahashi Y, Ushiba J. Muscle dependency of corticomuscular coherence in upper and lower limb muscles and training-related alterations in ballet dancers and weightlifters. J Appl Physiol. 2010;109:1086–95.
Vallence AM, Hammond GR, Reilly KT. Increase in flexor but not extensor corticospinal motor outputs following ischemic nerve block. J Neurophysiol. 2012;107:3417–27.
Williams ER, Baker SN. Renshaw Cell Recurrent Inhibition Improves Physiological Tremor by Reducing Corticomuscular Coupling at 10 Hz. J Neurosci. 2009;29:6616–24.
Witham CL, Riddle CN, Baker MR, Baker SN. Contributions of descending and ascending pathways to corticomuscular coherence in humans. J Physiol. 2011;589:3789–800.
Witte M, Patino L, Andrykiewicz A, Hepp-Reymond M, Kristeva R. Modulation of human corticomuscular beta-range coherence with low-level static forces. Eur J Neurosci. 2007;26:3564–70.
World Medical Association. WMA Declaration of Helsinki – Ethical Principles for Medical Research Involving Human Subjects [Internet]. 2008 [cited 2012 Jan 20]. Available from: <http://www.wma.net/en/30publications/10policies/b3/>.
Yang Q, Fang Y, Sun C-K, Siemionow V, Ranganathan VK, Khoshknabi D, et al. Weakening of functional corticomuscular coupling during muscle fatigue. Brain Res. 2009;1250:101–12.
Yao W, Fuglevand RJ, Enoka RM. Motor-unit synchronization increases EMG amplitude and decreases force steadiness of simulated contractions. J Neurophysiol. 2000;83:441–52.
Yue GH, Liu JZ, Siemionow V, Ranganathan VK, Ng TC, Sahgal V. Brain activation during human finger extension and flexion movements. Brain Res. 2000;856:291–300.

Clinical Neurophysiology 124 (2013) 5–7

Contents lists available at SciVerse ScienceDirect

Clinical Neurophysiology

journal homepage: www.elsevier.com/locate/clinph

Editorial

Resonance between cortex and muscle: A determinant of motor precision?

See Article, pages 136–147

Coherence is a traditional measure for quantifying the linear correlation between two signals in the frequency domain (Halliday et al., 1995). It provides both amplitude and phase information about the relationship between two oscillatory signals at a particular frequency (Varela et al., 2001; Fell and Axmacher, 2011). In the field of neurophysiology, the most beneficial feature of coherence analysis is that, unlike evoked potential assessments that determine neural characteristics from nervous system responses to an external change, coherence can be used to estimate the synchronisation between two distant neural sites during natural motor behaviour. It was first reported around 15 years ago in both monkeys (Baker et al., 1997) and humans (Conway et al., 1995) that oscillations in the 15–35 Hz frequency range (β-band) appeared over the sensorimotor cortex during weak-to-moderate intensity steady contraction, and that these oscillations were coherent with electromyogram (EMG) activity of contralateral limb muscles. Many research groups have attempted to elucidate the mechanism underlying the generation of the corticomuscular coherence, and its functional significance.

Initially, corticomuscular coherence had been assumed to be an efferent phenomenon simply reflecting the propagation of central oscillations to the periphery through the corticospinal tract. Such an interpretation was based on studies showing that the time lag between the cortical recordings and EMG, estimated from the coherence phase–frequency relationship, was consistent with a simple conduction delay from the cortex to the muscle (Salenius et al., 1997; Gross et al., 2000; Mima et al., 2000). However, more recent studies have reported that the coherence phase estimates did not always fit the value expected for a simple conduction delay (Riddle and Baker, 2005; Witham et al., 2011), suggesting that corticomuscular coherence is not a simple efferent phenomenon. In addition, it was demonstrated that manipulation of the peripheral neural feedback loop by ischaemia (Pohja and Salenius, 2003) or arm cooling (Riddle and Baker, 2005) modulated corticomuscular coherence and/or its phase. Thus, the current main assumption is that corticomuscular coherence is a complex phenomenon with contributions from both the motor and somatosensory pathways.

Corticomuscular coherence is known to be most prominent during steady contraction while being abolished by movement (Baker et al., 1997; Feige et al., 2000; Kilner et al., 2000; Riddle and Baker, 2006). Thus, one of the main interests regarding the functional role of corticomuscular coherence has been its relation to motor precision. For example, it was demonstrated that the error signal (i.e. the difference between target and exerted forces) was smaller in the periods with high coherence between sensorimotor cortex activity measured by electroencephalogram (EEG) and EMG during steady force output than in the periods with low coherence (Kristeva et al., 2007). In addition, some studies have reported an acute increment in the magnitude of EEG–EMG coherence following visuomotor skill learning with improvements in motor performance (Perez et al., 2006; Mendez-Balbuena et al., 2012). As such, these studies provided evidence supporting a potential positive influence of the resonant activity between cortex and muscle on motor precision.

Conversely, a potential negative impact of the resonant activity between cortex and muscle on motor precision has also been suggested, based on data on individual differences in the magnitude of corticomuscular coherence. It was recently reported that, even within the same population (i.e. healthy young adults), the magnitude of EEG–EMG coherence varied among 100 individuals, and showed a significant positive correlation with the extent of the β-band grouped discharge in EMG signals (Ushiyama et al., 2011). Another study demonstrated that, compared with untrained individuals, well-trained athletes (i.e. ballet dancers and weightlifters) showed smaller EEG–EMG coherence with no clear grouped discharge in their EMG signals (Ushiyama et al., 2010). Because the EMG shows the final output of motor system, these studies assumed that its prominent oscillations disturb steadiness of motor behaviour. Overall, it is still open to question whether the resonance between cortex and muscle influences motor precision positively or negatively.

This issue studied by Divekar and John (2013) approached the functional role for corticomuscular coupling by examining differences in the magnitude of EEG–EMG coherence and the steadiness of exerted force between antagonistic muscle sets, i.e. wrist flexors and extensors, in healthy individuals. They focussed on these muscle sets because, in the fields of sports science and rehabilitation medicine, it is thought that, compared with wrist extensors, wrist flexors show higher accuracy, faster motor learning and faster motor recovery from disorders such as stroke. As a result, they found that the magnitude of EEG–EMG coherence was significantly smaller in wrist flexors with better motor precision, i.e. lower force fluctuations.

One of the most important findings in the study of Divekar and John (2013) was that not only the β-band component of the force signal, which would be directly influenced by the β-band grouped discharge in EMG, but also the mean squared error of force, which would mainly reflect the major lower frequency (i.e. ⩽4–5 Hz) force fluctuation, were significantly greater during wrist extension than during wrist flexion. Although it is still unclear

1388-2457/$36.00
http://dx.doi.org/10.1016/j.clinph.2012.08.004

how the β-band EMG oscillations induced by corticomuscular coupling are related to the generation of larger lower frequency force fluctuations, the authors provided variable information suggesting that the extent of resonance between cortex and muscle, as estimated by the magnitude of corticomuscular coherence, is a determinant of motor precision. Further, it is also of interest to note that the subjects perceived it to be more difficult to stabilise the force output during the wrist extension task than during the wrist flexion task. Because the subjects found a steady wrist extension task to be more difficult owing to inexperience through their daily living, the magnitude of corticomuscular coherence in wrist extensors might increase to promote effective sensorimotor binding. Conversely, it is also possible that, because the magnitude of corticomuscular coherence is higher in wrist extensors than in wrist flexors owing to inherent factors such as a greater density of corticospinal projections (de Noordhout et al., 1999), enhanced β-band grouped discharges on EMG could induce greater force fluctuations. The subjects might have perceived the wrist extension task to be more difficult via the somatosensory feedback system detecting the muscle tremor and/or the visual feedback system detecting the visuomotor error between the exerted force and the target force level. Overall, the results of this study provide evidence supporting potential interactions among corticomuscular coherence, motor precision and the perceived difficulty of the task.

As mentioned above, it seems likely that inter-muscle or inter-subject differences in the magnitude of corticomuscular coherence are negatively related to motor precision. However, the observed variance in fluctuations of motor output would be just within the subclinical level, which would not cause any problems in performing activities of daily living. Considering this point, there are a couple of questions that should be addressed in future studies. First, at the expense of some motor precision, are there any physiological benefits for the muscles or subjects with higher corticomuscular coherence? Next, if there are, why does corticomuscular coherence during weak-to-moderate intensity steady contraction occur only in the β-band, but not in the α-band or the γ-band? Finally, which part of the nervous system generates the oscillation (i.e. does a specific neural site act as a pace maker for the oscillation or does the oscillation reflect the characteristic frequency of sensorimotor network)? Furthermore, although corticomuscular coherence has been suggested in the literature to reflect the process of sensorimotor binding, the actual physiological meaning of sensorimotor binding is not fully understood.

Further, the best methods for analysis of the corticomuscular coupling remain the subject of debate. As mentioned above, coherence estimation comprises both co-variation in the amplitude and synchronisation of the phases of two oscillatory signals (Varela et al., 2001; Fell and Axmacher, 2011). However, physiologically, we can suppose both situations where the amplitudes of two signals co-vary with the phase difference unlocked, and where the phase difference is constant throughout the performed task while the amplitude co-variance is lower as a result of independent inputs to two neural sites. Because of methodological constraints, we cannot distinguish between these situations using only coherence analysis. In some situations, it would be better to evaluate the phase synchronisation and amplitude co-variance separately for a deeper physiological consideration of the resonance between cortex and muscle.

While scalp EEG signals reflect the grouped potentials of cortical neurons, such as local field potentials, under the electrodes, surface EMG signals are recorded from electrodes positioned in the direction of propagated potentials. Thus, full-wave rectification for surface EMG signals is needed to detect the temporal pattern of grouped firing of motor units (Halliday et al., 1995; Myers et al., 2003). Although it is a common pre-processing step prior to calculation of coherence based on the theory of signal processing regarding the detection of amplitude-modulated waves, there is still continuing debate about whether EMG rectification is necessary (Boonstra, 2010; Halliday and Farmer, 2010) or unnecessary (Neto and Christou, 2010; McClelland et al., 2012) for calculation of corticomuscular coherence.

Overall, corticomuscular coherence analysis is widely used as a tool in systems neuroscience, and particularly studies of motor control under natural motor behaviour. To clarify the precise neurophysiological property of the resonant activity between cortex and muscle in more detail, researchers have attempted to modify and reconsider the methodology used for analysis mathematically. It is expected that, as the authors have attempted in this issue, research into how neural processing within the body (accompanying the resonant activity between cortex and muscle) characterises the output from the body to the environment will be more advanced in the future.

References

Baker SN, Olivier E, Lemon RN. Coherent oscillations in monkey motor cortex and hand muscle EMG show task-dependent modulation. J Physiol 1997;501:225–41.

Boonstra TW. The nature of periodic input to the muscles. J Neurophysiol 2010;104:576. author reply 7.

Conway BA, Halliday DM, Farmer SF, Shahani U, Maas P, Weir AI, et al. Synchronization between motor cortex and spinal motoneuronal pool during the performance of a maintained motor task in man. J Physiol 1995;489:917–24.

de Noordhout AM, Rapisarda G, Bogacz D, Gerard P, De Pasqua V, Pennisi G, et al. Corticomotoneuronal synaptic connections in normal man: an electrophysiological study. Brain 1999;122:1327–40.

Divekar NV, John LR. Neurophysiological, behavioural, and perceptual differences between wrist flexion and extension related to sensorimotor monitoring as shown by corticomuscular coherence. Clin Neurophysiol 2013;124:136–47.

Feige B, Aertsen A, Kristeva-Feige R. Dynamic synchronization between multiple cortical motor areas and muscle activity in phasic voluntary movements. J Neurophysiol 2000;84:2622–9.

Fell J, Axmacher N. The role of phase synchronization in memory processes. Nat Rev Neurosci 2011;12:105–18.

Gross J, Tass PA, Salenius S, Hari R, Freund HJ, Schnitzler A. Cortico-muscular synchronization during isometric muscle contraction in humans as revealed by magnetoencephalography. J Physiol 2000;527:623–31.

Halliday DM, Farmer SF. On the need for rectification of surface EMG. J Neurophysiol 2010;103:3547. author reply 8–9.

Halliday DM, Rosenberg JR, Amjad AM, Breeze P, Conway BA, Farmer SF. A framework for the analysis of mixed time series/point process data–theory and application to the study of physiological tremor, single motor unit discharges and electromyograms. Prog Biophys Mol Biol 1995;64:237–78.

Kilner JM, Baker SN, Salenius S, Hari R, Lemon RN. Human cortical muscle coherence is directly related to specific motor parameters. J Neurosci 2000;20:8838–45.

Kristeva R, Patino L, Omlor W. Beta-range cortical motor spectral power and corticomuscular coherence as a mechanism for effective corticospinal interaction during steady-state motor output. Neuroimage 2007;36:785–92.

McClelland VM, Cvetkovic Z, Mills KR. Rectification of the EMG is an unnecessary and inappropriate step in the calculation of corticomuscular coherence. J Neurosci Meth 2012;205:190–201.

Mendez-Balbuena I, Huethe F, Schulte-Monting J, Leonhart R, Manjarrez E, Kristeva R. Corticomuscular coherence reflects interindividual differences in the state of the corticomuscular network during low-level static and dynamic forces. Cereb Cortex 2012;22:628–38.

Mima T, Steger J, Schulman AE, Gerloff C, Hallett M. Electroencephalographic measurement of motor cortex control of muscle activity in humans. Clin Neurophysiol 2000;111:326–37.

Myers LJ, Lowery M, O'Malley M, Vaughan CL, Heneghan C, St Clair Gibson A, et al. Rectification and non-linear pre-processing of EMG signals for cortico-muscular analysis. J Neurosci Meth 2003;124:157–65.

Neto OP, Christou EA. Rectification of the EMG signal impairs the identification of oscillatory input to the muscle. J Neurophysiol 2010;103:1093–103.

Perez MA, Lundbye-Jensen J, Nielsen JB. Changes in corticospinal drive to spinal motoneurones following visuo-motor skill learning in humans. J Physiol 2006;573:843–55.

Pohja M, Salenius S. Modulation of cortex-muscle oscillatory interaction by ischaemia-induced deafferentation. Neuroreport 2003;14:321–4.

Riddle CN, Baker SN. Digit displacement, not object compliance, underlies task dependent modulations in human corticomuscular coherence. Neuroimage 2006;33:618–27.

Riddle CN, Baker SN. Manipulation of peripheral neural feedback loops alters human corticomuscular coherence. J Physiol 2005;566:625–39.

Salenius S, Portin K, Kajola M, Salmelin R, Hari R. Cortical control of human motoneuron firing during isometric contraction. J Neurophysiol 1997;77: 3401–5.
Ushiyama J, Suzuki T, Masakado Y, Hase K, Kimura A, Liu M, et al. Between-subject variance in the magnitude of corticomuscular coherence during tonic isometric contraction of the tibialis anterior muscle in healthy young adults. J Neurophysiol 2011;106:1379–88.
Ushiyama J, Takahashi Y, Ushiba J. Muscle dependency of corticomuscular coherence in upper and lower limb muscles and training-related alterations in ballet dancers and weightlifters. J Appl Physiol 2010;109:1086–95.
Varela F, Lachaux JP, Rodriguez E, Martinerie J. The brainweb: phase synchronization and large-scale integration. Nat Rev Neurosci 2001;2:229–39.
Witham CL, Riddle CN, Baker MR, Baker SN. Contributions of descending and ascending pathways to corticomuscular coherence in humans. J Physiol 2011;589:3789–800.

Junichi Ushiyama *
Department of Rehabilitation Medicine,
Keio University School of Medicine,
35 Shinanomachi, Shinjuku-ku,
Tokyo 160 0016, Japan
**Tel.: +81 3 5363 3833; fax: +81 3 3225 6014.*

Graduate School of Fundamental Science and Technology,
Keio University,
3-14-1 Hiyoshi,
Kouhoku-ku, Yokohama,
Kanagawa 223 8522, Japan
Tel./fax: +81 45 566 1678.
E-mail address: ushiyama@bme.bio.keio.ac.jp

Junichi Ushiba
Department of Biosciences and Informatics,
Faculty of Science and Technology,
Keio University,
3-14-1 Hiyoshi, Kouhoku-ku,
Yokohama, Kanagawa 223 8522, Japan
Tel./fax: +81 45 566 1678.

Available online 20 September 2012